Pharmacological modulation and manipulation of cancer drug resistance

A thesis submitted for the degree of PhD.

By

Aoife Devery, B.Sc.

The experimental work described in this thesis was carried out under the supervision of

Prof. Martin Clynes and Dr. Robert O'Connor

National Institute for Cellular Biotechnology

Dublin City University

Glasnevin

Dublin 9

Ireland

January 2010

I hereby certify that this material, which I now submit for assessment on the programme of study leading to the award of Ph.D. is entirely my own work, that I have exercised reasonable care to ensure that the work is original, and does not to the best of my knowledge breach any law of copyright, and has not been taken from the work of others save and to the extent that such work has been cited and acknowledged within the text of my work.

Signed: _____   ID No.: _____

Date: _____

Acknowledgements

First and foremost I would like to thank my supervisor and co-supervisor, Dr. Robert O'Connor and Prof. Martin Clynes for giving me the opportunity to do a PhD, for always being there and for all the insight, support and encouragement over the past five and half years, especially towards the end.

Thanks to all the great researchers who have helped, encouraged and supported me over the years and who I have enjoyed working with. A special mention to Dr. Verena Murphy (for all the advice, cells, chats and smiles), Dr. Joanne Keenan (for the advice and bubbly early morning chats), Dr. Norma O'Donovan (who started me off back in A126 and followed through to the end with advice, understanding and availability even though she was very busy with her own students!), and finally Dr. Anne-marie Larkin (for all the chats, advice, insight and understanding).

To the many others who have helped me directly or indirectly with my work over the years. Dr. Finbarr O'Sullivan for all the help with the Confocal work. Micheal Henry for Mass Spec problem solving. Dr. Laura Breen for Western blots and much more. Dr. Britta Stordal for encouraging and going through ideas. Dr. Lisa Murphy for many of my queries, insight, support and for being there. Dr. Denis Collins for advice, encouragement, constant support and laughs from the beginning. Helena Joyce for her wonderful cell line and for the chats over early morning tea or in the corridor. To the other members of my group including my bench buddies, Grainne Dunne and Sandra Roche, for Western blots, all the MS help, and for putting up with stressed Aoife!

A very special thanks must go to my clean room and ex-clean room collegues; Alex, Brendan, Brigid, Zulfi, Martina, Norma, Dimitrius, and Thamir. Thank you for all the musical entertainment (!) and laughs in the clean room (especially late at night!), lab, lunch, tea, nights out and craic at the Tri-to-beat-Cancer triathalone (go team "in it not to win it"!). With a special thanks to Alex and Denis for help with the Western blots. And finally thanks for putting up with me when the stress really kicked in towards the end. Also, to Erica/Kishore and Joanne/Brendan/Zulfi/Britta/Paula for the use of their cleanroom when ours was booked up.

Aoife Devery

Abstract

The aim of this project was to investigate pharmacological methods of overcoming resistance in cancer. Novel compounds, targeted therapies and non-steroidal anti-inflammatory drugs (NSAIDs) were examined for their potential to modulate and manipulate specific forms of drug resistance.

Sixty one novel compounds were tested in combination with chemotherapeutic drugs in proliferation assays for their ability to overcome MRP1 and P-gp-mediated drug resistance. Two compounds were successful P-gp modulators in the DLKP-A cell line; the ditrifluoroacetyl resveratrol derivative, RBM15, and the macrocycle derivative, KG104.

A panel of nine therapeutic agents were evaluated for their potential to down-regulate multidrug resistant protein expression and thus, overcome P-gp, MRP1 or BCRP-mediated drug resistance, at and below pharmacologically-relevant concentrations. Two of these agents (indomethacin and 17-AAG) partially down-regulated the expression of P-gp in the A549-Taxol cell line but did not overcome P-gp-mediated resistance when combined with docetaxel simultaneously or in pre-treated proliferation assays. Three agents (lapatinib, sulindac sulphide and 17-AAG) reduced the expression of MRP1 in the A549 cell line. Only sulindac sulphide overcame MRP1-mediated resistance in the combination proliferations assays; however, this was due to the inhibitory mechanism of sulindac sulphide and not due to the down-regulation of the MRP1 protein. Five agents (17-AAG, lapatinib, indomethacin, elacridar and gefitinib) down-regulated the expression of BCRP in the DLKP-SQ/mitox cell line. Lapatinib, gefitinib, elacridar and 17-AAG overcame BCRP-mediated resistance in both the combination and pre-treatment proliferation assays. The data indicates that the amount of down-regulation resulting from treatment with these drugs was insufficient to overcome drug resistance. Up-regulation of the three MDR transporter proteins was observed with a variety of agents tested. This suggests that, long-term treatment with such agents could lead to the development and amplification of multidrug resistance, and therefore, reduce the effectiveness of substrate chemotherapies in patients.

Targeted therapies, including tyrosine kinase inhibitors (TKIs, such as lapatinib), are the latest significant development in the treatment of cancer. Lapatinib sensitised HER2-expressing cell lines to chemotherapeutic agents in the presence or absence of EGFR expression. This agent was also found to be a more active sensitiser in P-gp-expressing cell lines, while erlotinib was more active in BCRP-expressing cell lines. Gefitinib was the least active of three TKIs at modulating P-gp, MRP1 or BCRP. Following a 48 hours treatment, lapatinib up-regulated the expression and function of COX-2. It also stimulated COX-2 activity directly. This lapatinib-mediated COX-2 induction was independent of its TKI action on EGFR, and HER2 and could have serious therapeutic effects as COX-2 is known to increase cell growth, inhibit apoptosis, and enhance metastasis and angiogenesis.

A COX-2-specific inhibitor, celecoxib, overcame P-gp, MRP1 and BCRP-mediated resistance. At pharmacologically relevant concentrations, celecoxib significantly overcame MRP1 and BCRP-mediated resistance. And to a much lesser extent celecoxib overcame P-gp mediated resistance above pharmacologically relevant concentrations. The combination of lapatinib with celecoxib could be of therapeutic benefit, as the combination of these agents could collectively inhibit COX-2, P-gp, MRP1, BCRP, HER2 and EGFR activity in tumours expressing multiple oncoproteins resistant pathways and enhanced signalling pathways.

It is hoped that a novel treatment regimens, using these agents and TKI drugs with traditional chemotherapeutic agents, could improve current treatment strategies resulting in increased survival rates and decreased mortality.

Table of Contents

Section 1.

Introduction

1.1. Cancer: History and Treatment

Cancer is a term used for a group of diseases, in which abnormal cells divide uncontrollably and are able to invade other tissues. More than a hundred types of cancers have been identified and are generally named after the organ in which they are found, i.e. lung cancer, colon cancer, breast cancer, etc. As cancer has a high mortality rate, intelligent ways to inhibit its progress and development and therefore, increase the survival and remission for cancer patients, have been researched for the past 70 years. Current treatments include surgical excision of the tumour, radiotherapy, chemotherapy, immunotherapy and combinations of all of the above.

Research has identified a number of biological markers associated with the aggressive growth and drug resistance in cancer. Recent discoveries into the understanding of these biological markers or pro-oncoproteins, (such as; multi-drug resistant (MDR) proteins, epidermal growth factor receptors (EGFR), and cyclooxygenase enzymes (COX-2) (reviewed in sections 1.4, 1.5.1 and 1.6)) have led to a new approach in the anti-cancer strategy employed in the laboratory and clinic. Some recently developed drugs that were found to inhibit these oncoproteins include tyrosine kinase inhibitors (against EGFR family [1]), non-steroidal anti-inflammatory drugs (against COX-2 [2]) and ERK/P13K/Hsp90 [3] signalling pathway inhibitors. It is hoped that pharmacodynamic information and an intrinsic mechanistic understanding of how these targeted therapies function in individual patients will improve current treatment strategies resulting in increased survival rates and decreased mortality.

1.2. Cancer Chemotherapy

Conventional drug treatment of cancer involves treatment with cytotoxic chemotherapy drugs that directly cause cancer cell death. These cytotoxic drugs can damage cells in target organs in a variety of ways by causing cellular injury leading to a complex sequence of events. The eventual response may be reversible injury or an irreversible change leading to the death of the cell. These toxic compounds have proven very helpful in the reduction or cure of some cancers. Their action can be through interfering with cell growth, antagonising proteins associated with an aggressive phenotype, interfering with DNA repair mechanisms, preventing unzipping of the double helical strands of DNA, inhibiting mitosis and angiogenesis and by causing or promoting apoptosis (see table 1.2.1.).

Chemotherapy is generally most useful against tumours with a high proportion of dividing cells, such as leukaemia. Some of the more common malignant tumours, i.e. solid tumours including colorectal, lung and breast tumours, usually have a lower proportion of dividing cells that in some cases are less susceptible to treatment by chemotherapy. However, some normal tissues, i.e. bone marrow and gastrointestinal tract (GIT) [4], also have a high proportion of dividing cells. The side effects of chemotherapy are different depending on the person, the drugs, and the drug doses, and can be acute (short-term), chronic (long-term) or permanent. A few of these side-effects include: neurotoxicity, cardiotoxicity, nausea, vomiting, anemia, infertility or respiratory problems. The clinical effectiveness of a chemotherapeutic drug necessitates that the dose administered must allow enough cells in a patient's normal tissues (bone marrow, GIT etc) to survive and allow the patient to recover, while killing as many malignant tumour cells as possible [4].

1.2.1. Agents used in Cancer treatment.

A variety of chemotherapeutic agents are used in the treatment of malignancies. They vary in their cellular targets, mechanism of action and types of cancer they are used to treat. The major compounds are classified in table 1.2.1.1., along with the diseases that the chemotherapeutic agents are used to treat:

Table 1.2.1.1.: Below is a table that contains a list of chemotherapeutic drugs, their classes, names, primary mechanisms and types of cancers treated by them.

Class	Type of agent	Name	1º Mechanism of action	Cancer treated
Natural products	Antibiotics	Daunorubicin	intercalation of the planar ring with DNA and subsequent inhibition of DNA and RNA synthesis.	Acute myeloid leukemia; acute lymphocytic leukemia
		Doxorubicin	Intercalation of the planar ring with DNA and subsequent inhibition of DNA and RNA synthesis.	Osteogenic sarcoma, Hodgkin's & non-Hodgkin's disease, breast, lung, thyroid and stomach cancer, neuroblastoma and genitourinary cancer.
		Epirubicin	Intercalation of the planar ring with DNA and subsequent inhibition of DNA and RNA synthesis.	Breast; lung; lymph system; stomach; and ovaries
	Vinca Alkaloids	Vincristine	Inhibits formation of microtubules	Brain; breast; lung; leukaemia; melanoma and many more.
		Vinblastine	Inhibits formation of microtubules.	Breast; bladder; Hodgkin's; lung; testicular.
	Taxanes	Paclitaxel	Render microtubules resistant to depolymerisation.	Ovarian; non-small cell lung; prostate; and many more.
		Docetaxel	Render microtubules resistant to depolymerisation.	Breast; non-small cell lung; prostate; and more
	Epipodophyllotoxins	Etoposide Teniposide	Topoisomerase II inhibitors	Testicular, lung, and breast cancer, Hodgkin's and non-Hodgkin's disease, acute granulocytis carcinoma, Kaposi's sarcoma.
	Camptothecins	Topotecan Irinotecan	Topoisomerase I inhibitors	Ovarian, lung and colon cancer

Class	Type of agent	Name	1° Mechanism of action	Cancer treated
Miscellaneous	**Anthracenedione**	Mitoxantrone	Topoisomerase II inhibitor	Acute granulocytic carcinoma, pancreatic and breast cancer.
	Platinum complexes	Cisplatin Carboplatin	Inhibit DNA through covalent binding leading to intra-strand, inter-strand, and protein cross-linking of DNA.	Bladder; lung; breast; testicular; ovarian; brain and many more.
	Alkylating agents	Chlorambucil	Binds to DNA double helix, preventing it from unzipping and thus replicating hence cells cannot reproduce.	Immunosuppressive agent;
Antimetabolites	**Folic acid analogue**	Methotrexate	Folate synthase inhibitor	Acute lymphocytic leukaemia, breast, lung, head and neck cancer, estrogenic sarcoma.
	Pyrimidine analogue	Fluorouracil (5-Fu)	DNA destabilisation	Breast, colon, stomach, pancreatic, ovarian, head and neck cancer
		Gemcitabine	DNA destabilisation	Pancreatic and ovarian cancer.

This table was derived from the following references: [5] [6] [7] [8] [9] [10] [11] [12] [13] [14].

The Anthracycline, Epirubicin

Different anthracycline derivatives have been used successfully in the treatment of a wide spectrum of cancers for over two decades. Epirubicin is the 4`-epi-isomer of doxorubicin which is an anti-neoplastic antibiotic originally obtained from *Streptomyces peucetius* (see figure 1.2.1.1 for the structure of epirubicin) [15]. Intracellular production of free radicals along with intercalation with DNA and subsequent inhibition of topoisomerase II are generally accepted as the major mechanisms of anthracycline cytotoxicity [16] [17]. Anthracycline-produced free radicals can be generated by both enzymatic and non-enzymatic mechanisms [18] [19]. Free radicals may cause damage to biological molecules such as DNA. They can produce different kinds of DNA lesions, among which are free radical-modified DNA bases [20]. Base damage appears to be an important class of lesions because some of them may possess mutagenic properties and may lead to carcinogenesis [20] [21]. Thus, the observed mutagenicity of anthracyclines may be, at least in part, attributed to the generation of reactive oxygen species [16].
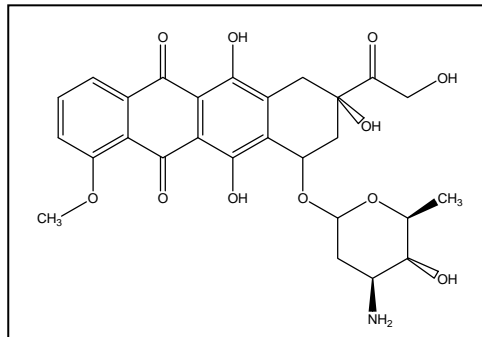
Figure 1.2.1.1.: The chemical structure of epirubicin [15].

Anthracyclines are widely used and effective anti-neoplastic drugs. Although active against a wide variety of solid tumours and haematological malignancies, their clinical use is hindered by tumour resistance and toxicity to healthy tissues [22]. Resistance to the three anthracyclines (daunorubicin, doxorubicin and epirubicin) is mainly established through over-expression of *mdr1* and its protein, P-glycoprotein (P-gp), in cancer cells [15] [23] (Discussed later in section 1.4.2.)

The two major side effects of the anthracyclines are cardio-toxicity following long-term treatment and haemo-toxicity experienced following acute exposure. Increased distribution in tumours, prolonged circulation and reduced free drug concentrations in plasma may increase anti-tumour activity and improve the tolerability of the anthracyclines [24]. Therefore, understanding the pharmacokinetics of epirubicin in patients is essential for treatment and management of side effects. The plasma concentration of epirubicin varies depending on the dose and method of administration. The most common form of administering epirubicin is by intravenous delivery. This can result in an area under the curve (AUC) of between 1.6 and 4.2 µg·h/mL and a Cmax of between 5.7 and 9.3 µg/ml with a half life of 30 to 35 hours [25]. All concentrations used in this project fall below the AUC values.

Taxanes

Paclitaxel and docetaxel are the most prominent members of the taxane family of cancer drugs. Paclitaxel is a natural product isolated from the bark of the Pacific yew tree, *Taxus brevifolia*. The anti-tumour activity of the yew bark extract was discovered through a plant screening program in the 1960s. Docetaxel is a semi-synthetic product derived from the needles of the European yew, *Taxus baccata*. Both share the tricyclic taxane skeleton but have different substitutes at the c-10 and c-13 side chains (Figure 1.2.1.2).

Figure 1.2.1.2.: Docetaxel and paclitaxel structures [26].

7
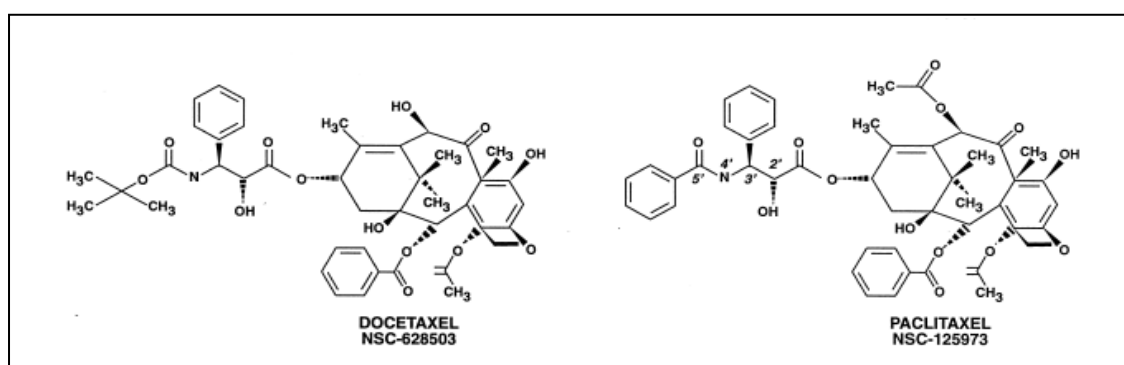
Despite similar structures, docetaxel and paclitaxel exhibit noticeable differences in pharmacological properties. Gligorov and Lotz [27], summarise the major differences.

Docetaxel:

- Exhibits greater uptake into, and slower efflux from, tumour cells (P388, murine leukaemia cell line).
- Exhibits greater affinity to the β-tubulin subunit of microtubules.
- Targets centrosome organisation.
- Acts on cells in the S/G2/M stages of the cell cycle.
- Demonstrates linear pharmacokinetics and no cardiotoxic effects in combination with anthracyclines.

Paclitaxel:

- Targets the mitotic spindle.
- Acts on cells in the G2/M phase of the cell cycle.
- Demonstrates non-linear pharmacokinetics and enhanced cardio-toxicity, especially in combination with the anthracyclines.

Docetaxel and paclitaxel share a unique mechanism of cytotoxic action. Both agents promote assembly of tubulin proteins into microtubules, and render them resistant to depolymerisation. Treated cells are blocked in the G2/M phase of the cell cycle giving rise to mitotic arrest [28]. Both taxanes bind to the β-subunit of tubulins, but the microtubules produced by docetaxel are larger than those produced by paclitaxel. This may explain why docetaxel appears to be two to four times more potent than paclitaxel [26].

 Both taxanes cause Bcl-2 phosphorylation leading to apoptosis but the concentration of docetaxel needed to cause apoptosis through Bcl-2 is 100 times less than paclitaxel [29]. Bcl-2 is an anti-apoptotic protein over-expressed in a number of tumours. Paclitaxel increases Raf 1, a serine/threonine protein kinase involved in the MAPK pathway and Bcl-x, leading to decreased levels of Bcl-2 [30]. Once activated, Raf-1 can phosphorylate to activate the dual specificity protein kinases MEK1 and MEK2 which

in turn phosphorylate to activate the serine/threonine specific protein kinases ERK1 and ERK2.

To date, two main mechanisms of taxane resistance have been identified; through increased expression of P-glycoprotein [31] [32] (discussed later in section 1.4.2.) and tubulin mutations leading to alterations in microtubule binding activity [33].

Similar to epirubicin, the main method of taxane administration in the clinic is through intravenous delivery. This method results in an AUC of between 6300 and 15007 µg.h/ml and a Cmax between 195 and 3650 µg/ml with a half life of 13 to 53 hours [25].

In 2008, data combined from eleven clinical trials showed that patients receiving taxanes (paclitaxel or docetaxel) for the treatment of newly diagnosed advanced breast cancer lived about as long as those receiving anthracyclines (epirubicin or doxorubicin). As single agents, however, the anthracyclines offered better progression-free survival. Combinations based on sensitising cancer cells to taxane treatment, by targeting epidermal growth factor receptor family or multidrug resistance, provided better response rates and also better progression-free survival than those based on anthracyclines [34].

1.3. Pharmacokinetics of cancer drugs

Pharmacokinetics is a branch of pharmacology dedicated to the determination of the fate of substances administered to a living organism. Pharmacokinetics includes the study of the mechanisms of absorption and distribution of an administered drug, the rate at which a drug action begins and the duration of the effect, the chemical changes of the substance in the body and the effects and route of excretion of the metabolites of the drug.

The majority of chemotherapeutic drugs are intravenously administered while many small molecule agents (discussed in section 1.4.5.) are orally administered. Biological factors that alter the distribution and elimination of intravenously administered drugs include plasma transport proteins (discussed in sections 1.3.4 and 1.3.5.), such as albumin and α_1-acid glycoprotein and ABC transport pumps [35] (discussed in section 1.4.) such as P-glycoprotein (P-gp), multidrug resistance protein-1 (MRP1) and breast

cancer resistance protein (BCRP) (see section 1.3.2.). The pharmacokinetics of orally administered drugs are influenced by tissue membranes [36], such as the gastrointestinal tract and liver, plasma transport proteins and ABC transport pumps. In relation to ABC transport pumps, it is clear that they are saturable, inducible, can be inhibited and display some degree of polymorphism – these are factors that need to be considered with respect to variability in drug disposition and response [37].

1.3.1. Role of the gastrointestinal tract in orally administered drug distribution

Drug absorption across the gastrointestinal tract can be highly dependent upon ABC transport pump affinity as well as lipophilicity. ABC transport pumps can be involved in the active absorptive (influx) of compounds, such as amino acids, oligopeptides, monosaccharides, mono- and dicarboxylic acids, bile acids, and several water-soluble vitamins from the lumen into the portal bloodstream [38] [39]. They are also responsible for the reduced absorption of anti-cancer agents. For example, the expression of BCRP in the gastrointestinal tract reduces the bioavailability of irinotecan [40]. Similarly, cyclosporine absorption in man is decreased by intestinal P-gp. There is a greater decrease in its absorption from the colon due to P-gp expression resulting in variations of its levels found in the blood [41]. Therefore, preclinical and clinical studies clearly demonstrate that P-gp-mediated intestinal efflux not only limits absorption of anti-cancer drugs, but also can result in variable and non-linear oral pharmacokinetics [42].

1.3.2. Role of the liver in cancer drug distribution

The liver plays a key role in the clearance and excretion of many cancer drugs. Hepatobiliary excretion of these agents from the blood, through the hepatocyte, and into the bile can be considered a three-step process.
The first step involves the uptake of anti-cancer drugs from blood into the hepatocyte. A significant number of anti-cancer drugs can be transported into hepatocytes via the sinusoidal (basolateral) membranes [43].

Once inside the hepatocyte the anti-cancer drug is transferred to metabolic sites and /or the biliary canalicular membrane, which is mediated by intracellular transfer proteins and passive diffusion [44]. The degree of metabolic biotransformation of anti-cancer drugs is highly dependent upon their physicochemical properties and structure-metabolism relationship [45].

The third step of biliary excretion, at the canalicular membrane, can involve mainly unchanged drug, metabolites or a combination of both parent drug and metabolites. Many carrier proteins have been shown to be present on the canalicular membrane to mediate this process [46] [47].

1.3.3. Transport of intravenous and orally administered anti-cancer agents via the blood system.

Serum transport proteins, such as serum albumin and α_1-acid glycoprotein (AAG), play a major role in the binding, distribution, and thus potency, of anti-cancer agents transported in the blood [48]. The average human has 5 litres of blood in his body. 55% of the blood is made up of plasma constituting the fluid part of the blood. The cells and platelets that are present in our blood make up the other 45%. Plasma is made up of water (90%), proteins, (8%) inorganic ions (0.9%) and organic substances (1.1%). The plasma proteins include serum albumin, serum globulin (including α_1-acid glycoprotein), fibrinogen, and prothrombin.

These proteins are mainly involved in:

- Transportation of substances with low solubility, such as drugs, around the body by allowing them to bind to protein molecules.
- Blood clotting
- Inflammatory response
- Protection from infection via gamma globulin function
- Balancing pH of the blood

1.3.5. The role of serum albumin in drug transport

Serum albumin is a highly soluble single polypeptide that is manufactured in the liver and isn't stored. It is present at approximately 40 mg/ml (600 μM) in the plasma. Serum albumin is important for the transport of drugs (including anti-cancer drugs), maintenance of colloidal osmotic pressure, free radical scavenging, platelet function inhibition and anti-thrombotic effects as well as control of vascular permeability. Serum levels of albumin can decrease due to decreased synthesis, increased catabolism, increased loss (nephrotic syndrome), exudative loss (in burns, haemorrhage), and redistribution (haemodilution, increased capillary permeability, decreased lymph clearance). Albumin has the highest affinity for drugs with acidic or strong electronegative functional groups and is less easily saturated than other transport proteins, such as AAG (see next section).

To date, it has been demonstrated that serum albumin is crucial for the distribution, elimination and effectiveness via binding of drugs such as digoxin, NSAIDs [49], midazolam, warfarin, thiopentone, tamoxifen, digitoin, and cancer drugs such as the anthracyclines [50] and taxanes etc. [51] [52].

1.3.6. The role of Alpha-1 acid glycoprotein (AAG) in drug transport

AAG (or orosomucoid) is a major glycoprotein of human plasma. It is produced by the liver and is an acute-phase reactant - i.e. its concentration in the blood can increase by up to 280-fold following stress, inflammatory response [53], pregnancy, and neoplasia. AAG has been reported to be taken up avidly in rats by tumours and granulomas [54]. The possibility that AAG regulates immune responses has been suggested by several findings [55] [56]. There is a strong similarity between the amino acid sequences in AAG and immunoglobulin. Detected on the surface of human lymphocytes, AAG inhibits proliferation of lymphocytes stimulated with the mitogen phytohemagglutinin or with allogeneic cells [57] and interferes with phagocytosis of bacteria by macrophages [58].

AAG is a 40 kDa protein present in the plasma at an approximate concentration of 0.8 mg/ml (20 μM). Basic drugs are often selectively bound to AAG with high affinity. Chassany O., *et al.* [59], investigated the *in vitro* binding potential of AAG to a range

of anthracycline derivatives and found that the hydrophobicity of the anthracycline derivatives was directly related with the percentage binding. Iododoxorubicin was the most highly bound (94%) while epirubicin (31%) had the least affinity for AAG. The impact of this variation on anthracycline distribution, bioavailability and potency has yet to be investigated.

Since a protein-bound drug is generally considered to be too large to pass through most cell membranes to exert pharmacological actions, protein binding can affect the potency of drugs that exert pharmacological actions intracellularly. Sham HL.*, et al,* [60] found that the magnitude of this effect could be estimated by the reduction of *in vitro* potency of a compound in the presence or absence of exogenously added serum.

1.4. MultiDrug Resistance in Cancer

MultiDrug Resistance (MDR) is a major cause of chemotherapeutic treatment failure. MDR is a phenomenon whereby tumour cells*,* which have been exposed to one cytotoxic agent, develop cross-resistance to a range of structurally and functionally unrelated compounds. This resistance is often due to elevation in the expression of cellular proteins, such as cell membrane transporters, which can result in an increased efflux of cytotoxic drugs from the cancer cells [61]. One such family of proteins are the transport proteins belonging to the ATP-binding cassette (ABC) family. Other mechanisms that can mediate the development of MDR include decreased drug uptake into the cell, activation of detoxifying enzymes (ROS), and defective apoptotic pathways [61].

Most of the drugs effluxed by MDR pump proteins are natural products derived from plants (taxanes) and micro-organisms; examination of their chemical structures reveals no common chemical features, but these drugs commonly display hydrophobic regions and are often positively charged at physiological pH [62].

The cytotoxic drugs that are most frequently associated with MDR are hydrophobic, amphipatic natural products, such as taxanes (paclitaxel, docetaxel), vinca alkaloids (vinorelbine, vincristine, and vinblastine), anthracyclines (doxorubicin, daunorubicin, and epirubicin), epipodophyllotoxins (etoposide, teniposide), topotecan, dactinomycin, and mitomycin C [32] [63].

1.4.1. ATP-binding-cassette (ABC) transport systems

The ATP-binding cassette (ABC) transport proteins are a superfamily consisting of a broad range of intra-cellular and transmembrane proteins that transport solutes in and out of the cell. The ABC transporters comprise of an extremely diverse class of membrane transport proteins that couple the energy of ATP hydrolysis to translocation of solutes across biological membranes [64]. The sequence and organisation of their ATP-binding domain(s) (nucleotide-binding folds (NBFs)) is the method by which these ABC transporters are classified (see figure 1.4.1.1.A). All ATP-binding domains have a characteristic motif (walker A and B domains) separated by 90-120 amino acids (see figure 1.4.1.1.B). This NBF also contains a signature (C) motif located upstream of the Walker B site [65]. In eukaryotic cells, the ABC genes are organised into a full transporter; containing two NBFs and two transmembrane (TM) domains, or a half transporter (see figure 1.4.1.2.); the latter must form either homodimers or heterodimers to become a fully functioning transporter. The specificity of each MDR transporter is determined by the TM domain. This domain comprises of 6-11 membrane-spanning α-helices. The NBFs are located in the cytoplasm and transfer energy to transport the substrate across the membrane. ABC transporter pumps are predominantly unidirectional. Most of the known functions of eukaryotic ABC transporters involve the shuttling of hydrophobic compounds either within the cell as part of a metabolic process or outside the cell for transport to other organs or for secretion from the body.
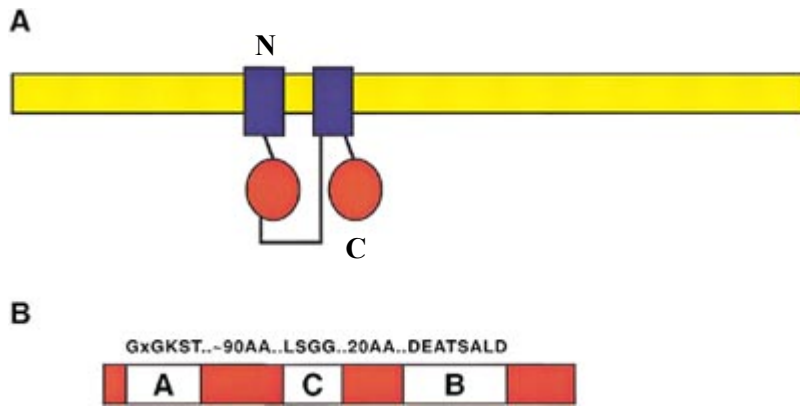
Figure 1.4.1.1.: Diagram of a typical ABC transporter protein. **A**. A diagram of the structure of a representative ABC protein is shown with a lipid bilayer in *yellow*, the TM domains in *blue*, and the NBF in *red*. Although the most common arrangement is a full transporter with motifs arranged N-TM-NBF-TM-NBF-C, as shown, NBF-TM-NBF-TM, TM-NBF, and NBF-TM arrangements are also found. **B**. The NBF of an ABC gene contains the Walker A and B motifs found in all ATP-binding proteins. In addition, a signature or C motif is also present [66].

Figure 1.4.1.2.: ABC gene structure. Above is a diagram of an ABC half transporter and a full transporter. The half transporter can form homo- or heterodimers, whereas the entire full transporter is found in one transcript [66].

ABC genes play an important role in MDR, and at least six genes are associated with drug transport. (For a recent review in this area refer to Lage H. [67]). Three ABC genes appear to account for a large majority of the MDR in tumour cells in both human and rodent cells. These are *ABCB1/P-gp/MDR1*, *ABCC1/MRP1*, and *ABCG2/MXR/BCRP* (see tables 1.4.1. to 1.4.3.). *In vitro*, scientists have been developing drug resistance variants in order to further study the mechanism by which these MDR pumps are over-expressed and how best to overcome this phenotype in the clinic [58]. The phylogenetic associations between each ABC transporter subfamily is illustrated in figure 1.4.1.3 below.
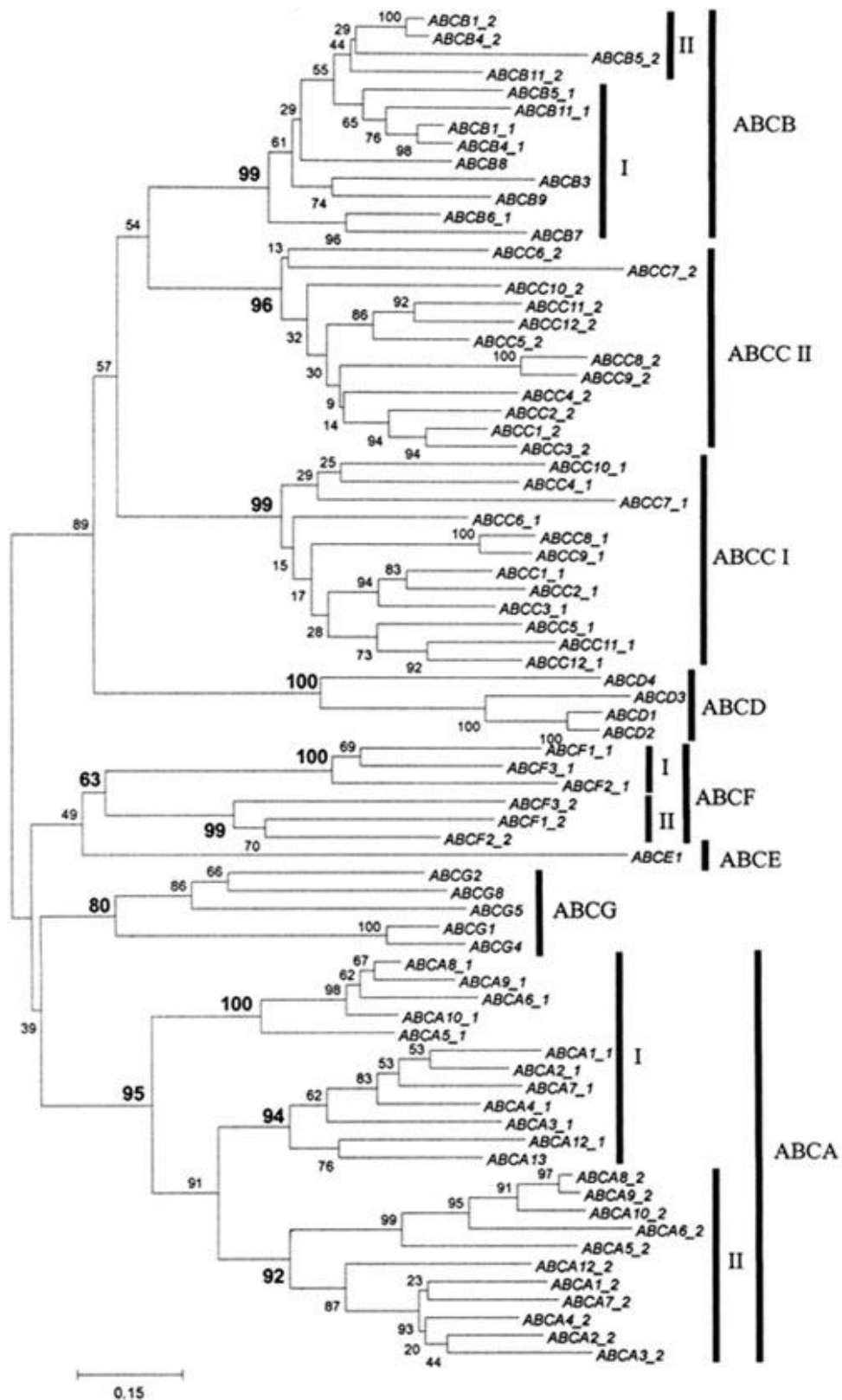
Figure 1.4.1.3.: The phylogenetic tree above illustrates the inter-relationship between each ABC transporter subfamily [68].

1.4.2. MultiDrug Resistance 1 (MDR1)

Multidrug resistance 1 (MDR1) or p-glycoprotein (P-gp) is a 170 kDa ATP-dependent membrane transporter that acts as a drug efflux pump (pumping drug out of the cell or into vesicles). Its gene, ABCB1/*mdr1*, maps to chromosome 7q21.1 and is the best characterised ABC drug pump. ABCB1 was the first transporter cloned and the first to be characterised for its ability to confer a multidrug resistant phenotype in cancer cells [69] [70].

A component of P-gp-mediated multidrug resistance may be due to alterations in membrane potential. This feature of P-gp-expressing cells is caused by changes in lipid-protein interactions on the intra-membranous surface of the transporter, which may be brought about by changes in the distribution of types of lipids (i.e. glucosylceramide) between the inner and outer leaflets of the plasma membrane giving rise to altered dipole potentials [71] and altered alkalinisation of the acidic compartments (endosomes and lysosomes). However, it is argued that resistance to weakly basic chemotherapeutic agents used in cancer treatment cannot be explained by changes in membrane potential and therefore trans-membranous distribution of those drugs [72] [73].

Several hypotheses have been developed to explain the mechanism by which this pump confers resistance to chemotherapy drugs. The classic model for drug transport by P-gp states that P-gp acts as a transmembrane pore-forming protein and interacts with anti-cancer drugs in the cytoplasm and expels them directly into the extracellular medium. According to the "hydrophobic vacuum cleaner" model, P-gp binds directly with substrates in the plasma membrane and pumps them out of the cell [74]. In the "flippase" model, P-gp encounters drugs in the inner leaflet of the plasma membrane and flips them to the other leaflet from which they diffuse into the extracellular medium [75]. In an alternative model, P-gp affects the intracellular pH and/or the plasma membrane electric potential of the cell by acting as a proton pump or a chloride channel [73], thereby indirectly reducing intracellular accumulation of weakly basic, cationic lipophilic anti-cancer drugs. However, this last model does not agree with studies done in the mid 90's that demonstrated direct drug transport by purified P-gp [76] (see figure 1.4.2.1.).
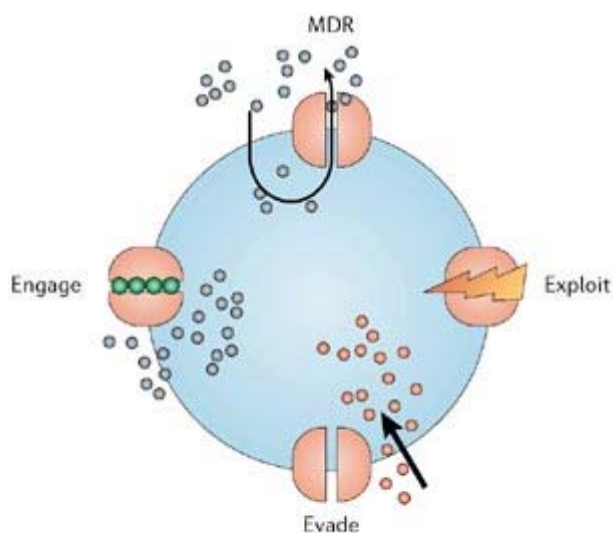
Figure 1.4.2.1.: An image to illustrate how the membrane bound P-gp transporter protein which pumps drug out is inhibited and evaded [77]. Engaging agents inhibit and prevent the efflux activity of the MDR pump. Agents unaffected by the expression of MDR pumps are known as evaders, while agents that use MDR pumps to enter the cell are known as exploiters.

Many of the first chemosensitisers identified were themselves substrates for P-gp and worked by competing with the cytotoxic substrate compounds for efflux by the P-gp pump; and high serum concentrations of the chemosensitisers were necessary to produce adequate intracellular concentrations of the cytotoxic drug [63] (see table 1.4.1 below).

Three generations of inhibitors have been developed and investigated but an effective and safe clinical P-gp inhibitor has yet to be described [61].

Many anti-cancer agents have been found to either have no effect on the function of the P-gp pump (work independently of P-gp), to be substrates (pumped by the transporter), or are inhibitors, (directly interfere with the mechanics of the pump preventing it from doing its job). These agents include a broad range of families; for example, the taxanes, vinca alkaloids and anthracyclines are P-gp substrates while some of the platinum drugs and 5-flourouracil operate independent of P-gp (see table 1.4.2.1.)

Some of these cytotoxic substrates include some epipodophyllotoxins, camptothecins and heavy metal anions [78] [79] [80] (see table 1.4.2.1.).

18

The ABCB1/P-gp protein is also expressed in normal tissue. It is highly expressed in haematopoietic stem cells, where it may serve to protect these cells from toxins [81]. The highest expression is found in secretory cell types such as kidney, pancreas, colon, liver, intestinal and adrenal glands, where the normal function is thought to involve the excretion of toxic metabolites [82] (discussed briefly in section 1.3.). Cancerous tissues originating from these cells express the highest levels of P-gp. This over-expression leads to the resistance of malignant tumours prior to treatment with chemotherapeutic drugs. However, cancer cells with low expression of P-gp can also develop an MDR phenotype following treatment with cytotoxic agents [62].

The general up-regulation of P-gp protein expression has been studied both *in vivo* and *in vitro*. Results indicate that MDR1 expression can be up-regulated by many extracellular stimuli including UV irradiation [83], heat shock [84], osmotic shock, low external pH, xenobiotics, differentiating agents, hypoxia (via HIF-1) [85], hormones [86] [87], radiotherapy, and growth factors, and by a number of drugs [88] [89]. There are a number of different mechanisms known for down-regulating P-gp including, degradation of its protein [3] and reducing intracellular reactive oxygen species (ROS) (ROS causes DNA damage and oxidises amino acids in proteins) [90].

Transcriptional regulation resulting in increased *mdr1* mRNA has been widely investigated and many studies provide evidence of complex mechanisms involving transcription factor recognition sites as MDR1 gene promoters [91]. SPI, NF-Y [83] and YB-1 [92] transcription factors have been shown to up-regulate MDR1 promoter activity. Also, inactivation of p53, by mutation, can cause resistance to doxorubicin *in vivo* and the mutational status of p53 might be associated with the up-regulation of P-gp-mediated drug resistance in human tumours [93] [94].

Transcription regulation resulting in a decrease in *mdr1* mRNA has also been investigated. A negative regulator of the MDR1 gene promoter was identified as a protein complex made-up of NF-kappaB/p63 and c-Fos that interacted with the CAAT region of the promoter [95]. Negative down-regulation can also be caused by the activation of the transcription factor, c-Jun [96].

Apart from interfering with the MDR1 protein at the gene level, blocking the function of the pump by inhibiting post-translational modifications such as phosphorylation, is also an effective way of overcoming P-gp mediated drug resistance [97]. Agents known to modulate the function of P-gp include calcium channel blockers, calmodulin

antagonists, steroidal agents, protein kinase C inhibitors, immunosuppressive drugs, antibiotics, tyrosine kinase inhibitors, non-steroidal anti-inflammatory drugs and surfactants. Calcium channel blockers, such as verapamil, have been shown to reverse P-gp-mediated MDR by blocking drug-pumping function of P-gp. However, Sikic BI., [98], found that these agents exhibit dose-limiting side effects that severely restrict their clinical utility.

Table 1.4.2.1: Below is a list of anti-cancer agents that have been shown to be substrates, inhibitors or to function independently of P-gp.

MDR pump	Substrate	Inhibitor	Non-substrates
P-glycoprotein	Actinomycin D	Cyclosporine A	Carboplatin
	Bisantrene	Elacridar (GF120918)	Cisplatin
	Cyclosporine A	Indole-3-carbinol	Cyclophosphamide
	Daunorubicin	Verapamil	Fluorouracil (5FU)
	Doxorubicin	Valspodar	Gemcitabine
	Homourringtonine	Zosuquidar	Ifosfamide
	Epirubicin	PSC833	Melphalan
	Etoposide	GG918	Methotrexate
	Imatinib	Pluronic L61	
	Irinotecan		
	Mitomycin c		
	Mitoxantrone		
	Paclitaxel		
	Docetaxel		
	Teniposide		
	Topotecan		
	Vinblastine		
	Vincristine		
	Vinorelbine		

This was compiled using the following references: [79] [99] [100] [101] [102].

1.4.3. MultiDrug Resistance Protein 1 (MRP1)

The first member of the MRP subfamily (MRP1) was identified in the NCI-H69 cell line [103]. Despite having a broad spectrum of drug resistance, this cell line did not express P-gp [103]. Although both MDR transporters share similar substrates, they have less than 15% identical amino acids [103]. Identification of MRP1 led to the discovery of 8 additional members (MRP2-9), with MRP1-6 being the best characterised to date [104].

Mature MRP1 protein has an apparent molecular weight of 190 kDa and its gene maps to chromosome 16p13.1. It is an organic anion transporter that couples ATP binding with hydrolysis to transport across the biological membrane. MRP1 transports a wide variety of anti cancer drugs [105].

The MRP transporter protein family can be found in both normal and tumour cells. MRP1 is predominantly expressed in lung [106] [107] [108], gastrointestinal tract [109], blood brain barrier (BBB) [110] and blood-testis barrier [103] [111] and has been identified in liver [112], kidney and at varying levels in the placenta [113]. MRP2 has also been located in all of these tissues except lung and testis (see review [78]). The function of MRP1 in normal tissues appears to be protective and maintenance of cell health through regulation of absorption, distribution and excretion of xenobiotics, nutrients, hormones, etc (see review [78] and discussed briefly in section 1.3.).

Because of the protective role MRP1 plays, over-expression is common in cancer cells and confers MDR. In general, MRP1 expression levels are found to be higher post-chemotherapy treatment compared to initial presentation of the tumour. For example, 62% of breast cancer patients presented MRP1 expression prior to treatment while 88% expressed it post-chemotherapy treatment [114]. MRP1 over-expression has been located in treated tumour types such as acute myeloid leukaemia, small cell lung cancer, T-cell leukaemia and neuroblastoma. Studies into MRP1 in breast cancer suggest no correlation exists between MRP1 expression and tumour size, lymph node status, histologic grade and type, hormone-receptor status, age, or menopausal status [114]. However, early expression of MRP1 correlates with a worse prognosis [114].

The regulation of MRP1 expression is not fully understood but tenuous links between transcription factors, nrf2, n-myc and c-myc (important in P13K pathway), and MRP1 transcriptional regulation have been suggested. Hypoxic conditions increase the phosphorylation of ERK/MAPK and increase HIF-1 activity. These factors cause the up-regulation of MRP1.

MRP1 inhibition might be a clinically relevant target for improving patient outcome in cancer treatment. Regardless of the resistance profile similarities between MRP1 and P-gp a whole new approach in developing and designing MRP1 inhibitors is called for. Also, unlike P-gp, MRP1 does not affect resistance to and/or transport of paclitaxel [80] [115] (see table 1.4.3.1.), mitoxantrone [100] (see table 1.4.3.1.), arabinofuranosylcytosine [116] or m-AMSA (amsacrine) [115]. Also membrane vesicle

assays [117] [118] (see figure 1.4.3.1.) of MRP1 transport demonstrated that MRP1 require acidic ligands such as glutathione (GSH), glucuronide, or sulphates for efficient transport of its substrates across biological membranes [100] [115] [105] [119]. Whether these acidic ligands bind to the MRP1 protein or the drug is unclear at present.

To date, competent MRP1 inhibitors include emtricitabine, MK571, probenecid, sulindac sulphide and indomethacin [78] [79] [99] [102] (see table 1.4.3.1.).

Table 1.4.3.1.: Below is a list of compounds associated with the functioning of the MRP1 pump.

MDR pump	Substrate	Inhibitor	Non-substrates
MRP1	Actinomycin D	Emtricitabine	Bisantrene
	Emtricitabine	MK571	Carboplatin
	Epirubicin	Probenasid	Cisplatin
	Etoposide	Sulindac sulphide	Cyclophosphamide
	Daunomycin	Indomethacin	Docetaxel
	Doxorubicin	Cyclosporine A	Fluorouracil (5FU)
	Methotrexate	V-104	Gemcitabine
	Menogaril		Ifosfamide
	Vincristine		Melphalan
	Vinorelbine		Methotmexate
			Mitoxantrone
			Paclitaxel
			Verapamil
			Vinblastine

This table was compiled using the following reference: [78] [79] [120] [121].

1.4.4. Breast Cancer Resistance Protein (BCRP/ABCG2)

BCRP (ABCG2; 72kDa membrane-protein) is the second member of the ABCG subfamily of ABC transporter proteins [122]. BCRP was first cloned from a breast cell line (MCF7/AdrVp) selected for its unique drug resistance in the presence of a P-gp inhibitor, verapamil [122]. Phylogenetic analysis of the relationship between BCRP and other members of the ABC transporter family revealed that it was more closely related to ABCG1 than MRP1 or P-gp. ABCG1 is also a member of the ABCG/white subfamily [123]. To date, there are 4 members of the G subfamily, ABCG1, ABCG2, ABCG5, and ABCG8.

There are two unique features of the ABCG family that imply a different transport mechanism compared to that of other ABC transporters. Firstly, the ABCG proteins are half transporters. Half transporters are composed of only one ABC and one transmembrane domain (TMD) unit within one polypeptide, the ABC domain being N-terminally located from the TMD. Increasing evidence suggests that ABCG proteins operate as either homodimer or heterodimers [124] [125]. The second unique characteristic is the configuration of the ABC and TMD domains to the N-terminal. In ABC transporter proteins such as MRP1 and P-gp, the TMD always precedes the ABC domain (ie. TMD is nearer the N-terminal than the ABC domain), whereas ABCGs' configuration is the opposite [126].

Several cell lines, from breast cancer, colon and gastric carcinoma, and fibrosarcoma, selected with drugs such as mitoxantrone, topotecan, daunorubicin, or verapamil, display resistance to a range of anti-cancer drugs (anthracyclines, topotecans and mitoxantrone). These resistant variants remain sensitive to cisplatin, taxanes, vinca alkaloids and other known P-gp/MRP1 substrates. This resistance profile is characteristic of BCRP. Inconsistencies in the resistance profile between wild and mutant/selected BCRP has been observed. The alteration to substrate specificity was found to be due to the conversion of arginine to threonine or glycine at position 482 [127]. It appears this single amino acid change enhances the export of anthracyclines; however, it also causes loss in the protein's ability to export methotrexate [128]. Extensive study has been carried out in amino acid substitution and authors speculate

that the intracellular change at position 482 is important for electrostatic interactions with some substrates at the membrane-cytosol interface [129] [130] [131] [132] [133].

Similar to other ABC transporter protein such as MRP1 and P-gp, BCRP can be found distributed around the body. A study carried out by Doyle L.A. *et al.* [134], found that BCRP is not expressed in heart, lung, skeletal muscle, kidney, pancreas, spleen, thymus, or peripheral blood leukocytes. However, Scheffer GL., *et al.* [107], detected low levels of BCRP in small endothelial capillaries in the lung. ABCCG2 was found to be highly expressed in the placenta [134], liver [134], blood brain barrier [135] and small intestines [134] [136] [137]. Low levels were detected in the blood-testis barrier. The role of BCRP appears to be solely a protective one; reducing exposure to xenobiotics primarily under hypoxic conditions. Hypoxia up-regulates the expression of BCRP by the hypoxia-inducible transcription factor complex HIF-1 [138].

The implications BCRP has on prognosis, survival and response to treatment have yet to be examined in many cancer types. Compared to P-gp, BCRP expression was found in a smaller proportion of childhood acute lymphoblastic leukaemia (ALL) [139] or nasophoryngeal tumours. However, on average 30% of acute myeloid leukaemia (AML) patients express BCRP at significantly high levels [140] and an unfavourable prognosis has been linked with BCRP over-expression in adult acute myeloid leukaemia (AML) and ALL [141] [142]. Studies carried out by Diestra J.E. [143] [144], on 140 untreated tumours found that more than 40% of tumours reacted to the immunoassay and that the digestive tract carcinomas (esophagus, colon, stomach) were the predominant expressers. Bladder carcinomas and osteosarcomas showed a low frequency of BCRP expression. Researchers have suggested that BCRP is predominantly expressed in a subpopulation and this may be the cause for treatment failure. Research by Hirschmann-Jax C., *et al.* [145], into BCRP expression in neuroblastomas suggests there is a highly expressing subpopulation which may represent the cancer stem cells and work carried out by Dean M. *et al.* [146], seconds this theory. They also revealed that neuroblastomas can be found in other solid tumours such as ovarian cancer, small-cell lung carcinoma, Ewing sarcoma, and prostate cancer. Therefore, despite the lack of clinical epidemiology the putative role BCRP plays in solid tumour resistance (hypoxic conditions promote BCRP expression [138] could still have prognostic value.

With BCRP's possible prognostic value the necessity to develop effective inhibitors is imperative. To date, a number of inhibitors have been identified and despite the structural difference between BCRP and P-gp they share a number of functional inhibitors and expression reducers. These include AG1478, lapatinib [147], erlotinib [148], gefitinib [149] [150] [151] [152], imatinib [153], sunitinib, wortmannin, LY294002 [154], elacridar [130], PD98059, FTC [155], and Ko143 [130] (see table 1.4.4.1). Some of these drugs have already proven beneficial (extended survival period) in the fight against multidrug resistance in treated tumours. Some agents can be both substrates and inhibitors, i.e. imatinib mesylate.

Table 1.4.4.1: A list of compounds associated with the functioning of the BCRP pump.

MDR pump	Substrate	Inhibitor	Non-substrates
BCRP	Aza-anthrapyrazole	Cyclosporine A	Carboplatin
	9-Aminocamptothecin	Elacridar/GF120928	Cisplatin
	Bisantrene	Flavonoids (chrysin, biochanin A)	Cyclophosphamide
	Daunorubicin#	Flavopiridol	Docetaxel
	Doxorubicin#	Fumitremorgin C (FTC)	Fluorouracil(5-FU)
	Epirubicin#	Gefitinib	Gemcitabine
	Etoposide	Imatinib mesylate	Ifosfamide
	Flavopiridol	Iressa	Melphalan
	Idarubicinol#	Ko143	Paclitaxel
	Imatinib	Novobiocin	Vinblastine
	Imatinib mesylate	Tamoxifen	Vincristine
	Irinotecan	VX-710	Verapamil
	J107088		
	Methotrexate (glu2, glu3)$^{\Psi}$		
	Mitoxantrone		
	Nb-506		
	parzocin		
	SN-38		
	statins		
	Topotecan		

Note:

symbol denotes the substrates transported by BCRP with the amino acid change at position 482.

Ψ symbol denotes the substrate transported by wild-type BCRP.

This table was compiled from the following references: [63] [99] [78] [80] [102] [156].

1.4.5. Interactions of modern targeted therapies with multidrug resistance proteins

The aim of modern therapies is to target overactive signalling pathways and growth factor receptors that are characteristic of aggressive tumours. Many of these targeted therapies interact with ABC transporter proteins, i.e. they are modulators, which mean they can be substrates, inhibitors of the function or expression of these proteins. Some of these P-gp, MRP1 and BCRP modulators, mentioned in table 1.4.5.1 below, will be briefly discussed in this section. The small molecule agents examined in the project range from a new class of targeted therapies as well as older drugs that are and were used for other diseases. These agents come from a range of families, such as, P13K/Akt inhibitor, ERK/Mek inhibitors, Hsp90 inhibitors, tyrosine kinase inhibitor and non-steroidal anti-inflammatory drugs (NSAIDs), and were selected for their MDR status and use in clinic. More traditional anti-neoplastic agents such as epirubicin, docetaxel, cisplatin, vincristine, or 5FU are not discussed in this section as they have either been discussed previously or are solely used as MDR substrates or MDR-independent agents throughout this project.

Table 1.4.5.1.: A selection of modern targeted therapies and their relationship with three MDR pumps (P-gp, MRP1 and BCRP).

Class	Drugs	P-gp		MRP1		BCRP	
		Modulation	*Reference*	*Modulation*	*Reference*	*Modulation*	*Reference*
Growth factor TKI	AG1478	Inhibit function		No effect	N/A	Inhibit function	157
	Lapatinib	Inhibitor	112	?	N/A	Inhibitor	97
	Erlotinib	Inhibitor	157	No effect	157, 158	Inhibitor	148
	Gefitinib	Inhibitor	150	?	N/A	Substrate, inhibitor & ↓expression	150
	Genistein	?	N/A	Inhibitor	159	?	N/A
	Imatinib	Substrate	160	?	N/A	Substrate	153
	Sorafenib	?	N/A	?	N/A	?	N/A
Src TKI	Dasatinib	substrate	161	?	N/A	substrate	161
Receptor TKI	Sunitinib	Inhibitor	162	?	N/A	Inhibitor	163
P13K/Akt	LY294002	Inhibitor & ↓expression	163, 164	Inhibitor, ↑expression??	163	↓Expression	163, 165
	Wortmannin	Inhibitor	166	↓expression	167	↓expression	168
	WO 04/007491	?	N/A	?	N/A	?	N/A
ERK/MEK	U0126	↓expression	3	↓expression, no effect	169	?	N/A
	PD98059	↓expression	3	Inhibitor, no effect??	163	↓expression	170
	PD184161	?	N/A	?	N/A	?	N/A
NSAID	Sulindac	Non-inhibitor	171	Inhibitor	172, 173	?	N/A
	Celecoxib	↓expression	160	↓expression	174	?	N/A
	Naproxen	↔Expression	96	?	N/A	↑expression	96
	Rofecoxib	↓Expression & inhibitor	175	?	N/A	?	N/A
	Valdecoxib	?	N/A	?	N/A	?	N/A

Class	Drugs	P-gp		MRP1		BCRP	
		Modulation	*Reference*	*Modulation*	*Reference*	*Modulation*	*Reference*
NSAID	Paracoxib	?	N/A	?	N/A	?	N/A
	Ketorolac	?	N/A	?	N/A	?	N/A
	NS-398	↓Expression & inhibitor	171	?	N/A	?	N/A
	Ibuprofen	Inhibitor	171	?	N/A	No inhibition	176
	Nimesulide	↓Expression & inhibitor	96	?	N/A	No interaction	176
	Indomethacin	↓Expression & inhibitor	96	Inhibitor	177	↑ expression	96
Hsp90	Radicicol	?	N/A	?	N/A	?	N/A
	17-AAG	↓expression	3	?	N/A	?	N/A
	Geldamycin	?	N/A	?	N/A	?	N/A
	NVP-AUY922	?	N/A	?	N/A	?	N/A
	17-DMAG	?	N/A	?	N/A	?	N/A
Fungal Toxin	FTC	Weak inhibitor	130	Weak inhibitor	130	Inhibitor	130
	FTC analogue: Ko143	Weak inhibitor	130	Weak inhibitor	130	Inhibitor	130
Chelating agent	FTI-277	↓Expression	3	?	N/A	?	N/A
Quinoline-type reversal agent	Dofequidar fumarate	Substrate & competitive inhibitor	178	Inhibitor	179	?	N/A
Ca$^+$ channel inhibitor	Verapamil	Inhibitor	180	No interaction	181	No interaction	182
	Diltiazem	Substrate & competitive inhibitor	183	?	N/A	No interaction	182

Class	Drugs	P-gp		MRP1		BCRP	
		Modulation	*Reference*	*Modulation*	*Reference*	*Modulation*	*Reference*
Immunosuppressive	Cyclosporine A	Inhibitor	184	Modulator	185	Modulator/Inhibitor	185
	Clycosporine analogue: PSC-833	Substrate, competitive inhibitor	185	No interaction	185	No interaction	185
	Tacrolimus (FK-506)	Substrate	186	?	N/A	Modulator	187
	Sirolimus	?	N/A	?		Modulator	187
Anti-inflammatory	MK-571	No interaction	188	Inhibitor	188	No interaction	188
Taxane	Orataxel	Modulator	189	Modulator	189	Modulator	189
Other	Tariquidar	Inhibitor	190	No interaction		Inhibitor	179
	Elacridar	Inhibitor	191	No interaction	192	Inhibitor	193
	Indole-3-carbinol	↓Expression	194	?	N/A	↑expression	195

Note:

An agent where mechanism is that of overcoming MDR-mediated resistance is termed a modulator.

Key: ?: status unknown   ↓: down-regulation of protein expression   ↑: up-regulation of protein expression   ↔: no change in protein expression

N/A: not applicable

Tyrosine kinase inhibitors:

The epidermal growth factor receptor (EGFR) family is composed of cell surface tyrosine kinase receptors that are involved in the regulation of cellular proliferation and survival of epithelial cells (this area is discussed further in section 1.5). EGFR and HER2 receptor activation leads to the phosphorylation of the intracellular catalytic domains, and ultimately activation of signal transduction pathways that promote proliferation and survival, including the phosphatidylinositol 3′-kinase (PI3K)/Akt/mTOR, the Erk1/2 mitogen-activated protein kinase (MAPK) and the Jak/Stat pathway [196]. As stated in table 1.4.4.1., most tyrosine kinase inhibitors interact with P-gp and BCRP. Three of these agents (lapatinib, erlotinib and gefitinib) are briefly discussed below.

Lapatinib:

At clinically relevant concentrations (below 3.77 µg/ml or 3.99 µM) lapatinib, the dual HER2/EGFR tyrosine kinase inhibitor, has been shown to increase P-gp expression [197] [112] while directly inhibiting the function of both the P-gp and BCRP transporter proteins (demonstrated using ATPase assays) [112] [97].

Conversely, Dai C-L., *et al.* [147], showed that lapatinib does not affect the expression of the P-gp and BCRP mRNA and protein expression (0.3 – 5 µM for 48 hours) in doxorubicin and vincristine-selected MCF7 cells and SI-M1-80 cells induced with P-gp and BCRP expression. However, they proved that lapatinib reverses P-gp and BCRP-mediated multidrug resistance by directly inhibiting their transport function (2.5 and 10 µM).

Erlotinib:

Erlotinib is a specific EGFR tyrosine kinase inhibitor. Erlotinib has been shown to be a substrate ([198] 1.3 and 15 µM of erlotinib used) and have direct inhibitory activity on both P-gp and BCRP ([157] [148] 2.5 and 10 µM of erlotinib used in Western blotting (36 and 72 hours), combination assays and accumulation/efflux assays). It does not alter the expression BCRP [157]. Erlotinib has no interaction with MRP1 [157] [158].

Gefitinib:

Gefitinib is also a specific EGFR tyrosine kinase inhibitor. A number of researchers, using ATPase and pharmacokinetic assays, observed the direct inhibition of both P-gp and BCRP by gefitinib (in human myelogenous leukaemia cells transfected with BCRP: [150] 10 μM caused 80-90% BCRP function inhibition while 1 μM caused ~10% inhibition [151] [199] [40]). No studies have been carried out to date with regard to effect on MRP1 activity.

The P13K/Akt inhibitors:

The P13K/Akt signal transduction cascade has been investigated extensively for its roles in oncogenic transformation. Initial studies implicated both P13K and Akt in prevention of apoptosis. More recent evidence has also associated this pathway with regulation of cell cycle progression. Uncovering the signalling network spanning from extracellular environment to the nucleus should illuminate biochemical events contributing to malignant transformation [200]. Therefore, by inhibiting the signal transduction, targeted anti-cancer agents such as wortmannin, and LY294002 could inhibit tumour progression. If these agents also have anti-MDR potential scheduling regimens could provide improved patient treatment while minimizing the number and dose of drugs necessary and therefore side-effects.

LY294002:

LY294002 is a potent P13K/Akt inhibitor. Abdul-Ghan R., et al. [163], showed that 20 μM of this Akt inhibitor inhibited the function of MRP1, while 10 μM reduced P-gp-mediated resistance and down-regulated the expression of BCRP at the protein level. Using murine lymphoma cell lines (vincristine & doxorubicin variant), Garcia MG., et al. [164], demonstrated that 10 μM LY294002 reduced the efflux of daunorubicin from the P-gp expressing cell line. No protein characterisation was carried out. In 2006, Mantovani I., et al. [201], proved that the cleavage of the membrane bound P-gp protein following exposure to 50 μM LY294002 (no effect at 10 and 25 μM but large effect at 50 μM was observed in T-lymphoblastoid CEM cells and its vinblastine variant). The deactivation of functional protein is thought to be through the cleavage of 170kDa P-gp by caspase 3 (as part of the process of apoptosis). Katayama K., et al. [3], carried

out Western blots for changes in P-gp expression following a 12 hour treatment with 10 µM LY294002 in colon and breast cell lines. No change was observed.

Nakanishi T., *et al.* [165], observed a down regulation in BCRP protein expression following exposure to 10 µM LY294002 (K562 & BCRP variant, MCF7/AdrVp and Igrov1/T8 (ovarian); no change occurred with 2 µM, 10-20% reduction with 10 µM following a 14 hour exposure).

Therefore, LY294002 is either an inhibitor or competitive substrate for MRP1 and P-gp while being a down-regulator of the BCRP protein. The exact mechanism by which LY294002 acts is unknown (see table 1.4.5.1.). There is no clinical or pharmacological data on this drug therefore it is unclear if the concentrations used are clinically relevant.

ERK/Mek inhibitors:

Growth factors and mitogens use the Ras/Raf/MEK/ERK signalling cascade to transmit signals from their receptors to regulate gene expression, control cell proliferation, differentiation and prevent apoptosis. Some components of these pathways are mutated or abnormally expressed in human cancer (i.e., Ras, B-Raf) [202], [203]. Mutations also occur at genes encoding upstream receptors (i.e., EGFR and Flt-3) and chimeric chromosomal translocations (i.e., BCR-ABL) which transmit their signals through these cascades [204]. The activation of this pathway can lead to the unrestrained growth of cancer cells. The Ras/Raf/MEK/ERK and Ras/PI3K/PTEN/Akt pathways have been shown to interact with each other to regulate growth and in some cases tumourigenesis. The ERK/Mek pathways have also been linked with a multidrug resistance phenotype [205]. Some anti-ERK/Mek inhibitors affect the expression of MDR transporter proteins (see table 1.4.5.1.). U0126 and PD98059 down-regulate P-gp. No research has been published on the newest ERK/Mek inhibitor, PD184161, in relation to MDR.

<u>U0126:</u>

This drug is an ERK/Mek inhibitor. In 2006, Abdul-Ghani R., *et al.* [163], demonstrated no interaction between this ERK/Mek inhibitor and MRP1 (at 20 µM). However, a year later, using Western and RT-PCR techniques, Zhu H., *et al.* [106], found that, in hepatocellular carcinoma cell lines, a 12 hour treatment down regulated

both MRP1 and P-gp protein and RNA levels but did not affect BCRP. No data regarding concentrations or magnitude of effect is available as the article is in Chinese. Katayama K., *et al.* [3], carried out Western blots for changes in P-gp expression following a 12 hour treatment with 10 µM U0126 in colon and breast cell lines. An 80-100% reduction was observed and in some cases this reduction was better than 17-AAG (a Hsp90 inhibitor derivative of geldamycin, described later in this section). Therefore, U0126 down-regulates both P-gp and MRP1 but does not affect BCRP protein expression. U0126 affects MRP1 at the transcriptional level (see table 1.4.5.1.). However, the mechanism by which U0126 down-regulates P-gp protein expression is unknown. There is no clinical or pharmacological data on this drug.

Non-steroidal anti-inflammatory drugs (NSAIDs):

NSAIDs are drugs commonly used in the treatment of pain and inflammation. Their primary mode of action is the blockage of one or both of the cyclooxygenase enzymes, COX-1 and COX-2. These enzymes play an intrinsic role in the synthesis of prostaglandins (see section 1.6.2. for further details). COX expression has been directly related with tumour initiation, progression and metastasis (see section 1.6.3.). To date, substantial evidence suggests that COX-2 could contribute to the development of resistance to the pharmacological treatment of tumour cells (see section 1.6.3.: COX expression and Multidrug resistance). A number of NSAIDs have proven to be effective modulators of P-gp and MRP1. See table 1.4.5.1 for a selected list of NSAIDs and their known interactions with P-gp, MRP1 and BCRP.

Sulindac:

Sulindac is a non-specific COX-1/COX-2 inhibitor. Tatebe S*., et al.* [207], investigated the effect of sulindac exposure on the MRP gene family. They found that 24 hour treatment with 100-1200 µM sulindac increased the gene expression levels. O'Connor R., *et al.* [172], suggested that sulindac would be a good therapeutic MRP1 inhibitor. Sulindac does not reverse P-gp-mediated resistance in the human doxorubicin-resistant uterine sarcoma cells [171]. No studies with regard to sulindac's effect on BCRP have been published to date. There are no publications with regard to sulindac's active form, sulindac sulphide, and MDR [25].

With a 300 mg dose the peak plasma concentration for this drug is about 2 µg/ml and it has a half life ranging from 7 hours to 16 hours depending on health and diet of the patient [25].

Celecoxib:

Celecoxib is a COX-2 specific inhibitor that has been shown to down-regulate the expression of MRP1 and P-gp. Arunasree KM., et al. [160], demonstrated a 50% down regulation in P-gp protein expression (imatinib resistance) with 10 µM celecoxib following a 24 hour exposure time. Kang H-K., et al. [174], showed no change in MRP1 expression with 5 µM celecoxib for 24 hours but a 50 µM exposure for 24 hours caused an 80% down regulation of MRP1 expression. However, this concentration is exorbitant compared to achievable plasma concentrations (a maximum of 2 µg/ml).

No data has been published on celecoxib relationship with BCRP.

Therefore, celecoxib down-regulates P-gp at pharmacological concentration but its mechanism is unknown. It only affects the expression of MRP1 at extremely high, non-clinically relevant concentrations, and has not been linked with BCRP transport or function (see table 1.4.5.1.).

For a dose of 200 mgs, the peak plasma concentration can reach 0.705 µg/ml with a half life of 11 hours [25]. Higher doses have caused an increase in plasma concentrations of up to 2 µg/ml.

Ibuprofen:

This non-selective COX inhibitor was found to overcome P-gp mediated resistance below its therapeutic plasma concentration by Angelini A., et al. [171]. Nozaki Y., et al. [176], found that concentrations ranging from 1 to 100 µM did not inhibit the function of BCRP in human kidney slices. Neither authors examined the mechanism by which it modulates P-gp. (See table 1.4.5.1.)

The dosage for ibuprofen is between 1.2 g and 3.2 g. The peak plasma concentration reached with this dosage is 10 µg/ml with a half life of 1.8 hours to 2 hours [25].

Naproxen:

This NSAID is a COX-1 and COX-2 inhibitor. It has been shown not to affect the function of BCRP (in human kidney splices, at 1-100 μM [176]) but instead cause an increase in BCRP protein (6 μM exposure for 24, 48 and 72 hours resulted in an increase of 30%, 70% and 100% respectively) and mRNA levels (a 150% increase with 6 μM for 24 hours [96]) at clinically relevant concentrations. Zrieki A., *et al.* [96], observed no change in the expression of P-gp protein or levels of mRNA with the same treatments. No data was located for MRP1. (See table 1.4.5.1.)

The peak plasma concentration obtained with a typical dose is between 90 μg/ml and 98 μg/ml with a half life of 12 to 17 hours [25].

Nimesulide:

This preferential COX-2 inhibitor has been shown to decrease P-gp at the transcriptional level. No change in BCRP was observed and no data for MRP1 has been published. (See table 1.4.5.1.)

Zrieki A., *et al.* [96], studied the effect of 10 μM nimesulide on P-gp and BCRP protein expression and levels of mRNA in a colorectal cell line (CaCo-2). With 10 μM exposure for 24 hours they observed no change in P-gp protein expression but a 40% decrease in mRNA levels. However, by increasing the exposure time by 24 or 48 hours a 20% decrease in protein expression was observed. Using the same treatment times and concentration, no change was observed in BCRP mRNA levels and protein expression.

The peak plasma concentration for nimesulide is 1.93 μg/ml [25].

Indomethacin:

Indomethacin (non-selective COX inhibitor) has been shown to inhibit both MRP1 and BCRP but not P-gp. However, this only occurs at concentrations exceeding the peak plasma concentration (1 μg/ml to 2 μg/ml) [25]. It has been shown to decrease the expression of P-gp transporter protein and mRNA level at clinically relevant concentrations. (See table 1.4.5.1.)

Zrieki A., *et al.* [96], studied the effect of 0.4 μM indomethacin on P-gp and BCRP protein expression and levels of mRNA in a colorectal cell line (CaCo-2). 24, 48 and 72 hour exposures resulted in a 10%, 30% and 40-50% down-regulation of P-gp expression. While a 24 hour exposure reduced the P-gp mRNA level by 40%. The

same exposure saw a 10-40% increase in BCRP protein expression but no change in mRNA level. Nozaki Y., *et al.* [176], found that 1 μM had no inhibitory effect on BCRP function, but 10 μM caused a 30% decrease in activity in human kidney splices. Draper MP., *et al.* [177], showed that 10 μM indomethacin inhibited MRP1 but not P-gp. Gedeon C*., et al.* [208], also demonstrated this.

NS-398:

NS-398 is a selective COX-2 inhibitor. To date, no work has been carried out on its interaction with MRP1 and BCRP. Kim SK., *et al.* [209], indicated that NS-398 could impede the function of P-gp (using efflux assays/combination assays) and down regulate P-gp protein expression (by Western blot) (see table 1.4.5.1.). Zatelli M.C. *et al.* [175], showed that 1 μM NS-398 prevents the development of P-gp resistance due to doxorubicin exposure over a 10 day period. And also, that this concentration could, to a small extent, down-regulate doxorubicin induced P-gp expression. Combination and efflux assays further demonstrated the drugs ability to inhibit the function of P-gp at this concentration in MCF7-doxorubicin selected breast cells.

No clinical toxicological data is available but *in vitro* toxicological data would suggest its IC_{50} values lies between 100-200 μM. No clinical or pharmacological data is available for this NSAID.

Heat shock protein 90 (Hsp90) inhibitors:

Heat shock protein 90 (Hsp90) is a molecular chaperone required for the stability and function of several conditionally activated and/or expressed signalling proteins. Many of these client proteins such as Akt, HER2, Bcr-Abl, c-Kit, EGFR and PDGFR-α are oncoproteins and important cell-signalling proteins [210]. As signal transducers and molecular switches, these client proteins are inherently unstable. Hsp90 keeps unstable signalling proteins poised for activation until they are stabilised by conformational changes associated with the formation of signal transduction complexes. As such, it is a single molecular target that is a central integrator of multiple pathways important to cancer.

17-AAG:

17-AAG is a derivative of geldamycin that retains its Hsp90 inhibitory function. Katayama K., *et al.* [3], demonstrated the potent ability of 0.1 µM 17-AAG to down-regulate the expression of P-gp (~80% after a 12 hour treatment in colon (SW620 MDR selected) and breast cell lines (MCF7 and MDA-MB-231 MDR induced)). Zhang H., *et al.* [211], presented *in vitro* and *in vivo* work to show that 17-AAG is a P-gp and MRP1 substrate. No information has been published to suggest 17-AAG modulates BCRP. The pharmacologically achievable levels of 17-AAG range from 0.15 - 17 µM depending on dosage [212].

Therefore, 17-AAG is a substrate of both P-gp and MRP1 and is also potent down-regulator of P-gp protein expression (mechanism of down-regulation is unknown). For details of other Hsp90 inhibitors see table 1.4.5.1.

Other:

Indole-3-Carbinol:

This drug is a natural elastase enzymatic inhibitor that also down regulates vinblastine induced P-gp [194] and up-regulates BCRP expression (1 µM had no effect while 10 µM doubled the expression of BCRP after a 72 hour treatment [195]). The authors [194] used 10 mM for 24 hours to reduce the P-gp expression by ~50%.

Elacridar:

This lipophilic compound has proven to be a potent inhibitor of both P-gp and BCRP. No effect was observed on function or expression of MRP1. Den Ouden D., *et al.* [191], demonstrated that elacridar could reverse P-gp-mediated resistance in AML cells. Elacridar was found to directly inhibit the function of BCRP at 2 µM and 10 µM [193] [213]. Evers R., *et al.* [192], established that 5 µM elacridar had no effect on MRP1-mediated resistance.

1.5. Tyrosine kinase inhibitors

1.5.1. Epidermal growth factor receptor family

The epidermal growth factor receptor (EGFR) family is composed of cell surface tyrosine kinase receptors that are involved in the regulation of cellular proliferation, survival and differentiation during development, tissue homeostasis, and tumourigenesis of epithelial cells. The EGFR family includes four receptors: EGFR/ErbB1, HER2/ErbB2, HER3/ErbB3 and HER4/ErbB4. Each receptor has an extracellular domain (ECD), a transmembrane region and an intracellular domain with tyrosine kinase activity. The binding of receptor-specific ligands to the ectodomain of EGFR, HER3 and HER4 results in the formation of homodimeric and heterodimeric kinase-active complexes. HER2 signalling is potentiated by HER2-containing heterodimers, and/or increases in the binding affinity of receptor ligands to EGFR and HER3/4 [214]. HER2 receptor activation leads to the phosphorylation of the intracellular catalytic domains, and ultimately activation of signal transduction pathways that promote proliferation and survival, including the phosphatidylinositol 3′-kinase (PI3K)/Akt/mTOR, the Erk1/2 mitogen-activated protein kinase (MAPK) and the Jak/Stat pathway [196].

HER2 is over-expressed and/or amplified in one-fourth of breast tumours and confers a more aggressive clinical course and a worse survival [215]. The clinical outcome for these highly aggressive tumours has markedly improved with the development of anti-HER2 therapies, i.e. trastuzumab (see table 1.5.2.1 below). Recently a number of these therapies, alone and in combination with more conventional chemotherapeutic agents, have been evaluated in randomised trials. Results from these trials indicate activity with the single agent and also improved survival in patients with advanced disease [216] [217] [218] [219]].

1.5.2. ErbB inhibitors

Inhibition of the EGFR family can be at their extracellular and intracellular domains. Small molecule targeted antibodies target the extracellular domain while tyrosine kinase inhibitors (TKIs) target the intracellular domain (refer to table 1.5.2.1 for examples of both antibodies and TKIs). These types of inhibitors are less toxic then commonly used chemotherapeutic drugs. They target a number of cell surface and intracellular markers, such as, EGFR, HER2, PDGFR, VEGF etc., which are found to be over-expressed in malignancies. A number of these inhibitors also have anti-multidrug resistance properties. Three TKIs (lapatinib, erlotinib and gefitinib) were found to directly inhibit the function of both P-gp [112] [157] [151] and BCRP [112] [157] [151] (for further information refer to sections 1.3 and 1.4.). Figure 1.5.2.1 below is a diagrammatical representation of the activation EGFR and the signal transduction pathways that lead to increased cell growth and reduced apoptosis. The legend for this figure discusses the site of action of tyrosine kinase inhibitor and the signal transduction cascades affected.
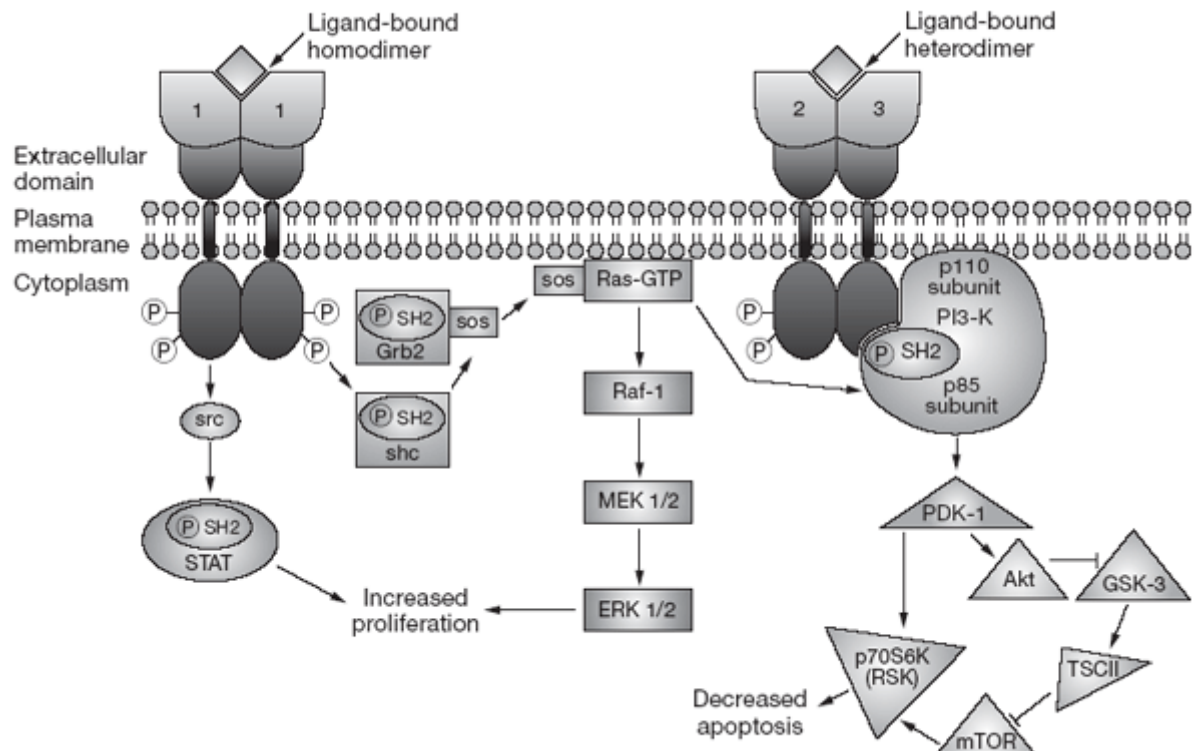
Figure 1.5.2.1.: This diagram represents the activation of EGFR and its down-stream signal transduction pathways. Tyrosine kinase phosphorylation occurs at intracellular docking sites. Tyrosine kinase inhibitors, such as lapatinib, erlotinib and gefitinib, prevent phosphorylation at these sites. This prevents EGFR tyrosine and protein binding and thus prevents the activation of pathways such as Ras/Raf/MEK/ERK. STAT protein activation is also inhibited by this method. The combined activation of ERK 1/2 and STAT leads to increased proliferation. Heterodimerisation with HER3 recruits PI3K, which activates a cascade that results in Akt phosphorylation. Inhibiting this dimerisation prevents the activation of downstream components of Akt that lead to decreased apoptosis. This image was obtained from medscape [220]. Table 1.5.2.1 below provides a list of tyrosine kinase inhibitors and antibodies targeted at members of the EGFR family.

Table 1.5.2.1.: The table below contains a list of targeted therapy antibodies and tyrosine kinase inhibitors for cell surface proteins, including their category, target and multidrug resistance status.

Inhibitor	Category	Targets	MDR status
Lapatinib (Tykerb)	TKI- Reversible	EGFR & HER2	Inhibits P-gp transport function.
Erlotinib	TKI- Reversible	EGFR	P-gp/BCRP substrate. P-gp/BCRP pump function inhibitor
Imatinib (Gleevec)		EGFR	BCRP & P-gp substrate
Imatinib mesylate		EGFR	BCRP substrate & functional inhibitor
Trastuzumab	Antibody	HER2	N/A
Gefitinib	TKI	EGFR	Inhibits P-gp/BCRP function.

Key:
N/A: unknown
This table was compiled from: [40] [147] [148] [150] [151] [157] [198] [199] [221].

1.6. Non-Steroidal anti-inflammatory drugs (NSAIDs)

Early in the nineteenth century, the active component of white willow bark (commonly used for the relief of inflammation and fever) was determined and acetyl salicylate (aspirin) was synthesised on an industrial scale for the first time. What evolved from this event was a new class of treatment for inflammation and pain, known as non-steroidal anti-inflammatory drugs (NSAIDs) (some of these agents have previously been discussed in relation to their MDR status in section 1.4.5). Modern NSAIDs include drugs such as sulindac and ibuprofen, and have become the most commonly used pharmaceutical compounds worldwide, especially for the outpatient management of pain and inflammation in a wide spectrum of diseases. Over 70,000 tons of aspirin are produced a year, reflecting the importance of this drug. In the US alone, 50 million people per year use NSAIDs for the treatment of a number of patho-physical conditions from the prophylaxis of cardiovascular disease or rheumatoid/osteoarthritis, to the relief of discomfort from minor injuries and headache (reviewed in reference [222]). Numerous clinical trials have taken place using a combination of chemotherapy with an NSAID in cancer treatment.

1.6.1. Classification and side-effects of NSAIDs

Classification:

NSAIDs primary mode of action is the blockage of one or both of the cyclooxygenase enzymes, COX-1 and COX-2, activity. These enzymes play an intrinsic role in the synthesis of prostaglandins. These prostaglandins (PGs or prostanoids) are ubiquitous lipid mediators that coordinate a wide variety of physiological and pathological processes via membrane receptors on the surface of target cells [223]. Prostanoids play an important biological function in the:

1. Activation and reduction of the inflammatory response, depending on their type,
2. Production of pain and fever,
3. Stimulation of blood vessel constriction or dilation,
4. Clotting of platelets or inhibition of blood clotting,
5. Regulation of the secretion of digestive juices and hormones,
6. Regulation of temperature and blood pressure,
7. Controlling cell division and growth,
8. Aiding in the introduction of labour and other reproductive processes including fertility, as well as,
9. Cytoprotection of the gastric mucosa, hemostasis, and renal hemodynamics

Prostanoid biosynthesis is induced in different pathological conditions, including inflammation and cancer [223] [224]. A broad spectrum of COX specific and non-specific inhibitors have been developed over the last 100 years. Table 1.6.1.1 below provides a comprehensive list of NSAIDs including their family subtype and COX selectivity.

Table 1.6.1.1.: The table below contains a list of the chemical classification, biological action of each drug, and specificity of a broad range of NSAIDs.

NSAID Family	Drug	COX-1, COX-2 selectivity
Salicylates	Acetylsalicylic acid (aspirin)	Non-selective COX.
	Benorylate/benorilate	Not specified
	Diflunisal	Non-selective COX
	Magnesium salicylate	Not specified
	Salicyl salicylate	Not specified
	Salicylamide	Not specified
Arylalkanoic acids		
	Diclofenac	Non-selective COX
	Aceclofenac	Non-selective COX
	Etodolac	Not specified
	Indomethacin	Non-selective COX.
	Nabumetone	Not specified
	Sulindac	Non-selective COX.
	Tolmetin	Not specified
2-Arylpropionic acids (profens)	Ibuprofen	Non-selective COX
	Dexketoprofen	Not specified
	Fenoprofen	Not specified
	Flurbiprofen	Not specified
	Ketoprofen	Non-selective COX
	Ketorolac	COX-1
	Loxoprofen	Non-selective COX
	Naproxen	Cox-1 and Cox-2.
	Oxaprozin	Not specified
	Tiaprofenic	Not specified
***N*-Arylanthranilic acids (fenamic acids)**	Mefenamic acid	Non-selective COX
	Flufenamic acid	Not specified
	Meclofenamic acid	Not specified
	Tolfenamic acid	Not specified
Pyrazolidine derivatives	Ampyrone	Not specified
	Metamizole	Not specified
	Phenazone	Not specified
Oxicams	Piroxicam	Non-selective COX
	Lornoxicam	Not specified
	Meloxicam	Cox-2 preference
	Tenoxicam	Not specified
COX-2 inhibitors	Celecoxib	Cox-2
	Etoricoxib	Cox-2
	Lumiracoxib	Cox-2
	Parecoxib	Cox-2
	Rofecoxib	Cox-2
	Valdecoxib	Cox-2

This list was compiled using google, pubmed and sciencedirect searches.

Side-effects of NSAIDs:

Given the important role of prostanoids in the body, one can imagine preventing their synthesis may result in some significant side effects. The most common adverse effect of NSAID-use are respiratory problems, cutaneous [225], gastrointestinal (GI) [226] [227] [228] [229] and cardiovascular [230] complications. Typically these manifest as:

- asthma attacks,
- heart attacks,
- increased mucosal permeability,
- anemia and acute blood loss,
- protein loss,
- active bleeding, GI/stomach perforations
- mucosal ulceration,
- stricture due to diaphragm disease

- urticaria,
- strokes,
- mucosal inflammation,
- malabsorption,
- illeal dysfunction,
- diarrhoea,

The therapeutic effects of NSAIDs are primarily related to their ability to inhibit COX-2, whereas some of their most frequent adverse effects may be caused by COX-1 inhibition. In contrast to most "classic" NSAIDs which block both isoforms, the so-called coxibs preferentially inhibit COX-2. These coxibs (such as celecoxib, rofecoxib, valdecoxib, etoricoxib, etc.) were developed in the hopes of overcoming some of the undesirable side-effects of non-selective COX inhibitors. To date, these coxibs have been associated with reduced gastrointestinal toxicity from the upper and lower GI tract compared to that of non-selective COX inhibitors. COX-2 inhibitors selectively reduce vascular prostacyclin synthesis without disrupting COX-1-derived thromboxane synthesis in platelets. However, removal of prostacyclin's capacity to restrain endogenous compounds contributing to platelet activation and vasoconstriction is a well-recognised mechanism for coxib action in the cardiovascular system [231]. The severity of this side-effect appears to depend on the drug, dose and duration of use.

Capone ML., *et al.* [231], performed an etoricoxib (coxib) versus diclofenac (old NSAID) gastrointestinal evaluation study in patients with OA (osteoarthritis) and showed that etoricoxib significantly reduced the rate of discontinuation by 50% due to adverse gastrointestinal events versus diclofenac. Rates of discontinuation due to hypertension-related adverse effects were higher on etoricoxib than diclofenac.

Similar to other COX-2 inhibitors, etoricoxib is contradicted in patients with ischaeme heart disease or stroke and should be used with caution in patients with risk factors for heart disease.

Graham DJ., *et al.* [230], suggested that coxibs may confer an elevated risk for acute myocardial infarction and sudden cardiac death after long-term therapy. As a result the Food and Drug Administration (FDA) met to discuss the future of cyclooxygenase-2 inhibitors in April of 2005 and controversially approved rofecoxib, celecoxib, and valdecoxib use but placed a black-box warnings on their labels [232].

Around the same time as this meeting, randomised clinical trials and observational studies showed an increased risk of myocardial infarction, stroke, hypertension and heart failure during treatment of patients with coxibs [231], leading to the withdrawal of rofecoxib and valdecoxib from the market. Furthermore, several cases of severe liver-toxicity led to a halt in the approval of lumiracoxib in the EU in November 2007. Rofecoxib has subsequently been removed from by market by Merck.

However, short term treatment with NSAIDs have little side-effects. Therefore, the availability of coxibs would be advantageous for non-COX selective intolerant patients, patients with risk of heart disease and for osteoarthritis or rheumatoid arthritis patients who are unable to tolerate the gastrointestinal side effects of other drugs.

1.6.2. PGE pathway and COX proteins

1.6.2.1. PGE pathway

Prostaglandins were first discovered and isolated from human semen in the 1930's by Ulf von Euler of Sweden. Thinking they had come from the prostate gland he named them prostaglandins (PG's).

Prostaglandin and thromboxane production from arachidonic acid (AA) is mediated by two cyclooxygenase (COX) enzymes, also referred to as prostaglandin H synthases, or prostaglandin endoperoxide synthases. AA is a 20 carbon polyunsaturated fatty acid that is released from membrane-bound phospholipids, usually by the action of phospholipase enzyme A2, prior to oxygenation by the COX enzymes.

Both of these enzymes possess two activities, cyclooxygenase and peroxidase, that act sequentially, thus converting AA to an unstable intermediate prostaglandin G_2 (PGG_2) and then the product prostaglandin H_2 (PGH_2). PGH_2 is subsequently converted to other prostaglandins (PGs: PGD_2, PGE_2, PGF_2alpha, PGI_2) or thromboxanes (TXAs). The array of PGs produced varies according to the downstream enzymatic machinery present in particular cell type. See figure 1.6.2.1.
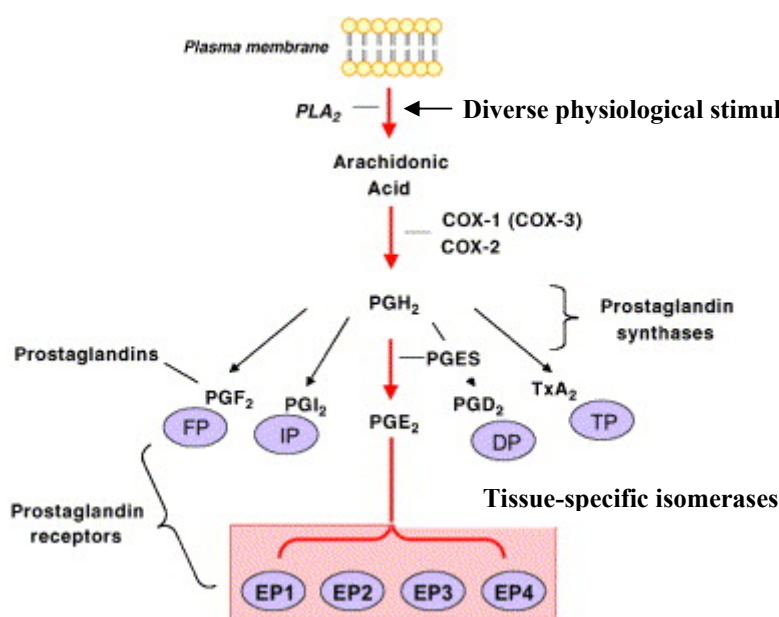
Figure 1.6.2.1.: The Arachidonic acid pathway.

In the last 10 years, studies have suggested that PGEs and tissue specific isomerases (prostaglandin receptors (EP)) 1-4 types may play a role in tumourigenesis. For example, increased mPGES-1 expression has been associated with human cancers of the lung [233], uterus [234], stomach [235], colon [236], penis [237], and head and neck [238], whereas studies using EP-knockout mice have suggested a role for each receptor subtype in murine intestinal tumour formation [239] [240].

COX-2 derived prostaglandins were demonstrated to promote tumour growth by accelerating the cellular proliferation rate, inhibiting apoptosis and enhancing metastasis and angiogenesis [241] [193].

Based on knowledge of the pathway of PGE_2 generation, a number of targets for selective inhibition come to light. For example, PGE_2 is formed by the isomerisation of PGH_2 by the action of three specific PGE_2 synthases (PGEs), after which it is able

to signal through any one of four G protein-coupled E-prostanoid receptors, and ultimately, four different signal transduction pathways [242] (figure 1.6.2.1. previous). PGE_2 is also cleared from the extracellular environment by a specific prostaglandin transporter [243] and metabolised to ligands with diminished biological activity by further catabolic enzymes [244] which lead to the rapid attenuation of stimulated response. Such stimulated responses are suggested to include the transactivation of growth factor receptors such as EGF receptor [245] and nuclear receptors such as NR4A2 [246] and PPARs [247].

Non-steroidal anti-inflammatory drugs (NSAIDs), which are widely prescribed as analgesics and anti-inflammatory agents, inhibit the biosynthesis of PGs. Their mechanism of action includes inhibition of both COX-1 and COX-2 isoenzymes [224] [248] [249]. COX-2, but not COX-1, is characterised by an accessible side pocket that is an extension to the hydrophobic channel [250] thus allowing for drugs to have selectivity.

There are still a number of targets yet to be evaluated for selectively inhibiting the functions of PGE_2 that may prove less harmful to the individual than inhibiting all prostaglandin production. Through COX-2 inhibition targeting such differences may be a more suitable approach for long term applications, such as cancer chemo-prevention.

1.6.2.2. COX proteins

As discussed in section 1.6.2.1., cyclooxygenase (COX) enzymes (COX-1, COX-2 and COX-3) catalyze prostaglandin synthesis from arachidonic acid. The two isoforms that have been almost fully characterised to date are COX-1 and COX-2. COX-1 is a homeostasis protein constitutively expressed in a variety of tissues. The COX-2 protein is induced by growth factors, cytokines and oncogenes (for review see [251]).
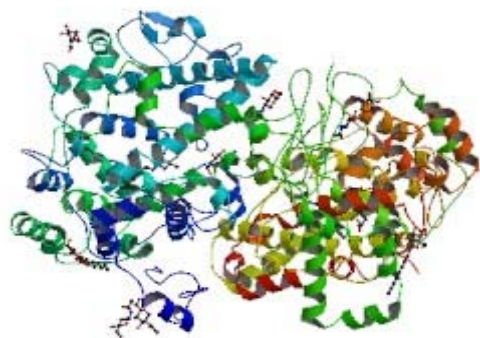
Figure 1.6.2.2.: The structure of the COX-1 enzyme.

COX enzymes are proteins with a molecular weight of about 68 kDa in an unmodified condition, which increases to 72-74 kDa after post-translation glycosylation [252]. The structure of COX enzymes consists of three distinct domains: an N-terminal domain with a conformation that is highly similar to that of epidermal growth factor, a domain containing a series of amphipathic helices, which comprise the membrane attachment site, and a C-terminal catalytic domain, which contains the cyclooxygenase and peroxidase active sites. Although the two enzymes are highly similar in structure and enzymatic activity they have different genomic structures and different gene regulations and expressions.

COX-1:

COX-1 was first purified and characterised in the 1970s and the gene was isolated in 1988 [253], COX-1 and COX-2 are encoded by separate genes located on different human chromosomes. The gene encoding for COX-1 enzyme is located on

chromosome 9 (9q32-9q33.3) and is approximately 40 kilobase (kb) pairs, contains 11 exons and its mRNA is 2.8 kb [254]. This gene exhibits the features of a housekeeping gene, it lacks a TATA box [255], and is generally not subject to transcriptional induction, but it is constitutively expressed with near-constant levels and activity in most tissues and cell types.

COX-2:

The COX-2 gene was cloned in 1993 [256]. The gene encoding for COX-2 is located on chromosome 1 (1q25.2-25.3), contains 10 exons and is approximately 8.3 kb with a 4.5 kb transcript [257]. COX-2 is an inducible or early-response gene, whose expression is undetectable in most normal tissues. COX-2 is highly induced in response to a broad spectrum of stimuli such as bacterial lipopolysaccharide (LPS) [258], cytokines [259], and growth factors [260].

Transcriptional control of the COX-2 gene is cell-specific, and it is evident that more than one pathway may co-operate to regulate COX-2 expression.

COX-3:

It has been suggested that there is another COX enzyme formed as a splice variant of COX-1 [261], referred to as COX-3. COX-3 is made from the COX-1 gene but retains intron 1 in its mRNA. Its expression was initially reported in the canine cerebral cortex and in lesser amounts in other analyzed tissues [261]. Recent molecular biology studies revealed that indeed three distinct COX-1 splicing variants exist in human tissues [262]. The most prevalent of these variants, called COX-1b1, would make the expression of a full-length protein impossible; therefore a catalytically active form of the enzyme might not exist in humans. However, the other two variant types, called COX-1b2 and COX-1b3, encode predicted full-length and probably COX-active proteins, as suggested by functional studies, which revealed that COX-1b2 is able to catalyse the synthesis of PGF2a from AA [262].

1.6.3. Relationship between COX expression and cancer

COX-1, COX-2 and their major metabolites involved in tumour progression are frequently up-regulated in many cancer types. The homeostasic protein COX-1, which is constitutively expressed in a variety of tissues, is over-expressed in human breast [263], prostate [264], cervical [265], hepatocellular carcinoma (HCC) [266] and ovarian cancer [267] [268], but not in colorectal adenocarcinoma. Chulada PC., *et al.* [269], showed that a loss of the COX-1 gene reduced intestinal tumourigenesis in mice. It has been suggested that COX-1 may be involved in the early stages of HCC tumour growth, as expression levels are significantly higher in well-differentiated HCC compared to poorly-differentiated tissues [269] [270] [271]. Sugimoto T., *et al.* [272], found that COX-1 expression levels in endometrial cancer patient samples were significantly up-regulated compared to mRNA levels. They also found that levels of COX-2 expression differed among cell lines, although no COX-2 mRNA elevation was found in their patients samples. These results indicate that the up-regulation of COX-1 rather than COX-2 may have an important role in tumour development in endometrial cancer.

COX-2 protein, which cannot be detected in the majority of normal tissues, is not only up-regulated in 80-90% of colorectal cancer [273], but is also up-regulated in gastric [274], lung [275], prostate [264], breast, ovarian [276] [277], liver, bladder, osteosarcoma, melanoma [278] and bone cancer. Several lines of evidence suggest the critical role of COX-2 in tumourigenesis [279] [280]. COX-2 has been demonstrated to promote cell growth, inhibit apoptosis, increase angiogenesis and enhance cell motility and adhesion [279] [281] [282].

In addition, it is known that PGE_2 (a COX-2 derived product) can have immunosuppressive properties allowing tumour to escape host surveillance mechanisms [280]. It has been reported that COX-2 inhibition reverses the tumour-induced increase in the immunosuppressive cytokine IL-10 from lymphocytes and macrophage and the suppression of the production of macrophage immune activator cytokine IL-12 [283].

Also, it is predominantly PGE_2 that is thought to be responsible for promoting colorectal tumourigenesis, with elevated levels reported in benign and malignant human and rodent colorectal tumours *in vivo* [284] [285].

COX-2 over-expression has been tentatively linked with poor prognosis, decreased survival and increase risk of re-occurrence in colorectal [286], ovarian [277] [287] and breast cancers [288]. In breast cancer, COX-2 up-regulation is associated with a high histological grade, a negative hormone receptor status, a high proliferation rate, high p53 expression, and the presence of HER-2 oncogene amplification, along with auxiliary node metastasis and a ductal type of histology (i.e. a poor prognosis) [286] [289].

Steffensen KD., *et al.* [276], revealed that COX-2 expression in epithelial ovarian cancer is only seen in a subset of ovarian carcinomas and that negative COX-2 expression is an independent prognostic factor for poor overall survival, however, others found that COX-2 expression was associated with significantly reduced median survival time [277] and levels were significantly higher in non-responding patients than patients responding to chemotherapy [287].

Elevated COX-2 expression in breast and colorectal cancer is associated with the more advanced stages and larger tumours. However, HCC and ovarian carcinoma portray a different expression pattern (high COX-2 expressed at pre-malignant and malignant lesions and well-differentiated carcinoma) [290].

In mouse and human adenomatous polyps of the colon, the earliest expression of COX-2 is detected in stromal cells, but in several types of cancers, COX-2 is found in multiple cells, i.e., epithelial, endothelial, stromal, and inflammatory cells [280].

1.6.3.1. Regulation of COX

A number of factors influence COX expression. The extracellular stimuli that induce COX-2 include growth factors, cytokines, tumour promoters, hypoxia (HIF-1 and NF-KappaB p65 transcription factor) [292] [293], ionizing radiation, carcinogens and chemotherapeutic drugs (cisplatin and taxanes up-regulate mRNA and protein) [294] [295] [296]. Hepatitis B (HBV) and hepatitis C (HCV) viral infections are risk factors associated with hepatocellular carcinoma (HCC). Studies have shown that both viruses promote COX-2 expression through activation of NF-KappaB and p38 MAPK pathways through the endoplasmic reticulum and reactivated oxygen species (ROS) [297]. Increased COX-2 expression has been noted in the presence of IFN-gamma [298], but to date, evidence to confirm its relationship has not been established. NF-kappaB co-regulates IL-4 while IFN-gamma inhibits the biological function of IL-4. Peng H.,

et al. [299], showed that endothelin-1 (ET-1) caused an increase in COX-2 protein expression as well as increased production of PGE_2. It also increased the production of IL-8 in A549 cells. Other factors influencing the expression of COX-2 mRNA and protein expression may include the combined de-regulation of Wnt and Ras pathways. Inhibition of COX-2 expression is caused by glucocorticoids [221], IL-4 [300], IL-13 [300], the anti-inflammatory cytokine IL-10 [301] and targeted therapies, such as erlotinib and gefitinib.

COX-2 expression can be regulated at the post-transcriptional level in tumours. This can occur through the binding of RAW [302a] or HuR [302b] to its RNA.

1.6.3.2. Relationship between COX expression and Angiogenesis

Angiogenesis, the development of new blood vessels, is an essential step in the growth of tumours, since the growth of malignant cells is limited by the availability of nutrients. Vascular endothelial growth factor (VEGF) is a well-characterised tumourigenic molecule and is known to potentiate tumour angiogenesis and invasion. A substantial body of evidence supports the role of COX-2 in angiogenesis, the "sprouting" of capillaries from pre-existing vasculature, in a variety of human malignancies [303] [304] [305] [306]. COX-2-expressing cells produce high levels of angiogenic factors that promote angiogenesis, mainly through the synthesis of prostanoids. These factors can induce tumour angiogenesis in an autocrine and/or paracrine fashion by stimulating the expression of pro-angiogenic factors [2]. COX-1 expression has been found to correlate with VEGF expression in ovarian [305] and endometrial cancer [272]. COX-2 expression has been linked with an angiogenic phenotype in colorectal carcinoma [280], bone [280], liver [307], intestinal epithelial cells [308] [309], pancreatic, cervical [305] [287] [310] and in patients with HVC- and HBV-associated HCC [311] [292] [312].

In vitro studies carried out by Kim MH., *et al.* [305], and Ferrandina G., *et al.* [287], demonstrate an association between COX-2 production, increasing VEGF, and subsequent angiogenesis. While Howe LR., *et al.* [264], showed that genetic abolition of the COX-2 gene product in HER2/nue knockout mice caused a decrease in tumour size, number and significantly reduced vascularisation as well as the expression of pro-angiogenic genes.

Lindstrom AK., *et al.* [310], reported that high COX-2 expression related to locally advanced disease, distant metastases, and decreased survival in cervical cancer patients. Multiple studies have shown that high COX-2 expression in conjunction with vascular endothelial growth factor (VEGF) or EGFR in cervical cancer correlates with poor prognosis and outcome [287]. Dai Y., *et al.* [313], confirmed over-expression of COX-2 and prostaglandins by immunohistochemistry and RT-PCR of pre-invasive cervical intraepithelial neoplasia [314] and invasive cervical cancer tissue compared to normal and inflamed cervical tissue (HPV negative) [313]. Head and neck squamous cell tumours show a similar pattern of co-existing COX-2 and VEGF over-expression as cervical disease [312]. Findings by Cervello M. *et al.* [311], suggest the hypothesis that selective inhibition of COX-2 by treatment with coxibs may contribute to inhibit HCC-associated angiogenesis.

To date, COX-2 inhibitors have been shown to induce apoptosis of transformed intestinal epithelial cells, inhibit angiogenesis *in vitro* [308] [310] [307], and inhibit invasion, growth and metastasis *in vivo* [2] [315] [316]. Other selective COX-2 inhibitors, including celecoxib, have anti-angiogenic activity in a variety of *in vitro* [299] and *in vivo* [317] [318] [319] models.

1.6.3.3. Relationship between COX expression and Invasion

A number of studies have shown that the expression of COX-1 and COX-2 is involved in VEGF [312] and metalloproteinase (MMP) activation [219] [320] [321]. MMPs play an important role in the control of cellular interactions with, and response to, their environment in conditions that promote tissue turnover be they physiological, such as normal development, or pathological, such as inflammation and cancer including invasion. Physiologically, MMP2 and MMP9 in coordination with other MMPs, play a role in normal tissue re-modeling events such as embryonic development, angiogenesis, ovulation, mammary gland involution and wound healing. In ovarian [305] and endometrial cancer [272], VEGF expression correlates with COX-1 expression and invasiveness. The COX-2/PGE$_2$ pathway plays a key role not only in bone, liver, breast, colon and ovarian metastasis but also in provoking angiogenesis and therefore progression of the tumour growth and survival. PGE$_2$ has been found to

stimulate growth, modulate apoptosis and enhance cell motility in colon carcinoma cell lines *in vitro* [322] [245].

Both COX-1 and COX-2 play a role in the activation of MMP2 by way of membrane-type 1 MMP induction in human breast cancer cell lines. In 2002, Dohadwala., *et al.* [323], showed that blockage of MMP expression by anti-sense oligonucleotides produced significant inhibition of PGE1-mediated CD44 expression. Singh B., *et al.* [324], showed that COX-2 over-expression correlated with increased production of IL-11 and increased bone metastasis.

In vitro and *in vivo* studies have proven that metastasis due to over-expression of COX-2 can be reversed by administering NSAIDs [241]. Diclofenac, nimesulide, celecoxib, valdecoxib, rofecoxib and sulindac sulphide all inhibited the expression and activation of MMP2 and MMP9 [241] [325]. Sulindac sulphide reduced MMP2-related invasion in COX-2 induced human colon cancer cells (Caco-2) [210]. Diclofenac sodium, nimesulide, celecoxib, valdecoxib, rofecoxib and etoricoxib down-regulated the expression of gelatinases (matrix metalloproteinase (MMP)-2 and MMP-9) in samples from early knee osteoarthritis (OA) of humans [325].

1.6.3.4. Relationship between COX expression and MultiDrug Resistance

Induction of COX-2 expression has been linked with the expression of multi-drug resistance proteins, such as P-gp, BCRP, MRP1, MRP2 and MRP3. Growing evidence indicates that COX-2 over-expression can up-regulate the expression of the multidrug resistance 1 (mdr1) gene and its protein, the multidrug resistance pump p-glycoprotein (P-gp) [326] [327] but this can be reversed by using NSAIDs and coxibs, such as celecoxib (for review see Sorokin A., [327]).

Using immunohistochemical analyses, a strong correlation between expression of COX-2 and P-gp was found in human breast tumour specimens [328]. Surowiak P., *et al.* [329], found a positive correlation between COX-2 and MDR1/P-gp expression and demonstrated that COX-2 and MDR/P-gp are unfavourable prognostic factors in breast cancers and unfavourable predictive factors in chemotherapy-treated breast cancer cases. In the P-gp-induced drug resistant cell line, MCF7, there was significant up-regulation of COX-2 expression as well as the up-regulation of transcription factors; protein kinase C (PKC) and activator protein 1 (AP1) subunits c-Jun and c-

Fos were also upregulated [328]. The inhibition of prostaglandin synthesis by COX-inhibitors could block this cascade resulting in a negative modulation of MDR1. This [329] and other evidence [326] [327] suggest that COX-2 could contribute to the development of resistance to pharmacological treatment by tumour cells. Zatelli MC., *et al.* [175], provided data to support the hypothesis that the COX-2 selective inhibitor, NS-398, can prevent and reduce the development of the chemo-resistance phenotype in breast cancer cells by inhibiting P-gp and function. Also using NS-398, Kim SK., *et al.* [209], suppressed the expression and function of P-gp and induced apoptosis in ependymomas (cancer derived from the ependyma, a tissue of the central nervous system). Patel VA., *et al.* [326], suggests that the up-regulation of COX-2 leads to increased P-gp expression and activity in RMC cells.

Puhlmann U., *et al.* [330], showed that doxorubicin-induced MDR1 over-expression was down-regulated by the COX-2-preferential inhibitor, meloxicam, in both HL-60 and primary AML blasts with subsequent improvement of cytostatic efficacy of doxorubicin. Arunasree KM., *et al.* [160], provided evidence that COX-2 and MDR-1 over-expression are responsible for the development of resistance to imatinib in IR-K564 cells. They showed that celecoxib, a selective COX-2 inhibitor, induced apoptosis by down-regulating the expression of COX-2 and MDR-1 via a mechanism involving the Akt pathway. Many other studies provide evidence that the non-steroidal anti-inflammatory drug, celecoxib, can increase the efficacy of chemotherapeutic [331] [332] [333] and neurotropic drugs [334]. Many of these drugs are substrates of P-gp, such as, doxorubicin, vincristine, etoposide, irinotecan, risperidone and reboxetine. Therefore, by acting on the expression of P-gp, it could be speculated that a selective inhibition of COX-2 activity could reinforce the anti-tumour act of conventional chemotherapy. The rationale behind the possible combination of traditional chemotherapy and selective COX-2 inhibitors is further supported by the fact that chemotherapy itself induces COX-2 expression [335].

Kang HK., *et al.* [174], examined the possibility that COX-2 expression is not only related to P-gp expression but also MRP1 expression. When the model chosen, A549 (a human epithelial lung cell line that highly expresses COX-2 and MRP1), was exposed to high levels of celecoxib (50 and 100 μM), MRP1 expression and function was down-regulated. They proved that MRP1 expression is not necessarily due to COX-2 expression as forced expression by transfection did not up-regulate MRP1. Incidentally, they also showed that induced COX-2 expression did not increase P-gp

expression, suggesting that the P-gp up-regulation observed by Patel VA., *et al.* [326], Puhlmann U., *et al.* [330], and Arunasree KM., *et al.* [160], may be carcinoma specific or it may not have happened as the cell line already expresses MRP1.

On the other hand, work carried out by Takaoka K., *et al.* [336], demonstrated that COX-2-transfected human epidermoid KB carcinoma cells, showed increased expression of MRP1 and MRP2 (shown by Western blot) which gave a 2.5-fold resistance to cisplatin, while maintaining sensitivity to vincristine, bleomycin and 5FU.

Using MRP1 expressing lung cell lines (A549, DLKP, HL60/Adr, COR L23P, COR L23R), Duffy CP. *et al.* [337], revealed that a specific subset of NSAIDs significantly increased the cytotoxicity of MRP1 substrates (anthracyclines, temiposide, VP-16 and vincristine), but not other vinca alkaloid (vinblastine and vinorelbine) or P-gp substrates (methotrexate, cytarabine, hydroxyurea, chlorambucil, cyclophosphamide, mitoxantrone, actinomycin D, bleomycin, paclitaxel and camptotecan). This demonstrates that some NSAID, such as, indomethacin and sulindac, are MRP1 inhibitors.

NSAIDs are currently being investigated for potential influences on multidrug resistant mechanisms. Ibuprofen overcame resistance in the human doxorubicin (doxo) resistant uterine sarcoma cells (MES-SA/Dx-5) expressing high levels of P-gp [171]. Similarly, NS-398 impeded the function and protein expression of P-gp in two primary cultured ependymoma cell lines [209]. However, sulindac, a non-specific COX-inhibitor, increased MRP1 and MRP3 expression levels while having no effect on MRP2, MRP4, MRP5 and MRP6 [207]. Tatebe S., *et al.* [207], suggested the mechanism was via the induction of ROS (and γ-glutamylcysteine synthetase heavy subunit gene which is a rate-limiting enzyme in glutathione biosynthesis), this was proven using down-regulation by NAC (N-acetylcysteine), a ROS suppression anti-oxidant.

COX-2-specific inhibitors, celecoxib [160], NS-398 [209], indomethacin [96] and nimesulide [96] reduce the expression and function of P-gp protein. Puhlmann U., *et al.* [330], down-regulated the expression and function of P-gp in doxorubicin-resistant cells, using meloxicam (COX-2 selective inhibitor), and suggested the mechanism is through the modulation of NF-KappaB.

1.6.3.5. Relationship between COX expression and Epidermal Growth Factor Receptors expression

Receptor tyrosine kinases, such as members of the EGFR family (i.e. HER2) via their over-expression and/or over-activation, mediate many of the characteristics of the malignant phenotype, such as decreased apoptosis, increased cell proliferation, metastasis, and resistance to chemotherapy and radiotherapy [338]. These receptors play a crucial role for the growth of both normal tissue and malignant tumours. The debate as to whether the expression of COX-2 is regulated or effected by EGFR/HER2 activation has been investigated since 1997 and remains a hot subject. Several studies reported that the epidermal growth factor receptor family can increase COX-2 protein expression and activity levels. This increase is suggested to occur through EGFR activation which increases COX-2 protein expression [339], paracrine/autocrine activation of HER2/HER3 heterodimers which leads to activation of the COX-2 promoter [340] [341], and a HER2/COX-2 promoter complex which stimulates COX-2 transcription [342].

HER2:

The correlation between COX-2 and HER2 co-expression with prognosis has been investigated in breast [343] [344] [345] ovarian [340], bladder [346], prostate [347] and endometrial cancer patients [348].

COX-2 expression is associated with increased angiogenesis, lymph node metastasis, and HER2-nue expression. Howe LR*., et al.* [349], found that tumour size, vascularisation, and expression of pro-angiogenic genes were down-regulated in COX-2 knockout mice that expressed HER2/neu compared to COX-2 and HER2/neu expressing mice.

COX-2 and HER2 co-expression is a poor prognostic marker in breast cancer. Dillon MF*., et al.* [343], found a link between membrane HER2, nuclear HER2 and COX-2 expression predicted a poor disease-free survival in breast cancer patients on endocrine treatment and had adverse side effects to tamoxifen treatment. Nassar A., *et al.* [344], found that the same co-expression also correlated with large tumour size and high tumour grade but not with outcome [350]. Zerkowski MP., *et al.* [345], showed that COX-2 expression was up-regulated in invasive breast tumours and that these patients had significantly worse disease-specific and overall survival. This was independent of

tumour size, nodal status, grade and ER levels. Despite this correlation, the combination of celecoxib and trastuzumab (an anti-HER2/neu monoclonal antibody) produced no change in response compared to trastuzumab treatment only [351]. However, *in vitro* research showed that 5 and 10 µM lapatinib (a dual EGFR/HER2 tyrosine kinase inhibitor (TKI)) reduced protein expression and function of TNFα, IL-1B and EGF stimulated COX-2 [352].

Using immunohistochemical analysis no prognostic significance was found with the expression of COX-2 and HER2 in ovarian [340] [353], bladder, prostate cancer [347] or NSCLC [354]. COX-2 and HER2 was co-expressed in 33% of invasive bladder cancer patients but this was independent of tumour stage, lymph node status and histological grade [346].

EGFR:

A link between COX-2 expression and EGFR expression and activation has been identified. A number of publications suggest that EGFR ligands potentiate and are required for COX-2 induction [355] [356]. Some of these ligands identified include, epidermal growth factor (EGF) and transforming growth factor-α (TGFα). These have been linked with ERK and Ras-Raf / Rac-PAKI-MEK signalling [357]. ERK interacts with the p38^{MAPK} pathway which leads to the phosphorylation of CREB and transcriptional activation of the COX-2 promoter [357] [358]. EGF-induced transcriptional activation of COX-2 and COX-2 mRNA was found to result from increased activator protein-1 (AP-1; c-Jun) activity, although some question exists as to whether this involves receptor signalling to JNK [356].

On the other hand, COX-2 activation has also been shown to lead to the transactivation of EGFR. The presence of PGE$_2$ leads to rapid EGFR phosphorylation and triggers the extracellular signal-regulated kinase 2 (ERK2) [245]. This PGE$_2$-induced EGFR transactivation involves signal transduction via TGF-alpha (likely released by c-Src-activated MMP(s)) [358] [281]. Al-Salihi MA., *et al.* [359], provided data demonstrating that COX-2 potentiates tumourigenesis in colon epithelial cells. They showed that COX-2 is not involved in initiation but instead, activation, of EGFR and the Akt signalling pathway, which may be responsible for the increase in tumour number and volume and in changes in morphological architecture and organisation.

Despite this cycle of regulation and activation, no significant correlation between COX-2/EGFR co-expression and survival has been identified. Brattstrom D., *et al.*

[360], demonstrated this in NSCLC while van Dyke AL., *et al.* [362], observed the same lack of trend in tumour status, prognosis and outcome in women with adenocarcinoma of the lung.

The combination of COX-2 inhibitors (celecoxib/NS-398) with erlotinib or gefitinib (EGFR tyrosine kinase inhibitors) increased apoptosis and decreased cell number *in vitro* [281] [362], while decreasing tumour size and number *in vivo* [363] [364]. Gadgeel SM., *et al.* [365], combined erlotinib/gefitinib with celecoxib in EGFR-wild and -mutant (moderate and high) expressing NSCLC cell lines. Both combinations had the greatest effect on the highly expressing EGFR-mutant-expressing cell line. This cell line also expressed high levels of COX-2. These results indicate that the combination would not be beneficial in EGFR-wild type-expressing NSCLC tumours.

Both erlotinib and gefitinib (EGFR-specific TKI's) down-regulate COX-2 expression and reduce its function in a non-small cell lung carcinoma cell line (H3255). A clinical trial investigating the efficacy of combined therapy with a COX-2 inhibitor with an EGFR inhibitor (erlotinib and gefitinib) found no additional benefit of combined treatment in platinum therapy unresponsive or chemotherapy-naïve patients in comparison with results from previous studies involving treatment with the TKI's alone [365] [366] [367].

1.7. *In vitro* assessment of anti-cancer agents' activity

As stated by Putnam KP., *et al.* [368], cytotoxicity is an important factor in understanding the mechanisms of action of chemicals on cells and tissues. Cytotoxicity is thought to play an important role in a number of pathological processes, including carcinogenesis and inflammation. It may also modulate the activity of other agents, including free radicals, irritants and genotoxins.

When testing a compound for cytotoxicity there are many biological endpoints that can be examined. These may be general mechanisms common to all cells or mechanisms specific to particular cell type. The use of cell culture systems has become common in the toxicological assessment of chemicals and chemical mixtures. Several large research groups have evaluated various *in vitro* assays and have recommended the use of cytotoxicity assays in toxicology.

There are many different types of cytotoxicity assays that suit various cell lines or toxic effects. Some use the breakdown of various tetrazolium salts to formazan by mitochondrial dehydrogenase in viable cells. Such assays include MTT, MTS, MTT-A, XTT, XTT-A, XTT (PMS) and WST-1.

Other assays that take advantage of the cell damage, which may be manifested by a loss of plasma membrane integrity or changes in influx and efflux systems through the cell membrane caused by toxins or drugs include; the neutral red assay (NR), Trypan blue exclusion assay, Lactate dehydrogenase assay (LDH), crystal violet dye elution (CVDE), kenacid blue and the resazurin system. Some of the above can determine the health of the cell by quantifying the amount of cellular protein. During normal cell growth, in an ideal environment, the protein levels within the cell will be constant. Once these standards are known, any change in cellular protein concentration can be directly related to the addition of drugs or toxins. ATP based assays, sulforhodamine B and the Acid Phosphatase (AP) assay are the only three that do not fall into the above categories. The ATP based assay determines changes in ATP levels within the cells at a given time, the sulforhodamine assay measures the amount of cellular protein, but does not require alterations in the structure or permeability of the cell membrane to do so. The AP assay is based on the amount of acid phosphatase enzyme on the cell membrane or on the lysosome. The AP assay requires lysis of the cell to release the acid phosphatase enzyme. The activity of acid phosphatase is quantified by

the catalysis of a substrate, p-nitrophenol (PNP), to p-nitrophenolate in the presence of NaOH producing as easily detectable colour change.

This highly sensitive, easy and direct colorimetric method of determining changes in cell proliferation, compared to the control wells, caused by small molecule and chemotherapeutic agents was employed throughout this project.

1.8. Aims of the thesis

The aims of this project were to:

1. Evaluate the anti-MDR and cytotoxicity of novel compounds in MRP1 or P-gp expressing cell models.

2. Identify a panel of MDR modulators that down-regulate the expression of MDR proteins while targeting other important signalling pathways and oncoproteins. To determine whether these agents cause the greatest anti-cancer effects in concurrent combination with traditional chemotherapeutic drugs or as a pre-treatment to the chemotherapeutic drugs.

3. Investigate the role of serum transport proteins, serum albumin and α_1-acid glycoprotein, may play in the availability and thus efficacy of epirubicin in normal versus cancer cells.

Focusing on two types of small molecule agents that modulate multidrug resistance:

4. Characterise the ability of three tyrosine kinase inhibitors (lapatinib, erlotinib and gefitinib) to sensitise EGFR/HER2-amplified breast cancer cell models and multidrug resistant cell lines to the chemotherapeutic drugs.

5. Determine the affect of lapatinib on COX-2 protein expression and activity.

6. Identify the relationship between the COX-2 inhibitor, celecoxib, and expression and function of multidrug resistant proteins.

Section 2.

Materials and Methods

2.1. Ultrapure water

Ultapure water (UHP) was used in the preparation of all media and solutions. This water was purified to a standard of 12-18 MΩ/cm resistance by a reverse osmosis system (Millipore Mill-RO 10 Plus, Elastat UHP).

2.2. Glassware

The solutions used in the various stages of cell culture were stored in sterile glass bottles. All sterile bottles and other glassware required for cell culture related applications were prepared as follows: glassware and lids were soaked in a 2% RBS-25 (AGB Scientific) for 1 hour. After this time, they were cleansed and washed in an industrial dishwasher, using Neodisher detergent and rinsed twice with UHP. The resulting materials were sterilised by autoclaving.

2.3. Sterilisation procedures

All thermostable solutions, water and glassware were sterilised by autoclaving at 121°C for 20 minutes at 15 p.s.i. Thermolabile solutions were filtered through 0.22 μm sterile filters (Millipore, Millex-GV SLGV025BS). Larger volumes (up to 10 litres) of thermolabile solutions were filter sterilised through a micro-culture bell filter (Gelman, 12158).

2.4. Preparation of cell culture media

Basal media used during cell culture was prepared as followed: 10X media was added to sterile UHP water, buffered with HEPES (N-(2-Hydroxyethyl) piperazine-N-(2-ethanesulfonic acid) and NaHCO$_3$ as required and adjusted through sterile 0.22μm bell filters (Gelman, 12158) and stored in sterile 500 ml bottles at 4°C. Sterility checks were performed on all bottles of media by inoculation of media samples on to Colombia blood agar (Oxoid, CM217), Sabauraud dextrose (Oxoid, CM217) and Thioglycolate broth (Oxoid, CM173). All sterility checks were then incubated at both

25°C and 37°C. These tests facilitated the detection of bacterial, yeast and fungal contamination. Basal media were stored at 4°C for up to three months. The HEPES buffer was prepared by dissolving 23.8 g of HEPES in 80 ml UHP water and this solution was then sterilised by autoclaving. Then 5 ml sterile 5 N NaOH was added to give a final volume autoclaving. Complete media was then prepared as follows: supplements of 2 mM l-glutamine (Gibco, 11140-0350) for all basal media and 1 ml 100X non-essential amino acids (Gibco, 11140-035) and 100 mM sodium pyruvate (Gibco, 11360-035) were added to MEM. Other components were added as described in Table 2.1. Complete media was stored at 4°C for a maximum of one month.

Sources of other types of media:

DMEM/Ham's F12 1:1 = represented by ATCC in this project and produced in house

RPMI-1640 (made in house)

McCoy5A (Lonza; 12-688F)

MEGM (Lonza; CC-3151 and CC-4136).

Table 2.4.1.: This table is a list of cell lines used during the life of this project. Including their basal media, percentage foetal calf serum and any additional requirements for growth.

Cell Line	Basel media	FBS (%)	Additions
DLKP	ATCC	5	None
DLKP-A	ATCC	5	None
A549	ATCC	5	None
A549-Taxol	ATCC	5	None
MDA-MB-453	RPMI-1640	10	None
MDA-MB-231	RPMI-1640	10	None
MCF7	RPMI-1640	10	None
NCI/Adr-res	RPMI-1640	10	None
BT20	RPMI-1640	10	None
HL60/s	RPMI (sigma;R8758)	10	None
HL60/adr	RPMI (sigma;R8758)	10	None
HL60/Mdr1	RPMI (sigma;R8758)	10	None
HL60/mxr	RPMI (sigma;R8758)	10	None
H1299	RPMI-1640	5	Sodium pyruvate
H1299-Taxol	RPMI-1640	5	Sodium pyruvate
2008/MRP1	RPMI-1640	10	None
M14	RPMI-1640	10	None
DLKP-SQ/mitox	ATCC	5	None
HMEC	MEGM	N/A	Lonza formula

2.5. Cells and cell culture

All cell culture work was carried out in a class II laminar airflow cabinet (Holten LaminAir). All experiments involving cytotoxic compounds were conducted in a cytoguard laminar airflow cabinet (Holten LaminAir Maxisafe). Before and after use the laminar airflow cabinet was cleaned with 70% industrial methylated spirits (IMS). Any items brought into the cabinet were also swabbed with IMS. Only one cell line was used in the laminar airflow cabinet at a time and upon completion of work with any given cell line the laminar airflow cabinet was allowed to clear for at least 15 minutes before use. This was to eliminate any possibility of cross-contamination between cell lines. The cabinets were cleaned weekly with industrial disinfectants (Virkon or TEGO). These disinfectants were alternated fortnightly. Details pertaining to the cell lines used for the experiments detailed in this thesis are provided in Table 2.5.1. All cells were incubated at 37°C with an atmosphere of 5% CO_2. Cell lines such

as, DLKP, DLKP-A, AsPC1, BxPC3 and HT1299-Taxol, did not have any CO_2 requirement. Cell were fed with fresh media or subcultured every 2-3 days in order to maintain active cell growth. All cell lines listed in Table 2.5.1. are anchorage dependent cell lines.

Table 2.5.1.: This table is a list of cell lines used during the life of this project, including the cancer type and where they were obtained.

Cell Line	Details	Source
DLKP	Non-small cell lung carcinoma (NSCLC)	NICB
DLKP-A	NSCLC, adriamycin-selected.	NICB [369]
DLKP-SQ/mitox	NSCLC, mitoxantrone-selected	NICB derived by Helena Joyce [unpublished]
A549	Lung	ECACC
A549-Taxol	Lung, paclitaxel-selected	ECACC derived by Dr. Laura Breen [370]
MDA-MB-453	Breast	ATCC
MDA-MB-231	Breast	ATCC
MCF7	breast	ATCC
NCI/Adr-res	Ovarian; Adriamycin-selected	NCI USA
HL60/S	Acute myeloid leukemia cells, non-MDR	ECACC
HL60/Adr	Acute myeloid leukemia cells, adriamycin-selected.	Melvin Center, Kansas State University [371]
HL60/Mdr1	Acute myeloid leukemia cells; Mdr1-transfected	Balazs Sarkadi, Hungary [371]
HL60/mxr	Acute myeloid leukemia cells; BCRP-transfected	Balazs Sarkadi, Hungary [372]
H1299-Taxol	Lung; paclitaxel-selected	NCTCC, derived by Dr. Laura Breen [370]
M14	Melanoma	NCI USA
2008/MRP1	Ovarian; MRP1-transfected	P. Borst, University Hospital, Amsterdam [373]
HMEC	Normal mammary	Lonza

2.5.1. Sub-culturing of cell lines

The cell culture medium was removed from the tissue culture flask and discarded into a sterile bottle. The flask was then rinsed out with 5 ml of PBS solution (Oxoid, BR14a) to ensure the removal of any residual media. Trypsin/EDTA solution (0.25% trypsin (Gibco, 043-05090), 0.01% EDTA (Sigma, E9884) solution in PBS (Oxoid, BRI4a)) was then added to the flask and was incubated at 37°C for the required period of time (dependant of each cell line) until all cells were detached from the inside surface of the tissue culture flask. The amount of trypsin used varies depending on flask size, i.e., 0.5 ml for T25cm^2, 1 ml for T75cm^2 and 2 - 4 ml for T175cm^2. The trypsin was deactivated by adding an equal volume of complete media to the flask. The cell suspension was removed from the flask and placed in a sterile universal container (Sterilin, 128a) and centrifuged at 160 x g for 3 minutes. The supernatant was then discarded from the universal and the pellet was suspended in complete medium. A cell count was performed. An aliquot of cells was then used to re-seed a flask at the required density, topping the flask up with fresh medium.

2.5.2. Assessment of cell number and viability

Cells were trypsinised, pelleted and resuspended in media. An aliquot of the cell suspension was then added to trypan blue (Gibco, 525) at a ratio of 5:1. The mixture was incubated for 3 minutes at room temperature. A 10μl aliquot of the mixture was then applied to the chamber of a glass coverslip enclosed haemocytometer. Cells in the 16 squares of the four grids of the chamber were counted. The average cell number, per 16 squares, was multiplied by a factor of 10^4 and the relevant dilution factor to determine the number of cells per ml in the original cell suspension. Non-viable cells stained blue, while viable cells excluded the trypan blue dye as their membrane remained intact, and remained unstained. On this basis, percentage viability was calculated.

2.5.3. Cryopreservation of cells

Cells for cryopreservation were harvested in the log phase of growth and counted as described in section (above). Cell pellets were resuspended in a suitable volume of FCS. An equal volume of a 10-20% DMSO/FCS solution was added dropwise to the cell suspension. A total volume of 1ml of this suspension was then placed in a cryovial (Greiner, 122278). These vials were then placed in the -20°C freezer for 20 minutes and then in the -80°C freezer overnight. Following this period the vials were removed from the -80°C freezer and transferred to the liquid nitrogen tanks for storage (-196°C).

2.5.4. Thawing of cryopreserved cells

A volume of 5 ml of fresh warmed growth media was added to a sterile universal. The cryopreserved cells were removed from the liquid nitrogen tank and thawed rapidly at 37°C. The cells were removed from the vials and transferred to the aliquoted media. The resulting cell suspension was centrifuged at 160 x g for 3 minutes. The supernatant was removed and the pellet resuspended in fresh culture medium. An assessment of cell viability on thawing was then carried out (see section: 2.5.2.). Thawed cells were then added to an appropriately sized tissue culture flask with a suitable volume of fresh growth media.

2.5.5. Monitoring of sterility of cell culture solutions

Sterility testing was performed on all cell culture media and related culturing solutions. Samples of prepared basal media were incubated at 37°C for a period of seven days. This ensured that no bacterial or fungal contamination was present in the media.

2.5.6. Serum Batch Testing

Batch to batch variation is a major problem associated with the use of FCS in cell culture. In extreme cases this variation may result in a lack of cell growth, whereas in more moderate cases growth may be retarded. To avoid the effects of the above variations, a range of FCS batches were screened for growth of each cell line. A suitable FCS batch was then purchased in bulk for a block of work with each particular cell line in use. Screening involved seeding cells into a 96 well plate and determining growth as a percentage of serum with known acceptance growth rate. Logarithmically growing cells were seeded into a 96 well plate (Costar; 3599) from a single cell suspension at a density of 10^3 cells/well in 100 µl of medium without FCS. 100 µl volumes of medium containing 10% or 20% FCS was added to respective wells on the 96 well plate, resulting in final dilutions of FCS to 5% or 10% respectively. The first column of each plate was maintained as a blank and the last column was maintained as a control where FCS resulting in known acceptance growth rate was used. Plates were placed at 37^oC in 5% CO_2, for 5 days, after which growth was assessed (see section: 2.7.2.).

2.6. Mycoplasma analysis of cell lines

Cell lines were tested for possible mycoplasma contamination in house by Mr. Michael Henry. The protocol is detailed in the following section.

2.6.1. Indirect staining procedure for Mycoplasma analysis.

Mycoplasma-negative NRK (Normal rat kidney fibroblast) cells were used as indicator cells for this analysis. The cells were incubated with a sample volume of supernatant from the cell lines in question and the examined for *mycoplasma* contamination. A fluorescent Hoechst stain was used in the analysis. The stain binds specifically to DNA and so stains the nucleus of the cells in addition to any *mycoplasma* present. *Mycoplasma* infection was indicated by fluorescent bodies in the cytoplasm of the NRK cells.

2.7. *In vitro* proliferation assays

Adherent cells in the exponential phase were harvested by trypsinisation as described in Section: 2.5.1. Cell suspensions containing 1×10^4 cell/ml were prepared in cell culture medium. Volumes of 100 µl/well of these cell suspensions were added to 96-well plates (Costar; 3599) using a multichannel pipette. Plates were agitated gently in order to ensure even dispersion of cells over a given well. Cells were then incubated overnight at 37^oC in an atmosphere containing 5% CO_2. Cytotoxic drug dilutions were prepared at 2X their final concentration in cell culture medium. Volumes of the drug dilutions (100 µl) were then added to each well using a multichannel pipette. Plates were then mixed gently as above. Cells were incubated for a further 6-7 days at 37^oC and 5% CO_2 until the control wells had reached approximately 80-90% confluency. Assessment of cell survival in the presence of drug was determined by the acid phosphatase assay (see section: 2.7.2.). The concentration of each drug which caused 50% cell kill (IC_{50} for that drug) was determined from a plot of the percentage cell proliferation (relative to the control cells) versus cytotoxic drug concentration using Calcusyn software.

2.7.1. Combination proliferation assays

Cells were harvested in the exponential phase of growth as described in Section: 2.5.1. The 96-well plates were seeded as described above and incubated overnight at 37^oC with 5% CO_2. Dilutions of cytotoxic drugs and other agents were prepared at 4X their final concentration in media. Volumes of 50 µl of the drug dilution and 50 µl of the combination drug dilution were then added to each relevant well so that each well had a final volume of 200 µl. All potential toxicity-enhancing agents were dissolved in DMSO, ethanol or media. Stock solutions were prepared at approximately 15 mg / 10 ml media; filter sterilised with a 0.22 µm filter (Millex-GV, SLGV025BS) and then used to prepare all subsequent dilutions. Cells were incubated for a further 6-7 days at 37^oC in an atmosphere of 5% CO_2. At this point the control wells would have reached approximately 80-90% confluency. Cell number was assessed using acid phosphatase assay (section: 2.7.3.).

2.7.2. Scheduled/pre-treated proliferation assays

Cells were harvested in the exponential phase of growth as described in Section: 2.5.1. The 96-well plates were seeded as described above and incubated overnight at 37°C with 5% CO_2. Dilutions of test agents were prepared at 2X their final concentration in media. Volumes of 100 µl of the agent dilution was added to each relevant well so that each well had a final volume of 200 µl. All potential toxicity-enhancing agents were dissolved in DMSO, ethanol or media. Stock solutions were prepared at approximately 15 mg / 10 ml media; filter sterilised with a 0.22 µm filter (Millex-GV, SLGV025BS) and then used to prepare all subsequent dilutions. Cells were incubated for 24 hours at 37°C in an atmosphere of 5% CO_2. At this point all media was removed from each well using a 12-channel multichannel pipette and 100 µl of warmed fresh media was added to each well. A 2X toxicity curve of the chemotherapeutic drug was prepared and 100 µl of each concentration was added to the appropriate wells. The plates were incubated at 37°C for 4 days. At this point the control wells would have reached approximately 80-90% confluency. Cell number was assessed using acid phosphatase assay (section: 2.7.3.).

2.7.3. Assessment of cell proliferation by the acid phosphatase assay

Following the incubation period of 6-7 days, media was removed from the plates. Each well was washed twice with 100 µl PBS. This was then removed and 100 µl of freshly prepared phosphatase substrate (10 mM p-nitrophenol phosphate (Sigma; 104-0) in 0.1 M sodium acetate (pH 5.5) (Sigma; S8625), 0.1%% triton X-100 (BDH; 30632)) was added to each well. The plates were then incubated in the dark at 37°C for 2 hours. The enzymatic reaction was stopped by the addition of 50 µl of 1 N NaOH. The plate was read in a dual beam plate reader (spectrophotometer, Synergy HT, Bio-Tek, USA) at 450 nm with a reference wavelength of 620 nm.

2.8. Safe handling of cytotoxic drugs

Cytotoxic drugs were handled with extreme caution at all times in the laboratory, due to the potential risks in handling them. Disposable nitrile gloves (Medical Supply Company Ltd) were worn at all times and all work was carried out in cytotoxic cabinets (Holten LaminAir Maxisafe). All drugs were stored in a safety cabinet at room temperature or in designated areas at 4°C. The storage and means of disposal of the cytotoxic drugs used in this work are outlined in Table 2.8.1.

Table 2.8.1.: This table contains a list of chemotherapeutic drugs and other drugs used in this project. All drugs were disposed of by incineration.

Cytotoxic Agent	Storage of liquid stock
Adriamycin	4°C in dark
Epirubicin	4°C in dark
Paclitaxel	Room temperature in the dark
Docetaxel	Room temperature in the dark
5-Fluorouracil	Room temperature in the dark
SN-38	-20°C
Vincristine	Room temperature in the dark
Vinblastine	Room temperature in the dark
Cisplatin	Room temperature in the dark
Celecoxib	4°C
Sulindac sulfide	4°C
Valdecoxib	Room temperature
Rofecoxib	Room temperature
Lapatinib	Room temperature in the dark
Elacridar/ GF	4°C
Tarceva/ Erlotinib	Room temperature in the dark
Iressa/Gefitinib	Room temperature in the dark

2.9. Safe handling and stock make-up of all novel compounds

All compounds were handled with extreme caution at all times in the laboratory, due to the potential risks of the unknown agents. Disposable nitrile gloves (Medical Supply Company Ltd) were worn at all times and all work was carried out in cytotoxic cabinets (Holten LaminAir Maxisafe).

All compounds were weighed in a fume hood and dissolved in media, DMSO or ethanol depending on their solubility. All compounds dissolved in media or ethanols

were stored in a safety cabinet at room temperature. All compounds in the DMSO suspension were stored in designated areas at 4°C. The storage and means of disposal of the non-characterised agents used in this work are outlined in Table 2.9.1.

Table 2.9.1.: A list of the novel chemistry compounds entered into the biological testing panel. The molecular weight (M.W.), solvent they were dissolved in, solubility, and storage. All drugs were disposed of by incineration.

Novel Compound	M.W. (g)	Vehicle	Solubility in Culture media with vehicle	Stock storage
PA1	464	DMSO	Soluble	-20°C
PA2	565	DMSO	Soluble	-20°C
PA3	202	DMSO	Not soluble	-20°C
PA4	218	Water	Soluble	-20°C
PA5	356	DMSO	Soluble	-20°C
PA6	272	DMSO	Soluble	-20°C
RF1	274	DMSO	Soluble	4°C
RF2	314	DMSO	Soluble	4°C
RF3	232	DMSO	Soluble	4°C
RF4	272	DMSO	Soluble	4°C
BM1	324	DMSO/Ethanol (50:50)	Not soluble	20°C
BM2	324	DMSO/Ethanol (50:50)	Soluble	20°C
BM3	306	DMSO/Ethanol (50:50)	Not soluble	20°C
BM4	306	DMSO/Ethanol (50:50)	Not soluble	20°C
BM5	444	DMSO/Ethanol (50:50)	Not soluble	20°C
RBM2	225	DMSO/Ethanol (50:50)	Soluble	20°C
RBM3	261	DMSO/Ethanol (50:50)	Not soluble	20°C
RBM4	231	DMSO/Ethanol (50:50)	Not soluble	20°C
RBM5	261	DMSO/Ethanol (50:50)	Not soluble	20°C
RBM6	231	DMSO	Soluble	20°C
RBM7	302	DMSO	Soluble	20°C
RBM8	344	DMSO	Soluble	20°C
RBM9	288	DMSO	Appeared soluble but may have had impurities	20°C
RBM10	233	DMSO	Soluble	20°C
RBM11	388	DMSO/Ethanol (50:50) & salts	Insoluble	20°C
RBM12	228	DMSO	Soluble	20°C

Novel Compound	M.W. (g)	Vehicle	Solubility in Culture media	Storage
RBM13	273	DMSO	Soluble	20°C
RBM14	312	DMSO	Soluble	20°C
RBM15	420	DMSO	Soluble	20°C
RBM16	288	Water	Soluble	20°C
RBM17	342	Water	Soluble	20°C
KG1	568	DMSO	Soluble, limitations	4°C
KG2	568	DMSO	Soluble, limitations	4°C
KG3	504	DMSO	Soluble	4°C
KG4	500	Ethanol	Soluble	4°C
KG5	568	DMSO	Soluble, limitations	4°C
KG6	568	DMSO	Soluble, limitations	4°C
KG100	170	Ethanol	Soluble	4°C
KG101	142	Water	Soluble	4°C
KG102	288	Water	Soluble	4°C
KG103	446	Ethanol	Soluble	4°C
KG104	446	Ethanol	Soluble	4°C
KG105	386	Ethanol	Soluble	4°C
KG200	162	N/A	Soluble	4°C
KG201	210	N/A	Soluble	4°C
KG202	258	N/A	Soluble	4°C
KG203	305	N/A	Soluble	4°C
KG204	240	N/A	Soluble	4°C
KG205	296	Water	Insoluble	4°C
KG206	344	Water	Soluble	4°C
KG207	400	Water & Salt	Insoluble	4°C
KG401	418	Ethanol	Not soluble	4°C
KG402	466	Ethanol	Soluble	4°C
KG403	457	Ethanol	Not soluble	4°C
KG404	458	Ethanol	Not soluble	4°C
KG405	459	Ethanol	Soluble	4°C
KG406	455	Ethanol	Soluble	4°C
KG408	418	Ethanol	Soluble, limitations	4°C
KG411	457	Ethanol	Soluble, limitations	4°C
KG413	455	Ethanol	Soluble	4°C
Titanocene Y	482	Provided in solution	Soluble	4°C

N/A: not applicable as the compounds are glycols and received in liquid form.

2.10. Chemistry compound screening

2.10.1. Compound solubilisation

Test compound (2 mg) was weighed out in a cryovial using the fine balance. DMSO, ethanol or water (1 ml) was added and the cryovial was shaken vigorously. The vial was then sonicated at 37°C for 1 hour.

If the compound was dissolved at this stage it was tested for its solubility in cell culture complete media (10 µl of the test solution in 40 µl of complete media or a dilution to make up 100 µM was carried out).

If the compound was found not to be soluble in media or if it didn't fully dissolve following sonication then another ml of DMSO, ethanol or water was added and the procedure was repeated.

Some compounds could not be fully dissolved and hence were not tested.

2.10.2. Compound combination proliferations with MDR substrates

The 96-well plates were prepared as described in section 2.7.1. Each novel compound was diluted to concentrations of 5 µM, 25 µM, and 50 µM. The first double combination to be carried out was with epirubicin and if an interesting result was found the double combinations was repeated with docetaxel and 5FU.

The plates were incubated for a further 6 days, at which time the acid phosphatase assay (see section 2.7.2.) was carried out in order to determine the cell density.

Results from this method gave information on the compounds short term stability in culture conditions, of its general toxicity and whether a synergistic combination with epirubicin was possible on either the DLKP or DLKP-A cell lines.

2.11. Protein investigations

2.11.1. Protein extraction

The tissue culture 10 mm^2 petri-dishes were seeded with $1x10^5$ cells in 10 mls of fresh complete media. The cells were allowed to grow at 37°C with 5% CO_5 until an 80% confluency was achieved. Media was removed and the petri dish was rinsed twice with cold PBS. Cold RIPA buffer (500 µl, Sigma; R0278) with 5µl 10X Protease Inhibitors (Sigma; P2714) and 50 µl 200 mM PMSF (348 mg in 10 ml 100% ethanol) was added to the cells and incubated on ice for 20 minutes. Following this period the lysed cells were removed, using a cell scraper, and transferred to a sterile eppendorf. The sample was passed through a 21-gauge needle (with a 1ml syringe) to shear and then centrifuged at 16100 x g for 5 minutes at 4°C. The supernatant was transferred to a new sterile eppendorf and stored at -20°C.

2.11.2. Protein quantification by bicinchoninic acid protein assay

The protein samples were diluted by 1 in 10 in cold PBS. Diluted sample (of 25 µl each) was added to the 96 well plate (in duplicate). Part A and part B of the bicinchoninic acid (BCA) kit (Pierce; # 23225) were mixed (1:50) when the 96 well plate was fully loaded. 200 µl of the part A/B mixture was added to each well. The plate was covered with tin-foil to block out the light and incubated for 20 mins at 37°C. The plate was gently swirled to ensure even mixture before reading on the plate reader. The protein concentrations were calculated on the plate reading using software.

2.11.3. Gel Electrophoresis

Proteins for Western blotting analysis were resolved using Sodium Dodecyl Sulphate-Polyacrylamide Gel Eletrophoresis (SDS-PAGE) gel electrophoresis (SDS-PAGE). The stacking and resolving gels were prepared as illustrated in Table 2.11.3.1. The gels were set in clean 9 cm x 8 cm gel cassettes, which consisted of 2 glass plates separated by a rubber gasket to a width of 1 mm. The resolving gel was added to the

gel cassette and allowed to set. Once the resolving gel had set, the stacking gel was poured on top. A comb was placed into the stacking gel after pouring, in order to create wells for sample loading (maximum sample loading volume of 20 µl for a 12 well gel and 25-30 µl for a 10 well gel). Some pre-gels were also purchased from Lonza (7.5% PAGEr gels, 12well, # 58501)

Table 2.11.3.1.: Preparation protocol for SDS-PAGE gels (2 x 0.75 mm gels)

Components		7.5% Gel	10% Gel	5% Stacking Gel
Acrylamide/bis-acrylamide solution (Sigma A-3574)	30%	3.8 ml	5.07 ml	840 µl
Ultrapure water		7.3 ml	5.94 ml	2.84 ml
1.5 M Tris-HCL pH 8.8		3.75 ml	3.75 ml	-
0.5 M Tris-HCL pH 6.8		-	-	1.25 ml
SDS solution 10% (w/v)		150 µl	150 µl	50 µl
Ammonium persulphate solution (Sigma A-3678)	10%	60 µl	60 µl	20 µl
TEMED (Sigma T-9281)		10 µl	10 µl	5 µl

In advance of samples being loaded into the relevant samples wells, 8-40µg of protein was diluted in 5X loading buffer and stored on ice. Molecular weight markers (Lonza; Prosieve color protein marker, # 50550) were loaded alongside the samples. The gels were run at 250V and 20mA (per gel) until the bromophenol blue dye front reached the end of the gel, at which time sufficient resolution of the molecular weight markers was achieved.

2.11.4. Western Blotting

Western blotting was performed by the method of Towbin H., *et al.* [374]. Once electrophoresis had been completed, the SDS-PAGE gel was equilibrated in transfer buffer (25mM Tris (Sigma; T8404), 192 mM gylcine (Sigma; G7126), pH 8.3-8.5) for approximately 15 minutes. Ten sheets of Whatman 3 mm filter paper and a nitrocellulose membrane (GE Healthcare; cat #: RPN303 2D) were soaked in freshly prepared transfer buffer for up to 15 minutes. Five of the filter papers were placed on top of each other on the plate of a semi-dry blotting apparatus (Bio-rad) followed by the nitrocellulose membrane and the air bubbles were removed. The SDS-PAGE gel was then placed on top and the air bubbles were removed again. Finally the last five

sheets of wetted filter paper were placed on top and air bubbles were removed. The proteins were transferred from the gel to the membrane at a current of 300 mA at 15 V for 60 - 75 minutes, until all colour markers had transferred.

Membranes were blocked for 2 hours with 5% blocking agent in PBS. Then they were treated with primary antibody overnight at 4°C. All antibodies were prepared in 3% blocking powder in PBS and are listed in Table 2.11.4.1. Primary antibody was removed after this period and the membranes were rinsed 3 times with PBS containing 0.5% Tween 20 (Sigma; P1379) for a total 15 - 30 minutes.

The secondary antibody (anti-mouse IgG, Sigma; A6782, used 1:1000) was then added for 1 - 1.5 hours at room temperature. The membranes were washed thoroughly in PBS containing 0.5% Tween for 15 minutes and finally washed in PBS for another 5 minutes.

Table 2.11.4.1.: Primary antibodies, including the company they were purchased from and the dilution used for probing.

Primary Antibody	Company	Catalogue #	Dilution
P-glycoprotein	Alexis	ALX-801-002-C100	1:250
MRP1	Santa Cruz	Sc-18835	1:100
BCRP	Alexis	ALX-801-029-C250	1:250
COX-1	Santa Cruz	Sc-52971	1:500
COX-2	Santa Cruz	Sc-19999	1:500

2.11.5. Enhanced chemiluminescence (ECL) detection

Immunoblots were developed using an Enhanced Chemiluminescence kit (Amersham, RPN2109), which facilitated the detection of bound peroxidase-conjugated secondary antibody. Following the final washing membranes were subjected to ECL. A volume of 2 ml of a 50:50 mixture of ECL reagents was used to cover the membrane. The ECL reagent mixture was removed after a period of one minute and the membrane placed between two plastic sheets, air bubbles were carefully removed. The membrane was then exposed to autoradiographic (Kodak, X-OMATS) for various

times (from 10 seconds to 10 minutes depending on the signal). The exposed autoradiographic film was developed in developer (Kodak; LX-24). The film was then briefly washed in water and transferred to a fixative (Kodak; FX-40) until clear. After another 5-10 minute wash in water, the film was left to dry at room temperature.

2.11.6. ELISAs

Samples were extracted and quantified as in Section 2.11.1. and 2.11.2. EGFR, pEGFR, HER2 and pHER2 levels were examined using developmental sandwich ELISA assay kits, DYC1854, DYC1095, DYC1129 and DYC1768 were purchased from R&D systems.

2.11.6.1. EGFR and HER2

The capture antibody was diluted to a working concentration of 0.8 μg/ml (EGFR) and 4.0 μg/ml (HER2) with PBS. The 96-well plates were coated with 100 μl of the diluted capture antibody. The plate was sealed and incubated overnight at room temperature. The capture antibody was aspirated vigorously and washed three times with wash buffer (0.05% Tween 20 in PBS, pH 7.2 − 7.4). The plate was blotted dry on clean paper towel then blocked for 1 − 2 hours at room temperature by adding 300 μl of block buffer (1% BSA, 0.05% NaN$_3$ in PBS, pH 7.2 − 7.4). The plate was aspirated and washed three times with wash buffer. A volume of 100 μl of each sample or standard, diluted in Diluent #12 (1% NP-40, 20 mM Tris (pH 8.0), 137 mM NaCl, 10% glycerol, 2 mM EDTA, 1mM activated sodium orthovanadate), was added to each well, sealed and incubated at room temperature for 2 hours. The plates were aspirated and washed three times with wash buffer. A volume of 100 μl of the diluted detection antibody (200 ng/ml) was added to each well, sealed and incubated for 2 hours at room temperature. The plates were aspirated and washed three times with wash buffer. The plates were incubated in darkness for 20 minutes at room temperature in the presence of 100 μl diluted Streptavidin-HRP (diluted in Diluent #14: 20 mM Tris, 137 mM NaCl, 0.05% Tween 20, 0.1% BSA, pH 7.2- 7.4). The plates were aspirated and washed three times. Substrate solution (100 μl) was added to each well and incubated in the dark for 20 minutes at room temperature. Stop

solution (50 µl) was added to each well. To mix, the plate was gently tapped. The plate was read at a wavelength of 450 nm.

2.11.6.2. Phospho-EGFR and Phospho-HER2

The capture antibody was diluted to a working concentration of 0.8 µg/ml (EGFR) and 4.0 µg/ml (HER2) with PBS. The 96-well plates were coated with 100 µl of the diluted capture antibody. The plate was sealed and incubated overnight at room temperature. The capture antibody was aspirated vigorously and washed three times with wash buffer (0.05% Tween 20 in PBS, pH 7.2 − 7.4). The plate was blotted dry on clean paper towel then blocked for 1 − 2 hours at room temperature by adding 300 µl of block buffer (1% BSA, 0.05% NaN_3 in PBS, pH 7.2 − 7.4). The plate was aspirated and washed three times with wash buffer. A volume of 100 µl of each sample or standard, diluted in Diluent #12 (1% NP-40, 20 mM Tris (pH 8.0), 137 mM NaCl, 10% glycerol, 2 mM EDTA, 1mM activated sodium orthovanadate), was added to each well, sealed and incubated at room temperature for 2 hours. The plates were aspirated and washed three times with wash buffer. A volume of 100 µl of the diluted detection antibody (200 ng/ml) was added to each well, sealed and incubated for 2 hours at room temperature. The plates were aspirated and washed three times with wash buffer. 100 µl of substrate solution was added to each well and incubated in the dark for 20 minutes at room temperature. 50 µl of stop solution was added to each well. To mix, the plate was gently tapped. The plate was read at a wavelength of 450 nm.

2.12. Pharmacokinetics studies

2.12.1. Determination of free versus protein-bound epirubicin

An aliquot of 1 ml of foetal calf serum, serum albumin or AAG was prepared and epirubicin was added to make a 2 µM solution. This solution was placed above the cellulose triacetate ultrafiltration membrane of the 20,000 Da Vivaspin 2 units (Sartorius; Cat #: VS02X1). The samples were centrifuged at 3200 x g for 20 minutes. The volume of the filtrate (filtered solution) was measured using a P1000 pipette and

made up to 1 ml. The remaining solution above the membrane was removed and the membrane was rinsed once with PBS. The final volume of solution above the membrane and the PBS containing the cake (protein/drug remaining on the surface of the membrane) was 1 ml. Samples were stored at -4°C for a maximum of 2 weeks. 200 µl of each sample was extracted (see section 2.12.3.) and the quantity of epirubicin that was protein bound or free was determined using LC-MS analysis (see table 2.12.5.1 for mass spectroscopy parameters).

Calculations:

Formula 1: Amount of protein-free drug bound to the membrane.
Membrane (ng) = Total (ng) – (retentate (ng) + filtrate (ng))

Formula 2: Percentage of protein-free drug.
Free (%) = Filtrate (ng) + membrane (ng) × 100
$\qquad$ Total (ng)

Formula 3: Percentage of drug bound to protein.
Bound (%) = retentate (ng) × 100
$\qquad$ Total (ng)

2.12.2. Cell Preparation

Vented T25 flasks were seeded with 5 mls of 3 x 10^4 cells/ml cell suspension and incubated at 37°C overnight to allow cells attach.

2.12.2.1. Accumulation assay:

Method as published by Wall R., *et al*. [339]. Cells were exposed to 2 µM epirubicin or 2.5 µM celecoxib, made-up in ATCC media containing 5% FCS, for 2 hours at 37°C. After 2 hours the media containing drug was removed and the cells were rinsed with sterile PBS. The cells were trypsinised and placed in extraction tubes. They were spun

for 3 minutes at 160 x g. The supernatant was removed and 1 ml of PBS was added. The cells were counted using the procedure described in section: 2.5.2 and the remaining cell suspension was centrifuged at 160 x g for a further 3 minutes. The supernatant was removed and the cell pellets were frozen for a maximum period of 2 weeks.

2.12.2.2. Efflux assay [339]:

Method as published by Wall R., *et a*l. [339]. Cells were exposed to 2 μM epirubicin or 10 μM celecoxib, made-up in ATCC media containing 5% FCS, for 3 hours. After 3 hours the media containing drug was removed, the cells were rinsed with warmed media and replaced with 5 mls of warmed media. At times 0, 30, 60, and 120 minutes cell pellets were prepared as described in section 2.12.2.1.

2.12.3. Anthracycline cell-drug extraction procedure:

2.12.3.1. Standards and solutions

Method as published by Wall R., *et a*l. [339]. Epirubicin (2 mg/ml) was purchased from Pfizer, Cambridge, MO, USA. The internal standard for epirubicin was daunorubicin (2 mg/ml). This was diluted to 1 μg/ml in MS grade water and protected from direct light prior to epirubicin extraction. For safe handling of all cytotoxic drugs see section (2.8).

2.12.3.2. Extraction procedure

Method as published by Wall R., *et a*l. [339]. The frozen cell pellets were thawed in the dark. The pellets were resuspended in 200 μl MS grade water. Then 20 μl of 33% silver nitrate was added and the sample was vortexed. 200 μl of the internal standard, daunorubicin, was added, followed by 700 μl ice cold isopropanol, 100 μl ammonium formate buffer. This mixture was mixed well before 1400 μl chloroform was added

using a glass pipette. The extraction tubes were mixed using a Stuart Scientific (UK) blood mixer for 5 minutes, and then they were centrifuged for 5 minutes at 3200 x g (Thermo (Ireland)). The bottom organic layer (1.1 ml) was removed and placed in a glass vial. The vials were evaporated to dryness using a Genevac EZ-2 (Ipswich, UK) evaporator at ambient temperature, without light. The samples were reconstituted in 30 µl of mobile phase with 20 µl injected automatically by the autosampler.

The standard curve was prepared in the same manner as the cell pellets. A broad range of standards (10 ng/ml, 30, 50, 100, 300, 500 and 1000 ng/ml or 10, 50, 100, 500, 1000, 3000, 5000 ng/ml) was prepared in MS grade water.

2.12.3.3. Mobile phase preparation

Method as published by Wall R., *et a*l. [339]. To 720 ml of MS grade water, 720 µl of formic acid was added using a starpette. (Performed in a fume cupboard). The pH, which was about 2.5, was very carefully brought up to pH 3.2 using concentrated ammonium formate (300 mg/ml, made up in MS grade water). Finally, 280 mls of MS grade acetonitrile was added and the bottle was gently shaken to mix.

2.12.4. Celecoxib cell-drug extraction procedure

2.12.4.1. Standards and solutions

Celecoxib, valdecoxib and rofecoxib were purchased from Sequoia (UK). Prior to drug-cell extraction primary stocks of 0.5 mg/ml rofecoxib, valdecoxib and celecoxib were prepared in acetonitrile. A primary stock of 7.6 mg/ml celecoxib was prepared in DMSO for use in the accumulation and efflux assays. All coxibs were stored at room temperature until use.

2.12.4.2. Extraction procedure

The frozen cell pellets were thawed and resuspend pellet 200 µl MS grade water. An aliquot of 50 µl of rofecoxib or valdecoxib internal standard and 50 µl 0.01M ammonium formate pH 5 buffer was added. Finally, 1400 µl chloroform was added using a glass pipette. The extraction tubes containing the mixture was inverted on a Stuart Scientific (UK) blood mixer for 5 minutes and then centrifuged for 5 minutes at 3200 x g (Thermo (Ireland)). The bottom organic layer was removed (1.1 ml) and placed in a glass vial. The vials were evaporated to dryness using a Genevac EZ-2 (Ipswich, UK) evaporator at ambient temperature, without light. The samples were reconstituted in 30 µl of mobile phase with 20 µl injected automatically by the autosampler.

The celecoxib standard curve was prepared in the same manner as the cell pellets. A broad range of standards (10 ng/ml, 30, 50, 100, 300, 500, 1000 and 2000 ng/ml) was prepared in MS grade water.

2.12.4.3. Mobile phase preparation

The pH of 350 ml 0.01 M formate buffer was reduced to pH 5.0 and 650 mls of acetonitrile was added. The mobile was gently shaken and allowed to settle. The method used for triplequad mass spectroscopy determination is modified from Satyanarayana U., *et al.* [375].

2.12.5. LC-MS (QQQ) analysis

For all drugs, chromatographic separation was achieved using a Prodigy reverse phase column (5u ODS3 100A, 150 × 4.60mm, 5 µm) from Phenomemex, UK. The mobile phase used per drug is described above (sections 2.12.3.3. and 2.12.4.3.). The mass spectrometer was operated using an ESI source in the positive ion detection mode. The ionisation temperature was 350°C, gas flow rate was 16 L/min and nebulizer pressure was 50 psi. Nitrogen was used as the ionisation source gas and ultrapure nitrogen as the collision cell gas. Quantification was based on the integrated peak area as determined by the Masshunter Quantification Analysis software which quantitates the peak areas of the MRM transitions of each analyte. The conditions for ideal separation of each drugs is listed in table (2.12.5.1.) below.

Table 2.12.5.1.: The mobile phase, flowrate, column and autosampler temperatures, retention times and MRM transitions for the anthracyclines and NSAID's (coxibs).

	Epirubicin	Daunorubicin	Valdecoxib	Rofecoxib	Celecoxib
Mobile phase (0.01M formic)	28% ACN, pH 3.2	28% ACN, pH 3.2	65% ACN, pH 5.0	65% ACN, pH 5.0	65% ACN, pH 5.0
Flowrate (ml/min)	0.25	0.25	0.2	0.2	0.2
Column temperature (^{o}C)	45	45	20	20	20
Autosampler temperature (^{o}C)	4	4	4	4	4
Retention time (mins)	9.5 ± 0.5	4.5 ± 0.5	3 ± 0.5	3.5 ± 0.5	6.5 ± 0.5
MRM transition (m/z)	$544 \rightarrow 397$	$528 \rightarrow 321$	$315 \rightarrow 192$	$315 \rightarrow 132$	$382 \rightarrow 362$

2.13. Determination of COX activity

Cyclooxygenase (COX, also called Prostaglandin H Synthase or PGHS) is a bifunctional enzyme exhibiting both COX and peroxidase activities. The COX component converts arachidonic acid to a hydroperoxy endoperoxide (PGG_2), and the peroxidase component reduces the endoperoxide to the corresponding alcohol (PGH_2), the precursor of PGs, thromboxanes, and prostacyclins.[1,2] It is now well established that there are two distinct isoforms of COX, namely COX-1 and COX-2. Cayman's COX Fluorescent Activity Assay provides a convenient fluorescence-based method for detecting COX-1 or COX-2 activity in both crude (cell lysates/tissue homogenates) and purified enzyme preparations. The assay utilizes the peroxidase component of COXs. In this assay, the reaction between PGG_2 and ADHP (10-acetyl-3,7-dihydroxyphenoxazine) produces the highly fluorescent compound resorufin that can be analyzed using an excitation wavelength of 530-540 nm and an emission wavelength of 585-595 nm. The kit includes isozyme-specific inhibitors for distinguishing COX-2 activity from COX-1 activity. As described in the kit booklet (Cayman; COX fluorescent activity assay kit, Cat #: 700200).

2.13.1. Lysate preparation

Cells grown in 90mm tissue culture petri-dishes were collected using a cell scraper when confluency had reached about 90%. The cells, suspended in PBS, were counted and then centrifuged at $1,000 \times g$ for 10 minutes at $4^{o}C$. The supernatent was removed and the appropriate volume of cold buffer (100 mM Tris-HCl, pH 7.5 containing protease inhibitors) was added to provide a cell suspension containing about 1×10^{7} cells/ml. The sample was pulsed 20 times using a sonicator and spun at $10,000 \times g$ for 15 minutes at $4^{o}C$. The supernatant was removed and stored on ice if performing the assay on that day. Otherwise, the sample was stored at $-80^{o}C$ (stable for up to one month).

2.13.2. Standard curve set-up

A standard curve was carried out in order to obtain the optimum GAIN (optimal fluorescent detector setting) for the assay on that day. A volume of 20 µl was removed from the resorufin vial (provided in the kit) and diluted with 1.98 ml diluted assay buffer. Following a 1 minute incubation the plate was analysed using a fluorometer (Bio-tek, Synergy HT from Mason technologies using KC4 software) with an excitation wavelength of 530-540 nm and an emission wavelength of 585-595 nm The curve was prepared are described in table 2.13.2.1 below.

Table 2.13.2.1.: The preparation of the resorufin standard curve.

Tube	Resorufin stock (µl)	Assay buffer (µl)	Final concentration (µM)
A	0	1,000	0
B	10	990	0.1
C	20	980	0.2
D	40	960	0.4
E	80	920	0.8
F	120	880	1.2
G	160	840	1.6
H	200	800	2

2.13.3. COX activity assay procedure:

This assay was performed according to the assay kit instruction (Cayman; COX fluorescent activity assay kit, Cat #: 700200). All samples were tested in duplicate wells. Each constituent of the assay was prepared as outlined in the manual provided with the assay kit.

1.   Standard wells – 180 µl of assay buffer was added to 10 ul of each resuforin standard, and read at excitation wavelength 530 – 540 and emission wavelength 585 – 595 after 5 minutes. The optimum GAIN was determined by setting the sensitivity to 'auto' and 'scale to highest wells'.

2. COX positive control wells – 150 µl of the assay buffer was added to 10 ul heme, 10 µl fluorescent substrate and 10 µl sample.

3. Sample wells – 160 µl of assay buffer was added to 10 µl heme, 10 µl fluorescent substrate and 10 µl sample.

4. Sample background wells – 160 µl of assay buffer was added to 10 µl heme, 10 µl fluorescent substrate and 10 µl sample.

5. Inhibitor wells – 140 µl of assay buffer was added to 10 µl heme, 10 µl fluorescent substrate, 10 µl sample and 10 µl of either DuP-697 or SC-560.

6. The reaction was initiated, only in the COX positive, sample and inhibitor wells, by adding 10 µl of Arachidonic acid solution.

7. The plate was read after one minute using the same excitation and emission wavelengths as the standard curve and the GAIN determined by the standard curve.

2.13.4. Calculating COX activity

The average fluorescence for each standard was calculated and the zero value was subtracted from each standard. Using excel, resorufin (µM) (x-axis) versus fluorescence (relative units) (y-axis) graph was plotted, a trendline and equation of the curve was added.

The average fluorescence for each sample was calculated and the background was subtracted. Using the equation of the curve from the standard curve the fluorophore concentration (µM) was calculated for each sample. To calculate the COX activity (nmol/min/ml) the follow equation was used:

$$\text{COX activity (nmol/min/}10^7 \text{ cells)} = \left[\frac{\mu M}{\text{Minute}}\right] \times \text{Sample dilution}$$

Note: At $22^{\circ}C$, one unit of enzyme causes the formation of 1 nmol of fluorophore per minute.

2.14. Statistical Analysis

Experimental *in vitro* data are presented as a mean ± standard deviations from three independent experiments, unless otherwise specified. For combination proliferation data where the three variables (i.e. drug 1, drug 2 and drug1 and 2 combined) had to statistically evaluated the difference in percentage proliferation between drug 1 and drug 2 (array 1) was paired against the difference between drug 1 and drug 1 and 2 (array 2). Levels of significance from these data were calculated using student's *t* test (two-tailed) (Excel ®, Microsoft). A p-value of less than 0.05 was considered significant in all statistical testing.

Section 3.

Results

3.1. Screening of potential novel anti-cancer agents

Multidrug resistance (MDR) proteins are expressed in a wide variety of tissue types, including, liver [42], gastrointestinal tract [35] and blood brain barrier, and help regulate the influx and efflux of substances required for normal cellular functioning [38] [39]. However, long-term treatment with chemotherapeutic drugs can lead to the over-expression of the MDR proteins and the development of the MDR phenotype. This phenotype and enhanced expression can be a major cause of treatment failure for traditional and modern anti-cancer drugs that are effluxed by MDR transporter proteins.

The search for agents that overcome this phenotype has been investigated for at least 30 years. An extensive range of MDR modulators has been identified (listed in tables 1.4.2.1, 1.4.3.1., 1.4.4.1, and 3.1.6.1.) and some of these have reached phase III of clinical trials [291] [180] [376]. However, the lack of improvement in outcome [291] [180] [376] and increased toxicity associated with the use of these agents [291] has hampered their entry into common clinical use.

In this project, we investigated a broad range of novel compounds designed and synthesised in the NICB (sixty compounds) and Conway institute (Dublin) (one compound) as well as some agents currently undergoing or entering clinical trial. These agents were tested by a quick screen for their potential as P-gp and MRP1 inhibitors and if an agent overcame resistance, further analysis took place. The *in vitro* models chosen for investigating this potential were DLKP and DLKP-A. The DLKP-A cell line is a daughter cell line of DLKP, a poorly differentiated squamous non-small cell lung carcinoma. The P-glycoprotein (P-gp) membrane pump is the main mechanism of multidrug resistance (MDR) in the DLKP-A cell line [369]. It highly over-expresses P-gp, while expressing very low levels of multidrug resistance protein 1 (MRP1). DLKP, on the other hand, expresses low, yet highly active, MRP1 levels, while lacking the P-gp cell membrane transporter [337].
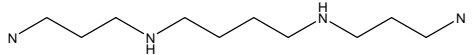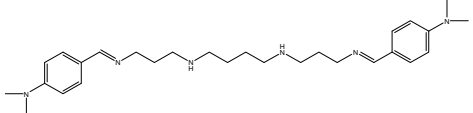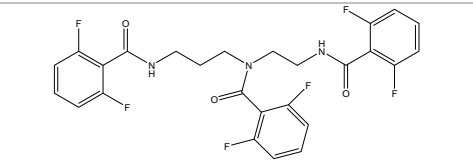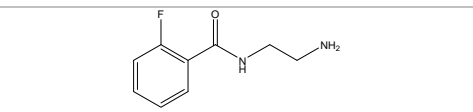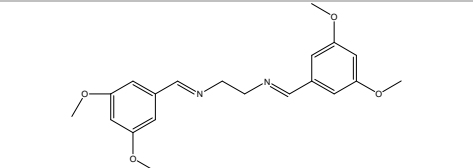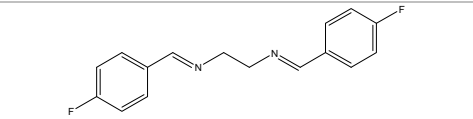
3.1.1. Polyamine derivatives

Polyamines are a group of organic compounds, with two or more primary amino groups, that are important in the regulation of gene expression, translation, cell proliferation, modulation of cell signalling, protein synthesis, and membrane stabilization in all known cell types [377] [378]. Adequate cellular polyamine levels are achieved by a careful balance between biosynthesis, degradation, and uptake of amines from the surrounding environment. Polyamines affect numerous processes in carcinogenesis. Increased polyamine levels are associated with increased cell proliferation, decreased apoptosis and increased expression of genes affecting tumour invasion and metastasis. Conversely, suppression/depletion of polyamine levels is associated with decreased cell growth [379], increased apoptosis and decreased expression of genes affecting tumour invasion and metastasis [380] [381]. Polyamines are often present at increased concentrations in tumour cells and tissues, for example, breast and colon cancer.

Several hundred polyamine synthesis inhibitors have been developed over the past 20-25 years with the main focus on decreasing cell growth [379]. However, the potential that these compounds could also inhibit MDR function has not been investigated. In this section, we used combination proliferation assay to investigate the possibility that spermine and 5 polyamine derivatives could inhibit the function of P-gp or MRP1 (for methodology see section 2.7.3. and 2.10.).

The five polyamine compounds tested were less toxic in both cell lines compared to their spermine parent (refer to table 3.1.1.1). Spermine had the greatest growth inhibitory effect in the DLKP (IC$_{50}$: 8 ± 1 μM) cell line. The PA1 structure is the most similar to spermine and had the greatest cytotoxic effect in both cell lines (10 ± 4 μM and 15 ± 2 μM). Spermine and four of the polyamine derivatives did not enhance the cytotoxicity of epirubicin in the DLKP cells, however, a mild increase was observed with spermine in the P-gp-expressing cell line, DLKP-A. The most toxic derivative, PA1, also slightly enhanced the anti-proliferative potential of the MRP1 and P-gp substrate, epirubicin, in both the DLKP and DLKP-A cell lines. This would suggest that PA1 maybe a weak modulator of both MRP1 and P-gp (see table 3.1.1.1 for details).

Table 3.1.1.1: The structure, molecular weight, IC_{50} values and enhancement of epirubicin cytotoxicity (combination result) by spermine and five polyamine derivatives in both the DLKP and DLKP-A cell lines. See graph 8.1.1.1. in section 8 for combaintion proliferation assays.

Compound	Structure	Molecular weight (Da)	DLKP (µM)	Cmb results	DLKP-A (µM)	Cmb results
Spermine		202	*8 ± 1	0	*<60	+
PA1		464	10 ± 4	+	15 ± 2	+
PA2		565	*110 ± 10	0	74 ± 21	0
PA4		218	*>200	0	*>200	0
PA5		356	34 ± 3	0	50 ± 40	0
PA6		272	*>200	0	130 ± 20	0

Key: Results presented above represent triplicate determinations carried out on separate days

*: single/double determination results **0:** no change in epirubicin cytotoxicity **+:** mild enhancement of epirubicin cytotoxicity

>: greater than value presented **<:** less than value presented

3.1.2. Resveratrol Analogues

Resveratrol has been shown to prevent and slow the progression of a wide variety of *in vitro* disease models, including cancer, cardiovascular disease and ischaemic injuries. It also enhances stress resistance and extends the lifespan of various organisms from yeasts to vertebrates [382]. *In vitro* and *in vivo* studies have identified resveratrol as an effective candidate for cancer chemoprevention as it blocks each step in the carcinogenesis process [383]. These properties are mainly due to its antioxidant activity on molecular targets involved in tumour initiation, promotion and progression [384].

A major limitation of resveratrol is its metabolic stability in the body. In the hope of increasing resveratrol's stability, toxicity and anti-MDR potential, our collaborators in the NICB, Dr. Frankie Anderson and Dr. Brian Moran, designed and synthesised a range of resveratrol derivatives. From this panel, a selection of analogues were tested for their anti-cancer toxicity and their potential to inhibit the function of P-gp and MRP1 (for methodology see section 2.7.3. and 2.10.).

Resveratrol and its ten derivatives had the greatest anti-proliferative activity in the DLKP cell line (see table 3.1.2.1 for details). RF1 (7 ± 1 μM), RF3 (6 ± 0.3 μM), and RBM17 (<10 μM) had a similar toxicity to resveratrol (10 ± 2 μM), in the DLKP cells. Whereas RF2 (25 ± 5 μM), RF4 (21 ± 5 μM), RBM12 (>50 μM), RBM13 (39 ± 2 μM), RBM14 (~50 μM), RBM15 (28 ± 4 μM) and RBM 16 (>50 μM) showed a decrease in cytotoxicity when compared to resveratrol in the DLKP cell line. Resveratrol (15 ± 3 μM) and RF1 (10 ± 2 μM) were the most potent anti-proliferation agents in the DLKP-A cell line. The 3,5-diacetyl analogue, RBM 14, and the 3,5-amino acid salt, RBM16**,** had an IC_{50} value greater than 50 μM, as did the *trans*-diamino stilbene RBM12, which lay beyond the range of this assay.

With regard to the MDR inhibitory status of resveratrol and its 10 analogues, resveratrol slightly increased the anti-proliferative potential of both MRP1 and P-gp substrate (epirubicin) while compound RBM15 caused a large enhancement of epirubicin toxicity in the P-gp expressing cell line, DLKP-A (see graph 3.1.2.1 and table 3.1.2.1. and 3.1.2.2. for details).

In both the DLKP and DLKP-A cell lines, resveratrol improved epirubicin cytotoxicity (Epi 0.01 μM and Res 10 μM). The combination of any of the 10 fluorinated resveratrol derivatives (10 μM) with the P-gp/MRP1 substrate, 0.01 μM epirubicin, resulted in no change in the anti-proliferative potential of epirubicin in the DLKP cells (see table 3.1.2.1.). Therefore, these compounds do not modulate the transporter function of MRP1.

On the other hand, a change in the potency of 1.5 μM epirubicin in the DLKP-A cells was observed when combined with compounds RF1, RF2, RF4, RBM12, RBM13 and RBM14. Compared to resveratrol, RBM17 caused a similar enhancement of epirubicin in this cell line. In graph 3.1.2.1, 1.5 μM epirubicin caused a 37% decrease in proliferation, 10 μM RBM15, a ditrifluoroacetyl derivative, caused a 16% reduction in proliferation, however, and when they were combined they collectively reduced proliferation by 80%. This is a significant enhancement of the P-gp substrate cytotoxicity, which would suggest RBM15 is a P-gp modulator [385]. The data on the RF1 to RF4 compounds were also presented as a poster at the IACR conference in 2006 and briefly discussed in the IACR newletter following the conference.

The combination of 3 resveratrol analogues with epirubicin in the DLKP-A cell line.
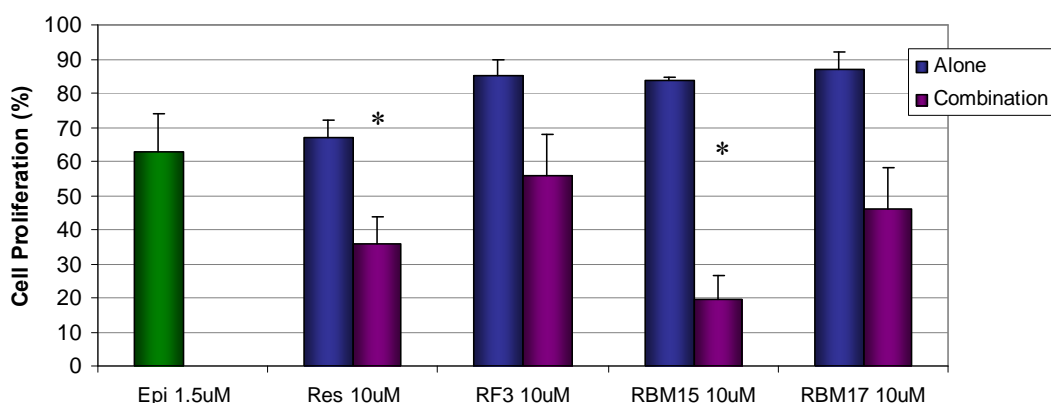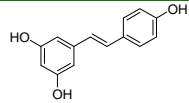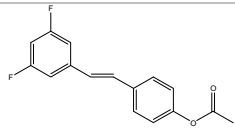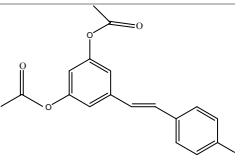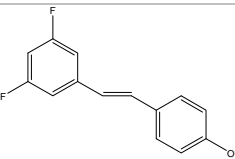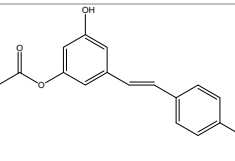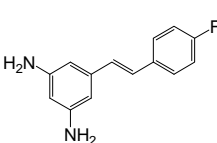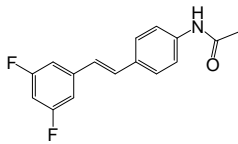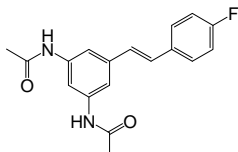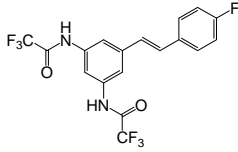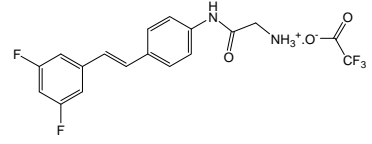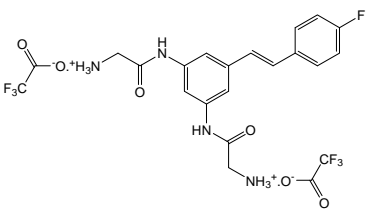
Graph 3.1.2.1: The bar chart above illustrates the effect of the combination of resveratrol, RF3, RBM15 and RBM17 with epirubicin in the DLKP-A cell line. No DMSO or ethanol toxicity was experienced at these concentrations. The other six compounds were also tested but did not enhance the cytotoxicity of epirubicin in either the DLKP or DLKP-A cell lines. This graph is the result of a single determination. Significance of combination result relative to drugs alone is represented by * ($p < 0.05$). Table 3.1.2.2 below depicts the percentage cell proliferation and standard deviations for this graph.

Table 3.1.2.2: This table provides data for the combination of epirubicin with resveratrol and 3 of its analogues in the DLKP-A cell line.

Compound	Cell Proliferation (%)			
	Alone	*St Dev (%)*	**Combination**	*St Dev (%)*
Epirubicin 1.5µM	63	*±11*		
Resveratrol 10µM	67	*±5*	36	*±7.6*
RF3 10µM	85	*±5*	56	*±12*
RBM15 10µM	84	*±0.7*	19	*±7*
RBM17 10µM	87	*±5*	46	*±12*

Table 3.1.2.1: The structure, molecular weight, IC$_{50}$ values and anti-P-gp/MRP1 activity of resveratrol and 10 resveratrol analogues in DLKP, and DLKP-A cell line. All IC$_{50}$ results represent duplicate independent determinations. Combination assays were carried out with epirubicin in both cell lines (see graph 3.1.2.1 for illustration of these results).

Compound	Structure	Molecular weight (Da)	DLKP (μM)	Cmb result	DLKP-A (μM)	Cmb result
Resveratrol		228	[#]10 ± 2	+	[#]15 ± 3	+
RF1		274	7 ± 1	0	10 ± 2	0
RF2		314	25 ± 5	0	19 ± 3	0
RF3		232	6 ± 0.3	0	14 ± 2	0
RF4		272	21 ± 5	0	21 ± 2	0
RBM12		228	> 50	0	> 50	0

Compound	Structure	Molecular weight (Da)	DLKP (μM)	Cmb result	DLKP-A (μM)	Cmb result
RBM13		273	39 ± 2	0	Not soluble	0
RBM14		312	50 ± 5	+	50 ± 3	0
RBM15		408	$28 \pm 4^{\Psi}$	0	$20 \pm 10^{\Psi}$	+++
RBM16		401	>50	+	>50	0
RBM17		567	>10	+	20 ± 10	+

Key: All IC$_{50}$ results are representative of duplicate independent determinations.

#: triplicate independent determinations Ψ: Duplicate independent determinations **0**: no change in epirubicin cytotoxicity

+: mild enhancement of epirubicin cytotoxicity +++: large enhancement of epirubicin cytotoxicity

3.1.3. Macrocyclic compounds

Cyclic peptides, such as cyclosporine, and macrocycle compounds, tacrolimus, and sirolimus, are immunosuppressants used in organ transplantation and can also act as P-gp inhibitors [386]. Polycyclic alkaloids have also been reported to act as P-gp inhibitors, but because of their cytotoxicity or other intrinsic pharmacological effects, almost all of them have been proven to be unsuitable for clinical use as P-gp inhibitors.

Due to the findings described above, six macrocyclic analogues (KG1 to KG6), designed and synthesised by Dr. Brian Deegan of the NICB, were investigated for their cytotoxicity and anti-MDR potential in two cells line, DLKP (MRP1-expressing) and DLKP-A (P-gp-expressing) (for methodology see section 2.7.3. and 2.10.). It was hoped that these ringed structures could additionally be designed to incorporate, and thus selectively delivery cytotoxic agents to cancer cells. A hydrolysis reaction would open the ringed structure producing MDR transporter pump modulators, therefore reducing the efflux of MDR substrates and thus enhancing their cytotoxicity.

KG3 and KG4 mildly enhanced the anti-proliferative potential of the P-gp substrate, epirubicin, in the DLKP-A cell line (see table 3.1.3.5, graph 3.1.3.2 and table 3.1.3.2 for details). These results were presented as a poster at the IACR conference in 2007. To determine whether the effect observed was due to the full macrocycle structure or a product of its hydrolysis, Dr. Deegan synthesised six further compounds (KG100 – KG105; see figure 3.1.3.1 for structure and sites of hydrolysis). These were also tested and three of the compounds had a similar effect on epirubicin cytotoxicity. KG103 and KG104, had a greater effect on the anti-proliferative potential of epirubicin than KG3 or KG4 (see graph 3.1.3.2 and tables 3.1.3.2 and 3.1.3.5 for details). Further hydrolysis of these compounds was possible and six more derivatives were synthesised and tested. However, with these later derivatives no change in epirubicin cytotoxic was observed. This would suggest that the active hydrolysed products of KG3 and KG4 are KG103 and KG104. Later, Dr. Ewa Kowalska of the NICB, designed and synthesised 6 more macrocyclic derivatives. Of these, only KG405 mildly enhanced the cytotoxic potential of epirubicin in the P-gp expressing cell line, DLKP-A. However, the effect was not significant.
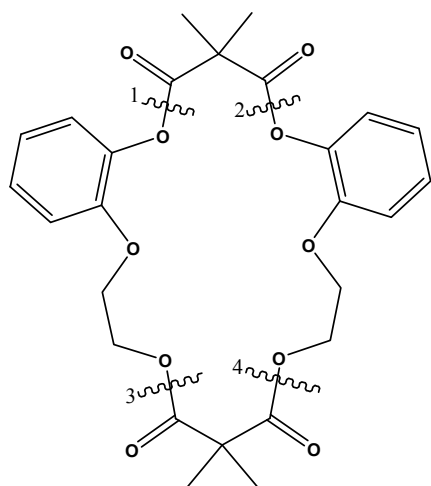
Figure 3.1.3.1.: The structure of KG4 and the location of four sites of hydrolysis. Hydrolysis across 1 and 2 gives KG104 and KG101. Hydrolysis across 3 and 4 gives KG103 and KG101. Hydrolysis across 1 and 3 gives KG100

KG100, KG101, KG102, KG105, KG200-KG206, KG408 and KG413 were found to be non-toxic (an IC_{50} above 50μM) in the DLKP-A cell line. KG411 (34μM) had the greatest growth inhibition followed by both KG103 (40 ± 18μM) and KG406 (40μM) and finally by KG104 (45 ± 11μM) in the DLKP-A cell line (see table 3.1.3.6 for details). For the DLKP cell line, five of the compounds tested were found to produce slight growth inhibition (see table 3.1.3.5 for details). KG413 (13 ± 3μM) was the most toxic followed closely by KG405 (19 ± 3μM) then KG411 (36μM), KG402 (42μM) and finally KG406 (48μM) in the DLKP cell line. We noticed that KG103 had a greater impact on the cell growth of DLKP-A compared to DLKP. We hypothesised that this might be due to the expression of P-gp in DLKP-A, therefore, we tested a small panel of other cell lines resistant due to P-gp over-expression. A549 expresses MRP1, while its daughter cell line, A549-Taxol, expresses P-gp. H1299 does not express P-gp while its paclitaxel-selected variant, H1299-Taxol, expresses low levels of P-gp. A difference in KG103 sensitivity between non-P-gp and P-gp expressing cell lines was not observed in A549 and H1299 cell lines and their variants (See graph 3.1.3.1 and table 3.1.3.1 for details).

KG3, KG4, KG103 (see graph 3.1.3.2 and table 3.1.3.2 and 3.1.3.5 for details), KG104 (see graph 3.1.3.3 and table 3.1.3.3 for details), KG105 (see graph 3.1.3.2 and table 3.1.3.2 and 3.1.3.5 for details) and KG405 (see graph 3.1.3.4 and table 3.1.3.4

for details) moderately enhanced the anti-proliferative potential of epirubicin, and in many cases also docetaxel, in the P-gp overexpressing cell line, DLKP-A. These compounds were only active in the P-gp expressing cell line, DLKP-A. KG3 and KG4 were the first macrocycles designed and synthesised for anti-cancer testing. Hydrolysis of the macrocycle KG3 produced non-macrocylic compounds KG100 to KG105. KG104 increased the cytotoxicity of epirubicin and docetaxel to the greatest extent in the P-gp expressing cell line, DLKP-A, at the lowest concentrations (see graph 3.1.3.2 and table 3.1.3.2 and 3.1.3.5 for details). But no change in the cyctotoxicity of the non-MDR substrate, 5FU, was observed suggesting KG104 effect is through P-gp modulation. Therefore, plans to investigate the mode of action by which KG104 overcame P-gp-mediated resistance were drawn up. Unfortunately, inconsistencies experienced with inter-batch solubility prevented this from being pursued (see section 8, graph 8.1.3.1 and table 8.1.3.1 for details). A number of attempts were made to dissolve the compound and while some worked, the solvent used actually interfered with normal P-gp function and therefore, work could not be continued (for details see section 8 graph 8.1.3.1 and table 8.1.3.1). This work was presented at the NICB conference in 2007.

Despite the interesting findings with KG104, no work is planned for the future due to the inter-batch variation.

The IC50 values of KG103 in a panel of lung cell lines.
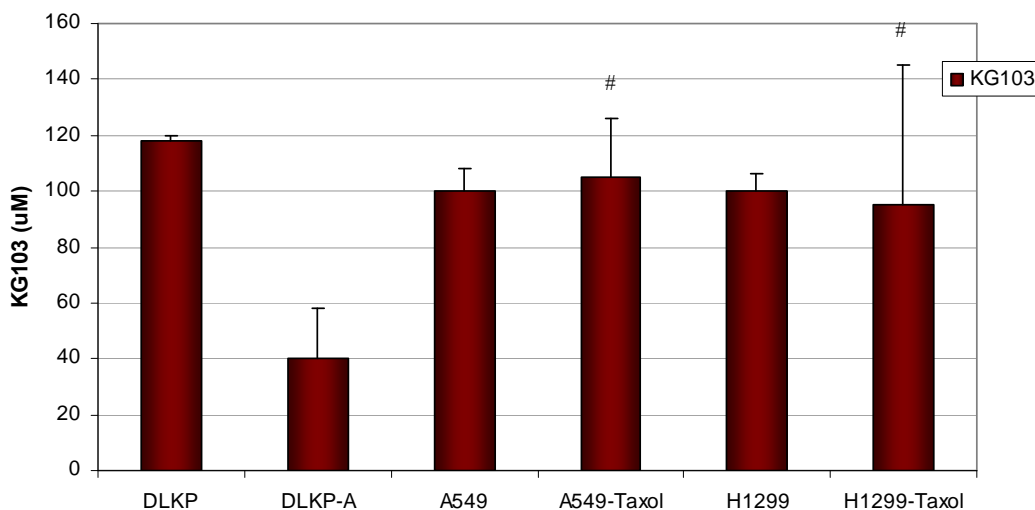
Graph 3.1.3.1: The IC$_{50}$ values of KG103 in a panel of lung cancer cell lines. No solvent vehicle (ethanol) anti-proliferative effects were experienced at the concentration used. Unless indicated ($^{#}$) each bar is representative of triplicate independent determinations. The IC$_{50}$ values and their standard deviations are presented in table 3.1.3.1 below.

Table 3.1.3.1: The IC$_{50}$ values of KG103 in a panel of lung cancer cell lines. All values represent triplicate independent determinations. $^{#}$ indicates duplicate independent determinations.

IC$_{50}$	DLKP	DLKP-A	A549	A549-T	H1299	H1299-T
KG103 (μM)	118	40	100	105$^{#}$	100	95$^{#}$
stdev (%)	±2	±18	±8	±21	±6	±50

Graph 3.1.3.2: The bar chart above illustrates the effect of the combination of 6 novel macrocyclic compounds with epirubicin in the DLKP-A cell line. No solvent vehicle (ethanol) anti-proliferative effects were experienced at the concentrations used. Significance of combination result relative to drugs alone is represented by * ($p<0.05$). Table 3.1.3.3 below depicts the percentage cell proliferation and standard deviations for this graph.

Table 3.1.3.2: This table provides the combination data of epirubicin with 6 macrocyline compounds in the DLKP-A cell line.

Compounds	Cell Proliferation (%)			
	Alone	St Dev (%)	Combination	St Dev (%)
Epirubicin 0.5μM	85	±12		
KG3 100μM	82	±3	59	±6
KG4 20μM	91	±9	55	±6
KG103 20μM	90	±5	11	±7
KG104 10μM	68	±10	11	±5
KG105 40μM	100	±4	54	±9
KG405 10μM	58	±10	39	±5

The combination **of KG104 with epirubicin, docetaxel and 5FU in the DLKP-A cell line.**

Graph 3.1.3.3: The bar chart above illustrates the effect of the combination of KG104 with epirubicin, docetaxel and 5FU in the DLKP-A cell line. No adverse ethanol effects were observed at concentrations used. This graph is the result of triplicate independent determinations. Significance of combination result relative to drugs alone is represented by * ($p < 0.05$). Table 3.1.3.4 below depict the percentage cell proliferation and standard deviations for this graph.

Table 3.1.3.3: This table provides the combination data of epirubicin, docetaxel and 5FU with KG104 on the DLKP-A cell line.

Compounds	Cell Proliferation (%)			
	Alone	*St Dev (%)*	**Combination**	*St Dev (%)*
KG104 10μM	68	*±10*		
Epirubicin 0.5μM	83	*±4*	11	*±5*
5FU 5μM	80	*±8*	66	*±5*
KG104 20μM	60	*±8*		
Docetaxel 0.005μM	95	*±3*	11	*±0.7*

The combination of KG405 with epirubicin, docetaxel and 5FU in the DLKP-A cell line.
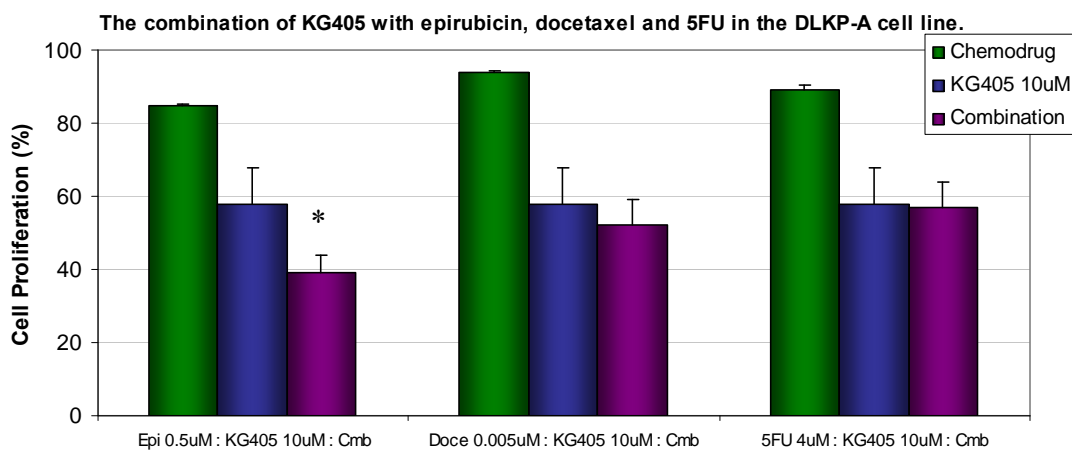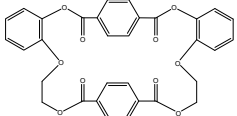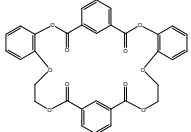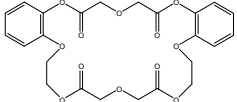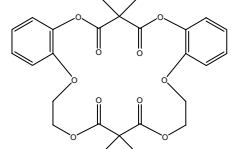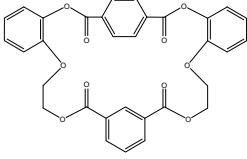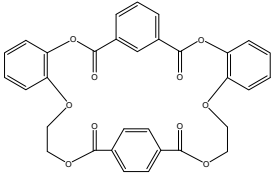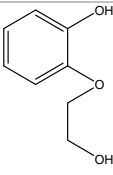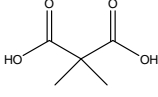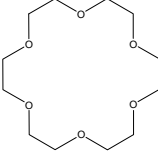
Graph 3.1.3.4: The bar chart above illustrates the effect of the combination of KG405 with epirubicin, docetaxel and 5FU in the DLKP-A cell line. No adverse ethanol effects were observed at the concentration used. Significance of combination result relative to drugs alone is represented by * ($p<0.05$). Table 3.1.3.5 below depicts the percentage cell proliferation and standard deviations for this graph.
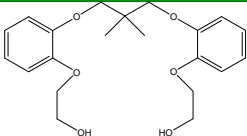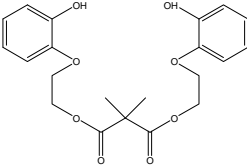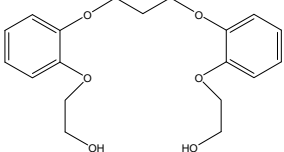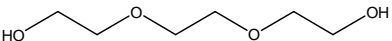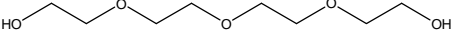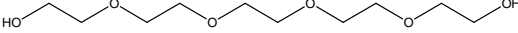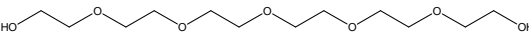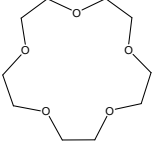
Table 3.1.3.4: This table provides the combination data of epirubicin, docetaxel and 5FU with KG405 on the DLKP-A cell line.
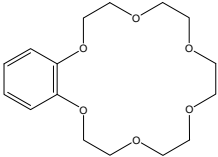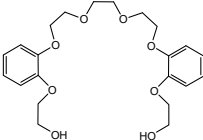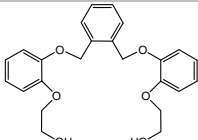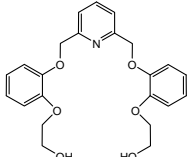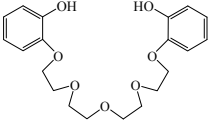
Compounds	Cell Proliferation (%)			
	Alone	*St Dev (%)*	**Combination**	*St Dev (%)*
KG405 10µM	58	*±10*		
Epirubicin 0.5µM	85	*±0.3*	39	*±5*
Docetaxel 0.005µM	94	*±0.5*	52	*±7*
5FU 4µM	89	*±1.6*	57	*±7*
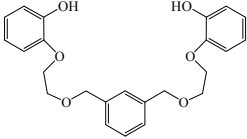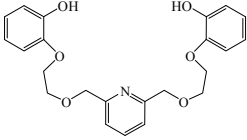
Table 3.1.3.5: This table provides the compound structure, molecular weights, IC$_{50}$ values and the level of epirubicin cytotoxicity enhancement of 24 macrocyclic compounds in both the DLKP and DLKP-A cell lines. Unless otherwise indicated, all results represent a single determination. The combination proliferation assays that enhanced substrate cytotoxicity the greatest are presented in graph 3.1.3.2 and table 3.1.3.2.

Compound	Structure	Molecular weight (Da)	DLKP IC$_{50}$ (µM)	Cmb result	DLKP-A IC$_{50}$ (µM)	Cmb result
KG1		569	N/A	0	N/A	0
KG2		569	N/A	0	N/A	0
KG3		504	N/A	0	N/A	*+
KG4		500	N/A	0	N/A	*+

Compound	Structure	Molecular weight (Da)	DLKP IC_{50} (μM)	Cmb result	DLKP-A IC_{50} (μM)	Cmb result
KG5		569	N/A	0	N/A	0
KG6		569	N/A	0	N/A	0
KG100		154	N/A	0	> 120	0
KG101		132	N/A	0	> 140	0
KG102		266	N/A	0	> 70	0

110

Compound	Structure	Molecular weight (Da)	DLKP IC_{50} (µM)	Cmb result	DLKP-A IC_{50} (µM)	Cmb result
KG103		405	118 ± 2	0	[#]40 ± 18	[#]+++
KG104		405	[#]88 ± 9	0	[#]45 ± 11	[#Ψ]++++
KG105		348	N/A	0	> 50	++
KG200		151	>250	0	>300	0
KG201		195	>115	0	>230	0
KG202		239	>95	0	>190	0
KG203		284	>80	0	>160	0
KG204		210	N/A	0	>210	0

Compound	Structure	Molecular weight (Da)	DLKP IC$_{50}$ (μM)	Cmb result	DLKP-A IC$_{50}$ (μM)	Cmb result
KG206		312	N/A	Not tested	>145	0
KG402		466	42	0	N/A	0
KG405		459	[#]19 ± 3	0	[#]34 ± 4	[#Ψ]+
KG406		455	48	0	40	0
KG408		418	N/A	Not tested	64 ± 20	0

Compound	Structure	Molecular weight (Da)	DLKP IC$_{50}$ (µM)	Cmb result	DLKP-A IC$_{50}$ (µM)	Cmb result
KG411		457	36	0	34	0
KG413		455	13 ± 3	0	58 ± 15	0

Key:
N/A   compound not tested
\#   triplicate independent determination
Ψ   combination proliferation assays of the test compound also carried out with docetaxel
0   no change in cytotoxic potential of epirubicin
+   mild enhancement of epirubicin cytotoxicity
++   moderate enhancement of epirubicin cytotoxicity
+++   large enhancement of epirubicin cytotoxicity
++++   large enhancement of epirubicin at lowest concentration
>   greater than the value indicated

3.1.4. Metal agents

Normally metal-based drugs, i.e. cisplatin, do not interact with multidrug resistance transport proteins (mentioned in section 1.0 in tables 1.4.1, 1.4.2, and 1.4.3). In this section, we determined if a titanium metal compound developed and synthesised by Dr. Matthias Tacke in the Conway Institute, UCD, was cytotoxic in MDR expressing cell lines (for methodology see section 2.7.3. and 2.10.). We chose two cell lines, DLKP and DLKP-A, for their expression of MRP1 and P-gp. Titanocene Y was selected from a panel of compounds.

The cytotoxicity of Titanocene Y was moderate in both the DLKP (25 ± 3 μM) and DLKP-A (18 ± 4μM) cell lines. Titanocene Y did not enhance epirubicin cytotoxicity in either cell line. Therefore, at the concentrations used, Titanocene Y does not modulate P-gp or MRP1 pump function and these cells are not sensitive to it. No further work is planned in this area.

Table 3.1.4.1.: This table provide the IC$_{50}$ values and combination proliferation assay results for Titanocene Y in both the DLKP and DLKP-A cell lines.

Compound (μM)	DLKP	Combination result	DLKP-A	Combination result
Titanocene Y	25 ± 3	No additivity	18 ± 4	No additivity
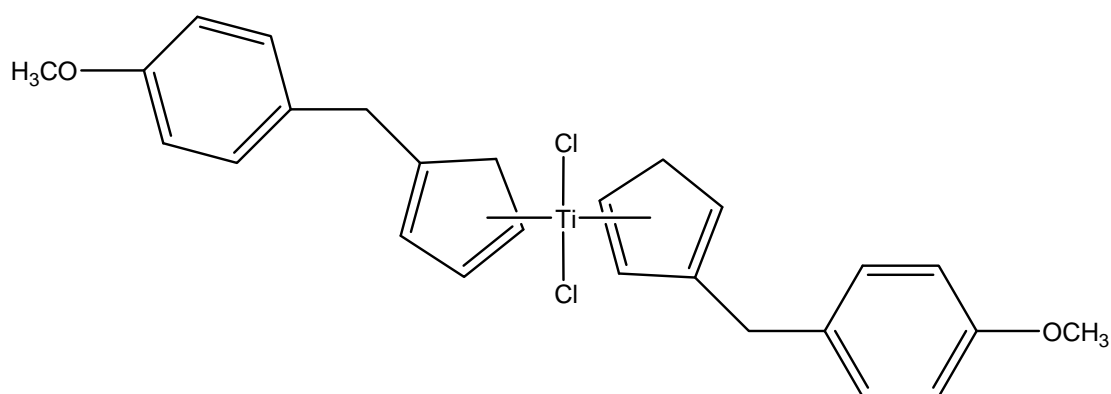
Figure 3.1.4.1.: The structure of Titanocene Y. The compound has a molecular weight of 482 Da.

3.1.5. Nano-particulate polymerised daunorubicin

In this section, we investigated the potential that surrounding daunorubicin with a polymer, poly(butylcyanoacrylate), could assist distribution and/or overcome/evade MDR efflux pumps [387] [388]. The full compound was synthesised by polymerising *n*-butylcyanoacrylate monomers in the presence of daunorubicin. To evaluate if this daunorubicin delivery system, which was designed and synthesised by our collaborators in DCU and the Conway institute, could evade P-gp and MRP1-dependent efflux *in vitro*, we carried out straight proliferation assays (for methodology see section 2.7.) of daunorubicin, nano-particulated polymerised daunorubicin, daunorubicin plus the particulate/polymer, and the particulate/polymer in both the DLKP and DLKP-A cell lines.

The straight proliferation assay of the polymerised daunorubicin particule in both the DLKP and DLKP-A cell line gave a similar toxicological response as unmodified daunorubicin (see table 3.1.5.1 for details). The particulate was less toxic than the test agents and the combination of daunorubicin with the particulate did not heighten the growth inhibition of daunorubicin (see table 3.1.5.1 for details). However, at high concentrations the encapsulation of daunorubicin reduced its potency in the P-gp overexpressing cell line, DLKP-A (see graph 3.1.5.1 for details). This work was published in Simeonova M., *et al.,* [389].
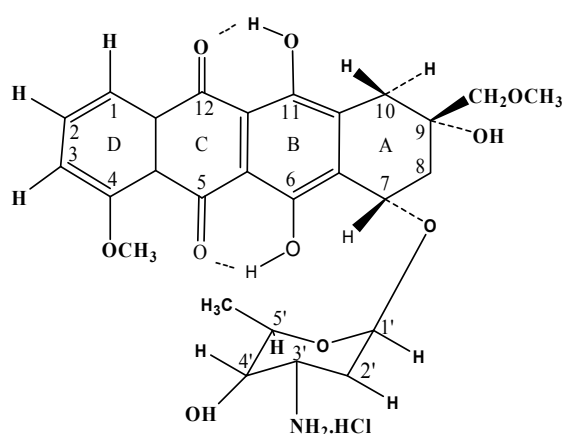
Figure 3.1.5.1.: The molecular structure of daunorubicin (M.W. 527.52 Da). Daunorubicin consists of a planar aglycon chromophore bearing an amino acid ring.
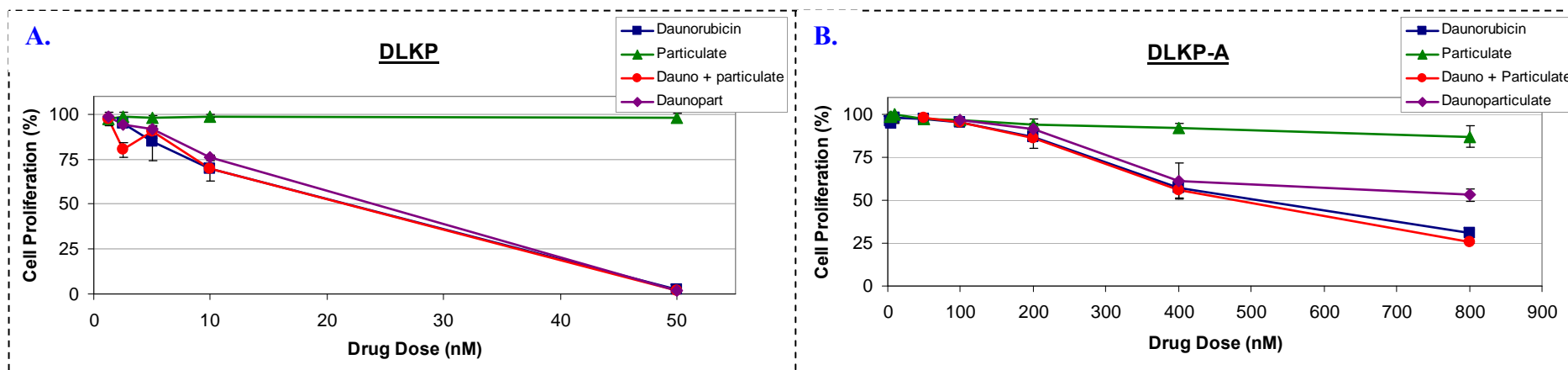
Graph 3.1.5.1.: The toxicity curves of daunorubicin (■), the nanoparticulate (▲), the nanoparticulate combined with daunorubicin (●) and the nanoparticulate encapsulating daunorubicin (◆) in the DLKP (**A**) and DLKP-A (**B**) cell lines. These graphs are the result of a single assay. For the IC_{50} of these curves please refer to table 3.1.5.1 below.

Table 3.1.5.1.: This table provides the IC_{50} values of daunorubicin and its nano-particulate modified version in both the DLKP and DLKP-A cell lines. Concentrations used were calculated using the molecular weight of daunorubicin.

Compound	DLKP IC_{50} (μM)	DLKP-A IC_{50} (μM)
Daunorubicin	0.024	0.5
Daunorubicin + Particulate	0.024	0.5
Daunopart	0.026	0.8
Particulate	>0.05	>0.8

116

3.1.6. MDR down-regulation

In this section, we investigated a range of small molecule agents that, according to the literature, modulate P-gp, MRP1 or BCRP expression. For this, we chose the lung cancer cell lines, A549, A549-Taxol, and DLKP-SQ/mitox. A549 expressed moderate levels of MRP1 and does not express P-gp or BCRP. A549-Taxol is the daughter cell line of A549 and was selected using paclitaxel (work carried out by Dr. Laura Breen [370]). A549-Taxol expresses moderate levels of P-gp but does not express MRP1 or BCRP. Both the A549 and A549-Taxol cell lines are moderately resistant due to the expression levels of their MDR proteins. DLKP-SQ/mitox is a squamous non-small cell lung carcinoma cell line that was selected from DLKP-SQ using mitoxantrone (work carried out by Helena Joyce of the NICB). DLKP-SQ/mitox does not express MRP1 or P-gp but expresses high levels of BCRP.

The selection of these agents (listed in table 3.1.6.1 below) was based on the availability of information in the literature, i.e. biochemical data, known interactions with MDR pumps and existing availability for use in a clinical trial setting. The doses used in this work are also presented in table 3.1.6.1 and fall below the maximum concentration achievable in the blood, with the exception of 10 µM celecoxib (2 µM) and 5 µM ibuprofen (2 µM). These doses have been used in the literature and allow a direct comparison between the findings presented herein and those already published. The cells were exposed to each agent for 24 hours; allowing the drug enough time to alter protein expression (for methodology see section 2.11.). For agents that reduced MDR protein expression by more than 20%, they were brought forward for further analysis. This included examining the stability of the alteration in expression induced by the agents, the toxicity of the agents and their ability to overcome MDR-mediated resistance in co-treatment and pre-incubation proliferation assays (for methodology see section 2.11., 2.7.1., 2.7.2., and 2.7.3.). Over the next year, this body of work will be submitted for publication.

Table 3.1.6.1: Below is a list of agents known to alter MDR protein expression. Included in the table is a range of doses employed in the assay, the duration of exposure and summary of published findings for each agent.

Class	Drug	Dose (µM)	Exposure (hr)	Summary effect on transporter
TKI	Lapatinib	0.3, 0.5, 1	24	P-gp [112] & BCRP [97] inhibitor
	Erlotinib	0.3, 0.5, 1	24	P-gp [197] & BCRP [148] inhibitor
	Gefitinib	0.3, 0.5, 1	24	P-gp & BCRP inhibitor [150]
NSAID	Sulindac (sulphide)	0.5, 2, 5	24	↓MRP1↑P-gp [171] [172] [173]
	Celecoxib	0.5, 2, 10	24	↓MRP1 [174]↓P-gp [160]
	Ibuprofen	0.5, 2, 5	24	P-gp inhibitor [171]
	Indomethacin	0.4, 1, 2	24	↓P-gp [96], MRP1 [177] & BCRP [96] inhibitor
Hsp 90	17-AAG	0.1, 0.5, 1	24	↓P-gp [3]
Other	Elacridar	0.3, 0.5, 1	24	P-gp [191] & BCRP [193] inhibitor

Key:
↑ up-regulation of protein expression
↓ down-regulation of protein expression

3.1.6.1. P-gp downregulation

A549-Taxol was the P-gp expressing cell line chosen for this work. Figure 3.1.6.1 outlines the P-gp (170 kDa) Western blots of A549-Taxol cells following a 24 hour exposure to each agent. β-actin (a 48 kDa house-keeping protein) was used as a control for protein loading and to show that the lysates were in good condition.

For the lapatinib, erlotinib, gefitinib and elacridar-treated cells (lane 1 − 3) the bands from treated cells were bigger than the control/untreated (C) bands. This indicated that the P-gp protein expression was up-regulated in the presence of these agents. Densitometric analysis of these blots (which is presented as percentage change in table 3.1.6.2) supports these visual findings. These Western blots were not repeated as they did not qualify for further testing. Celecoxib, indomethacin and 17-AAG-treated cells (lane 1 − 3) showed a decrease in P-gp protein expression when compared to their control bands (C). Only the highest concentration of celecoxib (10 μM) downregulated the expression of P-gp. Indomethacin affected expression at 1 and 2 μM but not with 0.4 μM. 17-AAG downregulated expression at 0.3, 0.5 and 1 μM. A 60% decrease in expression occurred when the A549-Taxol cells were exposed to 1 μM 17-AAG for 24 hours. The only small molecule agent that did not affect P-gp protein expression was ibuprofen. Densitometry was carried out on all the Western blots and is presented in table 3.1.6.2 in the form of percentage changes.

Western blotting and densitometric analysis demonstrated that two small molecule agents, indomethacin and 17-AAG, noticably down-regulated the expression of P-gp. To identify if this down-regulation was maintained following removal of the drug after 24 hours, and if the concentrations used reduced cell proliferation, further Western blots were carried out, as well as short term proliferation assays.

All concentrations of indomethacin down-regulated the expression of P-gp following a 24 hour exposure, however, this was not maintained once the drug was removed for 24 and 48 hours (see figure 3.1.6.1.2.). A concentration of 1 μM 17-AAG down-regulated the expression of P-gp in the A549-Taxol cells following a 24 hour exposure. This down-regulation was sustained for 24 and 48 hours in drug-free media (see figure 3.1.6.1.2.).

In 6-well plates, with cells seeded at a density of 7×10^4 cells/ml, all concentrations were found to be non-toxic following a 24 hour exposure (see graphs 8.1.6.1.1.A and 8.1.6.1.1.B for details).

Target Protein	Western blot	Summary effect
	C 1 2 3	
P-gp (170kDa) β-actin (48kDa)		↑ by Lapatinib after 24hrs[#]
P-gp (170kDa) β-actin (48kDa)		↑ by Erlotinib after 24hr[#]
P-gp (170kDa) β-actin (48kDa)		↑ by Gefitinib after 24hr[#]
P-gp (170kDa) β-actin (48kDa)		↓ by Celecoxib after 24hr
P-gp (170kDa) β-actin (48kDa)		↑ by Sulindac Sulphide after 24hr[#]
P-gp (170kDa) β-actin (48kDa)		↔ by Ibuprofen after 24hr[#]
P-gp (170kDa) β-actin (48kDa)		↓ by Indomethacin after 24hr
P-gp (170kDa) β-actin (48kDa)		↑ by Elacridar after 24hr[#]
P-gp (170kDa) β-actin (48kDa)		↓ by 17-AAG after 24hr

Key:
C: Control / untreated   ↑: Protein expression up-regulation
1: 1st drug concentration   ↓: Protein expression down-regulation
2: 2nd drug concentration   ↔: No change in protein expression
3: 3rd drug concentration   [#]: Single replicate

Figure 3.1.6.1.1.: The P-gp Western blots of A549-Taxol treated for 24 hours with a panel of agents listed in table 3.1.6.1. The drug concentrations used in this work are also presented in table 3.1.6.1. P-gp has a molecular weight of 170 kDa and the housekeeping protein, β-actin with a molecular of 48 kDa, used as a protein loading control. Each sample was incubated at 37°C for 24 hours in ATCC media containing 5% FBS. Control samples had no drug in their media. 40 µg of sample was loaded into each well. The positive control used was DLKP-A but is not included in these images (see figure 3.4.1.3. for P-gp expression). The densitometric analysis of these blots is represented in table 3.1.6.2. These Western blots are representative of duplicate or more independent determinations unless otherwise indicated ([#]).

Table 3.1.6.1.2.: Percentage changes in the expression of P-gp in A549-Taxol cells following exposure to a range of agents (listed above) for 24 hours. These percentage changes were determined using densitometric analysis of Western blots carried out on lysates of the exposed A549-Taxol cells. The numbers 1-3 represent increasing concentrations of each agent which are listed in table 3.1.6.1.

Percentage change			
Drug panel	**1st concentration**	**2nd concentrations**	**3rd concentration**
Lapatinib	40	130	130
Erlotinib	170	200	160
Gefitinib	200	140	90
Celecoxib	0	-10	-20
Sulindac S.	-10	0	30
Ibuprofen	-20	20	0
Indomethacin[$]	0	-20	-50
Elacridar	70	70	80
17-AAG[$]	-20	-10	-40

Key:
[$]   Indicates successful candidates that were brought forward for testing stability in expression alteration, toxicity and proliferation assay.
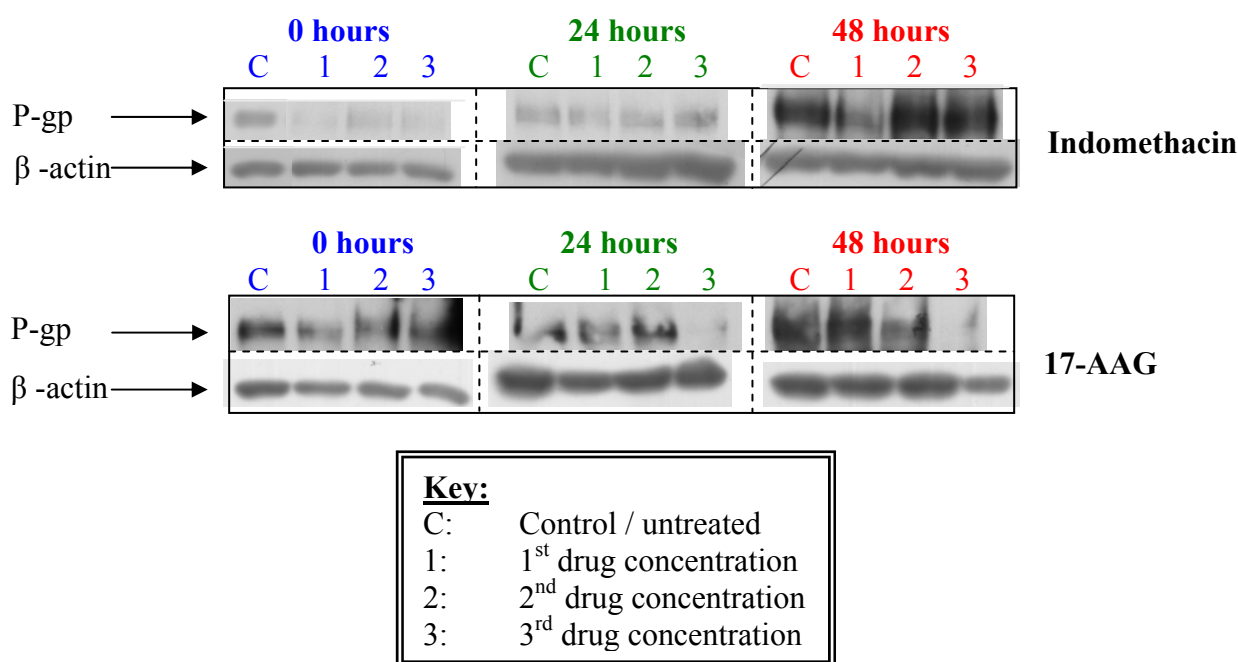
Figure 3.1.6.1.2.: The P-gp Western blots of A549-Taxol treated for 24 hours with indomethacin or 17-AAG. Drug was removed after the 24 hour exposure and the cells were rinsed and fresh media was added. The drug concentrations used in this work are presented in table 3.1.6.1. Samples were taken 0 hours, 24 hours and 48 hours after drug removal. P-gp has a molecular weight of 170 kDa and the housekeeping protein, β-actin with a molecular of 48 kDa, used as a protein loading control. Each sample was incubated at $37^{o}C$ for 24 hours in ATCC media containing 5% FBS. Control samples had no drug in their media. 40 μg of sample was loaded into each well. The positive control used was DLKP-A. These Western blots are the result of a single experiment and represent a trend over a period of 48 hours.

Combination and scheduled proliferation assays:

Using the two small molecule agents investigated in graph 8.1.6.1.1 (section 8) and figure 3.1.6.1.2, we examined if the down-regulation of P-gp protein could sensitise the A549-Taxol cells to the P-gp substrate, docetaxel.

We found that indomethacin did not heighten the anti-proliferative potential of docetaxel in either the direct combination (5 ± 0.3 µM) or as a pre-treatment (9 ± 0.5 µM) for docetaxel in the A549-Taxol cell line (see graph 3.1.6.1.1, 3.1.6.1.3 and table 3.1.6.1.2. for details). All concentrations of indomethacin were non-toxic in both the combination and scheduled proliferation assays (see graph 3.1.6.1.1 and table 3.1.6.1.2 for details).

When the A549-Taxol cells were exposed to 0.3, 0.5 and 1 µM 17-AAG for 5 days, all concentrations were highly toxic (1-3% proliferation detected, see graph 3.1.6.1.2 and table 3.1.6.1.2 for details). Therefore, when directly combined with docetaxel, no change in cell proliferation, compared to 17-AAG alone, was observed (see graph 3.1.6.1.2. When the cells were exposed to 17-AAG for only 24 hours, and incubated for a further 4 days, the toxic effects were greatly reduced. A concentration 0.3 µM 17-AAG allowed 49% (±18%), 0.5 µM 17-AAG allowed 43% (±18%) and 1µM 17-AAG allowed 29% (±18%) cell proliferation (see table 3.1.6.1.2 for details). Using a 24 hour pre-treatment method (scheduling proliferation assay), these concentrations reduced the IC_{50} of docetaxel, from 5 ± 0.4 µM to 0.7 ± 0.4 µM, 0.4 ± 0.2 µM and < 0.07 µM (see graph 3.1.6.1.2.B, 3.1.6.1.3 and table 3.1.6.1.2 for details).
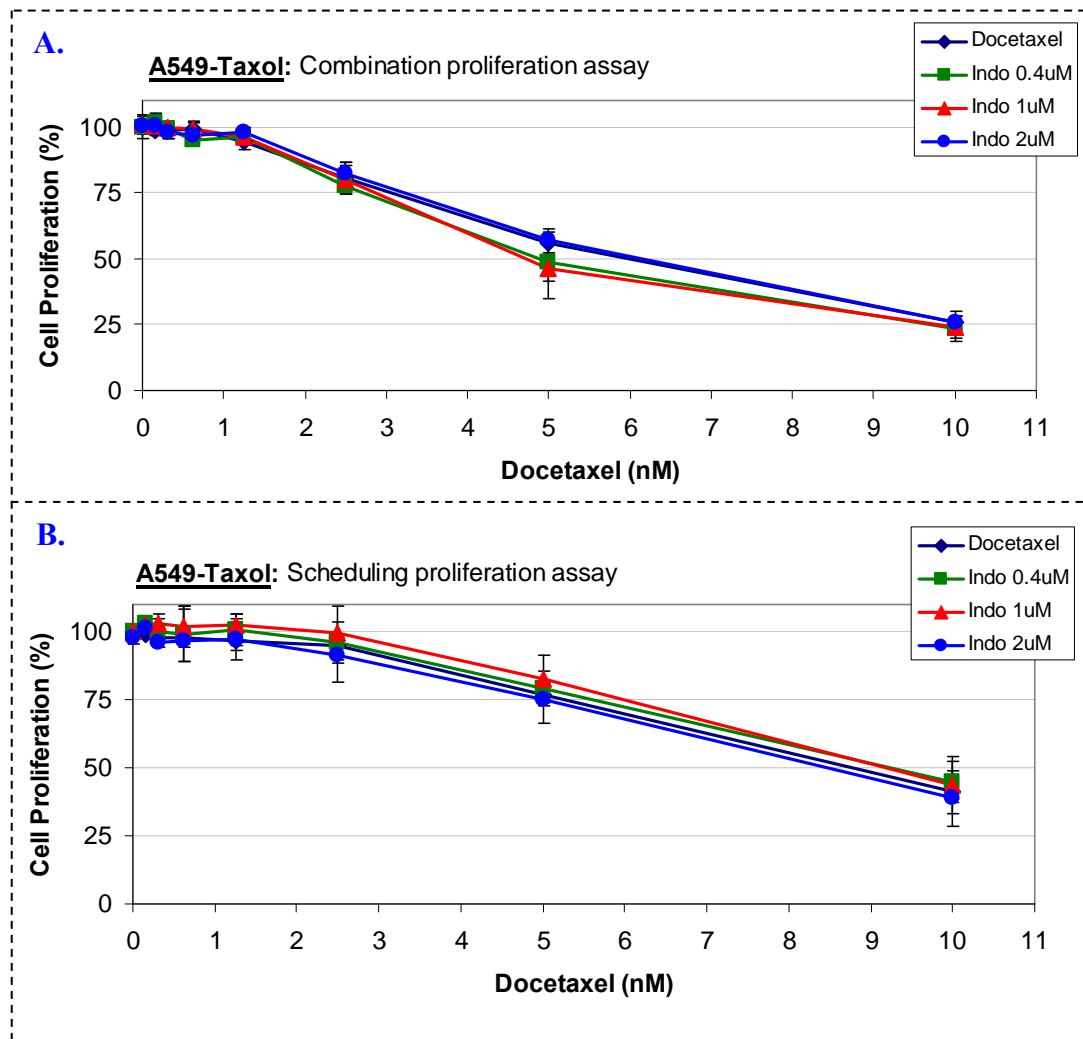
Graph 3.1.6.1.1.: The combination (**A**) and scheduling (**B**) assays of indomethacin and docetaxel (◆) in the A549-Taxol cell line. An IC_{50} curve of docetaxel combined or pre-treated with 0.5 (■), 1 (▲) and 2 μM (●) indomethacin over a 5 day period. The combination proliferation assay (**A**) is the combination of both drugs together on the cells at the same time. The 24 hour pre-treatment (**B**) is when the cells are exposed to indomethacin for 24 hours, removed and docetaxel is added for 4 days. Each graph is the result of a single assay with intra-day variation represented by error bars.
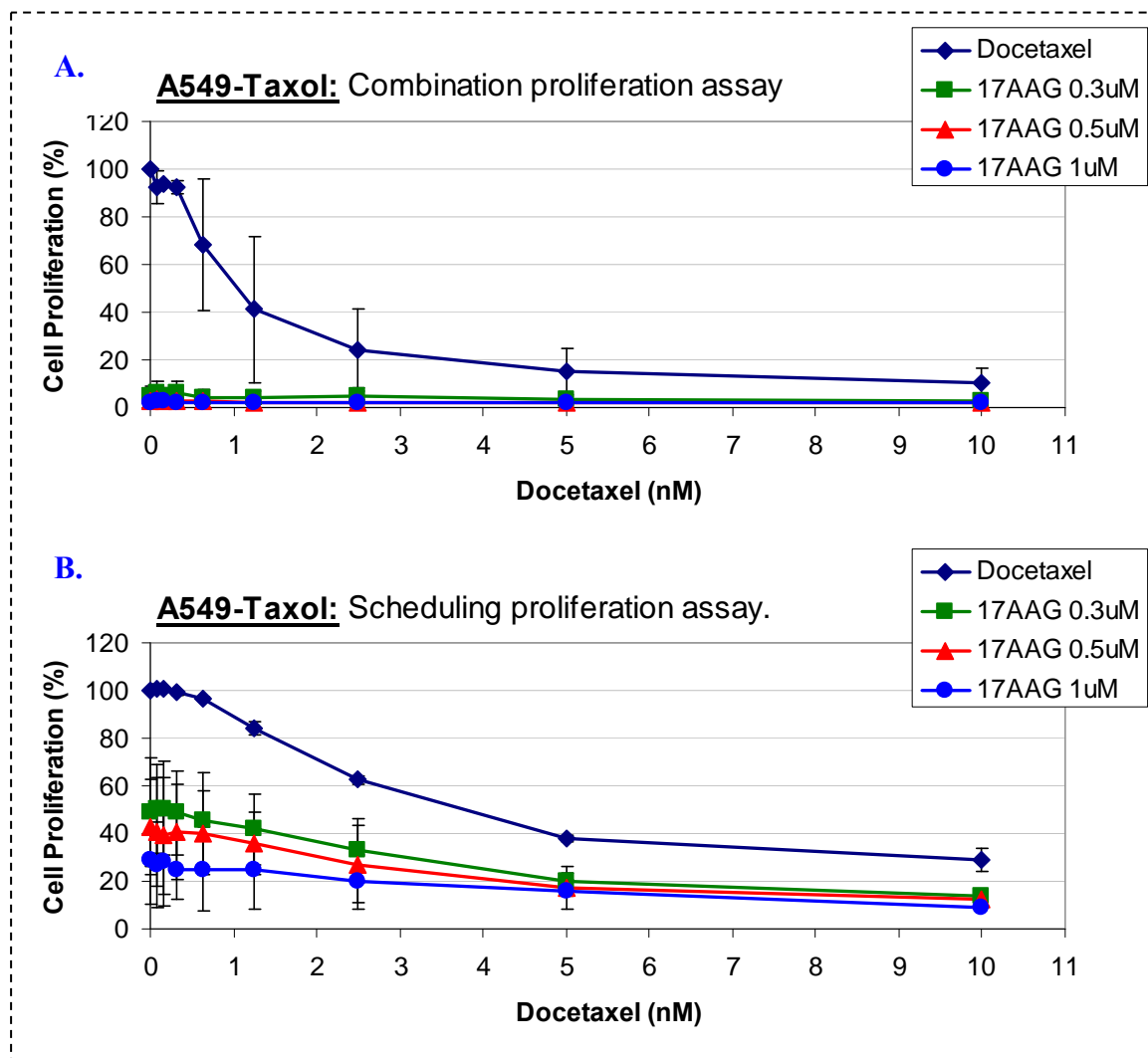
Graph 3.1.6.1.2.: The combination (**A**) and scheduling (**B**) assays of 17AAG and docetaxel (◆) in the A549-Taxol cell line. An IC_{50} curve of docetaxel when either co-incubated or pre-treated with 0.3 (■), 0.5 (▲) and 1µM (●) 17AAG over a 5 day period. The combination proliferation assay (**A**) used the combination of both drugs together on the cells at the same time. In the scheduling proliferation assay (**B**) the cells are exposed to 17-AAG for 24 hours, removed and docetaxel added for 4 days. Each graph is the result of duplicate independent determinations and inter-day variation is represented by error bars. The IC50 of docetaxel alone, incombination and following a 24 hour pre-treatment are presented in graph 3.1.6.1.4. and table 3.1.6.1.2.
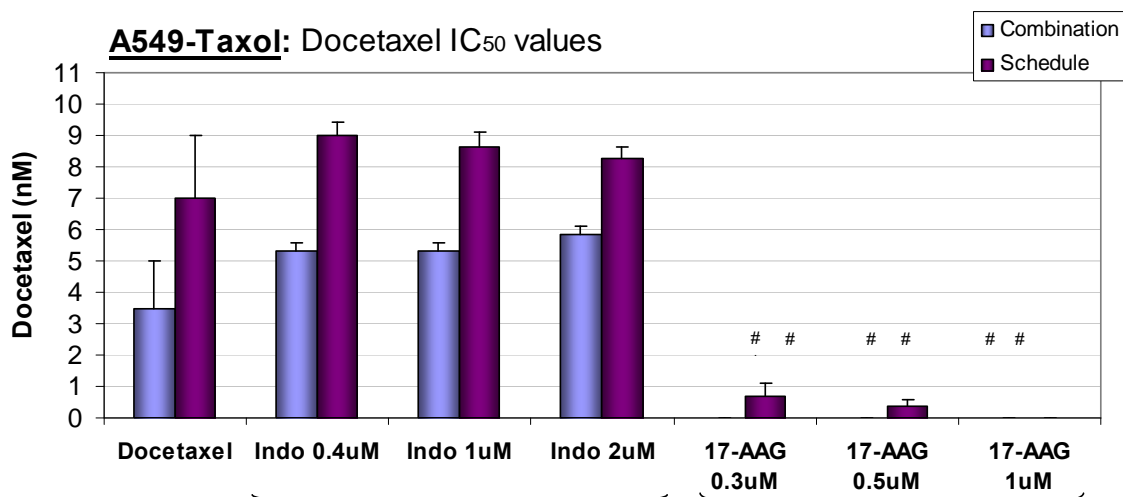
Graph 3.1.6.1.3.: The IC$_{50}$ values of docetaxel, alone and combined/scheduled with either indomethacin or 17-AAG, calculated using Calcusyn software. All values are the result of a duplicate determination. A star ($^{#}$) indicates where the small molecule agent caused significant cytotoxicity alone. Table 3.1.6.1.2 outlines that percentage cell proliferation for each agent and the change in IC$_{50}$ of docetaxel when combined or as part of a scheduled assay.

Table 3.1.6.1.2.: This table provides the percentage cell proliferation and the calculated average IC_{50} values (nM) of docetaxel for the duplicate combination and scheduled proliferation assays presented in graphs 3.1.6.2.1, and 3.1.6.2.2. These IC_{50} values are illustrated in graph 3.1.6.2.3. All results are due to duplicate independent determinations.
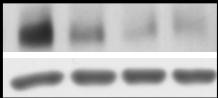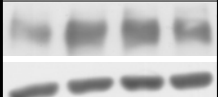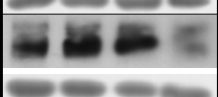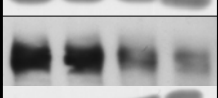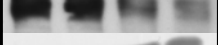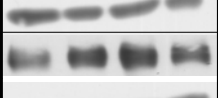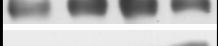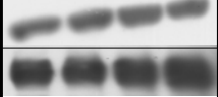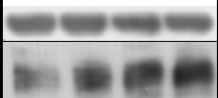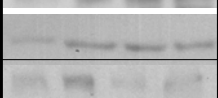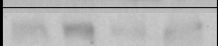
Drug	Combination assay Cell proliferation (%)	Combination assay IC_{50} value	Scheduling assay Cell proliferation (%)	Scheduling assay IC_{50} values
Docetaxel	**N/A**	**3.5 ± 1.5**	**N/A**	**7 ± 2**
Indomethacin 0.4	100	5 ± 0.3	100	9 ± 0.4
Indomethacin 1	100	5 ± 0.3	100	9 ± 0.4
Indomethacin 2	100	6 ± 0.3	100	8 ± 0.4
17-AAG 0.3	2 ± 2	< 0.07	49 ± 18	0.7 ± 0.4
17-AAG 0.5	1 ± 2	< 0.07	43 ± 18	0.4 ± 0.2
17-AAG 1	2 ± 1	< 0.07	29 ± 18	< 0.07

3.1.6.2. MRP1 down-regulation

As discussed in 3.1.7., A549 was the MRP1-expressing cell line chosen for this body of work. Figure 3.1.7.1 outlines the MRP1 (190 kDa) Western blots of A549 cells following a 24 hour exposure to each agent. β -actin (a 48 kDa house-keeping protein) was used as a control for protein loading and showed that the lysates were in good condition.

For the erlotinib, gefitinib, ibuprofen and indomethacin-treated cells (lane 1 − 3) the bands of the treated cells were bigger than the control/untreated (C) bands. This indicated that the MRP1 protein expression was up-regulated in the presence of these agents. Densitometric analysis of these blots (which is presented as percentage change in table 3.1.7.2) supports these visual findings. These Western blots were not repeated as they did not merit for further testing. Lapatinib, celecoxib, sulindac sulphide and 17-AAG-treated cells (lane 1 − 3) showed a decrease in MRP1 protein expression when compared to their control bands (C). Only the highest concentration of celecoxib (10 μM) downregulated the expression of MRP1. The only small molecule agent that did not affect MRP1 protein expression was elacridar. This Western blot was not repeated as it did not merit for further testing.

Densitometry was carried out on all the Western blots and is presented in table 3.1.7.2 in the form of percentage changes.

Target Protein ‖	Western blot ‖	Summary effect
	C 1 2 3	
MRP1 (190kDa) β-actin (48kDa)		↓ **by Lapatinib after 24hr**
MRP1 (190kDa) β-actin (48kDa)		↑ **by Erlotinib after 24hr**[#]
MRP1 (190kDa) β-actin (48kDa)		↑ **by Gefitinib after 24hr**[#]
MRP1 (190kDa) β-actin (48kDa)		↓ **by Celecoxib after 24hr**
MRP1 (190kDa) β-actin (48kDa)		↓ **by Sulindac Sulphide after 24hr**
MRP1 (190kDa) β-actin (48kDa)		↑ **by Ibuprofen after 24hr**[#]
MRP1 (190kDa) β-actin (48kDa)		↑ **by Indomethacin after 24hr**[#]
MRP1 (190kDa) β-actin (48kDa)		↑ **by Elacridar after 24hr**[#]
MRP1 (190kDa) β-actin (48kDa)		↓ **by 17-AAG after 24hr**

Key:

C:	Control / untreated	↑:	Protein expression up-regulation
1:	1st drug concentration	↓:	Protein expression down-regulation
2:	2nd drug concentration	↔:	No change in protein expression
3:	3rd drug concentration	#:	Single replicate

Figure 3.1.6.2.1.: The MRP1 Western blots of A549 treated for 24 hours with a panel of agents listed in table 3.1.7.1. The drug concentrations used in this work are presented in table 3.1.6.1. MRP1 has a molecular weight of 190 kDa and the housekeeping protein, β-actin with a molecular weight of 48 kDa, used as a protein loading control. Each sample was incubated at 37°C for 24 hours in ATCC media containing 5% FBS. Control samples had no drug in their media. 40 μg of sample was loaded into each well. The positive control used was 2008/MRP1 but is not shown (for proof of expression see figure 3.4.1.2.). The densitometric analysis of these blots is represented in table 3.1.7.2. These Western blots are the result of duplicate or more experiments unless otherwise indicated ([#]).

Table 3.1.6.2.1.: Percentage changes in the expression of MRP1 in A549 cells following exposure to a range of agents (listed above) for 24 hours. These percentage changes were determined using densitometric analysis of Western blots carried out on lysates of the exposed A549 cells. The numbers 1-3 represent increasing concentrations of each agent which are listed in table 3.1.7.1.

Drug Panel	Percentage change		
	1st concentration	2nd concentration	3rd concentration
Lapatinib*	-60	-80	-70
Erlotinib	110	90	40
Gefitinib	110	140	270
Celecoxib	30	40	-20
Sulindac Sulphide#	50	30	-40
Ibuprofen	50	60	30
Indomethacin	-10	0	-10
Elacridar	260	320	260
17-AAG#	-40	-60	-70

Key:
Indicates successful candidates that were brought forward for testing stability in expression alteration, toxicity and proliferation assay.

Key:
C: untreated
1: 1st concentration of drug
2: 2nd concentration of drug
3: 3rd concentration of drug
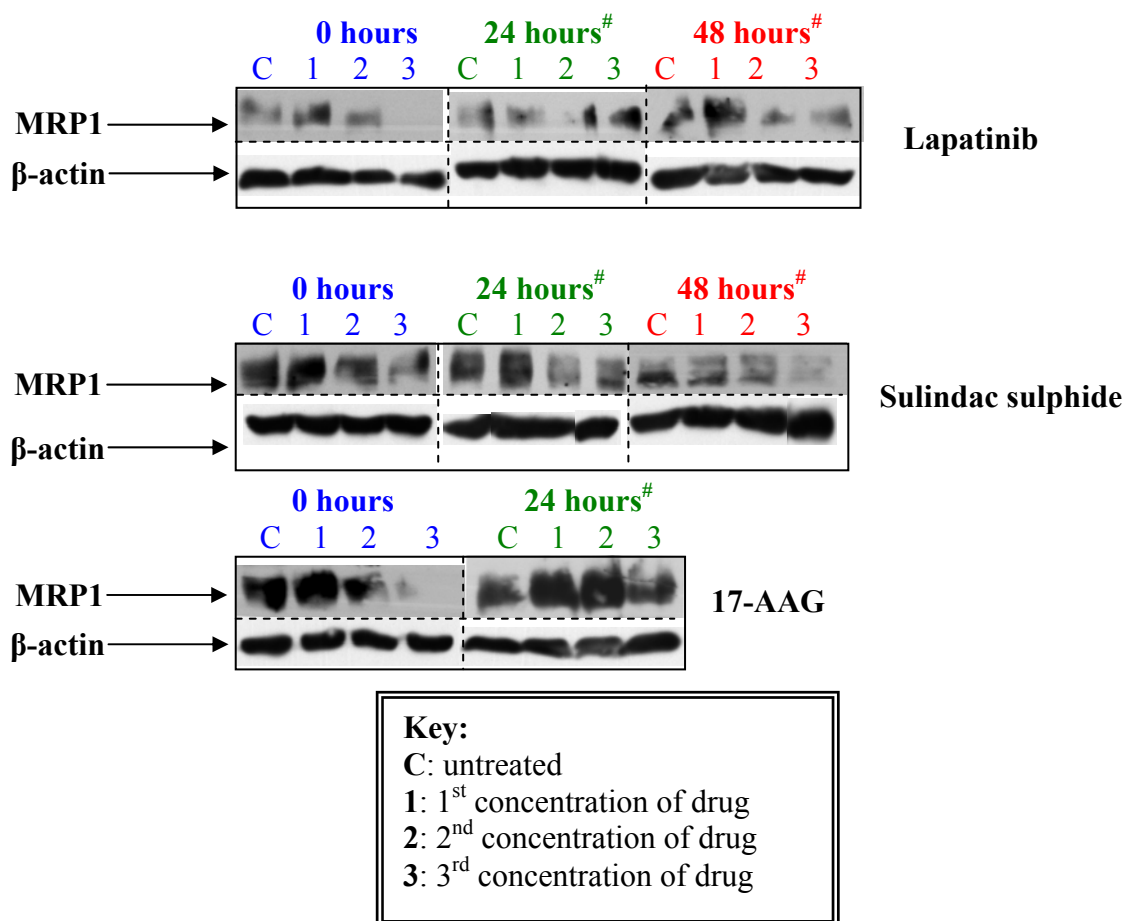
Figure 3.1.6.2.2.: The MRP1 Western blots of A549 treated for 24 hours with lapatinib, sulindac sulphide or 17-AAG. Drug was removed after the 24 hour exposure and the cells were rinsed and fresh media was added. Samples were taken 0 hours, 24 hours and 48 hours after drug removal. The concentrations used in this work are presented in table 3.1.6.1. MRP1 has a molecular weight of 190 kDa and the housekeeping protein, β-actin with a molecular weight of 48 kDa, used as a protein loading control. Each sample was incubated at 37°C for 24 hours in ATCC media containing 5% FBS. Control samples had no drug in their media. 40 μg of sample was loaded into each well. The positive control used was 20 μg of 2008/MRP1 but is not shown (for proof of expression see figure 3.4.1.2.). These Western blots are the result of duplicate or more independent Western blots unless otherwise indicated ([#]).

Table 3.1.6.2.2.: Percentage changes in the expression of MRP1 in A549 cells following exposure to the selected small molecule agents (listed above) for 24 hours with samples taken 24 and 48 hours later (Western blots are preseted in figure 3.1.6.2.2.). These percentage changes were determined using densitometric analysis of Western blots carried out on lysates of the exposed A549 cells. The numbers 1-3 represent increasing concentrations of each agent which are listed in table 3.1.7.1.

Treatment	Percentage change		
	1st concentration	2nd concentration	3rd concentration
Lapatinib 0 hr	28	22	-100
Lapatinib 24 hr	-50	-44	-10
Lapatinib 48 hr	209	-33	-10
Sulindac S. 0 hr	29	-20	-60
Sulindac S. 24 hr	-20	-36	-62
Sulindac S. 48 hr	-45	-39	-80
17-AAG 0 hr	19	-67	-93
17-AAG 24 hr	51	45	16

Combination and scheduled proliferation assays:

Using the two small molecule agents investigated in graph 8.1.6.2.1 (see section 8) and figure 3.1.6.2.2, we examined if the down-regulation of MRP1 protein could sensitise the A549 cells to the MRP1 substrate, vincristine.

We found that the lapatinib combination with vincristine mildly decreased cell proliferation and therefore reduced the IC_{50} of vincristine from 12 ± 4 nM to 6 ± 4 nM (see graph 3.1.6.2.1, 3.1.6.2.4 and table 3.1.6.2.3 for details). In some cases, this potentiation can be attributed to the anti-proliferative potential of lapatinib itself (between 1 and 10 % growth inhibition, see table 3.1.6.2.3 for details). However, with the highest concentration of lapatinib (1 μM), the enhancement was slightly greater than could be attributed to either drug alone (see graph 3.1.6.2.1.**A** for illustration). This would suggest that lapatinib may mildly modulate MRP1. The use of lapatinib in the scheduling assay was less effective. When both replicates are integrated they indicate there is no effect on the IC_{50} value of vincristine (see graph 3.1.6.2.1.**A**, 3.1.6.2.4 and table 3.1.6.2.3 for details).

Sulindac sulphide had a moderate effect on the IC_{50} value of vincristine. It reduced the IC_{50} from 12 ± 4 nM to 8 ± 2 nM at the biologically achievable concentration of 2 μM (see graph 3.1.6.2.2.**A**, 3.1.6.2.4 and table 3.1.6.2.3 for details). While there was a very mild effect using the scheduling assay method, it was not as marked or statistically significant (see graph 3.1.6.2.2.**A** and **B**.). The IC_{50} value remained close to 18 ± 2 nM.

Due to the high cytotoxic nature of 17-AAG in these cells, a set of lower concentrations (0.02, 0.05 and 0.1 μM) were also tested. 17-AAG concentrations above 0.02 μM (35% cell proliferation) were highly toxic (0 – 8% cell proliferation). Therefore, in the combination proliferation assays no change in vincristine toxicity could be observed. However, the enhancement of vincristine cytotoxicity by 0.02 μM 17-AAG was not due to MRP1 modulation but due to the anti-proliferative potential of 17-AAG alone. The low concentrations employed were less toxic when exposed to the A549 cells for only 24 hours of the 5 day period. The doses in graph 3.1.6.2.3.B.1 (0.03, 0.05 and 0.1 μM) had similar affects on growth inhibition (18, 22 and 26%), while the higher concentrations (0.3, 0.5 and 1 μM) in graph 3.1.6.2.3.B.2 inhibited cell proliferation by over 60% (see graph 3.1.6.2.3, 3.1.6.2.4 and table 3.1.6.2.3 for details).

A.

A549: Combination proliferation assay

Legend:
- Vincristine (uM)
- Lap 0.3uM
- Lap 0.5uM
- Lap 1uM

Y-axis: Cell Proliferation (%)
X-axis: Vincristine (nM)

B.

A549: Scheduling proliferation assay

Legend:
- Vincristine (uM)
- Lap 0.3uM
- Lap 0.5uM
- Lap 1uM

Y-axis: Cell Proliferation (%)
X-axis: Vincristine (nM)
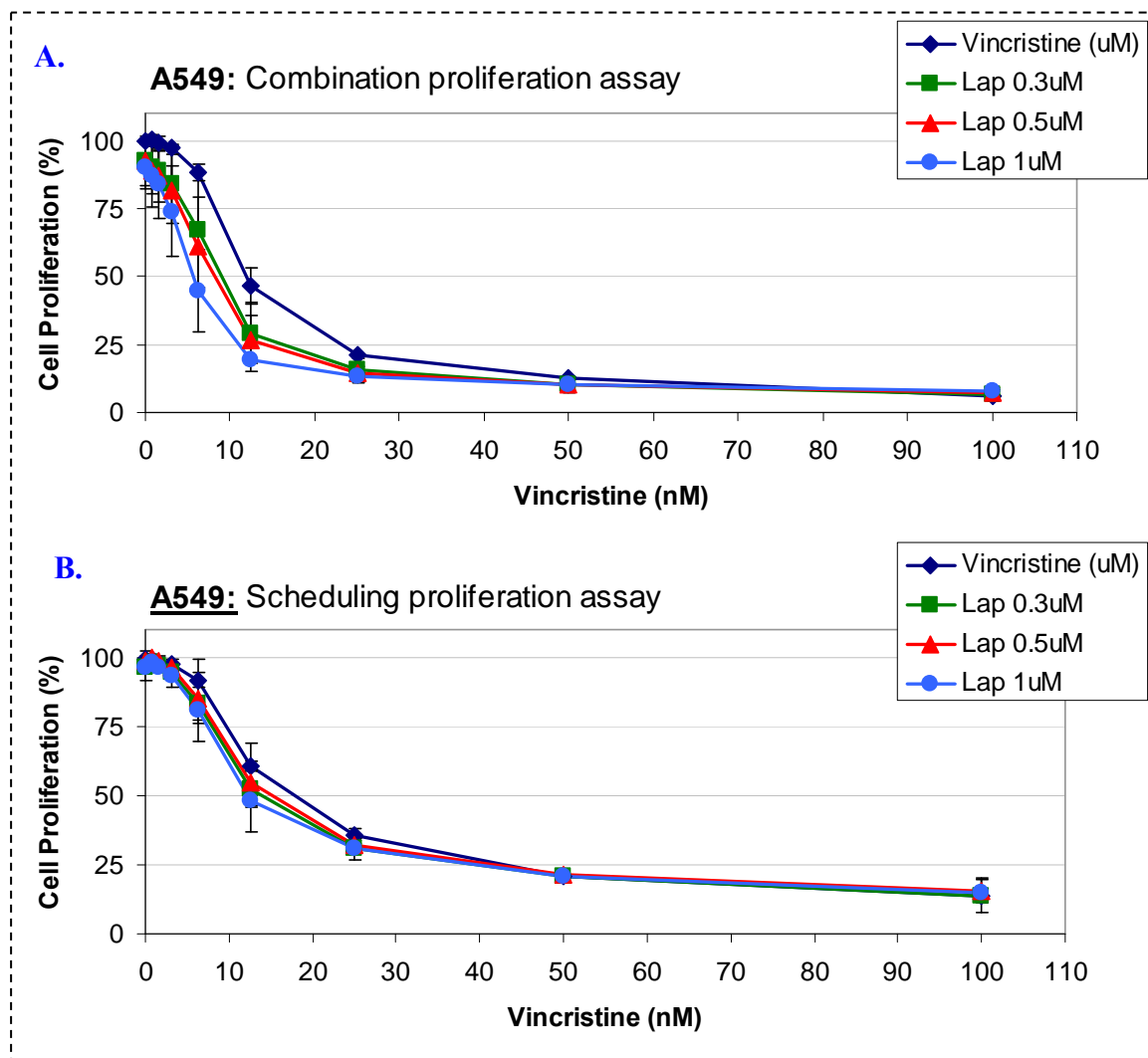
Graph 3.1.6.2.1.: The combination (**A**) and scheduling (**B**) assays of lapatinib and vincristine (◆) in the A549 cell line. An IC_{50} curve of vincristine is combined or scheduled with 0.3 (■), 0.5 (▲) and 1μM (●) lapatinib over a 5 day period. The combination proliferation assay (**A**) is the combination of both drugs together on the cells at the same time. The scheduling proliferation assay (**B**) is when the cells are exposed to lapatinib for 24 hours, removed and vincristine was added for 4 days. Each graph is the result of a duplicate independent determinations with inter-day variations represented by error bars. Table 3.1.6.2.3 below provides the IC_{50} values calculated using calcusyn software.
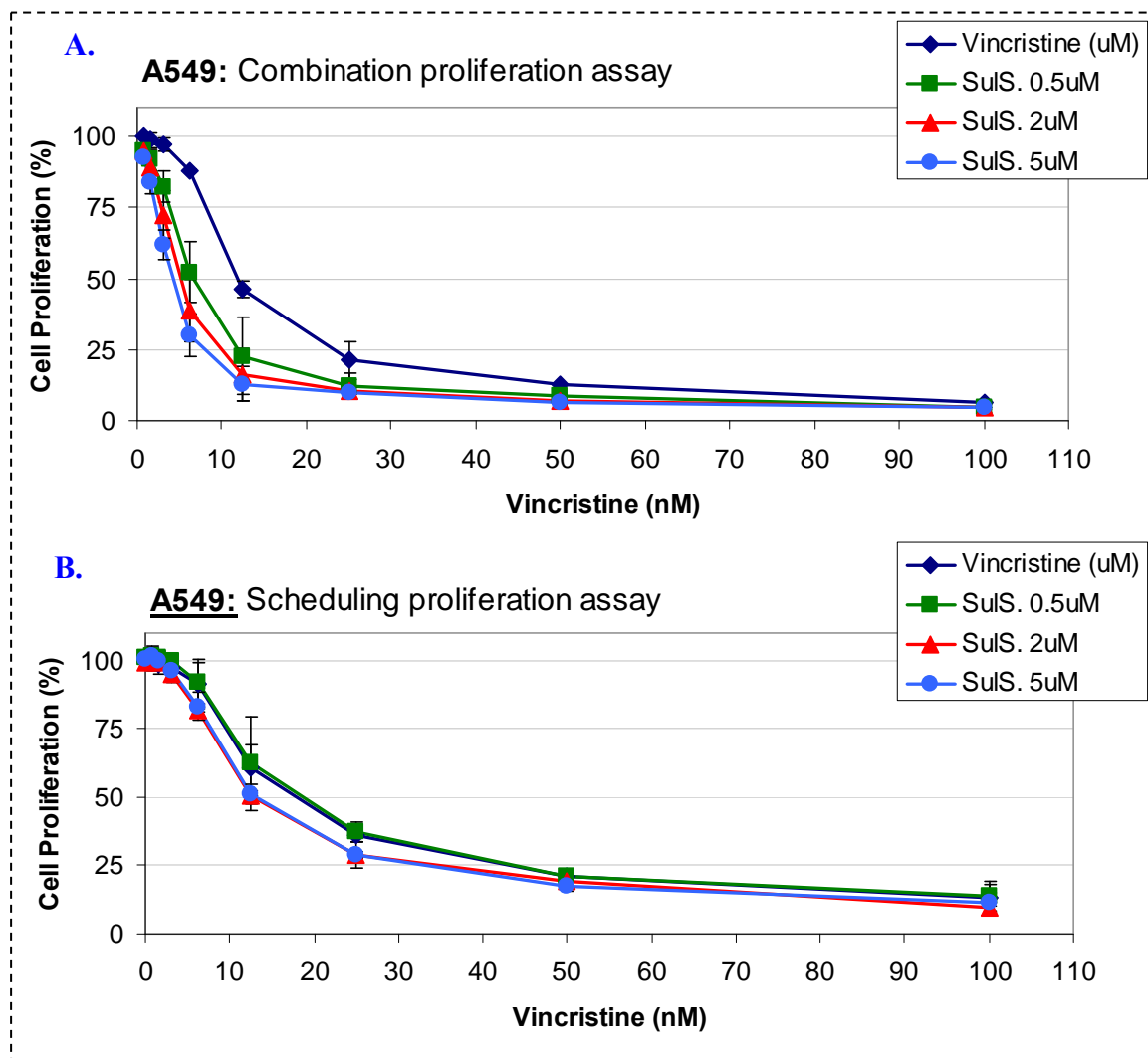
Graph 3.1.6.2.2.: The combination (**A**) and scheduling (**B**) assays of sulindac sulphide and vincristine (◆) in the A549 cell line. An IC_{50} curve of vincristine is combined or scheduled with 0.5 (■), 2 (▲) and 5μM (●) sulindac sulphide over a 5 day period. The combination proliferation assay (**A**) is the combination of both drugs together on the cells at the same time. The scheduling proliferation assay (**B**) is when the cells are exposed to sulindac sulphide for 24 hours, removed and vincristine is added for 4 days. Each graph is the result of a duplicate independent determinations with inter-day variation represented by error bars. Table 3.1.6.2.3 below provides the IC_{50} values calculated using calcusyn software.
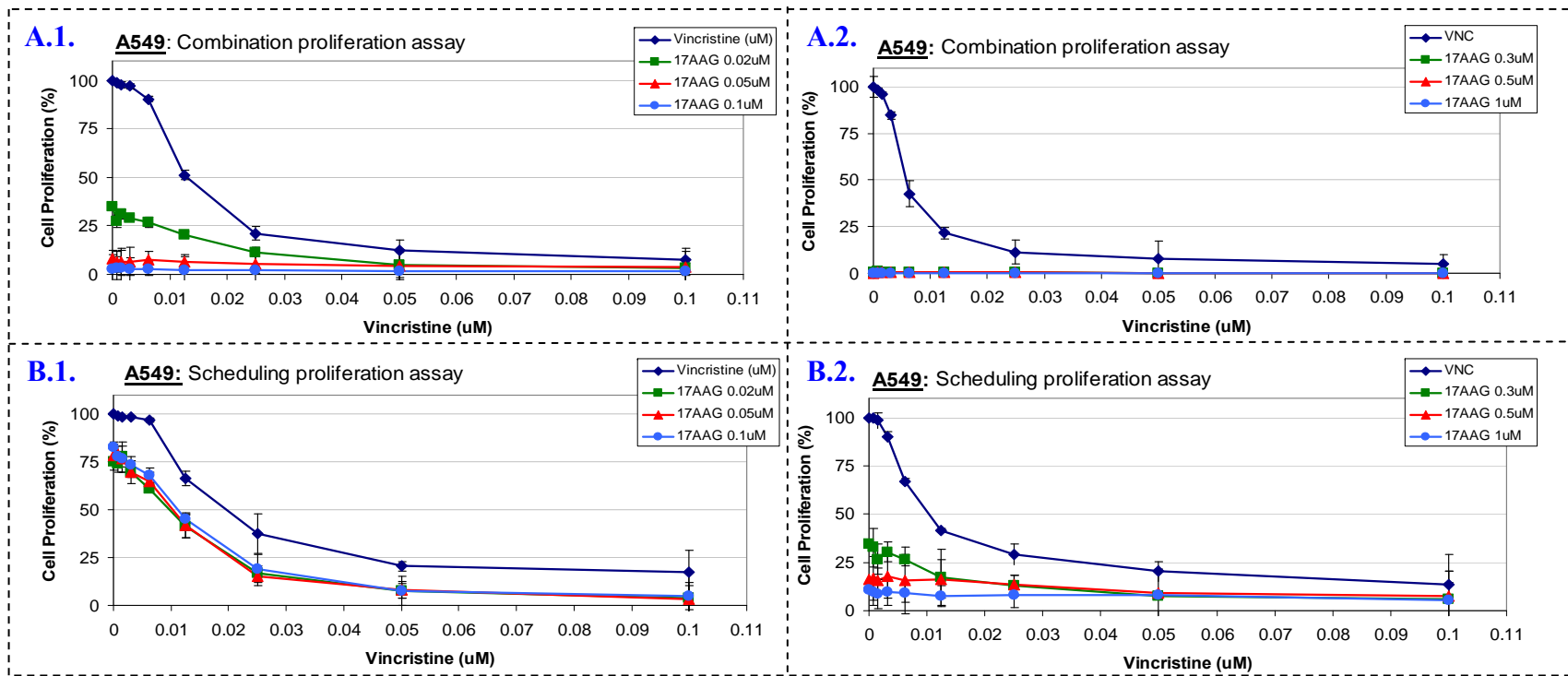
Graph 3.1.6.2.3.: The combination (**A.1** (low dose batch) and **A.2.** (high dose batch)) and scheduling (**B.1.** (low dose batch) and **B.2** (high dose batch)) assays of 17AAG and vincristine (◆) in the A549 cell line. An IC_{50} curve of vincristine is combined (**A.1**.) or scheduled (**B.1**.) with 0.02 (■), 0.05 (▲) and 0.1 μM (●) 17AAG over a 5 day period. An IC_{50} curve of vincristine is combined (**A.2**.) or scheduled (**B.2**.) with 0.3 (■), 0.5 (▲) and 1μM (●) 17AAG over a 5 day period. The combination proliferation assay (**A.1.** and **A.2.**) is the combination of both drugs together on the cells at the same time. The scheduling proliferation assay (**B.1.** and **B.2.**) is when the cells are exposed to 17-AAG for 24 hours, removed and vincristine is added for 4 days. Each graph is the result of a single assay with intra-day variation represented by error bars.

A549: Vincristine IC$_{50}$ values.
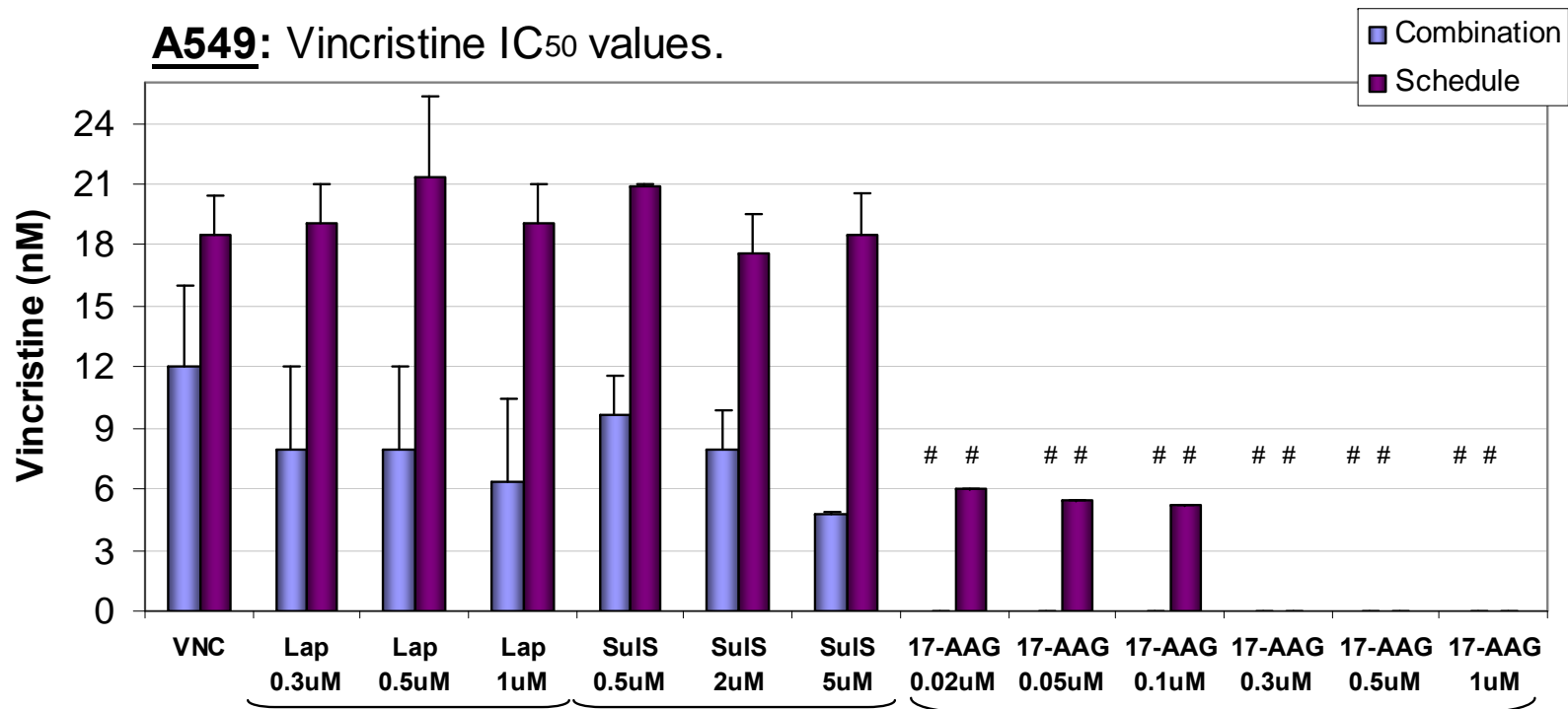
Graph 3.1.6.2.4.: The IC$_{50}$ values of vincristine calculated using Calcusyn software. All values are the average of two independent determinations and the standard deviations of this average is represented by error bars. A star ($^{\#}$) indicates where the small molecule agent caused significant cytotoxicity alone. IC$_{50}$ values below 0.7 μM were not determined and are not presented in this graph. Table 3.1.6.2.3 below outlines percentage cell proliferation for each agents and the change in IC$_{50}$ of vincristine when combined or as part of a scheduled assay.

Table 3.1.6.2.3.: This table provides the percentage cell proliferation and the calculated average IC_{50} values (nM) of vincristine for the duplicate combination and scheduled proliferation assays presented in graphs 3.1.6.2.1, 3.1.6.2.2 and 3.1.6.2.3. These IC_{50} values are illustrated in graph 3.1.6.2.4. All results are due to duplicate independent determination.

A549	Combination assay Cell proliferation (%)	Combination assay IC_{50} (nM)	Scheduling assay Cell proliferation (%)	Scheduling assay IC_{50} (nM)
Vincristine	N/A	12 ± 4	N/A	18 ± 2
Lapatinib 0.3μM	99 ± 9	8 ± 4	96 ± 1	19 ± 2
Lapatinib 0.5 μM	92 ± 9	8 ± 4	99 ± 3	21 ± 4
Lapatinib 1 μM	90 ± 8	6 ± 4	96 ± 4	19 ± 2
Sul. Sulphide 0.5 μM	90 ± 1	9 ± 2	100 ± 1	21 ± 0.2
Sul. Sulphide 2 μM	98 ± 2	8 ± 2	99 ± 1	17 ± 3
Sul. Sulphide 2 μM	98 ± 1	5 ± 1	100 ± 1	18 ± 2
17-AAG 0.02 μM	$^{\$}$35	$^{\$}$< 0.7	$^{\$}$74	$^{\$}$6 ± 0
17-AAG 0.05 μM	$^{\$}$8	$^{\$}$< 0.7	$^{\$}$78	$^{\$}$5 ± 0
17-AAG 0.1 μM	$^{\$}$3	$^{\$}$< 0.7	$^{\$}$82	$^{\$}$5 ± 0
17-AAG 0.3 μM	$^{\$}$0.3	$^{\$}$< 0.7	$^{\$}$34	$^{\$}$< 0.7
17-AAG 0.5 μM	$^{\$}$0.6	$^{\$}$< 0.7	$^{\$}$16	$^{\$}$< 0.7
17-AAG 1 μM	$^{\$}$0	$^{\$}$< 0.7	$^{\$}$11	$^{\$}$< 0.7

Key:

N/A: Not Applicable $:   single determination   <: IC_{50} value lies below the figure indicated

3.1.6.3. BCRP down-regulation

As discussed in 3.1.7., DLKP-SQ/mitox was the BCRP-expressing cell line chosen for this body of work. Figure 3.1.7.1 outlines the BCRP (72kDa) Western blots of DLKP-SQ/mitox cells following a 24 hour exposure to each agent. β -actin (a 48kDa house-keeping protein) was used as a control for protein loading and showed that the lysates were in good condition.

For 2 and 5 µM sulindac sulphide-treated cells (lane 2 – 3) the bands were bigger than the control/untreated (C) bands. This indicated that the BCRP protein expression was upregulated in the presence of this agent. Densitometric analysis of these blots (which is presented as percentage change in table 3.1.8.2) supports this visual finding. This Western blot was not repeated as it did not merit for further testing.

Gefitinib, indomethacin, elacridar and 17-AAG-treated cells (lane 1 – 3) decreased BCRP protein expression when compared to their control bands (C). For all concentrations of elacridar, gefitinib and indomethacin there was a 80 – 70% decrease in BCRP protein expression. 17-AAG had the greatest impact on BCRP protein expression in this cell line. There was a 50, 80 and 70% reduction in protein expression with 0.3, 0.5 and 1 µM exposures for 24 hours.

A number of the small molecule agents had varying effect of on BCRP protein expression. For instance, 0.3 and 0.5 µM erlotinib decreased BCRP expression but increased it at 1 µM. The lowest concentration of celecoxib (0.5 µM) nearly tripled the BCRP expression but 10 µM decreased it (20% reduction). Ibuprofen caused a very similar reaction. A dose of 0.5 µM ibuprofen increased BCRP by 360% but increasing concentrations (2 and 5 µM) caused less of an increase (130% increase) to a decrease (20% decrease) in protein expression. Sulindac sulphide behaved in the opposite manner to both celecoxib and ibuprofen, with 0.5 µM there was a reduction (20% reduction) but 2 and 5 µM caused an increase (30 and 40% increase) in expression. Lapatinib, the final small molecule agent, presented a gradual decrease in BCRP expression. Densitometry was carried out on all the Western blots and is presented in table 3.1.7.2 in the form of percentage changes.

Western blotting and densitometric analysis demonstrated that five small molecule agents, lapatinib, gefitinib, indomethacin, elacridar and 17-AAG, noticably down-regulated the expression of BCRP. To identify if this down-regulation was maintained

following removal of the drug after 24 hours, and if the concentrations used reduced cell proliferation, further Western blots were carried out, as well as short term proliferation assays.

When the DLKP-SQ/mitox cells were exposed to lapatinib for 24 hours in the biological replicate, lapatinib did not reduce the expression of BCRP (this was repeated a number of times). In fact, a slight increase was observed immediately after exposure as well as after a period of 24 and 48 hours in drug-free media (see figure 3.1.6.3.2.).

The reduction in BCRP expression following a 24 hour exposure to gefitinib was repeated and found to remain at the reduced level for 24 and 48 hours after drug removal.

All concentrations of indomethacin caused a reduction in BCRP expression following a 24 hours exposure. Expression levels returned to normal with the lowest concentration after 24 hours in drug-free media and expression recovered for all concentrations after 48 hours in drug-free media (see figure 3.1.6.3.2 for details). In fact, BCRP expression increased slightly after 48 hours in drug-free media.

A dose-dependent reduction in BCRP expression occurred following a 24 hours exposure to elacridar. Expression recovered after 24 and 48 hours in drug-free media (see figure 3.1.6.3.2.).

The largest reduction in BCRP expression was caused by a 24 hour exposure to pharmacologically relevant concentrations of 17-AAG (0.3, 0.5 and 1 μM) (ref: www.rxlistcom). A mild restoration of expression was observed after 24 and 48 hours in drug-free media (see figure 3.1.6.3.2.).

In 6-well plates, with cells seeded at a density of 7×10^4 cells/ml, all concentrations were found to be non-toxic following a 24 hour exposure (see section 8, graphs 8.1.6.3.1.A, B, C, D and E).

Target Protein ‖	Western blot ‖	Summary effect
BCRP (70kDa) β-actin (48kDa)	C 1 2 3	↓ by Lapatinib after 24hr
BCRP (70kDa) β-actin (48kDa)		↔ to ↓ by Erlotinib after 24hr[#]
BCRP (70kDa) β-actin (48kDa)		↓ by Gefitinib after 24hr
BCRP (70kDa) β-actin (48kDa)		↑ to ↓ by Celecoxib after 24hr[#]
BCRP (70kDa) β-actin (48kDa)		↑ by Sulindac S. after 24hr[#]
BCRP (70kDa) β-actin (48kDa)		↑ to↓ by Ibuprofen after 24hr[#]
BCRP (70kDa) β-actin (48kDa)		↓ by Indomethacin after 24hr
BCRP (70kDa) β-actin (48kDa)		↓ by Elacridar after 24hr
BCRP (70kDa) β-actin (48kDa)		↓ by 17-AAG after 24hr

Key:

C:	Control / untreated	↑:	Protein expression up-regulation
1:	1st drug concentration	↓:	Protein expression down-regulation
2:	2nd drug concentration	↔:	No change in protein expression
3:	3rd drug concentration	#:	represents single Western blots

Figure 3.1.6.3.1.: The BCRP Western blots of DLKP-SQ/mitox treated for 24 hours with a panel of agents listed in table 3.1.8.1. The concentrations used in this work are presented in table 3.1.6.1. BCRP has a molecular weight of 70 kDa and the housekeeping protein, β-actin with a molecular weight of 48 kDa, used as a protein loading control. Each sample was incubated at 37°C for 24 hours in ATCC media containing 5% FBS. Control samples had no drug in their media. The positive control used was HL60/mxr (see figure 3.4.1.1.). The densitometric analysis of these blots is represented in table 3.1.8.2. Due to the level of BCRP expression in these cells only 4 μgs of protein was initially loaded but this was increased to 8 μg (as seen in the indomethacin, elacridar and 17-AAG Western blots) in order to obtain a band consistency in the β-actin. These Western blots are representative of two or more independent biological replicates unless otherwise indicated ([#]).

Table 3.1.6.3.2.: Percentage changes in the expression of BCRP in DLKP-SQ/mitox cells following exposure to a range of agents (listed above) for 24 hours. These percentage changes were determined using densitometric analysis of Western blots carried out on lysates of the exposed DLKP-SQ/mitox cells. The numbers 1-3 represent increasing concentrations of each agent which are listed in table 3.1.8.1 above.

Drug Panel	Percentage Change		
	1st concentration	2nd concentration	3rd concentration
Lapatinib[#]	-30	-45	-45
Erlotinib	-20	-40	90
Gefitinib[#]	-20	-35	-25
Celecoxib	170	0	-20
Sulindac Sulphide	-20	30	40
Ibuprofen	360	130	-40
Indomethacin[#]	-40	-40	-30
Elacridar[#]	-35	-35	-40
17-AAG[#]	-50	-80	-70

Key:
[#] Indicates successful candidates that were brought forward for testing stability in expression alteration, toxicity and proliferation assay.
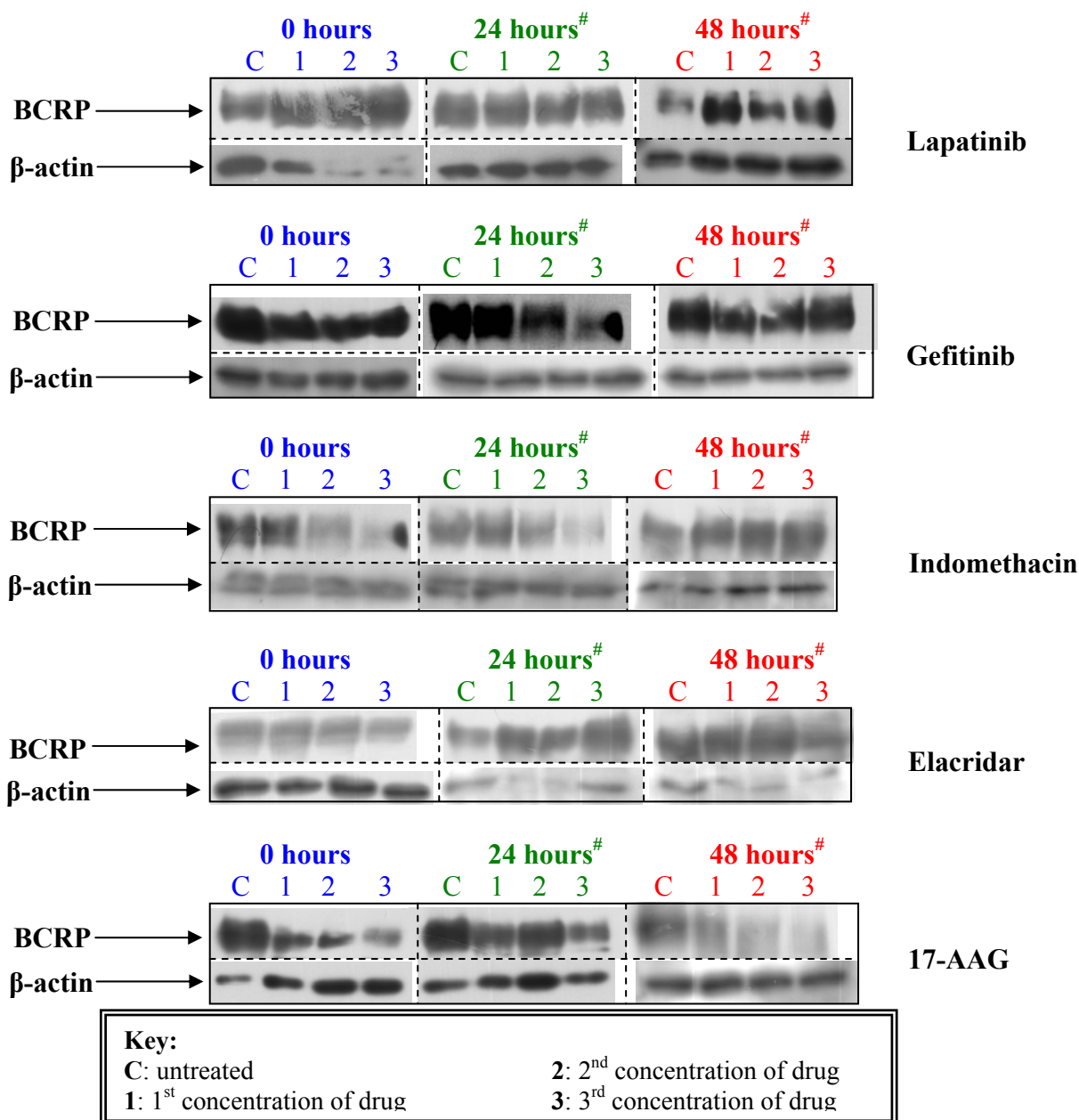
Figure 3.1.6.3.2.: The BCRP Western blots of DLKP-SQ/mitox treated for 24 hours with lapatinib, gefitinib, indomethacin, elacridar or 17-AAG. Drug was removed after the 24 hour exposure and the cells were rinsed and fresh media was added. The concentrations used in this work are presented in table 3.1.6.1. Samples were taken 0 hours, 24 hours and 72 hours after drug removal. BCRP has a molecular weight of 72 kDa and the housekeeping protein, β-actin with a molecular weight of 48 kDa, used as a protein loading control. Each sample was incubated at 37°C for 24 hours in ATCC media containing 5% FBS. Control samples had no drug in their media. 8 μg of sample was loaded into each well. The positive control used was 20 μg DLKP-SQ/mitox. These Western blots are representative of two or more independent biological replicates unless otherwise indicated ([#]).

Combination and scheduled proliferation assays

Using the five small molecule agents investigated in graph 8.1.6.3.1 (see section 8) and figure 3.1.6.3.2, we examined if the down-regulation of BCRP protein could sensitise the DLKP-SQ/mitox cells to the BCRP substrate, SN38.

The use of lapatinib in straight combination and scheduling proliferation assays was highly successful. The IC_{50} value of SN38 in the combination assay dropped from 45 ± 7 nM to 1 ± 0.1 nM with only 0.5 µM lapatinib (see graph 3.1.6.3.1.A, 3.1.6.3.5 and table 3.1.6.3.2 for details). The scheduling assay was also very successful; it reduced the IC_{50} of SN38 from 60 ± 10 nM to 2 ± 0 nM with the amount of lapatinib (1µM) (see graph 3.1.6.3.1.B, 3.1.6.3.5 and table 3.1.6.3.2 for details). All concentrations of lapatinib caused less than 10% cell growth inhibition.

Gefitinib was also highly effective in combination with SN38. A concentration of 1µM gefitinib reduced SN38's IC_{50} value from 45 ± 7 nM to 3 ± 0.7 nM (see graph 3.1.6.3.2.A, 3.1.6.3.5 and table 3.1.6.3.2 for details). However, the scheduling assay was not as effective. The IC_{50} was reduced from 60 ± 10 nM to 41 ± 3 nM (see graph 3.1.6.3.2.B, 3.1.6.3.5 and table 3.1.6.3.2 for details). The standard deviations for the scheduling proliferation assay IC_{50}'s are such that the strength of these results is weakened considerably. All concentrations of gefitinib used, caused less than 5% cell growth inhibition.

The pre-treatment of DLKP-SQ/mitox cells with indomethacin had no affect on the anti-proliferative potential of SN38. The presence of indomethacin did not heighten the cytotoxicity of SN38 in these cells. All concentration of indomethacin were non-toxic (see graph 3.1.6.3.3, 3.1.6.3.5 and table 3.1.6.3.2 for details). All concentrations of indomethacin used caused less than 6% cell growth inhibition.

Similar to lapatinib, the combination and scheduling proliferation assay of elacridar and SN38 on the DLKP-SQ/mitox cell line resulted in significant enhancement of SN38's cytotoxicity. There was a dramatic reduction in the IC_{50} value of SN38 in both assay types. A concentration of 0.5 µM elacridar reduced the IC_{50} value of SN38 from 45 ± 7 nM to 2 ± 0.6 nM (see graph 3.1.6.3.4.A, 3.1.6.3.5 and table 3.1.6.3.2 for details) when both drugs were simultaneously combined on this BCRP cell line. The same dose of elacridar (0.5 µM) had a near identical impact on the IC_{50} of SN38 in the scheduled proliferation assay; causing a reduction from 60 ± 10 nM to 3 ± 0 nM (see graph 3.1.6.3.4.B, 3.1.6.3.5 and table 3.1.6.3.2 for details).

The last small molecule agent tested was 17-AAG. Due to the cytotoxicity of 17-AAG on this cell line, DLKP-SQ/mitox, a lower set of concentrations (0.02, 0.05 and 0.1 µM) were also tested. The presence of 0.05 and 0.1 µM 17-AAG dramatically enhanced the cytotoxicity of SN38; reducing its' IC_{50} from 45 ± 7 nM to 12 ± 2 and 8 ± 3 nM. These concentrations of 17-AAG caused 3% and 23% cell growth inhibition. Concentrations above 0.1 µM were highly toxic alone and therefore the change in SN38s' IC_{50} was solely due to this. All concentrations of 17-AAG were less toxic when exposed to the DLKP-SQ/mitox cells for only 24 hours of the 5 day period. The low concentrations of 17-AAG (0.02, 0.05, and 0.1 µM) caused less than 10% cell growth inhibition while the higher concentrations (0.3, 0.5 and 1 µM) resulted in broader inhibition (32, 38 and 63%). Similar to the combination proliferation assays, 0.05 and 0.1 µM 17-AAG enhanced the anti-proliferative potential of SN38 (from 60 ± 10 nM to 44 ± 11 and 23 ± 3 nM) using the scheduling assay method. The concentrations 0.3, 0.5 and 1µM of 17-AAG also enhanced the cytotoxicity of SN38; from 60 ± 11 nM to 5, 1 and less than 0.7 nM.
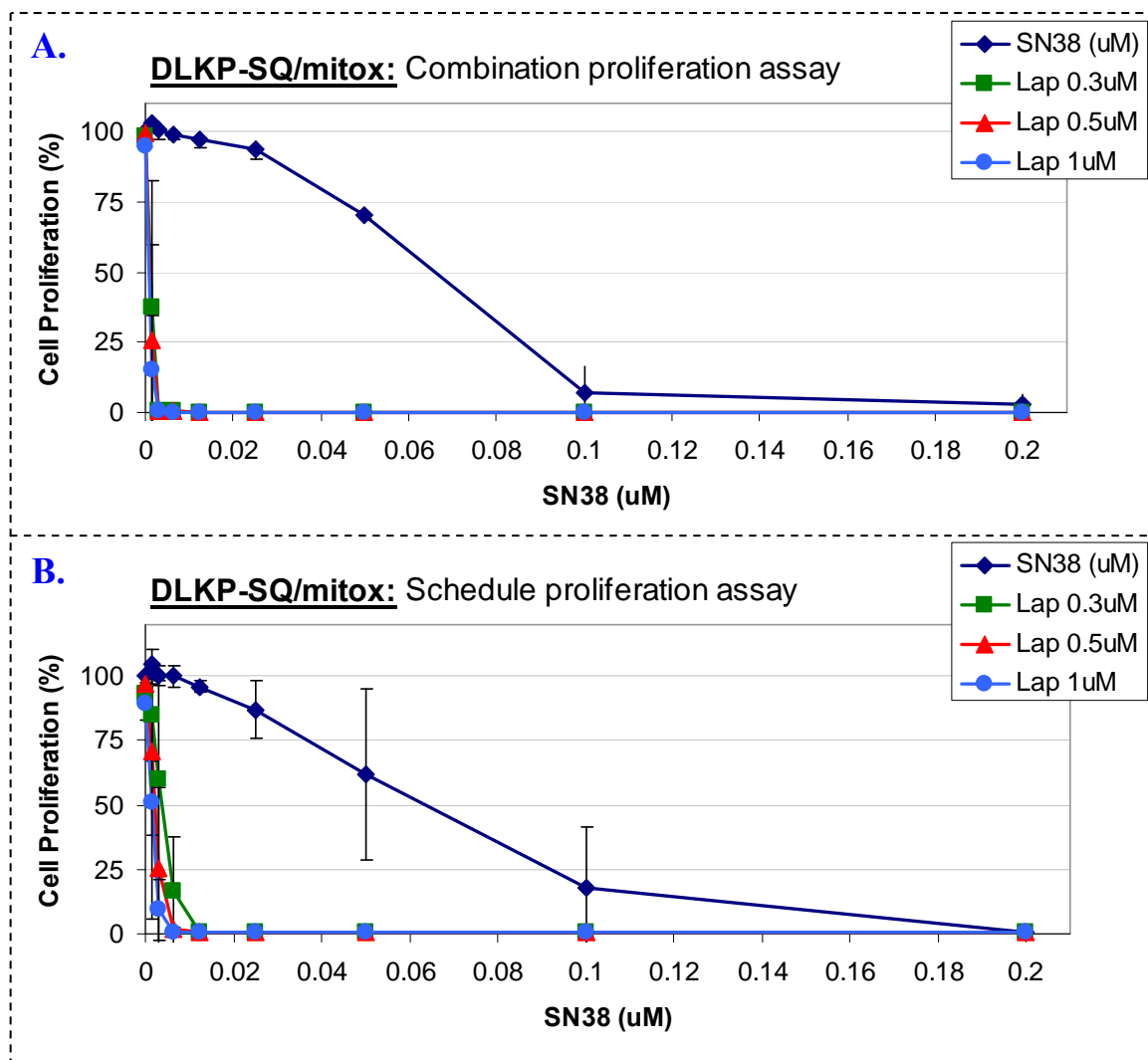
Graph 3.1.6.3.1.: The combination (**A**) and scheduling (**B**) assays of lapatinib and SN38 (◆) in the DLKP-SQ/mitox cell line. An IC_{50} curve of SN38 is combined or scheduled with 0.3 (■), 0.5 (▲) and 1μM (●) lapatinib over a 5 day period. The combination proliferation assay (**A**) is the combination of both drugs together on the cells at the same time. The scheduling proliferation assay (**B**) is when the cells are exposed to lapatinib for 24 hours, removed and SN38 is added for 4 days. These graphs are the result of duplicate independent determinations with inter-day variation represented by error bars. Table 3.1.6.3.2 provides the IC_{50} values calculated using calcusyn software.
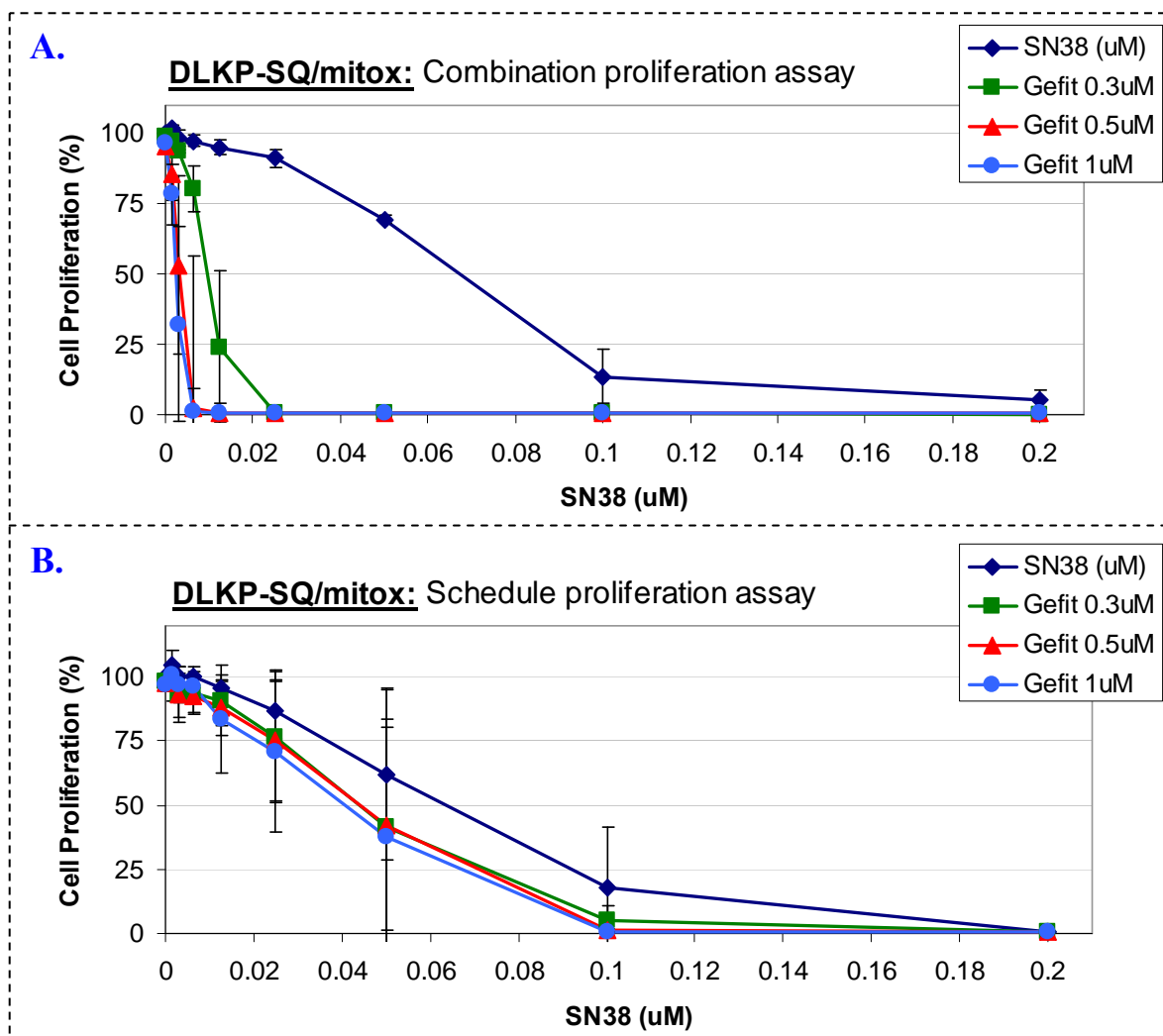
Graph 3.1.6.3.2.: The combination (**A**) and scheduling (**B**) assays of gefitinib and SN38 (◆) in the DLKP-SQ/mitox cell line. An IC$_{50}$ curve of SN38 is combined or scheduled with 0.3 (■), 0.5 (▲) and 1μM (●) gefitinib over a 5 day period. The combination proliferation assay (**A**) is the combination of both drugs together on the cells at the same time. The scheduling proliferation assay (**B**) is when the cells are exposed to gefitinib for 24 hours, removed and SN38 is added for 4 days. These graphs are the result of duplicate independent determinations with inter-day variation represented by error bars. Table 3.1.6.3.2 provides the IC$_{50}$ values calculated using calcusyn software.
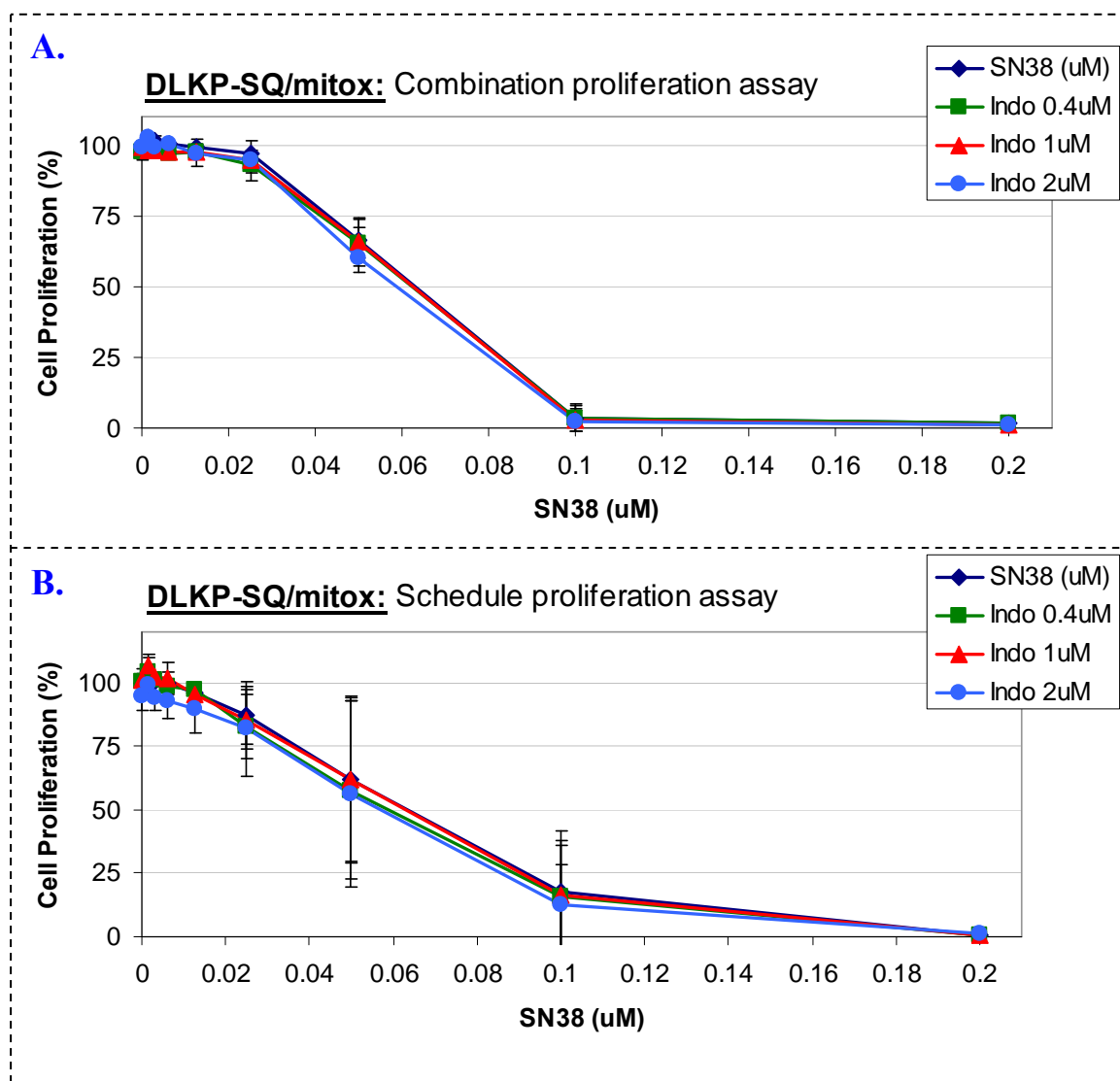
Graph 3.1.6.3.3.: The combination (**A**) and scheduling (**B**) assays of indomethacin and SN38 (◆) in the DLKP-SQ/mitox cell line. An IC_{50} curve of SN38 is combined or scheduled with 0.4 (■), 1 (▲) and 2μM (●) indomethacin over a 5 day period. The combination proliferation assay (**A**) is the combination of both drugs together on the cells at the same time. The scheduling proliferation assay (**B**) is when the cells are exposed to indomethacin for 24 hours, removed and SN38 is added for 4 days. These graphs are the result of duplicate independent determinations with inter-day variation represented by error bars. Table 3.1.6.3.2 provides the IC_{50} values calculated using calcusyn software.
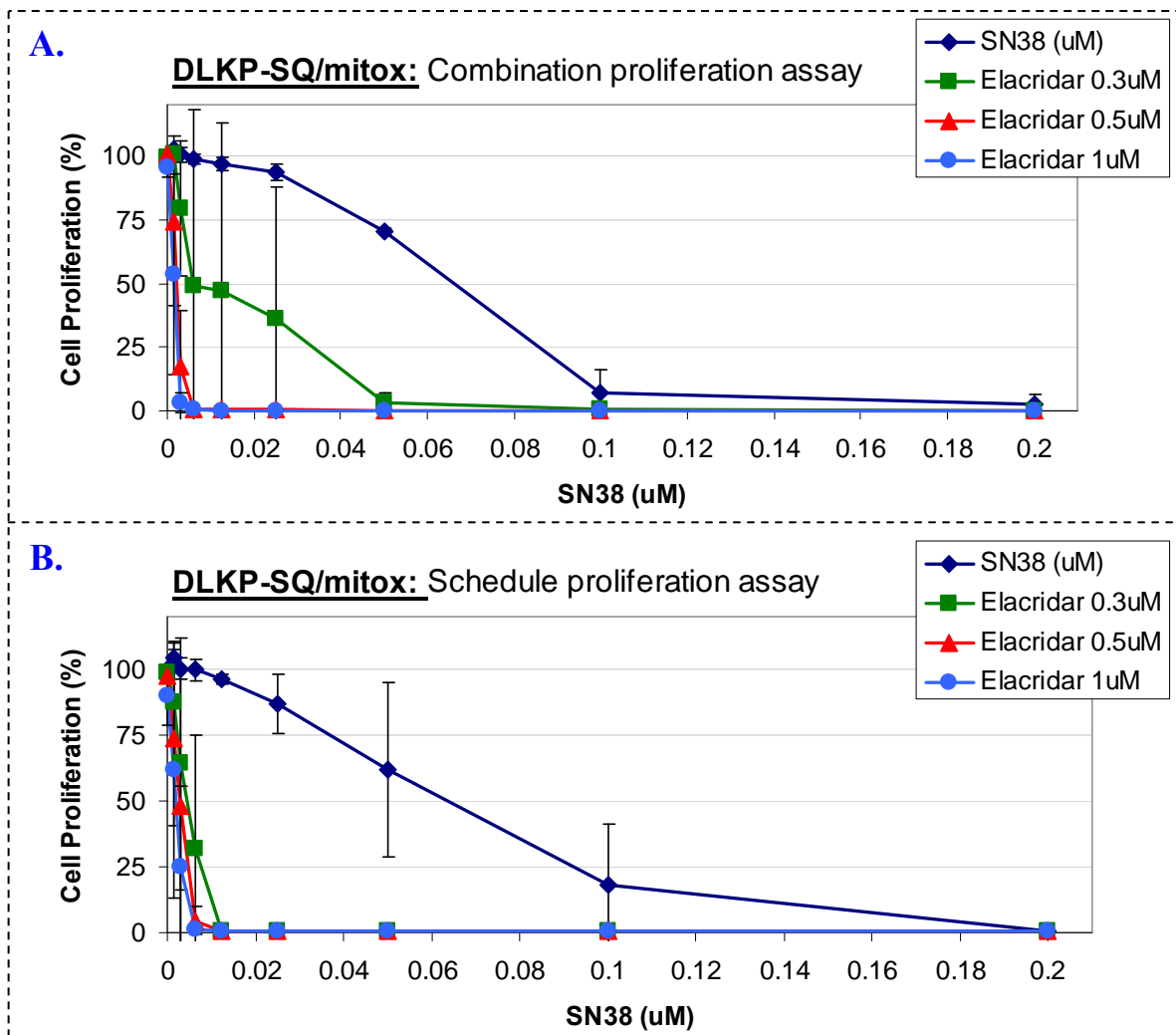
Graph 3.1.6.3.4.: The combination (**A**) and scheduling (**B**) assays of elacridar and SN38 (◆) in the DLKP-SQ/mitox cell line. An IC_{50} curve of SN38 is combined or scheduled with 0.3 (■), 0.5 (▲) and 1μM (●) elacridar over a 5 day period. The combination proliferation assay (**A**) is the combination of both drugs together on the cells at the same time. The scheduling proliferation assay (**B**) is when the cells are exposed to elacridar for 24 hours, removed and SN38 is added for 4 days. These graphs are the result of duplicate independent determinations with inter-day variation represented by error bars. Table 3.1.6.3.2 below provides the IC_{50} values calculated using calcusyn software.
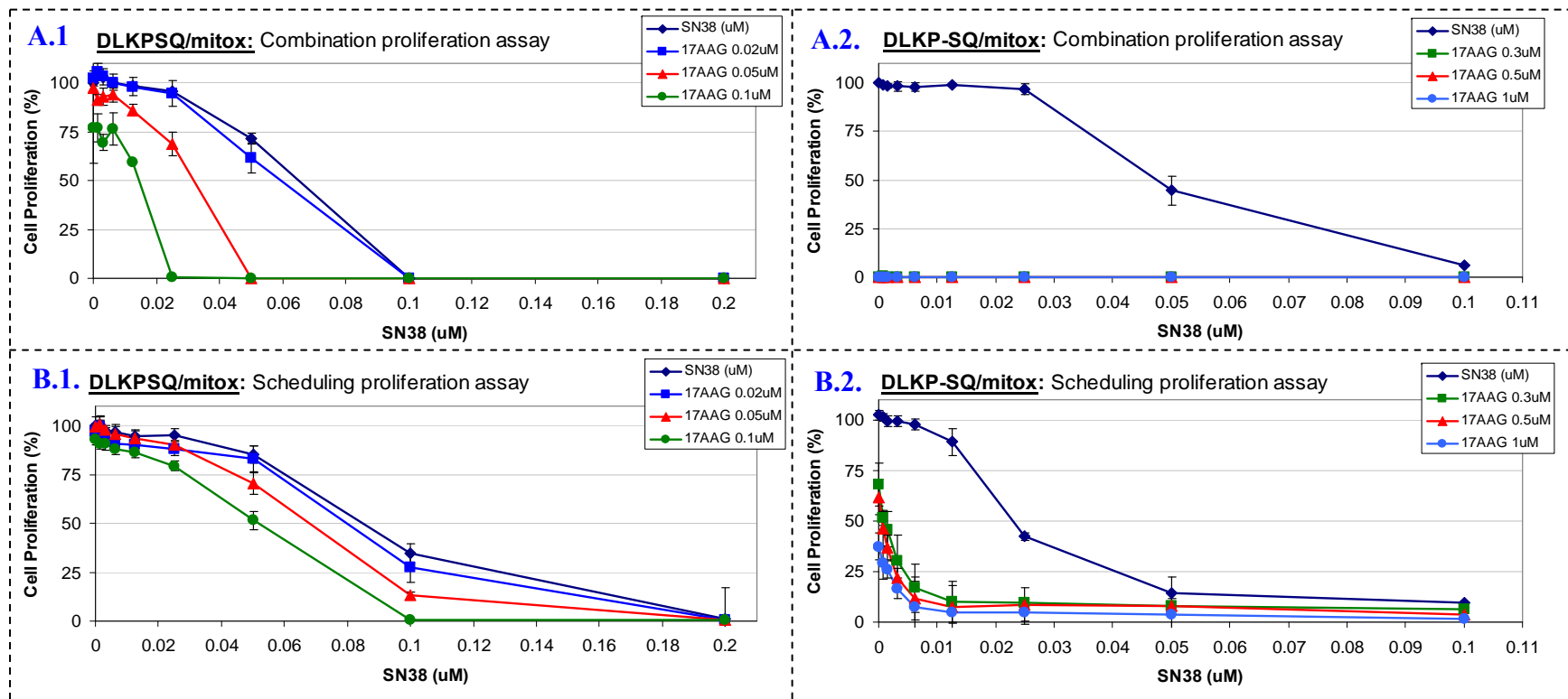
Graph 3.1.6.3.5.: The combination (**A**) and scheduling (**B**) assays of 17-AAG and SN38 (◆) on the DLKP-SQ/mitox cell line. An IC$_{50}$ curve of SN38 is combined (**A.1.**) or scheduled (**B.1.**) with 0.02 (■), 0.05 (▲) and 0.1 μM (●) 17-AAG over a 5 day period. An IC$_{50}$ curve of SN38 is combined (**A.2.**) or scheduled (**B.2.**) with 0.3 (■), 0.5 (▲) and 1μM (●) 17-AAG over a 5 day period. The combination proliferation assay (**A.1** and **A.2.**) is the combination of both drugs together on the cells at the same time. The scheduling proliferation assay (**B.1.** and **B.2.**) is when the cells are exposed to 17-AAG for 24 hours, removed and SN38 is added for 4 days. Each graph is the result of a single assay with intra-day variation represented by error bars. Table 3.1.6.3.2 below provides the IC$_{50}$ values calculated using calcusyn software.
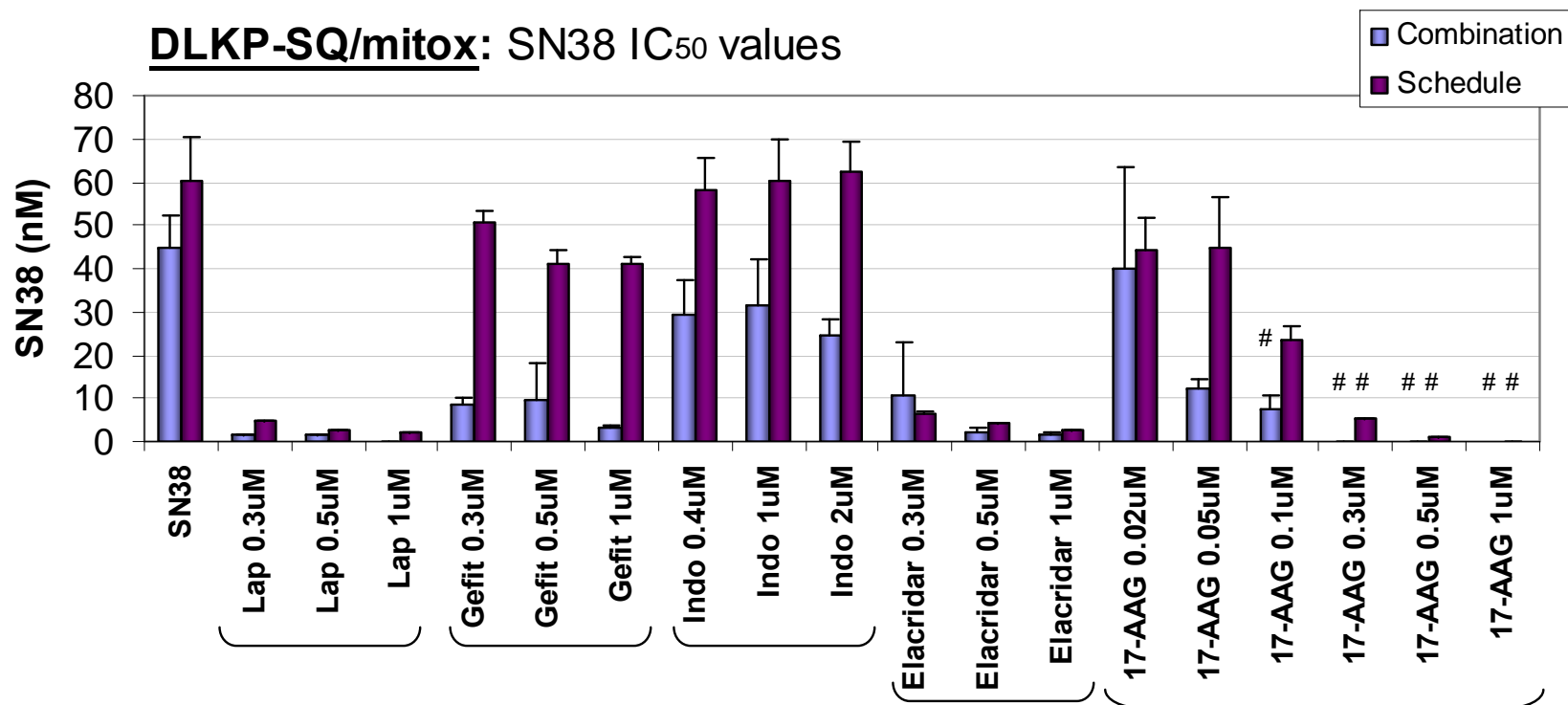
Graph 3.1.6.3.6.: The IC_{50} values calculated using Calcusyn software. All values are the average of two independent determinations and the standard deviations of this average is represented by error bars. A star ($^{\#}$) indicates where the small molecule agent caused significant cytotoxicity alone. Table 3.1.6.3.2 outlines that percentage cell proliferation for each agents and the change in IC_{50} of vincristine when combined or as part of a scheduled assay.

Table 3.1.6.3.2.: This table provides the calculated average percentage cell proliferation for each agent alone and the IC_{50} values (nM) for the duplicate combination and scheduled proliferation assays presented in graphs 3.1.6.3.2, 3.1.6.3.3 and 3.1.6.3.4. These IC_{50}s were calculated using calcusyn software. All values presented are the results of independent duplicate determinations plus and minus their standard deviations.

DLKP-SQ/mitox	Combination assay Cell Proliferation (%)	Combination assay IC_{50} (nM)	Scheduling assay Cell Proliferation (%)	Scheduling assay IC_{50} (nM)
SN38	N/A	$^{\Psi}45 \pm 7$	N/A	$^{\Psi}60 \pm 10$
Lapatinib 0.3 μM	93 ± 4	2 ± 0.2	99 ± 0.4	4 ± 0.3
Lapatinib 0.5 μM	96 ± 0.3	1 ± 0.1	99 ± 0.4	3 ± 0
Lapatinib 1 μM	89 ± 6	< 0.7	95 ± 0.3	2 ± 0
Gefitinib 0.3 μM	98 ± 1.4	8 ± 2	99 ± 0.3	51 ± 3
Gefitinib 0.5 μM	97 ± 1.7	10 ± 8	95 ± 0.1	41 ± 3
Gefitinib 1 μM	97 ± 2.3	3 ± 0.7	96 ± 1.3	41 ± 2
Indomethacin 0.4 μM	100 ± 3	29 ± 7	96 ± 0.3	58 ± 7
Indomethacin 1 μM	100 ± 4	31 ± 11	99 ± 0.7	60 ± 9
Indomethacin 2 μM	95 ± 6	24 ± 3	98 ± 0.03	62 ± 7
Elacridar 0.3 μM	99 ± 1	10 ± 12	99 ± 0.7	7 ± 0.4
Elacridar 0.5 μM	98 ± 1	2 ± 1	100 ± 0.3	4 ± 0.2
Elacridar 1 μM	90 ± 12	1 ± 1	96 ± 4	3 ± 0
17-AAG 0.02 μM	$^{\$}102$	40 ± 23	97	44 ± 7

DLKP-SQ/mitox	Combination assay Cell Proliferation (%)	Combination assay IC_{50} (nM)	Scheduling assay Cell Proliferation (%)	Scheduling assay IC_{50} (nM)
17-AAG 0.05 μM	[$]97	12 ± 2	99	44 ± 11
17-AAG 0.1 μM	[$]77	8 ± 3	90	23 ± 3
17-AAG 0.3 μM	[$]0	< 0.7	[$]68	[$]5
17-AAG 0.5 μM	[$]0	< 0.7	[$]62	[$]1
17-AAG 1 μM	[$]0	< 0.7	[$]37	[$]< 0.7

Key:

N/A   not applicable

Ψ   Values are the average of 8 independent determinations

[$]   Value are the result of a single assay determination..

3.2. Cellular Pharmacokinetics of Epirubicin

Two serum plasma proteins, serum albumin and α_1-acid glycoprotein (AAG), are important transport proteins for the majority of cancer drugs. Albumin has the highest affinity for drugs with acidic or strong electronegative functional groups. Albumin has been shown to be crucial for the distribution, elimination and effectiveness of many conventional pharmaceuticals and anti-cancer drugs including anthracyclines and taxanes etc. [50] [390].

Serum albumin is a highly soluble single polypeptide that is present in the plasma at an approximate concentration of 40mg/ml (600μM). AAG is a 40kDa protein present in the plasma at an approximate concentration of 0.8mg/ml (20μM). For a brief review on each plasma protein please refer to section 1.3.5 and 1.3.6.

Protein-bound drug is generally considered to be too large to pass through most cell membranes to exert pharmacological actions and therefore, limits their cytotoxic potential. In 1998, Sham HL., *et al,* [60] found that plasma protein drug binding can reduce the *in vitro* potency of a compound, ABT-378 (a highly potent inhibitor of the human immunodeficiency virus protease), in the presence of exogenously added serum.

3.2.1 Free versus Bound drug

To determine if drug-protein binding was affected the accumulation of epirubicin in normal versus cancer cells, we first examined the levels of free versus bound anthracycline in solutions with or without the serum proteins, albumin and AAG. We selected a Vivaspin 2 ultrafiltration membranes with molecular weight cut off of 20,000Da, supplied by Sartorius. Analysis indicated that the membrane material (cellulose triacetate) had high affinity for free epirubicin and this was taken into consideration when calculating the proportion of bound and unbound epirubicin. The formulae for calculating the amount of protein-free drug bound to the membrane, and the percentage of free and bound drug was described in section 2.12.1. with the extraction method described in section 2.12.3.2.

3.2.1.1. Free versus bound drug in solution containing serum proteins.

In this section, we used membrane filters to separate out the free and bound drug in various solutions and in the presence of foetal calf serum, serum albumin or α_1-acid glycoprotein (AAG). Initial testing demonstrated that the filter membrane material had high affinity for unbound epirubicin and this was exploited to allow calculation of the levels of free and bound epirubicin.

As expected, we found that over 99% of epirubicin was free in solutions of water (UHP) and PBS, while 94% was free in cell growth media (ATCC). As depicted in graphs 3.2.1.1.2 and 3.2.1.1.3 increasing levels of FCS and serum albumin resulted in a concentration-dependent increase in the percentage of bound epirubicin (epirubicin binding to FCS increased from 6% up to 100% and from 6% to 80% in the presence of serum albumin). However, while an increase in epirubicin binding was observed in the presence of AAG (graph 3.2.1.1.4) the trend was not as dramatic (epirubicin binding increased from 6% to 14% in the presence of increasing levels of AAG). This was also expected as the concentrations of AAG used in this experiment are significantly lower than the concentrations of serum albumin.

The concentrations of albumin and AAG were chosen to correlate with the amount present in serum, for example, 10% of FCS contains 40 mg/ml of albumin and 0.8 mg/ml of AAG. The total (ng/ml) is the amount of epirubicin that was spiked into each solution. The retentate (ng/ml) is the bound epirubicin that remains above the membrane. The filtrate (ng/ml) is the free epirubicin that passed through the membrane without sticking to it while the membrane (ng/ml) is the amount of epirubicin that was not protein bound but that stuck to the membrane material. For an example of calculation working please refer to section 2.12.1.

The portion of free versus bound epirubicin in a range of medium.
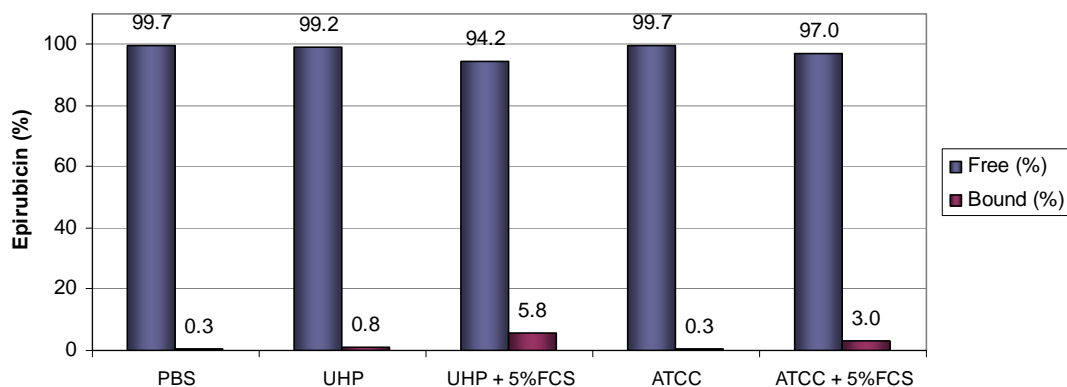
Graph 3.2.1.1.1.: Illustrates the proportion of free and bound epirubicin in solutions containing or lacking foetal calf serum (FCS). A concentration of 2 μM or 1.16 mg/ml of epirubicin was used in this experiment. This graph represents a single determination. The table below depicts the values (epirubicin ng) used to calculate the percentage of free and bound epirubicin in this graph.

Table 3.2.1.1.1.: Raw data for the calculation of the percentage free versus bound epirubicin in a variety of solutions.

Sample	Total (ng)	Retentate (ng)	Filtrate (ng)	Membrane (ng)	Free (%)	Bound (%)
PBS	1160	3	453	704	99.7	0.3
UHP	1160	9	1	1150	99.2	0.8
UHP + 5 % FCS	1160	67	48	1046	94.2	5.8
Cell growth media	1160	4	32	1124	99.7	0.3
Cell growth media + 5 % FCS	1160	34	105	1021	97.0	3.0

156
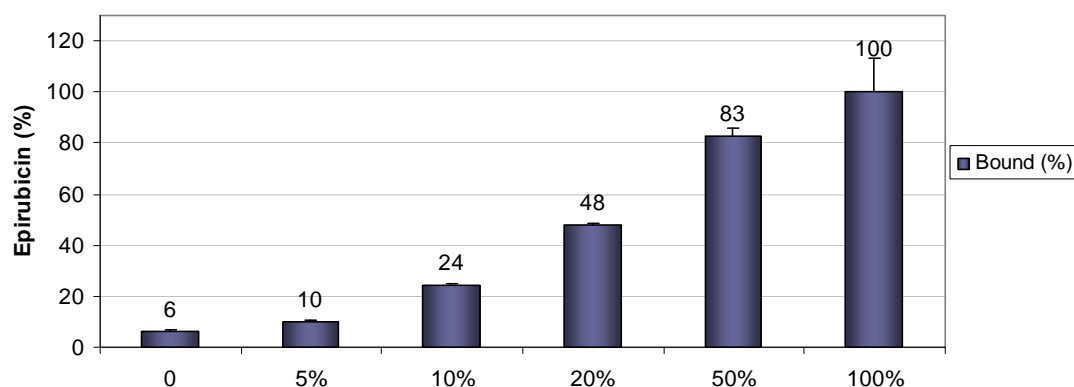
Foetal Calf Serum

Graph 3.2.1.1.2.: Illustrates the proportion of bound epirubicin in cell growth media in the presence of increasing levels of foetal calf serum (FCS). A concentration of 2 µM or 1.16 mg/ml epirubicin was used. This graph represents duplicate intraday results. The table below depicts the values (epirubicin (ng)) used to calculate the percentage of free and bound epirubicin in this graph.

Table 3.2.1.1.2.: Raw data for the calculation of free versus bound epirubicin, plus and minus their standard deviations (±), in cell growth media in the presence of increasing levels of foetal calf serum (FCS).

Foetal calf serum	Total (ng)	Retentate (ng)	Filtrate (ng)	Membrane (ng)	Bound (%)	Free (%)
0 %	1160	72	28	1060	6.2 ± 1	93.8 ± 1
5 %	1160	115	76	969	9.9 ± 0	90.1 ± 0
10 %	1160	284	207	669	24.5 ± 0	75.5 ± 0
20 %	1160	555	246	359	47.8 ± 0	52.2 ± 0
50 %	1160	959	196	4	82.7 ± 3	17.3 ± 3
100 %	1160	1160	0	0	100 ± 13	0 ± 13

Serum Albumin.
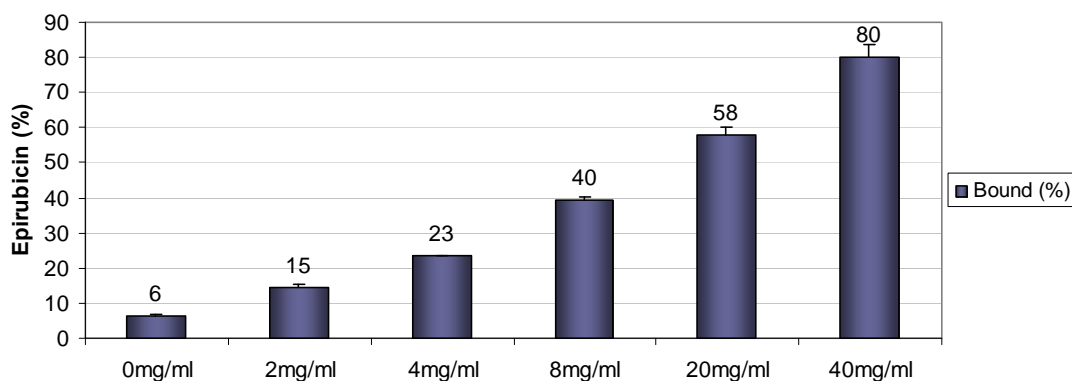
Graph 3.2.1.1.3.: Illustrates the proportion of bound epirubicin in cell growth media in the presence of increasing levels of albumin. A concentration of 2 μM or 1.16 mg/ml epirubicin was used. This graph represents duplicate intraday results. The table below depicts the values (epirubicin (ng)) used to calculate the percentage of free and bound epirubicin in this graph.

Table 3.2.1.1.3.: Raw data for the calculation of free versus bound epirubicin, plus and minus their standard deviations (±), in cell growth media in the presence of increasing levels of albumin.

Albumin	Total (ng)	Retentate (ng)	Filtrate (ng)	Membrane (ng)	Bound (%)	Free (%)
0 mg/ml	1160	72	28	1060	6.2 ± 1	93.8 ± 1
2 mg/ml	1160	170	61	930	14.6 ± 1	85.4 ± 1
4 mg/ml	1160	272	53	836	23.4 ± 0	76.6 ± 0
8 mg/ml	1160	458	54	648	39.5 ± 1	60.5 ± 1
20 mg/ml	1160	671	73	416	57.9 ± 2	42.1 ± 2
40 mg/ml	1160	928	118	114	80.0 ± 3	20.0 ± 3

Alpha-1 acid-glycoprotein
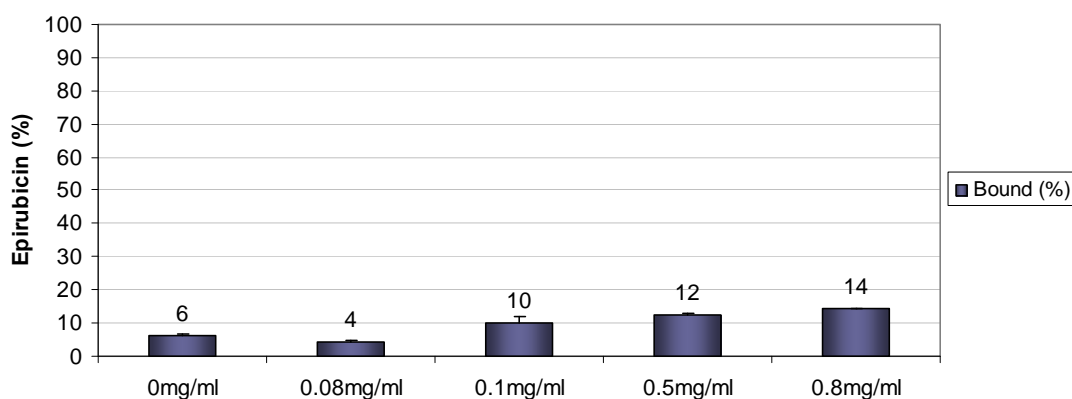
Graph 3.2.1.1.4.: Illustrates the proportion of bound epirubicin in ATCC media in the presence of increasing levels of α_1-acid glycoprotein. A concentration of 2 µM or 1.16 mg/ml epirubicin was used. This graph represents duplicate intraday results. The table below depicts the values (epirubicin (ng)) used to calculate the percentage of free and bound epirubicin in this graph.

Table 3.2.1.1.4.: Raw data for the calculation of free versus bound epirubicin, plus and minus their standard deviations (±), in ATCC media in the presence of increasing levels of α_1-acid glycoprotein.

α_1 acid-glycoprotein	Total (ng)	Retentate (ng)	Filtrate (ng)	Membrane (ng)	Bound (%)	Free (%)
0 mg/ml	1160	72	28	1060	6.2 ± 1	93.8 ± 1
0.08 mg/ml	1160	50	44	1065	4.4 ± 0	95.6 ± 0
0.1 mg/ml	1160	119	96	945	10.3 ± 2	89.7 ± 2
0.5 mg/ml	1160	143	74	943	12.3 ± 1	87.7 ± 1
0.8 mg/ml	1160	165	83	912	14.3 ± 0	85.7 ± 0

3.2.1.2. The effect of serum proteins on the uptake of epirubicin in normal mammalian epithelial cells and in breast and lung cancer cells.

As outlined in section 3.2.1.1, the presence of AAG, and, particularly, albumin in serum affect the proportion of free and bound levels of epirubicin in cell culture medium. In this section, we studied the impact this binding had on the accumulation of epirubicin in normal human mammary epithelial cells (HMEC), and in a breast (MCF7) and a lung (DLKP) cancer cell lines. Methodology for this body of work is described in section 2.12.2., 2.12.2.1., and 2.12.3.

We found that the presence of low levels of FCS had little impact on epirubicin accumulation in HMEC cells, while in the presence of 20%, 50% and 100% FCS there was a 3 fold decrease in drug accumulation. Little change was observed in the MCF7 cells with drug dissovled in medium containing 5%, 10% and 20% FCS but accumulation decreased in the presence of 50 % FCS and halved with 100% FCS compared to 0% FCS. On the other hand, there was a significant increase in accumulation of epirubicin in the presence of FCS in the DLKP cells. The accumulation peaked at 10% (4501 ± 590 ng/million cells) and remained higher in the presence of 100% FCS than 0% FCS.. A very similar trend was observed in all cells in the presence of serum albumin. This data is illustrated in graph 3.2.1.2.1 and in table 3.2.1.2.1.

With low levels of albumin (2 mg/ml and 4 mg/ml) in the media a slight increase in drug accumulation occurred, while higher levels reduced the accumulation of epirubicin in the HMEC cells. Little change was observed with the MCF7 cells at 2 mg/ml and 4 mg/ml of albumin but this accumulation decreased with 20mg/ml and almost halved with 40 mg/ml serum albumin. Similar to FCS, the presence of serum albumin significantly increased the accumulation of epirubicin in the DLKP cells. The accumulation peaked at 4mg/ml (3465 ± 917 ng/million cells) and did not drop to minimum drug accumulation with 40mg/ml of albumin in media (see graph 3.2.1.2.2 and table 3.2.1.2.2.). These trends would suggest that the binding of epirubicin to the proteins in FCS and to serum albumin impact greatly on the accumulation of epirubicin in all three cell types. However, as demonstrated in section 3.2.1.1 with

levels of protein normally found in the plasma, the majority of epirubicin is bound to serum protein (100% FCS solution bound 100% of the epirubicin while 40mg/ml of albumin bound 80% of the epirubicin) while a much smaller proportion of epirubicin is bound to AAG (0.8mg/ml bound 14% of the epirubicin). The results in graph 3.2.1.2.3 illustrate the affect the presence of AAG has on the acccumulation of epirubicin in the three cell types. In both the HMEC and DLKP cells there was a slight increase in the accumulation of epirubicin with low levels of AAG, however, this decreased at higher concentrations. Conversely, the accumulation doubled with the highest concentration of AAG in the MCF7 cells (see graph 3.2.1.2.3). This would suggest that AAG plays more complex role in cellular epirubicin accumulation.

As serum deprivation has a negative impact on cell growth the toxicological consequences of these alterations could not be evaluated.
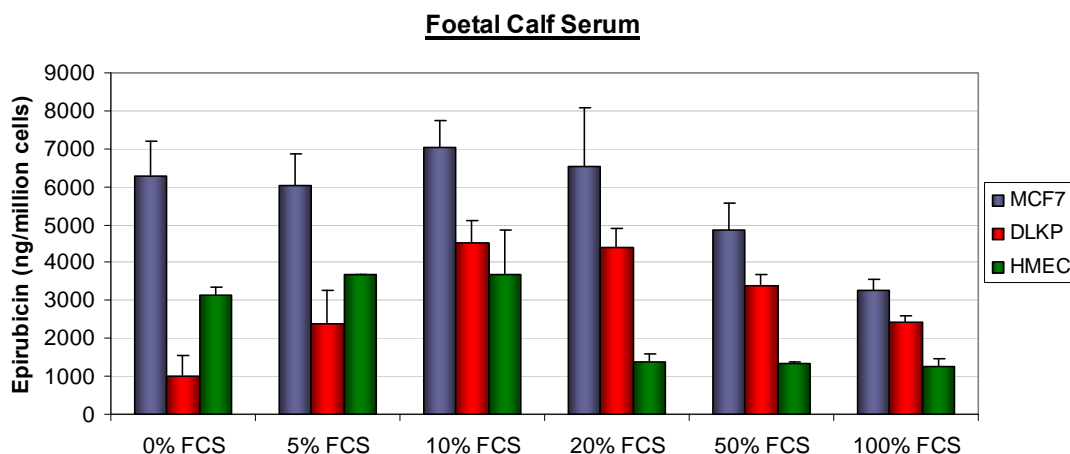
Foetal Calf Serum

Graph 3.2.1.2.1.: This bar chart illustrates the accumulation of epirubicin in human mammary epithelial cells (HMEC) and in a breast (MCF7) and lung (DLKP) cell line in the presence of increasing levels of foetal calf serum (FCS). This graph represents triplicate intra-day results. The table below depicts the quantity of epirubicin (ng/million cells) accumulated in each sample.

Table 3.2.1.2.1.: This table supplies the quantitative data for the accumulation of epirubicin in the presence of increasing levels of FCS in the three cell types.

FCS (%)	0	5	10	20	50	100
MCF7						
Epi (ng/10^6 cells)	6281	6012	7038	6539	4842	3270
St dev	± 911	± 842	± 725	± 1535	± 711	± 305
DLKP						
Epi (ng/10^6 cells)	1025	2400	4501	4392	3393	2431
St dev	± 529	± 865	± 590	± 525	± 286	± 171
HMEC						
Epi (ng/10^6 cells)	3150	3699	3663	1366	1358	1268
St dev	± 184	± 0	± 1198	± 238	± 19	± 190
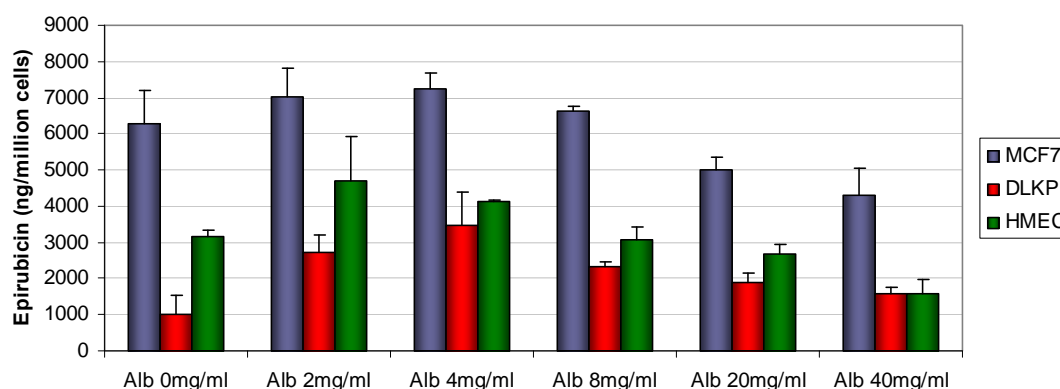
Graph 3.2.1.2.2.: This bar chart illustrates the accumulation of epirubicin in human mammary epithelial cells (HMEC) and in a breast (MCF7) and lung (DLKP) cell line in the presence of increasing levels of serum albumin. This graph represents triplicate intra-day results. The table below depicts the quantity of epirubicin (ng/million cells) accumulated in each sample.

Table 3.2.1.2.2.: This table supplies the quantitative data for the accumulation of epirubicin in the presence of increasing levels of serum albumin in the three cell types.

Albumin (mg/ml)	0	2	4	8	20	40
MCF7						
Epi (ng/10^6 cells)	6281	7035	7231	6627	5000	4317
St dev	± 911	± 768	± 447	± 128	± 362	± 748
DLKP						
Epi (ng/10^6 cells)	1025	2733	3465	2335	1907	1564
St dev	± 529	± 469	± 917	± 127	± 244	± 212
HMEC						
Epi (ng/10^6 cells)	3150	4704	4137	3057	2669	1588
St dev	± 184	± 1228	± 24	± 389	± 264	± 394

Alpha1 acid-glycoprotein
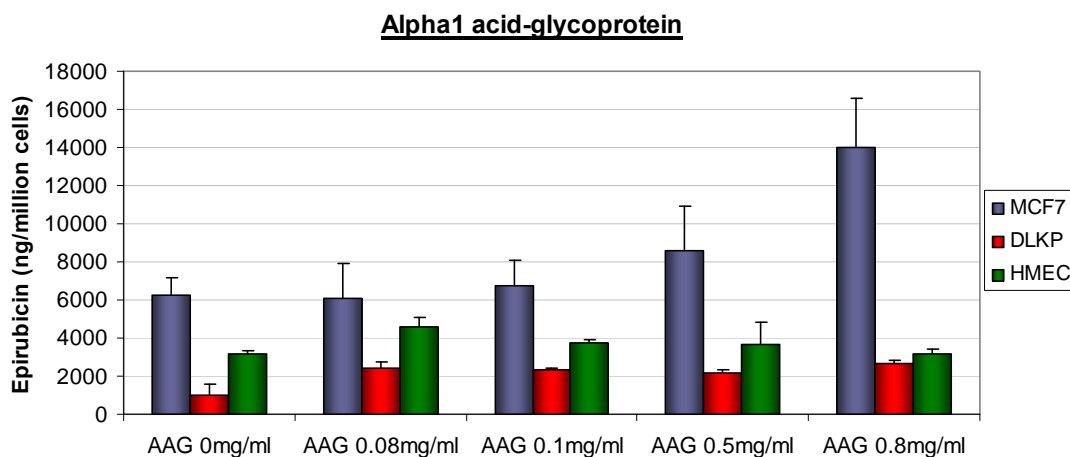
Graph 3.2.1.2.3.: This bar chart illustrates the accumulation of epirubicin in human mammary epithelial cells (HMEC) and in a breast (MCF7) and lung (DLKP) cell line in the presence of increasing levels of α_1-acid glycoprotein. This graph represents triplicate intra-day results. The table below depicts the quantity of epirubicin (ng/million cells) accumulated in each sample.

Table 3.2.1.2.3.: This table supplies the quantitative data for the accumulation of epirubicin in the presence of increasing levels of α_1-acid glycoprotein in the three cell types.

AAG (mg/ml)	0	0.08	0.1	0.5	0.8
MCF7					
Epi (ng/10^6 cells)	6281	6108	6714	8599	14011
St dev	± 911	± 1790	± 1360	± 2350	± 2537
DLKP					
Epi (ng/10^6 cells)	1025	2446	2318	2145	2670
St dev	± 529	± 281	± 113	± 185	± 150
HMEC					
Epi (ng/10^6 cells)	3150	4586	3770	3660	3131
St dev	± 184	± 495	± 149	± 1180	± 286

3.3. Effect of tyrosine kinase inhibitors on the function and expression of epidermal growth factor receptors, EGFR and HER2, multidrug resistance transporter and cyclooxygenase proteins.

3.3.1. TKI interference with EGFR and HER2 activity and heightened sensitivity to chemotherapeutic drugs.

In this section, we investigated if inhibition of the activity and function of EGFR and/or HER2, with TKI's (lapatinib, erlotinib and gefitinib), could sensitise breast cancer cells to chemotherapy (epirubicin and docetaxel). For this, we selected an HER2 over-expressing cell line that lacked EGFR (MDA-MB-453), a cell line with amplified levels of EGFR while lacking HER2 (MDA-MB-231) and finally a cell line that expressed both EGFR and HER2 at low levels (MCF7). Firstly, we carried out combination proliferation assays (see section 2.7.1 and 2.7.3) of lapatinib, erlotinib and gefitinib with epirubicin and docetaxel and finally ELISA immunoassays (see section 2.11.6 and 2.11.7.) to quantitate the effect of lapatinib on EGFR and HER2 expression and activation levels.

No decrease in cell proliferation was observed with the combination of lapatinib, erlotinib or gefitinib with epirubicin or docetaxel in the EGFR-overexpressing cell line, MDA-MB-231 (see graph 3.3.1.1 and table 3.3.1.1 for details), the HER2-overexpressing cell line, MDA-MB-453 (See graph 3.3.1.2.A. and table 3.3.1.2 for further details) or the low EGFR/HER2 expressing cell line, MCF7 (see graphs 3.3.1.3 **A** & **B** and table 3.3.1.3.). This would suggest that the three TKIs do not sensitise these TKI insensitive breast cell lines to the chemotherapeutic treatment of epirubicin or docetaxel.
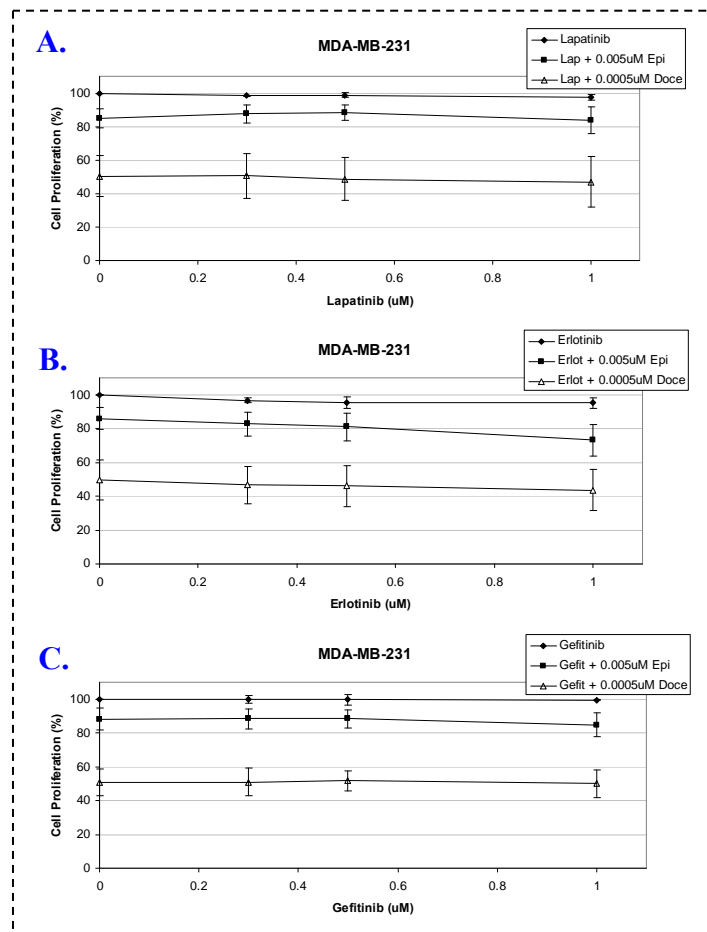
Graph 3.3.1.1.: The combination of epirubicin (■) or docetaxel (Δ) with lapatinib (**A**:◆), erlotinib (**B**:◆) and gefitinib (**C**:◆) on the MDA-MB-231 cell line (EGFR-amplified cell line). Clinically relevant concentrations of both the chemotherapeutic agents and TKIs were tested alone and combined over a 5 day period. The bar chart is the result of triplicate experiments carried out on separate days. The table below depicts the percentage cell proliferation and standard deviations illustrated in this graph.

Table 3.3.1.1.: This table provides the percentage cell proliferation and standard deviations for graph 3.3.1.1.

TKI (μM)	Cell Proliferation (%)							
	0	Stdev (%)	**0.3**	Stdev (%)	**0.5**	Stdev (%)	**1**	Stdev (%)
Lapatinib	100	± 0	98	± 1	99	± 1	97	± 2
Lap + 0.005μM Epi	85	± 6	87	± 5	88	± 5	84	± 8
Lap + 0.0005μM Doce	50	± 12	50	± 13	48	± 13	47	± 15
Erlotinib	100	± 0	96	± 1	95	± 3	95	± 3
Erlot + 0.005μM Epi	86	± 6	82	± 7	81	± 8	73	± 9
Erlot + 0.0005μM Doce	50	± 12	47	± 11	46	± 12	43	± 12
Gefitinib	100	± 0	99	± 12	99	± 3	99	± 0.2
Gefit + 0.005μM Epi	88	± 7	88	± 3	88	± 5	85	± 7
Gefit + 0.0005μM Doce	50	± 8	51	± 5	52	± 6	50	± 8
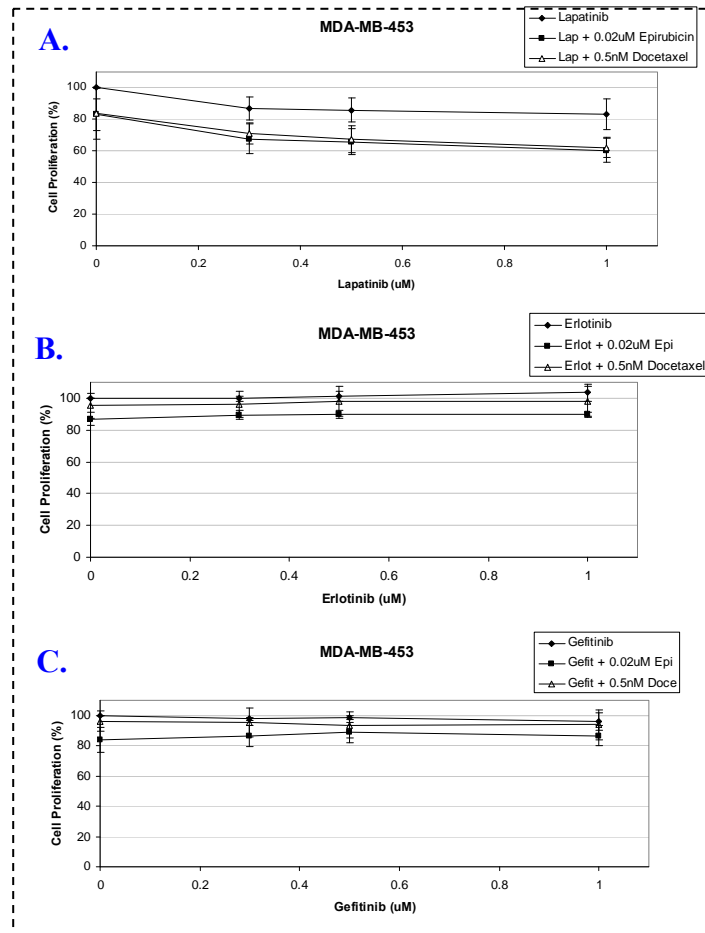
Graph 3.3.1.2.: The combination of epirubicin (■) or docetaxel (Δ) with lapatinib (**A**:◆), erlotinib (**B**:◆) and gefitinib (**C**:◆) on the MDA-MB-453 cell line (HER2-amplified cell line). Clinically relevant concentrations of both the chemotherapeutic agents and TKIs were tested alone and combined over a 5 day period. The bar chart is the result of triplicate experiments carried out on separate days. The table below depicts the percentage cell proliferation and standard deviations illustrated in this graph.

Table 3.3.1.2.: This table provides the percentage cell proliferation and standard deviations for graph 3.3.1.2 above.

TKI (μM)	Cell Proliferation (%)							
	0	Stdev (%)	**0.3**	Stdev (%)	**0.5**	Stdev (%)	**1**	Stdev (%)
Lapatinib	100	±0	87	±7	86	±7	83	±10
Lap + 0.02μM Epi	83	±10	68	±9	66	±8	60	±7
Lap + 0.5nM Doce	84	±16	71	±6	68	±8	62	±6
Erlotinib	100	±0	100	±2	101	±3	103	±5
Erlot + 0.02μM Epi	87	±4	90	±3	90	±2	90	±1
Erlot + 0.5nM Doce	95	±8	96	±8	98	±9	98	±9
Gefitinib	100	±0	98	±1	99	±1	96	±5
Gefit + 0.02μM Epi	84	±8	86	±7	89	±7	87	±6
Gefit + 0.5nM Doce	96	±7	95	±10	94	±9	94	±10
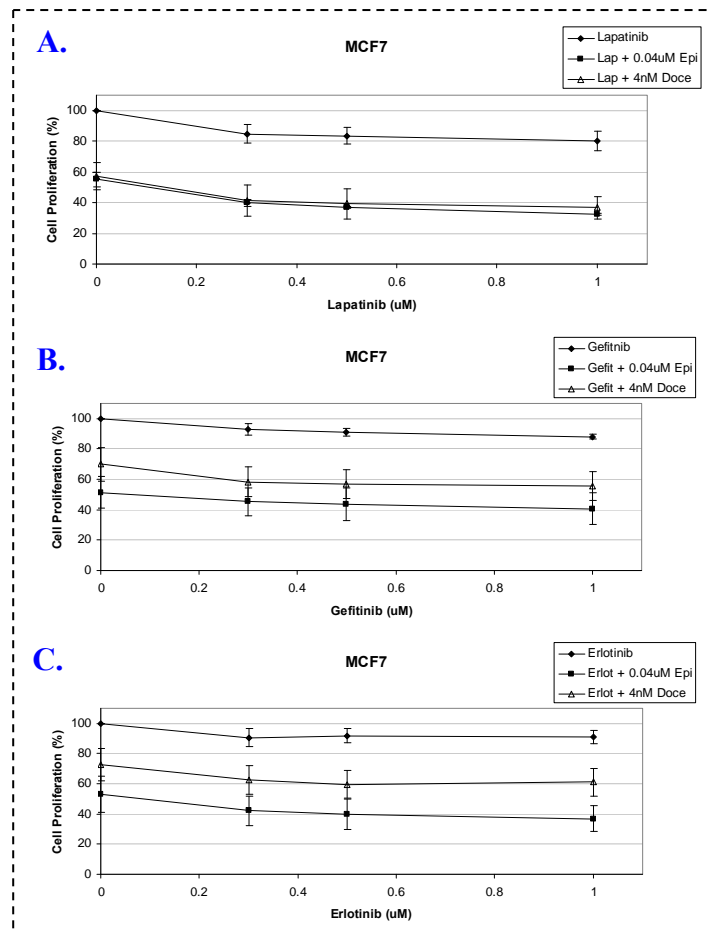
Graph 3.3.1.3.: The combination of epirubicin (■) or docetaxel (Δ) with lapatinib (**A**:◆), erlotinib (**B**:◆) and gefitinib (**C**:◆) on the MCF7 cell line (low EGFR/HER2-expressing cell line). Clinically relevant concentrations of both the chemotherapeutic agents and TKIs were tested alone and combined over a 5 day period. The bar chart is the result of triplicate experiments carried out on separate days. The table below depicts the percentage cell proliferation and standard deviations illustrated in this graph.

Table 3.3.1.3.: This table provides the percentage cell proliferation and standard deviations for graph 3.3.1.3.

TKI (μM)	Cell Proliferation (%)							
	0	Stdev (%)	**0.3**	Stdev (%)	**0.5**	Stdev (%)	**1**	Stdev (%)
Lapatinib	100	±0	85	±6	84	±6	80	±6
Lap + 0.04μM Epi	55	±5	40	±2	37	±1	32	±1
Lap + 4nM Doce	57	±9	41	±10	39	±10	37	±7
Erlotinib	100	±0	91	±6	92	±5	91	±5
Erlot + 0.04μM Epi	53	±12	42	±10	40	±10	37	±9
Erlot + 4nM Doce	73	±11	62	±10	60	±9	61	±9
Gefitnib	100	±0	93	±4	91	±3	88	±2
Gefit + 0.04μM Epi	51	±10	45	±9	44	±11	41	±10
Gefit + 4nM Doce	70	±11	58	±10	57	±9	55	±9

3.3.4. Effect of tyrosine kinase inhibitors on COX protein expression and activity

In this section, we considered the potential that lapatinib could affect the function and expression of the cyclooxygenase enzyme, COX-2 (see section 1.6.3. for review). We investigated the effect of four tyrosine kinase inhibitors (lapatinib, erlotinib, gefitinib and AG825) and the HER2 monoclonal antibody (trastuzumab) on the expression and activity of COX proteins (for methodology see section 2.11. and 2.13.). For this, we selected a human lung cell line, A549, which is known to express detectable levels of COX-1 and COX-2 protein. A549 also expresses low levels of EGFR and HER2 [97].

We exposed the A549 cells to 2.5, 5, 7.5 and 10 µM lapatinib or AG825 and 0.25, 0.5, 0.75 and 1 µM trastuzumab for 48 hours and ran Westerns blots to detect changes in the expression levels of COX-1 and COX-2 protein. We also evaluated the effect 10 µM erlotinib and gefitinib had on the expression of COX-2 compared to lapatinib. We found that lapatinib, the dual EGFR/HER2 TKI, caused mild down-regulation of COX-1 expression levels (see figure 3.3.4.1 for details) but up-regulated COX-2 protein expression (see figure 3.3.4.2 and table 3.3.4.1 for details). AG825, HER1/HER2 TKI, did not alter COX-1 or COX-2 protein expression (see figure 3.3.4.1, 3.3.4.3 and table 3.3.4.1 for details). Trastuzumab, HER2 monoclonal antibody, up-regulated the expression of COX-1 but down-regulated the expression of COX-2 in the A549 cell line (see figure 3.3.4.1, 3.3.4.2 and table 3.3.4.1 for details).

A panel of HER2-expressing cells lines, MDA-MB-453 (high HER-2-expressing and lapatinib insensitive), MCF7 (low EGFR/HER2-expressing and lapatinib insensitive) and BT474 (low HER-2-expressing and lapatinib sensitive), were also exposed to lapatinib, AG825 and trastuzumab (data not shown). However, COX-2 expression was not detected in either the untreated or treated cells.

In figure 3.3.4.3, we exposed A549 cells to 10 µM lapatinib, erlotinib, gefitinib and celecoxib (COX-2 specific inhibitor) and found that erlotinib, gefitinib and celecoxib down-regulated the expression of COX-2 and only lapatinib up-regulated the expression of COX-2 in the A549 cells.

Following a 48 hour exposure to 2.5 and 5 µM lapatinib, total COX activity was increased (from 8 nmol/min/10^7 to 13 and 15 nmol/min/10^7 cells) (graph 3.3.4.1.). This increase corresponded with an increase in COX-2 activity (from 2 nmol/min/10^7

to 4 and 7 nmol/min/10^7 cells) (graph 3.3.4.1.A). The higher concentrations of lapatinib (7.5 and 10 μM) returned total COX and COX-2 activity to normal levels. COX-1 activity was unaltered by lapatinib. All concentrations of AG825 mildly reduced COX-1 (from 7.5 nmol/min/10^7 cells to 6 nmol/min/10^7 cells) and COX-2 (from 2 nmol/min/10^7 cells to 1 nmol/min/10^7 cells) activity and thus total COX (from 9 nmol/min/10^7 cells to 7 nmol/min/10^7 cells) activity, following a 48 hour exposure (graph 3.3.4.1.B.). A same exposure to all concentrations of trastuzumab mildly reduced COX-1 (from 7.5 nmol/min/10^7 cells to 5 and 6 nmol/min/10^7 cells) and thus total COX activity (from 9 nmol/min/10^7 cells to 6 nmol/min/10^7 cells) (graph 3.3.4.1.C.). Concentrations of 0.5, 0.75 and 1 μM trastuzumab also reduced COX-2 activity (from 2 nmol/min/10^7 cells to 1 and 0.25 nmol/min/10^7 cells). COX-2 activity was unchanged in the presence of 0.25 μM trastuzumab (graph 3.3.4.1.C.).

In the direct COX activity assay, DMSO (the solvent control for lapatinib) reduced COX activity. However, 10 μM of lapatinib increased COX-1 (from 4 nmol/min/10^7 cells to 7 nmol/min/10^7 cells), COX-2 (from 3.5 nmol/min/10^7 cells to 7 nmol/min/10^7 cells) and thus total COX activity (from 5 nmol/min/10^7 cells to 14 nmol/min/10^7 cells) (graph 3.3.4.2.A.). Only the highest concentration of AG825 (10 μM) reduced COX-1 (from 3.5 nmol/min/10^7 cells to 2.2 nmol/min/10^7 cells) and COX-2 (from 3.8 nmol/min/10^7 cells to 1.2 nmol/min/10^7 cells) activity (graph 3.3.4.2.B.). Only the highest concentration of trastuzumab (1 μM) was tested and this reduced COX-1 (from 3.5 nmol/min/10^7 cells to 2.8 nmol/min/10^7 cells and COX-2 (from 3.8 nmol/min/10^7 cells to 2.8 nmol/min/10^7 cells) active levels (graph 3.3.4.2.B.). Celecoxib, a specific COX-2 inhibitor, was included as a control for this assay. As expected, 0.5 and 2 μM celecoxib only sufficiently inhibited COX-2 active levels (from 4 nmol/min/10^7 cells to 2.5 and 2 nmol/min/10^7 cells) while 10 μM celecoxib inhibited both COX-1 (from 5 nmol/min/10^7 cells to 3.5 nmol/min/10^7 cells), COX-2 (from 4 nmol/min/10^7 cells to 2.8 nmol/min/10^7 cells) activity (graph 3.3.4.2.C.) and total COX.

To determine if a general COX inhibitor could sensitise lapatinib-insensitive breast cell lines to lapatinib we carried out combination proliferation assays (for methodology see section 2.7.1. and 2.7.3.) of a non-specific COX inhibitor, sulindac, with lapatinib in three breast cell lines. These cell lines were chosen for their growth factor receptor status. One cell line expresses high levels of HER2 (MDA-MB-453),

and other expresses high levels of EGFR (MDA-MB-231). Neither cells express COX-2 and the third cell line expresses low levels of both EGFR and HER2 (MCF7). COX-2 expression was not found in MDA-MB-453 or MCF7 (graph 3.3.4.3. and table 3.3.4.2.).

The combination proliferation assay of sulindac with lapatinib, in the EGFR-overexpressing cell line MDA-MB-231, resulted in no increased growth inhibition (see graph 3.3.4.3.**A** and table 3.3.4.2 for details). Neither drugs had inhibitory effects alone. However, there was a mild effect (of about 5%) coming into view with 15 µM sulindac and 1 µM lapatinib.

When sulindac (non-specific COX inhibitor) and lapatinib (dual EGFR/ErbB2 inhibitor) were combined in the HER2-overexpressing cell line, MDA-MB-453, it was clear that sulindac potentiated the anti-proliferative affect of lapatinib by up to 33% (see graph 3.3.4.3.**B** and table 3.3.4.2 for details).

Similar to the result observed in the MDA-MB-231 cells, sulindac did not enhance the anti-proliferative potential in the low EGFR/HER2-expressing cell line, MCF7 (see graph 3.3.4.3.**C** and table 3.3.4.2 for details).

Target Protein ‖	Western blot ‖	Summary effect

0 2.5   5 7.5 10 μM   Tyrosine kinase inhibitor

COX-1 (70kDa)

β-actin (48kDa)   ↓ by Lapatinib after 48 hours

COX-1 (70kDa)

β-actin (48kDa)   ↔ by AG825 after 48 hours

0 0.25 0.5 0.75 1 μM   Antibody

COX-1 (70kDa)

β-actin (48kDa)   ↑ by Trastuzumab after 48 hours
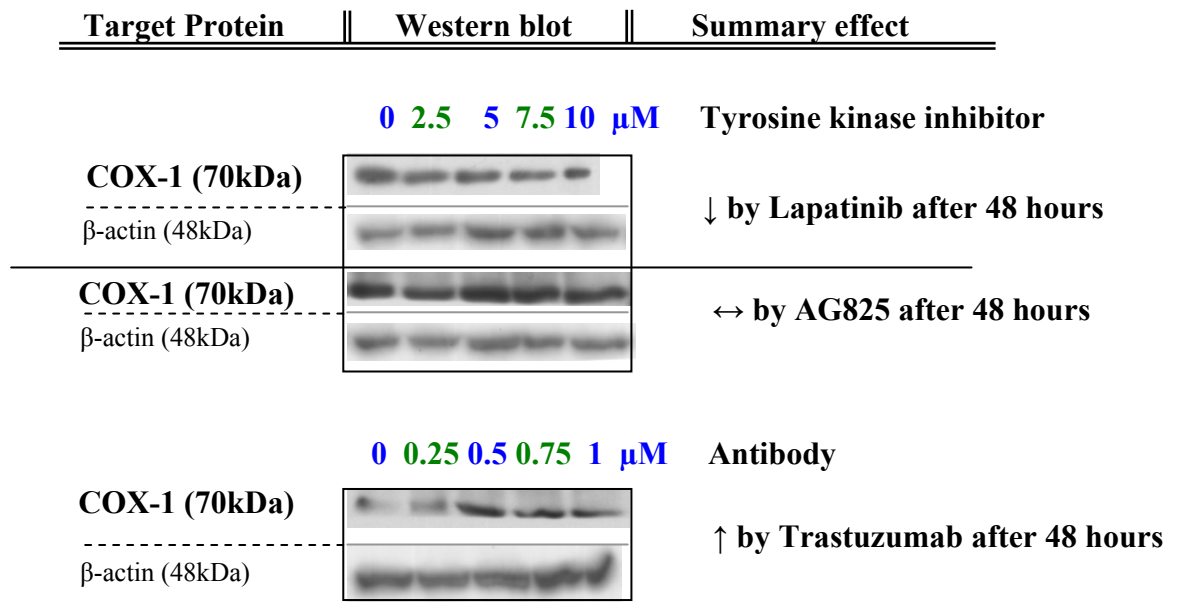
Figure 3.3.4.1.: COX-1 expression, by Western blotting, in the A549 cells following a 48 hour exposure to lapatinib, AG825 or trastuzumab. COX-1 has a molecular weight of 70 kDa and the housekeeping protein, β-actin with a molecular weight of 48 kDa, was used as a protein loading control. The same concentration of DMSO was included in all lapatinib samples (including the untreated sample) equal to that of the 10 μM concentration. A similar control for AG825 was not required as the levels of DMSO were less than 0.1%, while trastuzumab was in its clinical formulation. These Western blots represent a single determination. The concentrations used in the treatments are indicated in the legend above each band.
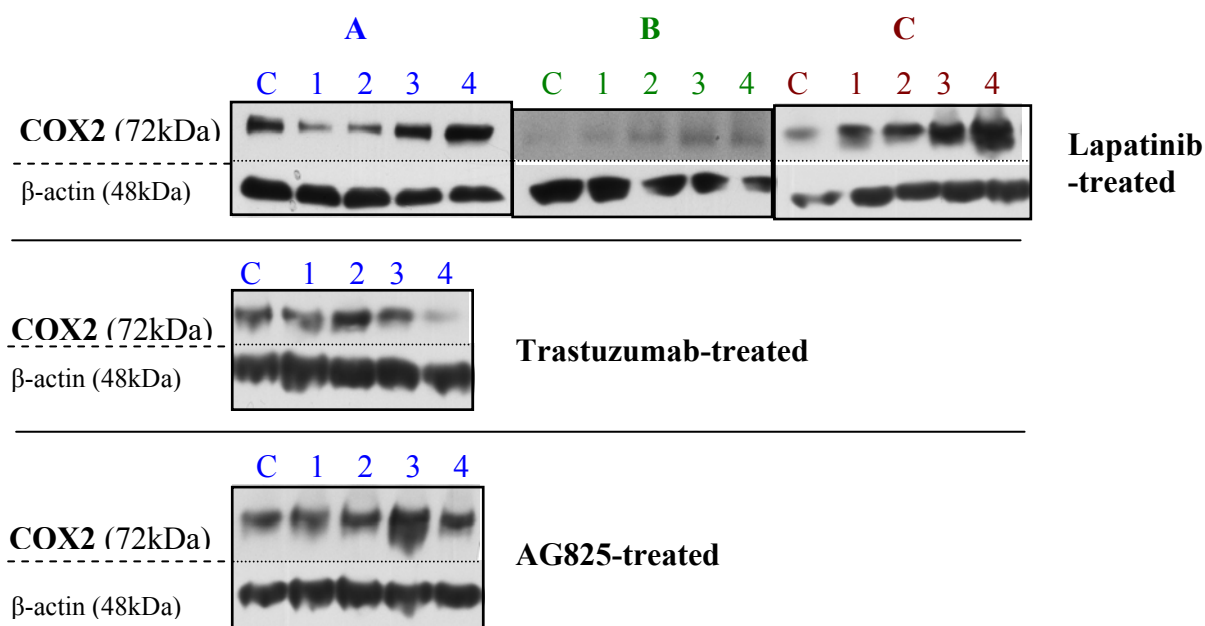
Figure 3.3.4.2.: COX-2 Western blots for A549 cells treated with a range of concentrations of lapatinib, AG825 and trastuzumab for 48hrs. COX-2 has a molecular weight of 72 kDa and the housekeeping protein, β-actin with a molecular weight of 48 kDa, was used as a protein loading control. The same concentration of DMSO was included in all lapatinib samples (including the untreated sample) equal to that of the 10 μM concentration. A similar control for AG825 was not required as the levels of DMSO were less than 0.1%, while trastuzumab was in its clinical formulation. The lapatinib western were carried out in triplicate biological experiments and is represented in **A**, **B** and **C**. The concentrations used in the treatments are indicated in the key below the Westerns blots. This table all presents the densitometry results of these westerns.

Table 3.3.4.1.: Fold changes in the expression of COX-2 in A549 cells following exposure to a lapatinib, AG825 and trastuzumab for 48 hrs. These fold changes were determined using densitometric analysis of Western blots carried out on lysates of the exposed A549 cells.

Sample	C	1	2	3	4
TKI dose (µM)	**0**	**2.5**	**5**	**7.5**	**10**
Lapatinib A	1	0.4	0.7	1.6	2.2
Lapatinib B	1	1.6	3.1	6.8	7.4
Lapatinib C	1	1.4	1.4	1.5	2.0
AG825	1	0.9	0.9	1.5	0.9
Antibody dose (µM)	**0**	**0.25**	**0.5**	**0.75**	**1**
Trastuzumab	1	0.7	1.3	0.8	0.2
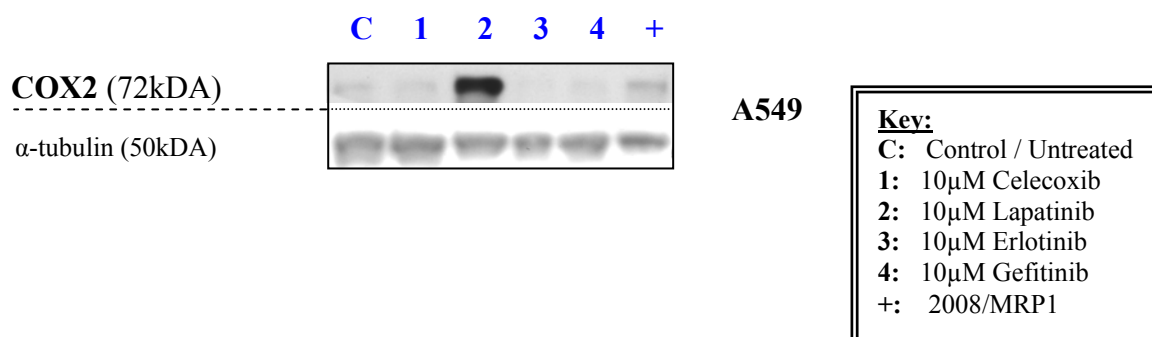
Figure 3.3.4.3: The protein expression of COX-2 in A549 following 48hr treatments with 10 µM celecoxib, lapatinib, erlotinib, and gefitinib. COX-2 has a molecular weight of 72 kDa and the housekeeping protein, β-actin with a molecular weight of 48 kDa, was used as a protein loading control. Due to the low expression of COX-2 in this cell line, 40µg of protein was loaded. The positive control for COX-2 was 2008/MRP1 (which we found to express COX-2 during a screening of a panel of cell lines, see section 3.4.1 and figure 3.4.1.4 for details). A technical replicate verified this result.
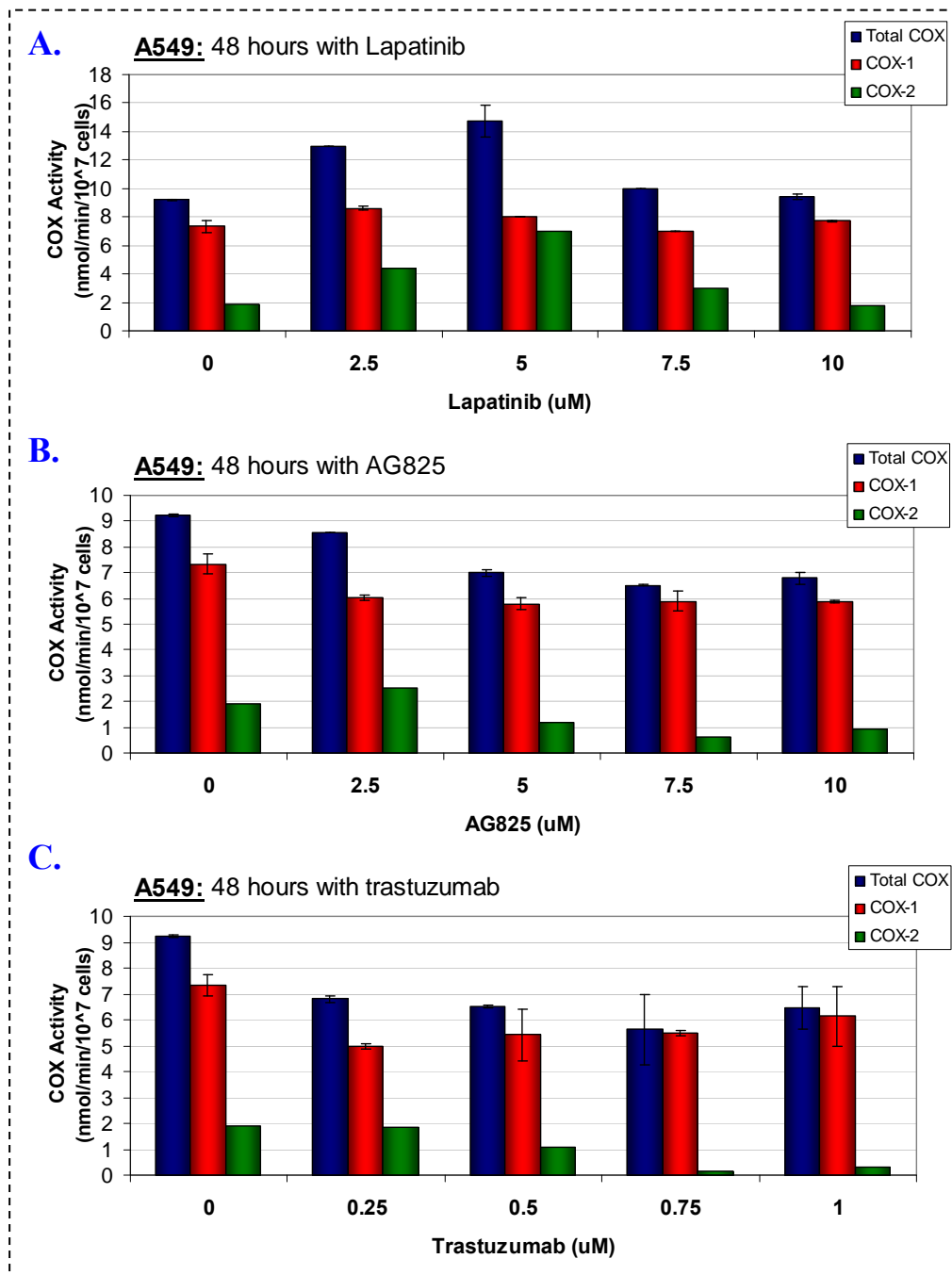
Graph 3.3.4.1.: The activity of total COX (navy), COX-1 (red) and COX-2 (green) in A549 cells following exposure to lapatinib (**A**), AG825 (**B**) or trastuzumab (**C**) for 48 hours. The same concentration of DMSO was included in all lapatinib samples (including the untreated sample) equal to that of the 10 μM concentration. A similar control for AG825 was not required as the levels of DMSO were less than 0.1%, while trastuzumab was in its clinical formulation. A concentration of 10μM celecoxib, a specific COX-2 inhibitor, was included as a control and decreased COX-2 activity was established. These graphs are the result of duplicate inter-assay replicates.
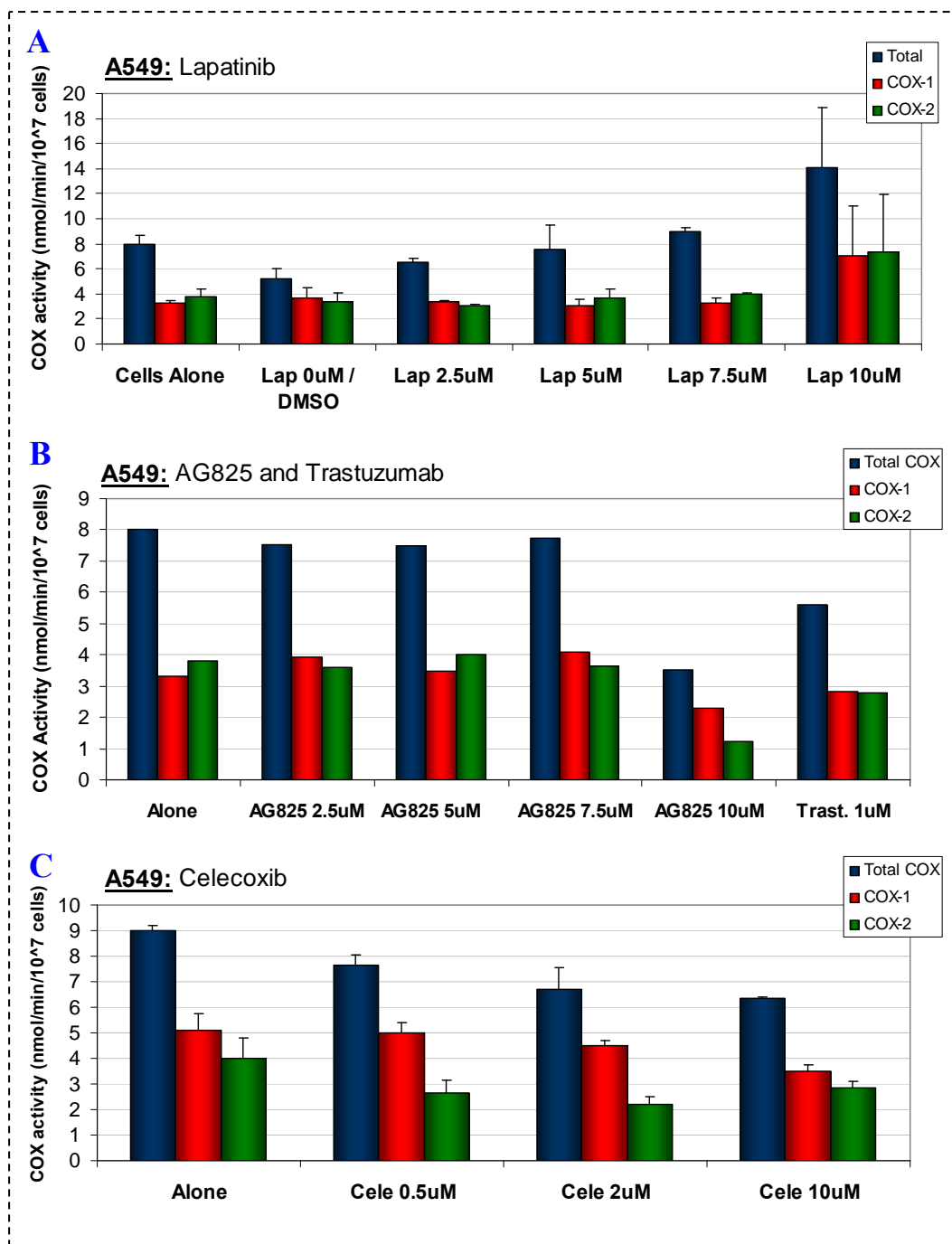
Graph 3.3.4.2.: The activity of total COX (navy bar), COX-1 (red bar) and COX-2 (green bar) in the A549 cell lysate in the presence of lapatinib (**A**), AG825 or trastuzumab (**B**) or celecoxib (**C**) for 48 hours. The same concentration of DMSO was included in all lapatinib samples (including the untreated sample) equal to that of the 10 μM concentration. A similar control for AG825 was not required as the levels of DMSO were less than 0.1%, while trastuzumab was in its clinical formulation. Graphs **A** and **C** are the result of duplicate inter-assay replicates while **B** is the result of a single assay
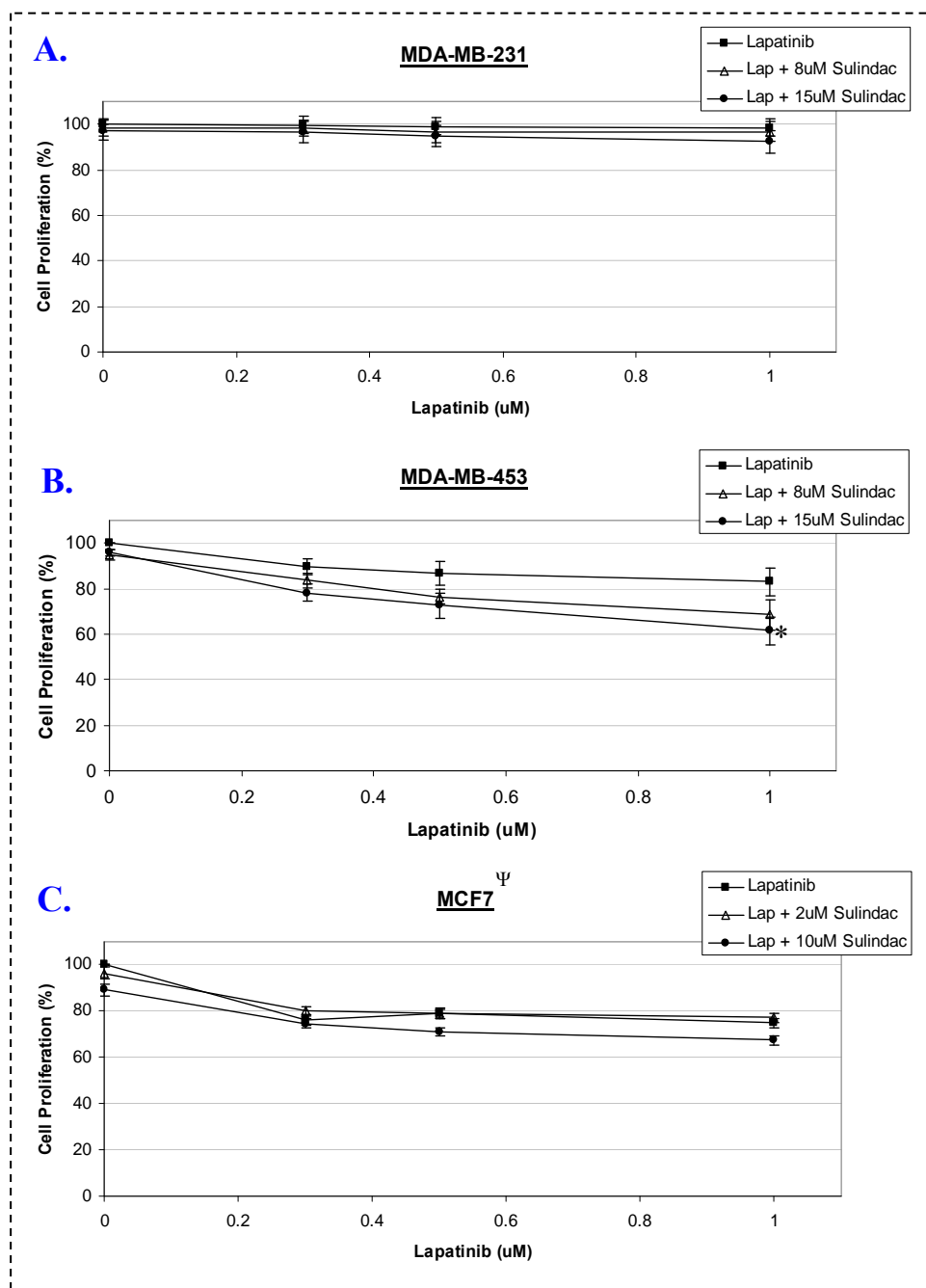
Graph 3.3.4.3.: The combination of lapatinib (■) with sulindac (Δ and ●) in the EGFR-amplified (MDA-MB-231; **A**.), HER2-amplified (MDA-MB-453; **B**.) and low EGFR/HER2-expressing (MCF7; **C**.) cell lines. These graphs depict the proliferation combination assays of clinically relevant concentrations of lapatinib with the non-specific COX inhibitor, sulindac, over a 5 day period. All results are representative of triplicate independent determinations unless otherwise indicated ($^{\Psi}$). Significant changes between each drug alone and the combination of both drugs is indicated by * (p<0.05). Table 3.3.4.2 outlines the percentage cell proliferation and standard deviations for this graph.

Table 3.3.4.2.: This table provides data for the combination of lapatinib and sulindac in the MDA-MB-453 cell line (see graph 3.3.4.1.**A**, **B** and **C**).

Cell line	Agents	Cell Prolfieration (%)							
	Lapatinib (µM)	**0**	StDev (%)	**0.3**	StDev (%)	**0.5**	StDev (%)	**1**	StDev (%)
MDA-MB-231	Lapatinib	100	±0	100	±4	99	±4	98	±4
	Lap + 8µM Sulindac	99	±4	98	±4	97	±5	97	±4
	Lap + 15µM Sulindac	97	±4	97	±5	95	±5	92	±5
MDA-MB-453	Lapatinib	100	±0	90	±3	87	±5	83	±6
	Lap + 8µM Sulindac	95	±2	84	±3	77	±3	68	±7
	Lap + 15µM Sulindac	96	±1	78	±4	73	±5	62	±6
MCF7	Lapatinib	100	±0	76	±2	79	±2	75	±2
	Lap + 2µM Sulindac	96	±3	80	±2	79	±2	77	±2
	Lap + 10µM Sulindac	89	±2	75	±2	71	±2	67	±2

3.3.5. TKI-mediated modulation of MDR protein.

In this section, we compared the efficacy of three tyrosine kinase inhibitors in overcoming resistance due to the amplified expression of multidrug resistance (MDR) transporter proteins (P-gp, MRP1 and BCRP). To date, a number of researchers have shown that lapatinib [97], erlotinib [198] and gefitinib [199] inhibit the function of the three transporters. However, none have compared their efficacy to overcome P-gp, MRP1 and BCRP-mediated drug resistance.

We selected a panel of cell lines that express P-gp, MRP1 and/or BCRP followed by a panel of MDR substrates and non-substrates. With each proliferation assay a control was carried out. This control included the MDR substrate combined with that particular MDR specific inhibitor, to ensure the MDR protein, in the chosen models, were transporting as normal during each assay.

Combination TKI – Cytotoxicity proliferation assays in P-gp-expressing cell models.
Three P-gp-overexpressing models, NCI/Adr-res, A549-Taxol and H1299-Taxol, were chosen for their differing expression levels of the P-gp protein. NCI/Adr-res (an ovarian cell model) expresses very high levels of P-gp while A549-Taxol (lung cell line) expresses moderate levels and H1299-Taxol (lung cell line) expresses low levels. Two P-gp substrates were used in these proliferation assays, epirubicin and docetaxel.

The combination proliferation assays of biologically-relevant concentrations of lapatinib in the ovarian P-gp-overexpressing cell line, NCI/Adr-res, significantly potentiated the cytotoxic effects of epirubicin and docetaxel (see graph 3.3.5.1.**A** and table 3.3.5.1.). Neither erlotinib nor gefitinib enhanced the anti-proliferative potential of epirubicin or docetaxel to the same degree as lapatinib in this cell line. However, when combined the total cell growth was reduced compared to each drug individually. This would suggest that erlotinib and gefitinib did not overcome P-gp-mediated resistance. However, lapatinib overcame P-gp-mediated resistance in this cell line.
Similar to the combination findings of lapatinib with epirubicin and docetaxel in the NCI/Adr-res cell line, lapatinib potentiated the cytotoxic effects of both chemotherapeutic drugs in the moderately-expressing P-gp cell line, A549-Taxol (see graph 3.3.5.2.**A**. and table 3.3.5.2.). However, the combination proliferation assays

using clinically relevant concentrations of erlotinib and gefitinib showed potentiation of the cytotoxic effect of epirubicin and docetaxel in this cell line (refer to graph 3.3.5.2 **B** and **C** and table 3.3.6.2).

Once again, the combination proliferation assays of lapatinib in the low-expressing P-gp cell line, H1299-Taxol, moderately potentiated the cytoxicity of epirubicin and docetaxel (see graph 3.3.5.3.**A**. and table 3.3.5.3.). However, this same trend wasn't evident with erlotinib and gefitinib. The combination of epirubicin with both erlotinib and gefitinib had no effect on cell growth while only a very mild reduction was observed when docetaxel and erlotinib combination in this cell line (see graph 3.3.5.3.**B** and **C** and table 3.3.5.3.).

This data indicates that, compared to erlotinib and gefitinib, lapatinib is the most efficient at sensitising P-gp-overexpressing cells to P-gp substrate cytoxic agents.
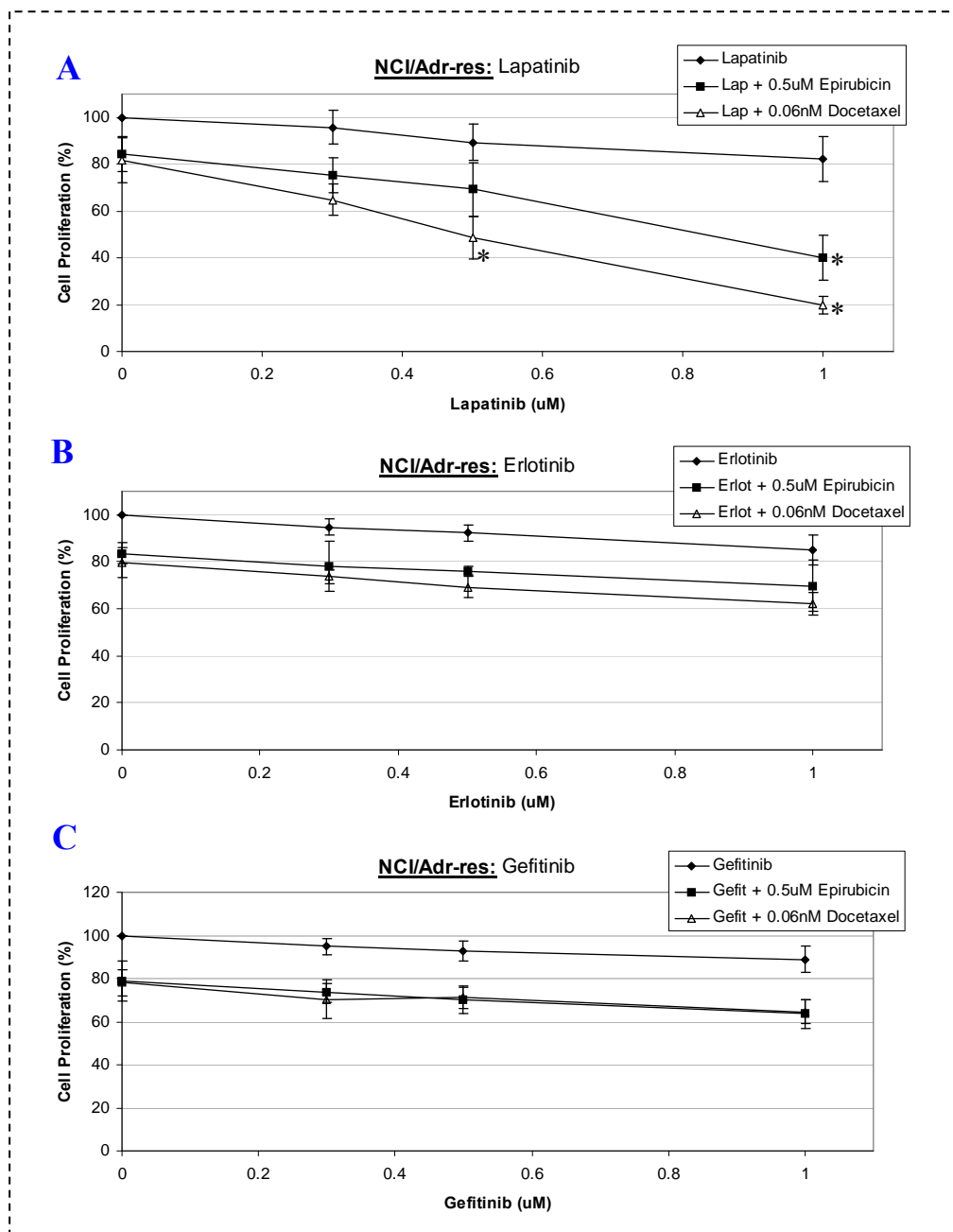
Graph 3.3.5.1.: The combination of epirubicin (■) or docetaxel (Δ) with lapatinib (**A**:◆), erlotinib (**B**:◆) and gefitinib (**C**:◆) in the NCI/Adr-res cell line. This proliferation assay combined clinically relevant concentrations of the TKI's with epirubicin or docetaxel over a 5 day period. The bar chart is the result of triplicate experiments carried out on separate days. Significant changes between each drug alone and the combination of both drugs is indicated by * ($p < 0.05$). Table 3.3.5.1 below depicts the percentage cell proliferation and standard deviations for this graph.

Table 3.3.5.1.: Data for the combination of epirubicin or docetaxel with the three TKI's in the NCI/Adr-res cell line.

TKI (µM)	Cell Proliferation (%)							
	0	StDev (%)	0.3	StDev (%)	0.5	StDev (%)	1	StDev (%)
Lapatinib	100	±0	96	±7	89	±8	82	±10
Lap + 0.5µM Epi	84	±7	75	±8	69	±11	40	±10
Lap + 0.06nM Doce	82	±10	65	±7	49	±9	20	±4
Erlotinib	100	±0	95	±3	92	±3	85	±6
Erlot + 0.5µM Epi	84	±5	78	±11	76	±2	70	±11
Erlot + 0.06nM Doce	80	±6	74	±3	69	±4	62	±5
Gefitinib	100	±0	95	±4	93	±5	89	±6
Gefit + 0.5µM Epi	79	±9	73	±4	70	±6	64	±7
Gefit + 0.06nM Doce	78	±6	70	±9	71	±5	65	±6
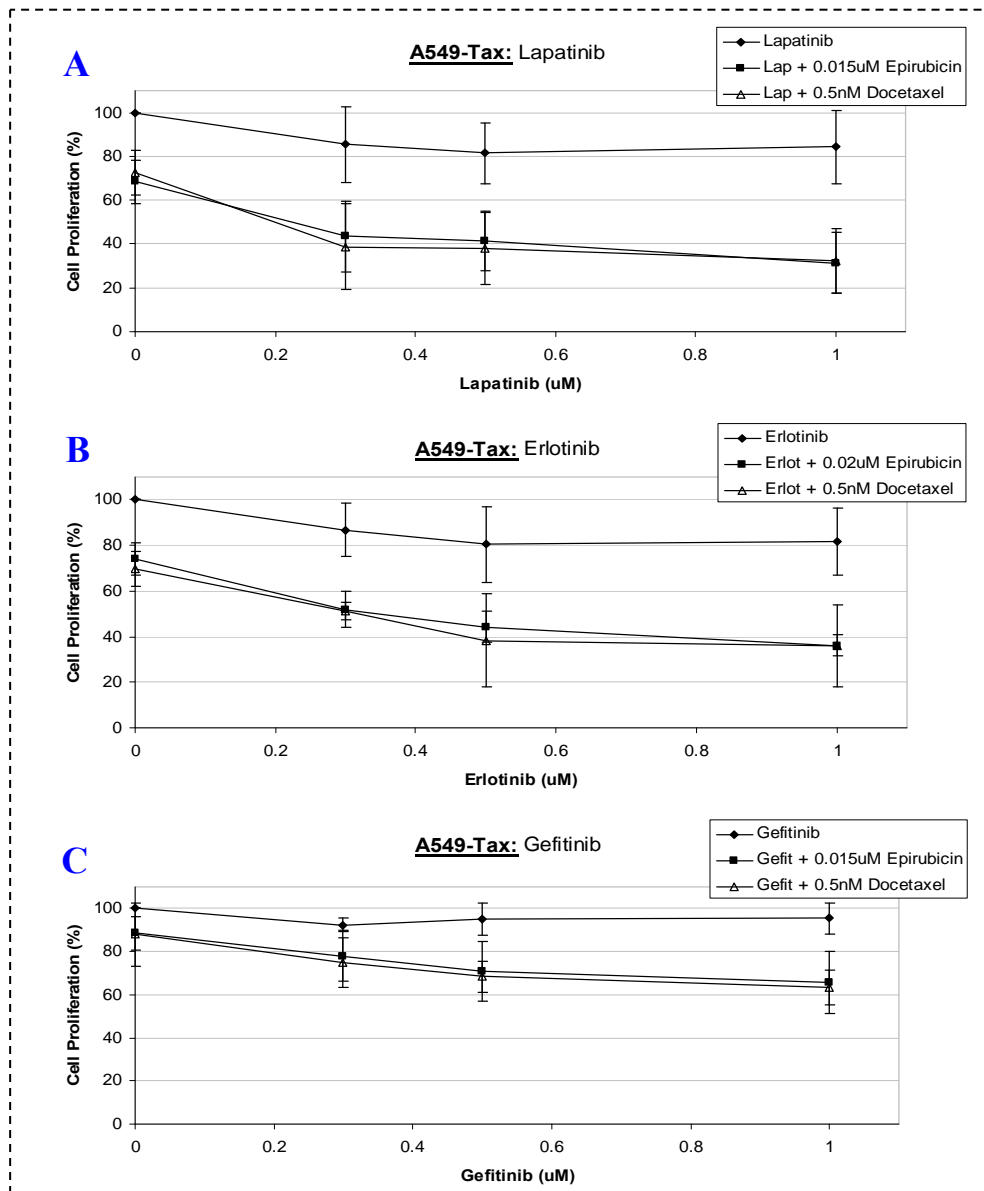
Graph 3.3.5.2.: The combination of epirubicin (■) or docetaxel (Δ) with lapatinib (**A**:◆), erlotinib (**B**:◆) and gefitinib (**C**:◆) in the A549-Taxol cell line. This proliferation assay combined clinically relevant concentrations of the TKI's with epirubicin or docetaxel over a 5 day period. The bar chart is the result of triplicate experiments carried out on separate days. Table 3.3.5.2 depicts the percentage cell proliferation and standard deviations for this graph.

Table 3.3.5.2.: Data for the combination of epirubicin or docetaxel with the three TKI's in the A549-Taxol cell line.

TKI (μM)	Cell Proliferation (%)							
	0	StDev (%)	**0.3**	StDev (%)	**0.5**	StDev (%)	**1**	StDev (%)
Lapatinib	100	±0	86	±17	81	±14	84	±17
Lap + 0.015μM Epi	69	±10	43	±16	41	±13	31	±14
Lap + 0.5nM Doce	73	±10	39	±20	38	±17	32	±15
Erlotinib	100	±0	87	±12	80	±17	82	±15
Erlot + 0.02μM Epi	74	±7	52	±8	44	±7	36	±5
Erlot + 0.5nM Doce	70	±8	51	±4	38	±20	36	±18
Gefitinib	100	±0	92	±3	95	±8	95	±7
Gefit + 0.015μM Epi	88	±8	78	±12	71	±14	66	±14
Gefit + 0.5nM Doce	88	±15	75	±11	68	±7	63	±8
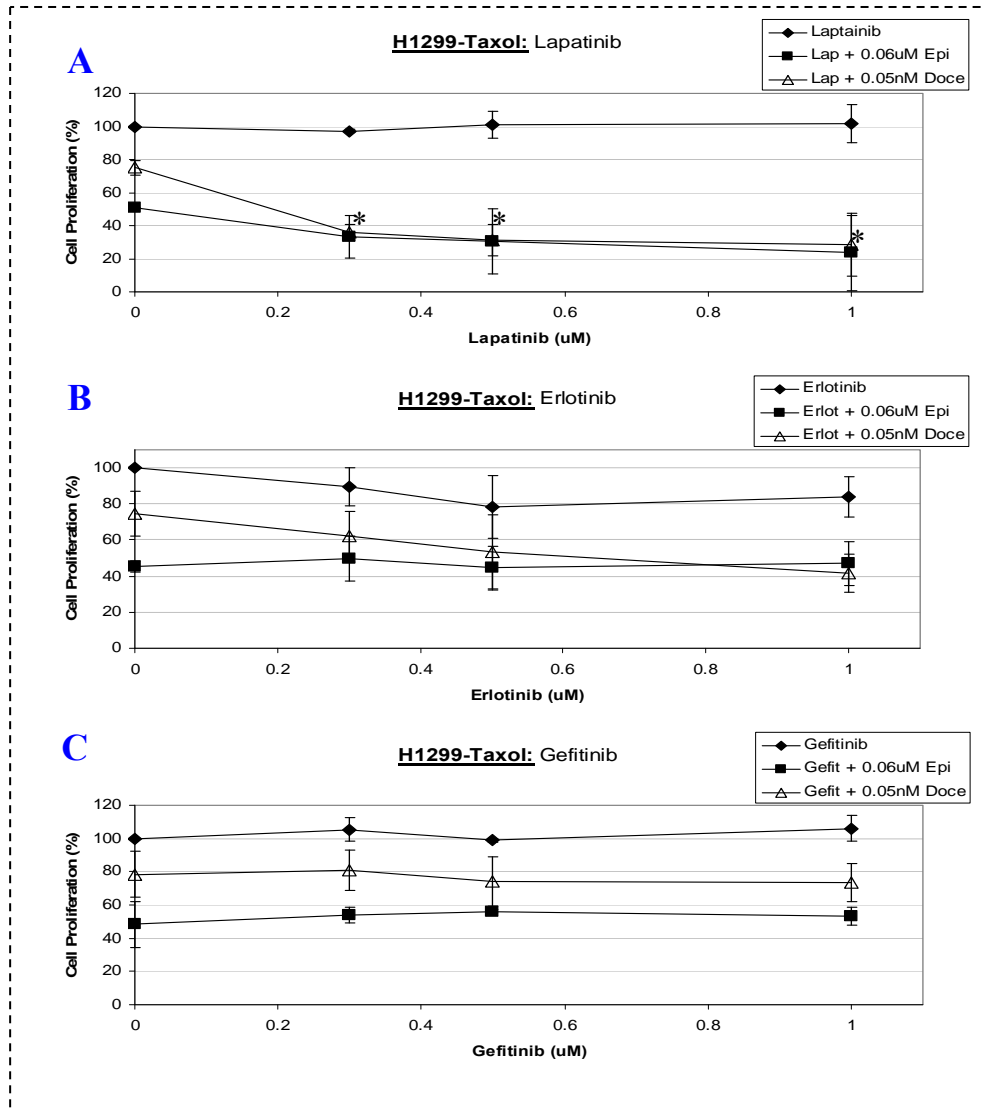
Graph 3.3.5.3.: The combination of epirubicin (■) or docetaxel (Δ) with lapatinib (**A**:◆), erlotinib (**B**:◆) and gefitinib (**C**:◆) in the H1299-Taxol cell line. This proliferation assay combined clinically relevant concentrations of the TKI's with epirubicin or docetaxel on the low P-gp-expressing lung cell line, H1299-Taxol, over a 5 day period. The bar chart is the result of triplicate experiments carried out on separate days. Significant changes between each drug alone and the combination of both drugs is indicated by * (p<0.05). Table 3.3.5.3 below depicts the percentage cell proliferation and standard deviations for this graph.

Table 3.3.5.3.: Data for the combination of epirubicin and docetaxel with the three TKI's in the H1299-Taxol cell line.

TKI (µM)	Cell Proliferation (%)							
	0	Stdev (%)	**0.3**	Stdev (%)	**0.5**	Stdev (%)	**1**	Stdev (%)
Lapatinib	100	±0	97	±1	101	±8	102	±11
Lap + 0.06µM Epi	51	±0	33	±13	31	±20	24	±23
Lap + 0.05nM Doce	75	±5	36	±5	31	±9	28	±19
Erlotinib	100	±0	90	±11	78	±17	84	±11
Erlot + 0.06µM Epi	45	±3	50	±12	45	±12	47	±12
Erlot + 0.05nM Doce	75	±12	62	±14	53	±21	42	±11
Gefitinib	100	±0	105	±7	99	±1	106	±8
Gefit + 0.06µM Epi	48	±14	54	±4	56	±1	53	±5
Gefit + 0.05nM Doce	78	±14	81	±12	74	±15	73	±11

Combination TKI – Cytotoxic proliferation assays in MRP1-expressing cell model.

In this case, a cell line of ovarian origin with transfected MRP1 was chosen, 2008/MRP1 [391]. The 2008/MRP1 cell line was chosen for its stability of MRP1 expression, rapid growth and because no one had employed for such purposes previously. To determine if any effect observed was due to MRP1-inhibition a single substrate, epirubicin, and a non-substrate, docetaxel, were chosen.

The combination proliferation assays of a clinically relevant concentration of docetaxel and epirubicin with lapatinib, erlotinib and gefitinib in the MRP1-expressing ovarian cell line, 2008/MRP1, were comparable (see graphs 3.3.5.4.**A**, **B** and **C** and table 3.3.5.4 for details). Combined, no significant decrease in cell proliferation that would indicate the TKIs ability to overcome MRP1-mediated resistance was observed. However, compared to each individual drug alone the combination was more effective at reducing cell proliferation.

This data suggests that these three TKI's do not overcome MRP1-mediated resistance in the selected model.
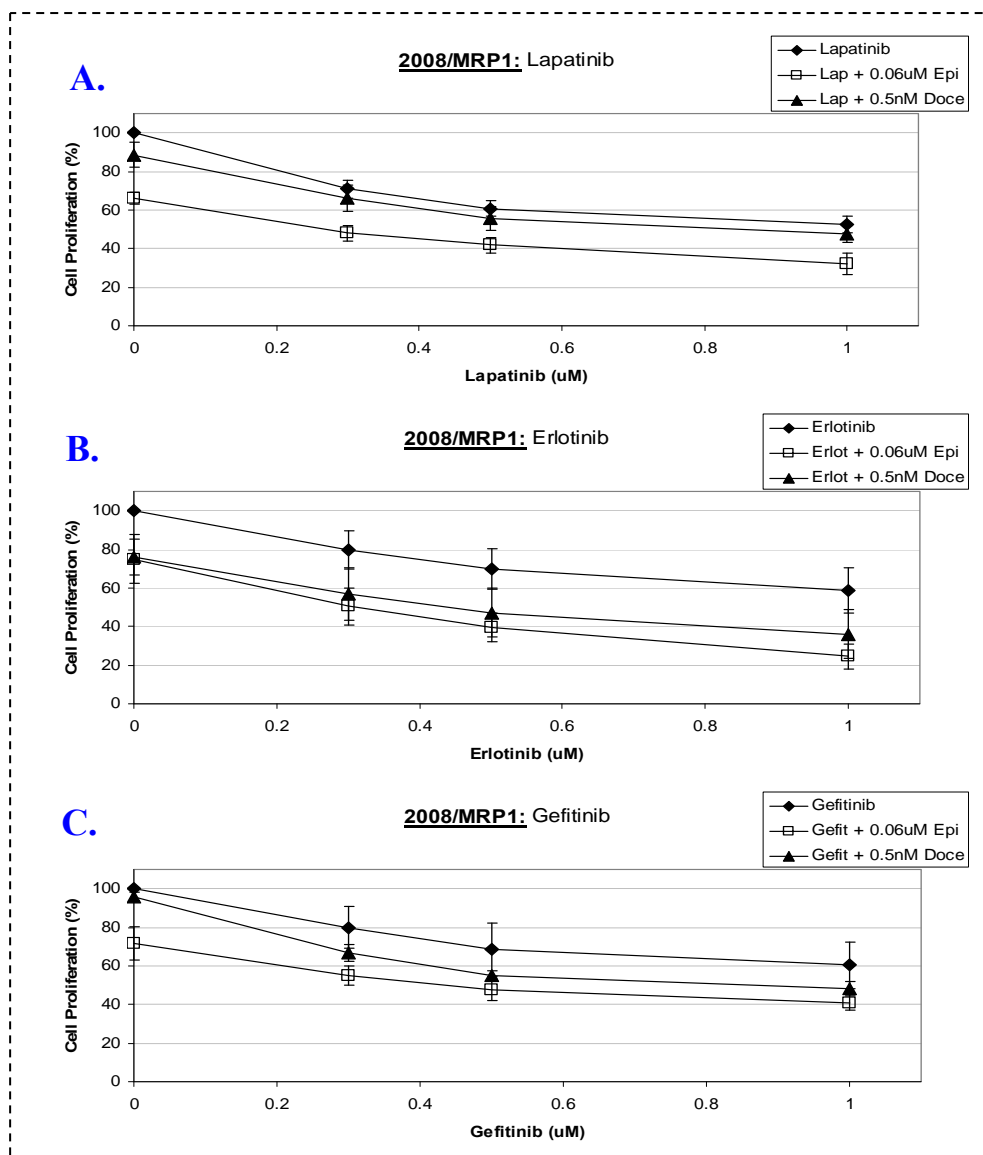
Graph 3.3.5.4.: The combination of epirubicin (□) or docetaxel (▲) with the three TKI's, lapatinib (**A**:◆), erlotinib (**B**◆) and gefitinib (**C**◆), in the 2008/MRP1 cell line. This proliferation assay involved the combination of a single concentration of epirubicin or docetaxel with the three TKI's, in the MRP1-overexpressing cell line, 2008/MRP1, over a 5 day period. This bar chart is the result of triplicate assays on separate days. Table 3.3.5.4 below depicts the percentage cell proliferation and standard deviations for this graph.

Table 3.3.5.4.: Data for the combination of epirubicin or docetaxel with lapatinib, erlotinib and gefitinib in the 2008/MRP1 cell line.

TKI (µM)	Cell Proliferation (%)							
	0	StDev (%)	**0.3**	StDev (%)	**0.5**	StDev (%)	**1**	StDev (%)
Lapatinib	100	±0	71	±5	61	±4	53	±4
Lap + 0.06µM Epi	66	±3	48	±4	42	±4	32	±6
Lap + 0.5nM Doce	89	±7	66	±7	56	±6	48	±4
Erlotinib	100	±0	80	±10	70	±10	59	±12
Erlot + 0.06µM Epi	75	±13	50	±10	40	±7	25	±6
Erlot + 0.5nM Doce	76	±9	57	±13	47	±13	36	±12
Gefitinib	100	±0	80	±11	68	±14	60	±12
Gefit + 0.06µM Epi	72	±9	55	±5	47	±5	41	±4
Gefit + 0.5nM Doce	96	±2	67	±4	55	±2	48	±4

Combination TKI – Cytotoxicity proliferation assays in a BCRP-expressing cell model.

We compared the efficacy of the TKI's to inhibit, and thus sensitise, BCRP-expressing cells to BCRP substrate cytotoxic agents. The model chosen (DLKP-SQ/mitox), has stable and high expression of BCRP and was developed in the NICB by Helena Joyce. Western blots demonstrated the presence of this protein in the cell line (see figure 3.4.1.1.).
The substrate chosen for this work was SN38 (the active metabolite of irinotecan [373]).

We found that all three TKI's hugely potentiated the cytotoxicity of SN38 when combined in the DLKP-SQ/mitox cell line (see graph 3.3.5.5 and table 3.3.5.5 for details). Lapatinib caused the greatest effect, followed closely by erlotinib and finally gefitinib.
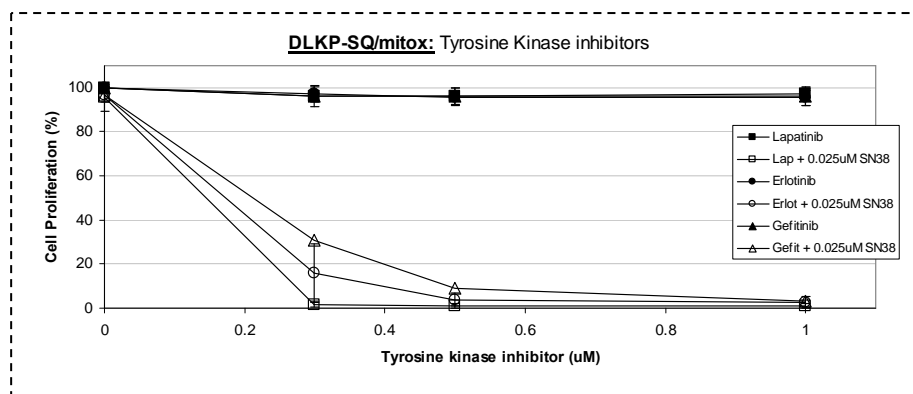
Graph 3.3.5.5.: The combination of SN38 with lapatinib (alone: ■, combined: □), erlotinib (alone: ●, combined: ○) or gefitinib (alone: ▲, combined: Δ) in the DLKP-SQ/mitox cell line. This proliferation assay involved the combination of a single concentration of SN38 with the three TKI's, in the BCRP-overexpressing cell line, DLKP-SQ/mitox, over a 5 day period. The bar chart is the result of a triplicate assays and all combination results are statistically significant when compared to each drug alone. Table 3.3.5.5 below depicts the percentage cell proliferation and standard deviations of this graph.

Table 3.3.5.5.: Data for the combination of SN38 with three TKI's, lapatinib, erlotinib and gefitinib in the DLKP-SQ/mitox cell line.

TKI (µM)	Cell Proliferation (%)							
	0	StDev (%)	**0.3**	StDev (%)	**0.5**	StDev (%)	**1**	StDev (%)
Lapatinib	100	±0	96	±2	96	±2	97	±1
Lap + 0.025µM SN38	96	±6	2	±1	1	±1	1	±1
Erlotinib	100	±0	97	±4	96	±4	96	±4
Erlot + 0.025µM SN38	97	±3	16	±13	4	±3	3	±2
Gefitinib	100	±0	96	±4	96	±4	96	±4
Gefit + 0.025µM SN38	97	±3	31	±35	9	±9	3	±3

3.3.6. The impact of short-term TKI exposure on protein expression levels of P-gp, MRP1 and BCRP.

In this section, we compared the extent, if any, to which the three TKI's altered the expression of three multidrug resistant transporter proteins, P-gp, MRP1 and BCRP. For this we chose 3 cells lines each expressing one type of MDR protein. These cell lines were chosen for their levels of protein expression. We hypothesised that moderate transporter overexpression was likely to be amenable to increased and decreased expression.

In this case, A549-Taxol (a lung cell line expressing P-gp), A549 (a lung cell line expressing MRP1) and DLKP-SQ/mitox (the BCRP expressing daughter cell line to DLKP-SQ, the non-small cell lung carcinoma cell line) were chosen. A549 was chosen for this section over 2008/MRP1 as it is easier to obtain a distinct protein band by Western blotting therefore allowing for better evaluation of the results.

Following a 24 hr exposure to 0.3, 0.5 and 1 μM lapatinib, erlotinib or gefitinib, P-gp expression was increased from between 40% and 200% in the A549-Taxol cell line (see figure 3.3.6.1. and table 3.3.6.1 for details). The Western blots shown in figure 3.3.6.1 are the result of a single determination, however similar findings have been replicated by two members of our group [197] [112].

Following a 24hr exposure to 0.3, 0.5 and 1 μM erlotinib or gefitinib the expression of MRP1 in the A549 cell line was up-regulated (see figure 3.3.6.2 and table 3.3.6.2. for details, result also replicated by another member of out group [197]). However, lapatinib had the opposite effect causing a 70% reduction in MRP1 protein expression compared to the control sample (see table 3.3.6.2. for details).

The same exposure in the DLKP-SQ/mitox cells resulted in a less marked result (refer to figure 3.3.6.3 for details). Some down-regulation occurred in the 1st biological test of lapatinib but the replicate was not fully consistent with this. Erlotinib showed slight down-regulation at 0.3 and 0.5 μM but up-regulation with 1 μM (this was also replicated by another member of our group [112]). All concentrations of gefitinib reduced BCRP expression and this was confirmed in a biological replicate. The densitometry is presented in table 3.3.6.3. This table also includes the densitometry results for the replicate Western blots that are not presented in figure 3.3.6.3.

Effect of short-term TKI exposure on P-gp expression in the A549-Taxol cell line.
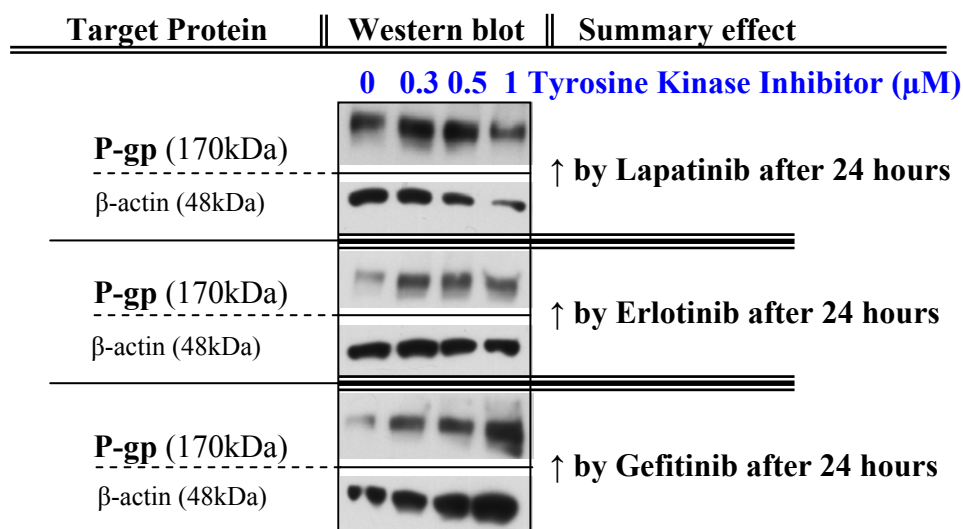
Figure 3.3.6.1.: Western blots illustrating changes in P-gp (170kDa) expression following 24hr exposures to 0, 0.3, 0.5 and 1 µM lapatainib, erlotinib or gefitinib in the moderately-expressing P-gp lung cell line, A549-Taxol. The arrows (↑) indicate that the P-gp protein was upregulated compared to control sample. Each sample loaded contained 40 µgs protein. These Western blots are the result of a single experiment. Densitometric analysis was carried out on these Westerns and the fold changes compared to control/untreated protein bands and normalised to β-actin are presented in table 3.3.6.1 below

Table 3.3.6.1.: Precentage changes in P-gp protein expression in the A549-Taxol cells following a 24 hr exposure to 0, 0.3, 0.5 and 1 µM lapatinib, erlotinib or gefitinib. These percentage changes were determined using densitometric analysis of Western blots carried out on lysates of the exposed A549-Taxol cells.

	Percentage Change			
TKI (µM)	0	0.3	0.5	1
Lapatinib	0	40	130	130
Erlotinib	0	170	200	160
Gefitinib	0	200	140	90

Effect of short-term TKI exposure on MRP1 expression in the A549 cell line.
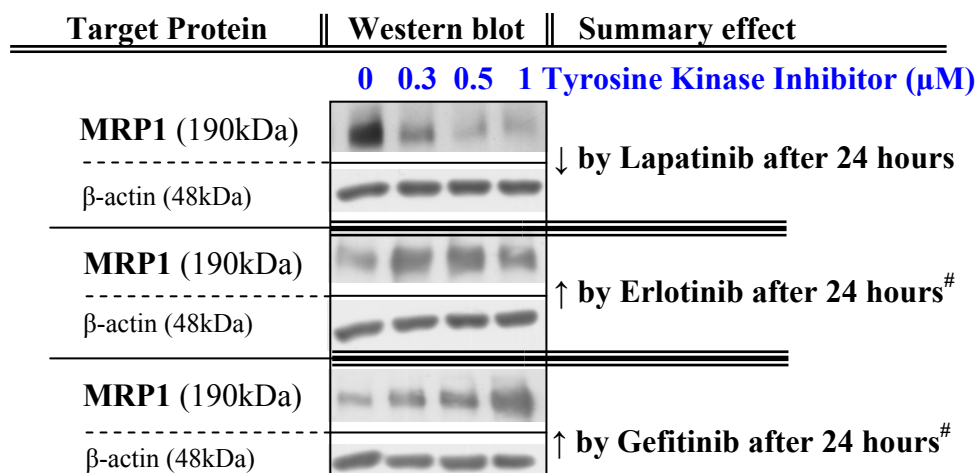
Figure 3.3.6.2.: Western blots showing changes in expression of MRP1 (190kDa) following 24hr exposures to 0, 0.3, 0.5 and 1μM lapatainib, erlotinib or gefitinib in the moderately expressing MRP1 lung cell line, A549. The arrows (↑ / ↓) indicate that the MRP1 protein was upregulated/downregulated compared to control sample. Each sample loaded contained 40 μgs protein. These Western blots are the result of duplicate or more Western blots, unless otherwise indicated ([#]). Densitometric analysis was carried out on these Westerns and the fold changes compared to control/untreated protein bands and normalised to β-actin are presented in table 3.3.6.2 below.

Table 3.3.6.2.: Fold changes in the expression of MRP1 in A549 cells following exposure to 0, 0.3, 0.5 and 1μM lapatinib, erlotinib and gefitinib for 24hrs. These fold changes were determined using densitometric analysis of Western blots carried out on lysates of the exposed A549 cells.

	Percentage Change			
TKI (μM)	**0**	**0.3**	**0.5**	**1**
Lapatinib	1	-60	-80	-70
Erlotinib	1	110	90	40
Gefitinib	1	110	140	270

Effect of short-term TKI exposure on BCRP expression in the DLKP-SQ/mitox cell line.

Target Protein	‖ Western blot ‖	Summary effect
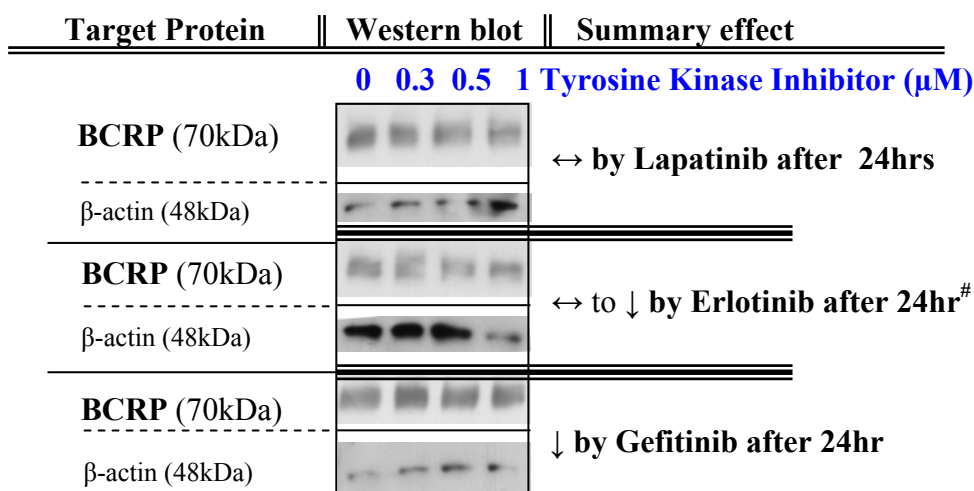
Figure 3.3.6.3.: These Western blots show changes in expression of BCRP (70kDa) following 24hr exposures to 0, 0.3, 0.5 and 1 µM lapatainib, erlotinib and gefitinib in the highly over-expressing BCRP lung cell line, DLKP-SQ/mitox. The arrows indicate that the BCRP protein is unchanged ($\leftrightarrow$) or downregulated ($\downarrow$) compared to control sample. 4 µgs of sample was loaded to each well. These Western blots are the represent duplicate or more independent Western blots, unless otherwise indicated ([#]). Densitometric analysis was carried out on these Westerns and the fold changes compared to control/untreated bands are presented in table 3.3.6.3 below.

Table 3.3.6.3.: Fold changes in the expression of BCRP in DLKP-SQ/mitox cells following exposure to 0, 0.3, 0.5 and 1 µM lapatinib, erlotinib and gefitinib for 24hrs. These fold changes (compared to the control/untreated samples) were determined using densitometric analysis of western blots carried out on lysates of the exposed DLKP-SQ/mitox cells. The westerns blots for lapatinib and gefitinib were carried out in duplicate and the densitometry for both blots is presented in this table.

TKI (µM)	Percentage Change			
	0	0.3	0.5	1
Lapatinib	1	-25	-45	-35
Erlotinib	1	-20	-40	90
Gefitinib	1	-20	-35	-25

3.4. Relationship between the COX-2 inhibitor, celecoxib, and expression and function of Multidrug resistant proteins.

This work was presented as a poster at the IACR conference in 2009. Over the next year, this body of work will be submitted for publication.

3.4.1. Cell Panel Characterisation

The purpose of this section was to verify the MDR and COX status of a panel of cell lines that were to be used in combination proliferation assays, pharmacokinetic and protein studies. Initially, 40 μgs of each protein sample was loaded; however, differences in target protein expression required alterations in the amount loaded for some samples.

Most cell lines gave the expected results with regard to their MDR status, i.e. DLKP-A expressed high levels of P-gp but did not express MRP1 or BCRP, HL60/S did not express P-gp, MRP1 or BCRP, etc (see table 3.4.1.1. and figure 3.4.1.1 to 3.4.1.3 for details). One cell line did not express the protein expected. From previous work done in the NICB (by Alex Eustace), BCRP expression was expected in lane 9 (M14) of figure 3.4.1.1. Later, BCRP-specific combination proliferation assays confirmed a lack of BCRP expression in this cell line.

Most cells in the body express COX-1, therefore it was not unexpected to find that every cell line in this panel expressed this protein (see table 3.4.1.1 and figure 3.4.1.4 for details).

However, expression of COX-2 was less common and the profile of this panel could not be predicted. Western blot analysis showed that 2008/MRP1 expressed very high levels of this protein while HL60/S and M14 expression was barely detectable (see table 3.4.1.1 and figure 3.4.1.5 for details).

Table 3.4.1.1.: Summary of the MDR and COX expression profile in the panel of cell lines used in this project.

Cell model	MRP1	P-gp	BCRP	COX-1	COX-2
HL60/S	-	-	-	+	+
M14	-	-	-	+	+
DLKP	+	-	-	+	-
2008/MRP1	+++	-	-	++	+++
HL60/Adr	++	-	-	+	-
DLKP-A	-	+++	-	+	-
H1299-T	-	++	-	++	-
HL60/mdr1	-	+++	-	+++	-
DLKP-SQ/mitox	-	-	+++	+	-
HL60/mxr	-	-	++	+	-

Key:

- No protein detected

+ Low protein expression

++ Moderate protein expression

+++ High protein expression

BCRP profiling:
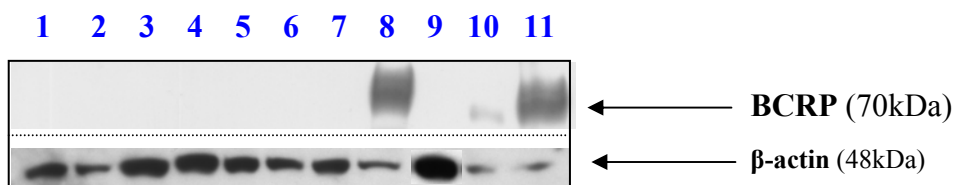
Figure 3.4.1.1.: The expression of BCRP in a panel of cell lines using the Western blotting technique. The positive control used in this blot was DLKP-SQ/mitox (lane 11). Lanes 1 to 7 (HL60/s, DLKP, 2008/MRP1, HL60/Adr, DLKP-A, H1299-Taxol, and HL60/Mdr1) did not express BCRP while lane 8 (DLKP-SQ/mitox) and 10 (HL60/mxr) expressed the protein. This Western blot is representative of duplicate independent determinations. Results are summarised in table 3.4.1.1.

Combination proliferation assays confirmed these results (see section 3.4.2 for details).

Western blot lane designation:

1. HL60/S (40μg)
2. DLKP (40μg)
3. 2008/MRP1 (40μg)
4. HL60/Adr (40μg)
5. DLKP-A (40μg)
6. H1299-Taxol (40μg)
7. HL60/mdr1 (40μg)
8. DLKP-SQ/mitox (10μg)
9. M14 (50μg)
10. HL60/mxr (10μg)
11. Positive control; DLKP-SQ/mitox (5μg)

MRP1 profiling:
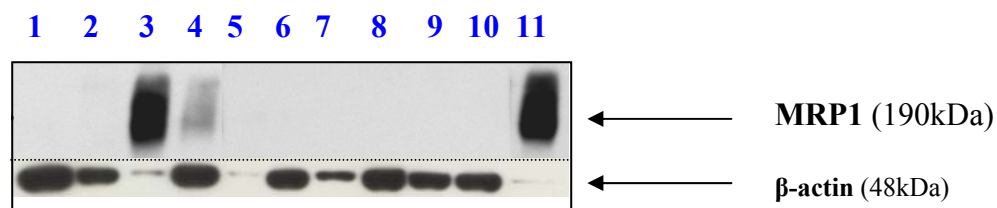
Figure 3.4.1.2.: Expression of MRP1 in a panel of cell lines using the Western blotting technique. Lanes 1 and 5 to 10 (HL60/s, DLKP-A, H1299-Taxol, HL60/Mdr1, DLKP-SQ/mitox, M14 and HL60/mxr) did not express MRP1 while lane 3 (2008/MRP1) and 4 (HL60/Adr) express the protein. Lane 2 (DLKP) had a very small amount and is barely evident. The positive control used in this blot is 2008/MRP1 and is located in lane 11. These results are summarised in table 3.4.1.1 above. This Western blot is representative of duplicate independent determinations. Results are summarised in table 3.4.1.1.

Combination proliferation assays also confirmed these results (see section 3.4.2 for details).

Western blotting lane designation:

1. HL60/S (40μg)
2. DLKP (40μg)
3. 2008/MRP1 (10μg)
4. HL60/Adr (40μg)
5. DLKP-A (10μg)
6. H1299-Taxol (40μg)
7. HL60/Mdr1 (20μg)
8. M14 (40μg)
9. DLKP-SQ/mitox (40μg)
10. HL60/mxr (40μg)
11. Positive control; 2008/MRP1 (10μg)

P-gp profiling:
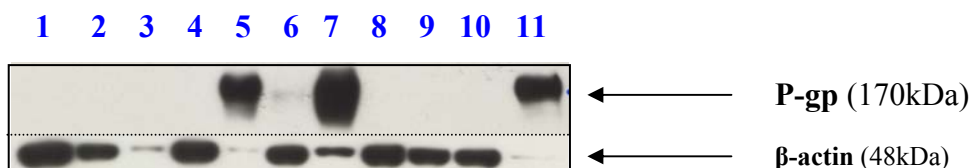
Figure 3.4.1.3.: Western blot show the expression of P-gp in a panel of cell lines. The positive control used in this blot is DLKP-A (lane 11). Lanes 1 to 4 and lane 8 to 10 (HL60/s, DLKP, 2008/MRP1, HL60/Adr, DLKP-SQ/mitox, M14 and HL60/mxr) did not express P-gp while lane 5 to 7 (DLKP-A, H1299-Taxol and HL60/mdr1) expressed the protein. DLKP-A had the highest expression of P-gp, followed closely by HL60/mdr1 and to a much lesser extent H1299-Taxol. These results are summarised in table 3.4.1.1 above. This Western blot is representative of duplicate independent determinations. Results are summarised in table 3.4.1.1. Combination proliferation assays confirmed these results (see section 3.4.2 for details).

Western blotting lane designation:
1. HL60/S (40µg)
2. DLKP (40µg)
3. 2008/MRP1 (10µg)
4. HL60/Adr (40µg)
5. DLKP-A (10µg)
6. H1299-Taxol (40µg)
7. HL60/Mdr (20µg)
8. M14 (40µg)
9. DLKP-SQ/mitox (40µg)
10. HL60/mxr (40µg)
11. Positive control; DLKP-A (10µg)

COX profiling:
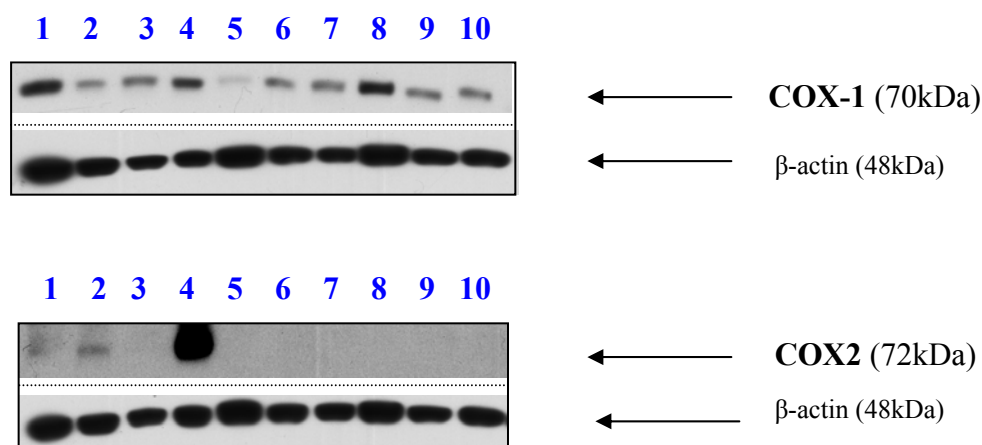
Figure 3.4.1.4.: Western blots show the expression of COX-1 and COX-2 in a panel of cell lines. The COX-1 positive control used was a mouse heart extract purchased from Santa Cruz. COX-2 positive control is A549. As COX-1 is known to be expressed in most tissue types it is not unexpected to discover every cell line in this panel express COX-1. On the other hand, COX-2 is not constitutively expressed but has been found to be expressed or up-regulated in cancer cells. Out of this panel HL60/S (lane 1), M14 (lane 2) and 2008/MRP1 (lane 4) expressed detectable levels of COX-2. The COX-1 blot was carried in duplicate (A and B) and the COX-2 Western is the result of a single experiment (A). These results are summarised in table 3.4.1.1 above.

Western blot lane designation:
1. HL60/S (40µg)
2. M14 (20µg)
3. DLKP (40µg)
4. 2008/MRP1 (40µg)
5. HL60/Adr (40µg)
6. DLKP-A (40µg)
7. H1299-Taxol (40µg)
8. HL60/Mdr1 (40µg)
9. DLKP-SQ/mitox (20µg)
10. HL60/mxr (20µg)

3.4.2. Effect of celecoxib on the inhibition of multidrug resistance transporter proteins.

The use of NSAIDs in the clinic for cancer treatment has been suggested and some agents such as, sulindac, are currently undergoing clinical trials (for review see section 1.4.3). The purpose of this body of work was to clarify the true relationship between celecoxib and its effect on the three MDR transporters. We selected a panel of MDR-expressing cell lines, two substrates, two non-substrates and an inhibitor for each MDR transporter. The cell lines were chosen for having established, reliable expression of their MDR proteins. The two substrates that were chosen for each MDR pump were selected in order to rule out the possibility of interacting with other MDR pumps and other non-MDR mechanisms. For example, epirubicin and docetaxel were chosen for the P-gp combination assays as docetaxel is a substrate for P-gp but not for MRP1 or BCRP, however, eprubicin is a substrate for P-gp, MRP1 and one mutant form of BCRP. A non-substrate for each MDR pump was selected to demonstrate that any additivity observed was due to that particular MDR transporter and not another.

Table 3.4.2.1.: Summary of the MDR cell lines, substrates, non-substrates and MDR-inhibitors used in this project.

MDR transporter	Cell line	Substrate	Non-substrate	MDR-inhibitor
P-gp	DLKP-A	Epirubicin	Cisplatin	Elacridar
	H1299-Taxol	Docetaxel	5FU	
	HL60/mdr1			
MRP1	DLKP	Epirubicin	Docetaxel	Sulindac Sulphide
	2008/MRP1	Vincristine	5FU	
	HL60/Adr			
BCRP	DLKP-SQ/mitox	SN38	Vinblastine	Elacridar
	HL60/mxr			

Note: The relationship of each drug with the multidrug resistance transporter proteins was discussed in section 1.4 and in tables 1.4.1, 1.4.2 and 1.4.3 of the introduction.

Interaction of celecoxib with P-gp-mediated resistance

As presented in section 3.4.1., the three P-gp expressing cell lines selected for this project were DLKP-A, H1299-Taxol and HL60/mdr1 (figure 3.4.1.3, table 3.4.2.1 and table 2.5.1 for for further details). The combination proliferation assays of epirubicin or docetaxel with celecoxib in the P-gp-overexpressing lung cell lines, H1299-Taxol and DLKP-A, demonstrated a moderate decrease in cell proliferation compared to celecoxib or the P-gp substrate alone. This effect only occurred with the highest concentration of celecoxib (10 µM). A milder effect was observed at biologically relevant concentrations (2 µM) (see graphs 3.4.2.1.**A** and **B** and table 3.4.2.1 for details). However, in graph 3.4.2.1.**C1** and **C2**, the combination proliferation assays of epirubicin and doctaxel with celecoxib in the HL60/mdr1 cell line demonstrated no change in growth proliferation. No interaction was observed by the combination of celecoxib with cisplatin or 5FU on these cell lines.

The decrease in cell proliferation observed with the P-gp substrates suggest that celecoxib overcomes P-gp-mediated resistance to a minor extent at biologically-relevant concentrations.
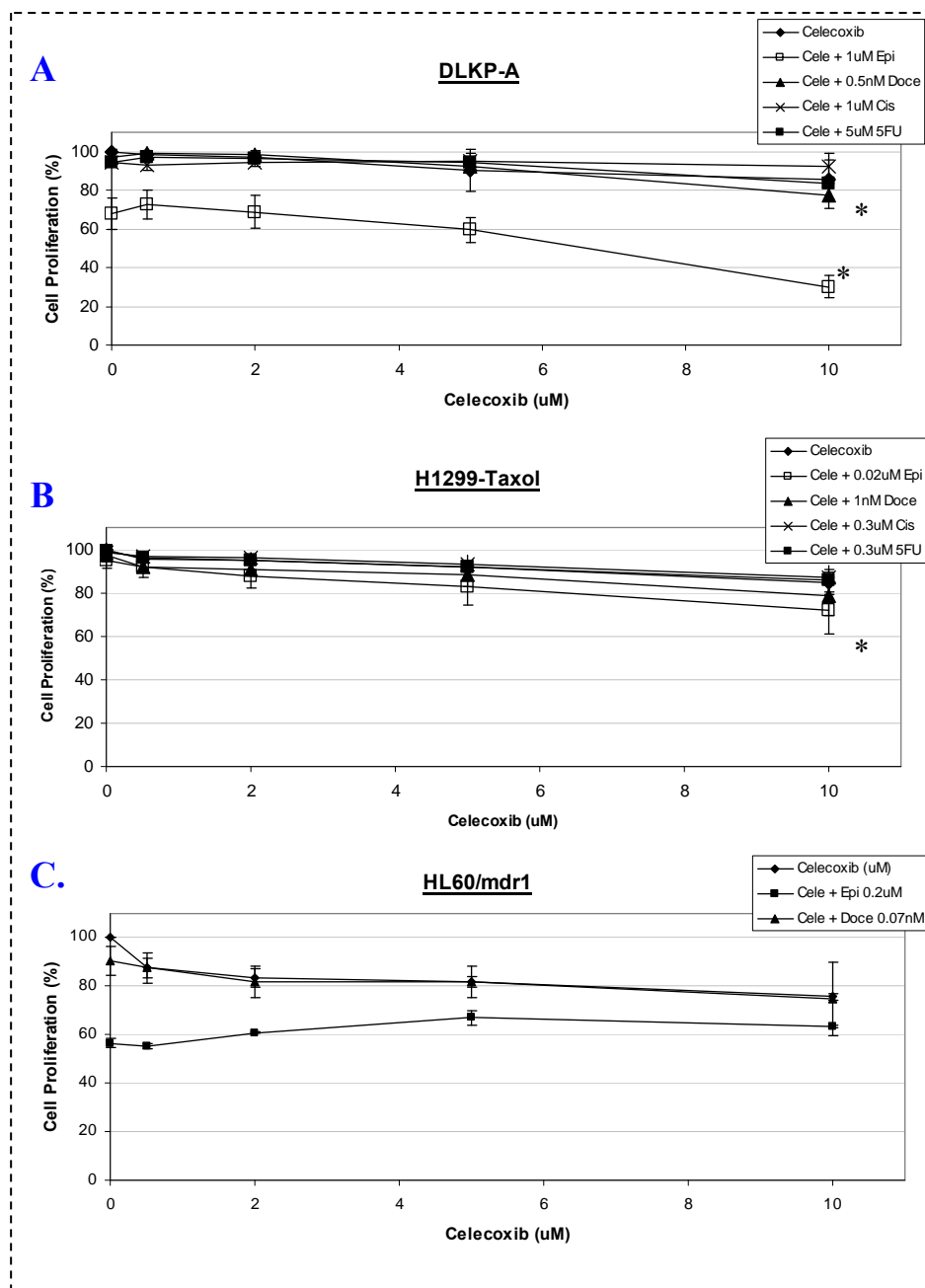
Graph 3.4.2.1.: The combination of epirubicin (□), docetaxel (▲), cisplatin (×) or 5FU (■) with celecoxib (◆) in the DLKP-A (**A**), H1299-Taxol (**B**) and HL60/mdr1 (**C**) cell lines. This proliferation assay involved the combination of one of 4 chemotherapeutic agents with celecoxib on the high, low and moderately expressing P-gp cell line, DLKP-A, H1299-Taxol and HL60/mdr1, over a 5 day period. Graph 3.4.2.1.**A** and **B** are the result of triplicate assays on separate days. Significant changes between each drug alone and the combination of both drugs is indicated by * ($p<0.05$). Graphs 3.4.2.1.**C** represents duplicate independent determinations Table 3.4.2.1 below depicts the percentage cell proliferation and standard deviations for this graph.

Table 3.4.2.1.: The percentage cell proliferation and standard deviations for the combination proliferation assays of epirubicin, docetaxel, cisplatin and 5FU with celecoxib in the three P-gp expressing cell lines. This table is illustrated in graph 3.4.2.1.

Cell line	Agents	Cell Prolfieration (%)									
	Celecoxib (µM)	0	StDev (%)	0.5	StDev (%)	2	StDev (%)	5	StDev (%)	10	StDev (%)
DLKP-A	Celecoxib	100	±0	98	±2	97	±2	91	±11	85	±10
	Cele + 1µM Epi	68	±8	73	±7	69	±8	60	±7	30	±6
	Cele + 0.5nM Doce	97	±4	99	±1	98	±3	92	±2	78	±7
	Cele + 1µM Cis	94	±1	93	±3	95	±2	95	±4	93	±6
	Cele + 5µM 5FU	94	±2	97	±0	97	±2	94	±0	84	±0
H1299-Tax	Celecoxib	100	±0	96	±1	95	±1	92	±2	84	±5
	Cele + 0.02µM Epi	95	±4	92	±5	88	±6	83	±8	72	±11
	Cele + 1nM Doce	97	±3	92	±2	91	±2	88	±5	78	±9
	Cele + 0.3µM Cis	99	±2	97	±1	96	±3	93	±4	87	±6
	Cele + 0.3µM 5FU	99	±2	96	±1	95	±1	92	±3	86	±5
HL60/mdr1	Celecoxib	100	±0	88	±6	83	±4	82	±6	76	±2
	Cele + 0.2µM Epi	57	±2	55	±1	61	±0	67	±3	64	±1
	Cele + 0.07nM Taxt	90	±6	88	±4	82	±7	82	±2	75	±15

Interaction of celecoxib with MRP1-mediated resistance

As presented in section 3.4.1., the three MRP1-expressing cell lines selected for this project were DLKP, 2008/MRP1 and HL60/Adr (figure 3.4.1.2, table 3.4.2.1 and table 2.5.1 for further details). The combination proliferation assays of vincristine with celecoxib in all three MRP1-expressing cell lines, DLKP (**A**), 2008/MRP1 (**B**) and HL60/Adr (**C1** and **C2**), gave a significant decrease in cell proliferation (see graphs 3.4.2.2.**A**, **B**, **C1** and **C2** and table 3.4.2.2. for details). The combination of epirubicin with celecoxib in the DLKP or 2008/MRP1 cell lines also had the same impact on cell growth. However, this combination caused no change in cell growth in the HL60/Adr cells.

The combinations of docetaxel and 5FU with celecoxib had no heightened decrease in the cell proliferation of DLKP or 2008/MRP1 therefore adding weight to thefact that these cells do not express P-gp and that the enhanced toxicity of the MRP1 substrates by celecoxib is the results of celecoxib overcoming MRP1-mediated resistance.

Graphs 3.4.2.2.**A** and **B** represent the average of three indepent determinations. Graph 3.4.2.2.**C1** and **C2** are duplicates of each other and represent single independent determinations. Table 3.4.2.2 contains the percentage cell proliferation and standard deviations for graphs **A**, **B** and **C** in graph 3.4.2.2.

In section 8, results for the combination assay of vincristine or epirubicin with celecoxib on the A549, moderately expressing MRP1, cell line are presented . This cell line does not express P-gp or BCRP [112]. The A549 cell line was included as it was later used to examine the effect of celecoxib on the expression of MRP1 (see section 3.4.3 for further details). The presence of celecoxib enhanced the anti-proliferative potential of both MRP1 substrates, epirubicin and vincristine (see section 8, graph 8.4.2.1 and table 8.4.2.1 for details). Therefore, celecoxib also overcomes MRP1-mediated resistance in the A549 cell line.
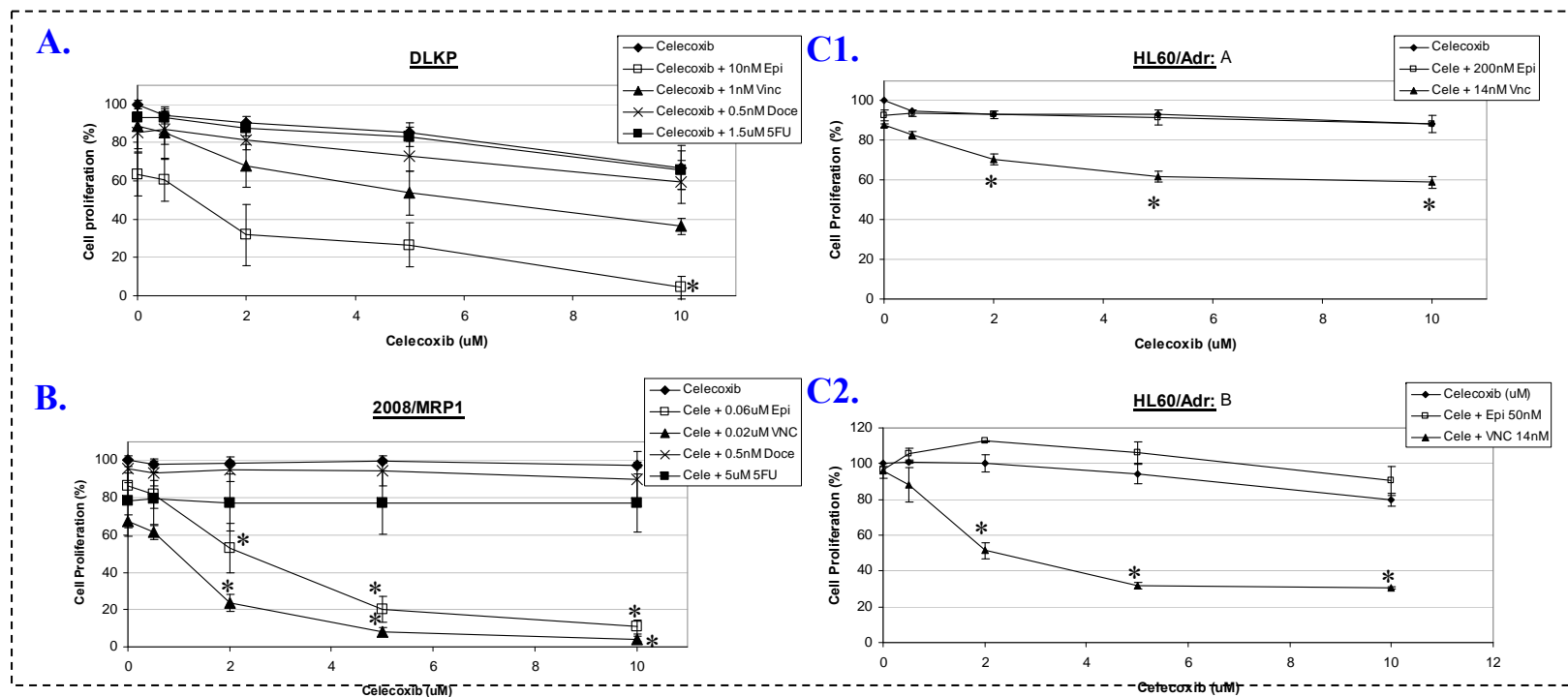
Graph 3.4.2.2.: The combination of epirubicin (□), vincristine (▲), docetaxel (×) or 5FU (■) with celecoxib (◆) in the DLKP (**A**), 2008/MRP1 (**B**) and HL60/Adr (**C1** and **C2**) cell lines. This proliferation assay involved the combination of one of 4 chemotherapeutic agents with celecoxib in very low, high and moderately expressing MRP1 cell lines, DLKP, 2008/MRP1 and HL60/Adr, over a 5 day period. Graph 3.4.2.2.**A**. and **B** are the result of a triplicate independent determinations. Significant changes between each drug alone and the combination of both drugs is indicated by * ($p<0.05$). Graphs 3.4.2.2.**C1** and **C2**. were single day replicates. Table 3.4.2.2 below depicts the percentage cell proliferation and standard deviations for this graph.

Table 3.4.2.2.: The percentage cell proliferation and standard deviations for the combination proliferation assays of epirubicin, vincristine, docetaxel, or 5FU with celecoxib in the three MRP1-expressing cell lines. This table is illustrated in graph 3.4.2.2.

Cell line	Agents	Cell Prolfieration (%)									
	Celecoxib (µM)	0	StDev (%)	0.5	StDev (%)	2	StDev (%)	5	StDev (%)	10	StDev (%)
DLKP	Celecoxib	100	±0	94	±3	90	±4	85	±5	67	±11
	Cele + 10 nM Epi	63	±11	61	±11	32	±16	26	±12	4	±6
	Cele + 1 nM Vinc	89	±13	85	±14	68	±11	54	±12	36	±4
	Cele + 0.5 nM Doce	85	±8	87	±8	81	±5	73	±8	59	±11
	Cele + 1.5 µM 5FU	93	±5	93	±3	87	±4	83	±5	66	±10
2008/MRP1	Celecoxib	100	±0	98	±2	99	±1	99	±1	97	±1
	Cele + 60 nM Epi	86	±7	82	±8	53	±13	20	±7	11	±4
	Cele + 20 nM Vinc	67	±3	61	±4	24	±5	8	±2	4	±1
	Cele + 0.5 nM Doce	95	±7	94	±7	95	±7	95	±8	90	±14
	Cele + 5µM 5FU	78	±19	80	±14	77	±15	77	±17	77	±16
HL60/Adr	Celecoxib	100	±0	95	±2	93	±6	93	±5	88	±5
	Cele + 0.05µM Epi	93	±3	94	±2	93	±2	92	±4	88	±4
	Cele + 0.14µM Vinc	88	±1	83	±2	70	±3	62	±3	59	±3

Interaction of Celecoxib with BCRP-mediated resistance:

Two cell lines were used in this section; DLKP-SQ/mitox and HL60/mxr (see figure 3.4.1.3, table 3.4.2.1 and table 2.5.1 for further details). The combination proliferation assay of SN38 with celecoxib in both cell lines, DLKP-SQ/mitox and HL60/mxr, gave a mild decrease in cell proliferation at the pharmacologically-relevant concentration of 2 µM and a much greater effect with 5 and 10 µM (see graphs 3.4.2.3.A, and table 3.4.2.3 for details).
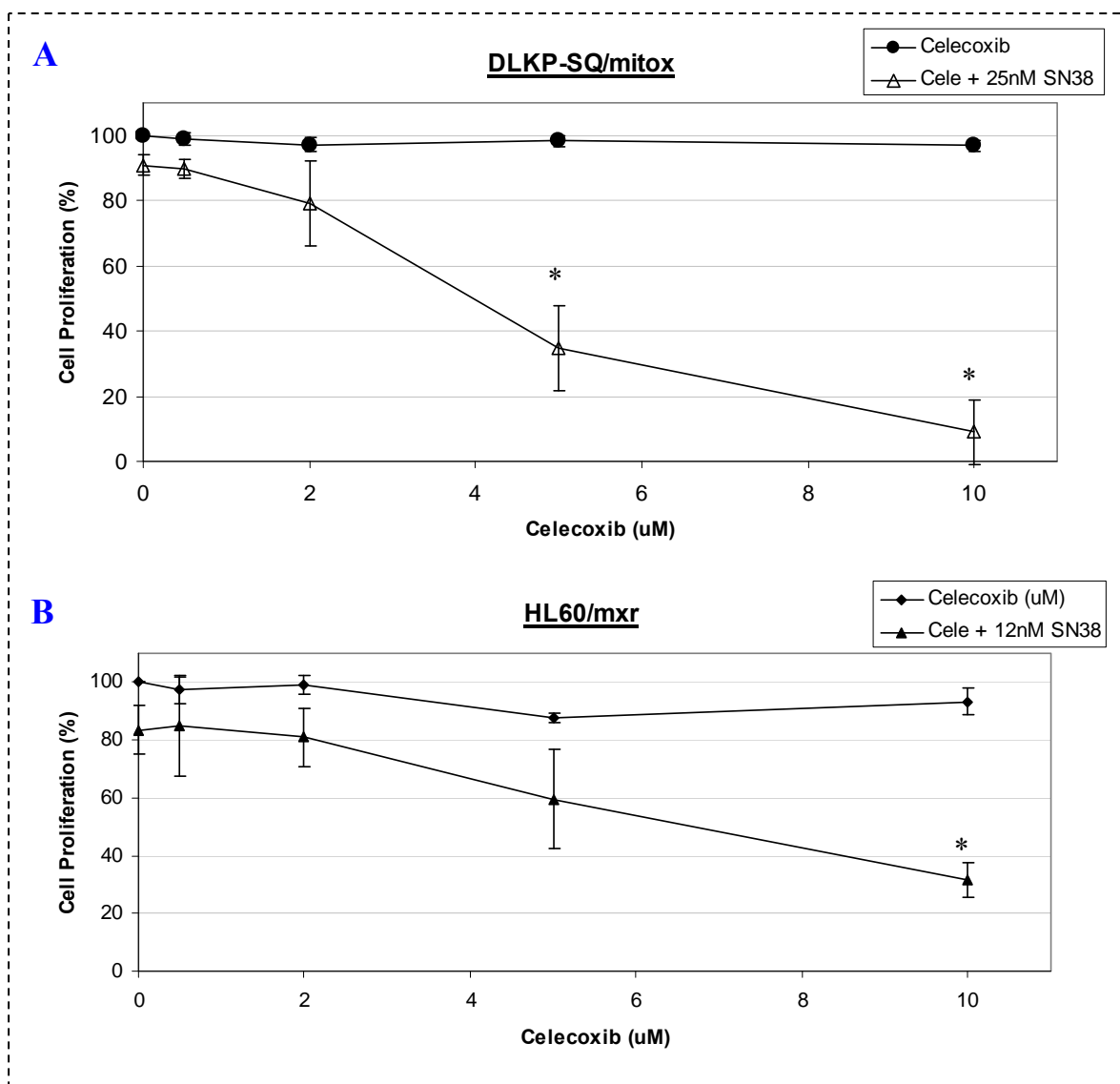
Graph 3.4.2.3.: Combination of SN38 (Δ) with celecoxib ($\bullet$) in the DLKP-SQ/mitox (**A**) and HL60/mxr (**B**) cell lines. This proliferation assay involved the combination of one of 2 chemotherapeutic agents with celecoxib in very high and moderately expressing BCRP cell lines, DLKP-SQ/mitox and HL60/mxr, over a 5 day period. Graph 3.4.2.3.**A**. was the result of a triplicate assay on separate days. Graph 3.4.2.3.**B**. was single day assays. Significant changes between each drug alone and the combination of both drugs is indicated by * ($p<0.05$). Table 3.4.2.3 below depicts the percentage cell proliferation and standard deviations for this graph.

Table 3.4.2.3.: The percentage cell proliferation and standard deviations for the combination proliferation assay of SN38 with celecoxib in the two BCRP expressing cell lines. This table is illustrated in graph 3.4.2.3.

Cell line	Agents	Cell Prolfieration (%)									
	Celecoxib (µM)	**0**	StDev (%)	**0.5**	StDev (%)	**2**	StDev (%)	**5**	StDev (%)	**10**	StDev (%)
DLKP-SQ/mitox	Celecoxib	100	±0	99	±2	97	±2	98	±2	97	±2
	Cele + 25nM SN38	91	±3	90	±3	79	±13	35	±13	9	±10
HL60/mxr	Celecoxib	100	±0	97	±5	99	±3	88	±2	93	±5
	Cele + 12nM SN38	84	±8	85	±17	81	±10	60	±17	32	±6

3.4.3. Effect of celecoxib on P-gp, MRP1, BCRP, COX1 and COX2 protein expression.

We investigated the extent to which celecoxib altered the expression of three multidrug resistant transporter proteins, P-gp, MRP1 and BCRP, and the cyclooxygenase enxymes, COX-1 and COX-2. For this we chose 3 MDR cells lines, each expressing one type of MDR protein. In this case, H1299-Taxol (a lung cell line expressing P-gp), A549 (a lung cell line expressing MRP1) and DLKP-SQ/mitox (a non-small cell lung carcinoma expressing BCRP) were chosen. H1229-Taxol and A549 express moderate to low levels of P-gp protein and are therefore more representative of what would be found *in vivo*. Unfortunately, a stable moderately-expressing BCRP cell line was not easily available so we chose DLKP-SQ/mitox (very high but stable expression of BCRP). The MRP1-transfected cell line, 2008/MRP1, was chosen for the COX-1 work and A549 (a well known COX-2 expressor) was used for the COX-2 protein expression work. All cells were exposed to 0, 0.5, 2 and 10 µM Celecoxib for 48 hours. 40 µg of protein was loaded for the P-gp, MRP1, COX-1 and COX-2 westerns. 4 µgs (for A) and then 8 µgs (for B) of the DLKP-SQ/mitox protein lysate were loaded for the detection of BCRP.

Following a 48hr exposure to 0.5, 2 and 10 µM celecoxib, the expression of P-gp in the H1299-Taxol cell line decreased slightly (see figure 3.4.3.1.i.A and B for details). Celecoxib caused a slight down-regulation of MRP1 at the highest concentration (10 µM) but had no impact at biologically relevant concentrations (0.5 and 2 µM) (see figure 3.4.3.1.ii.A and B for the image). Variations in the expression of BCRP occurred following the exposure of DLKP-SQ/mitox to celecoxib for 48 hours. The lowest concentration (0.5µM) slightly increased expression while the highest concentration (10µM) reduced its expression (see figure 3.4.3.1.iii.A and B for images).

COX-1 expression in the 2008/MRP1 cells was reduced with the highest concentration of celecoxib while there was little change in the expression of COX-2 across the board in the A549 cells (see figures 3.4.3.1.iv.A and B and figure 3.4.3.1.v. A for images).

<u>Effect of short-term celecoxib exposures on the P-gp, MRP1, BCRP, COX1 and COX2 expression in a panel of cell lines.</u>
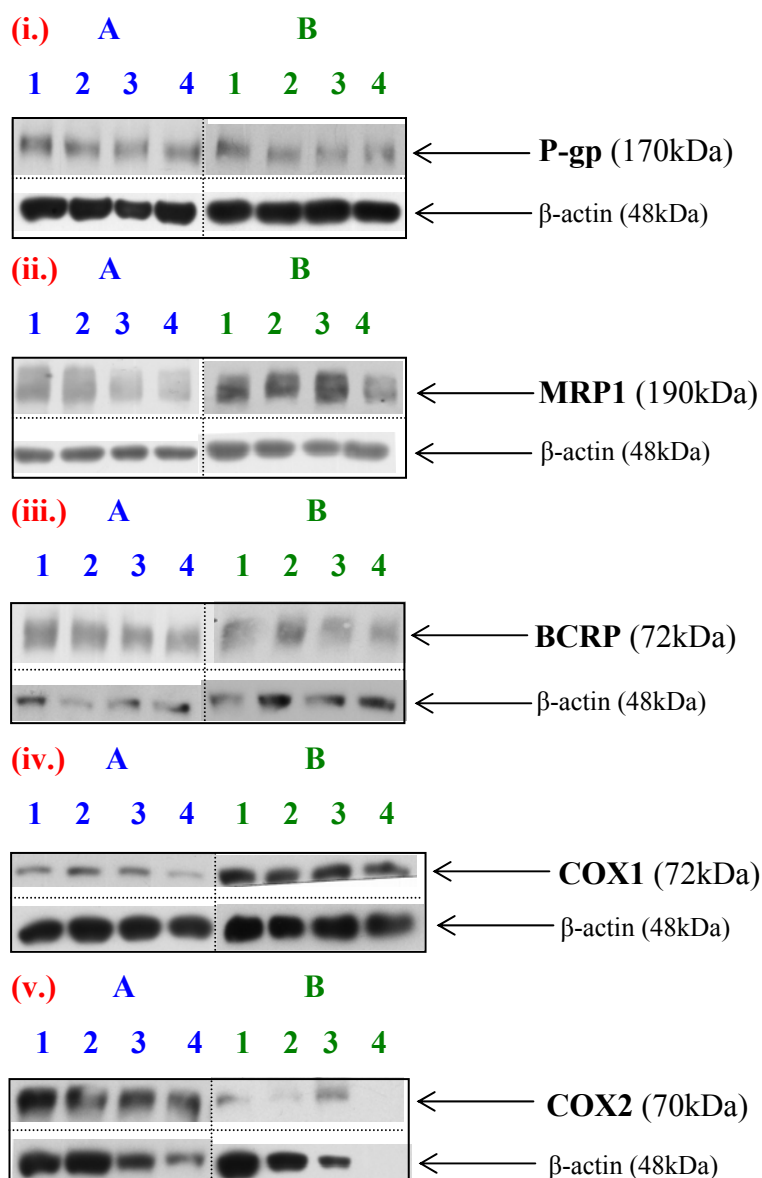
Figure 3.4.3.1.: These images represent the Western blots for P-gp (i.: 170kDa), MRP1 (ii.: 190kDa), BCRP (iii.: 70kDa), COX-1 (iv.: 72kDa) and COX-2 (v.: 70kDa) expression following exposure to 0, 0.5, 2 and 10 μM celecoxib for 48 hours. Blots **A** and **B** are biological replicates of each MDR/COX protein. 40 μg of protein was loaded for the P-gp, MRP1, COX-1 and COX-2 Westerns. 4 μg's (for **A**) and then 8 μg's (for **B**) of the DLKP-SQ/mitox protein lysate were loaded for the detection of BCRP.

3.4.4. Cellular pharmacokinetics of celecoxib in MDR-expressing cell models

In this section, we investigated the pharmacokinetics of celecoxib in MDR-expressing cell lines. This work was carried out to establish the relationship of celecoxib to each MDR transporter pump. For example, is celecoxib a substrate for MRP1, P-gp and /or BCRP?

We investigated the accumulation of celecoxib in the panel of cell lines (except for the suspension cells HL60/S, HL60/mdr1 and HL60/Adr). The cells were exposed to 2.5, 5 and 10 µM celecoxib for 2 hours. 2008/MRP1 had the greatest accumulation where the level of celecoxib nearly reached 2782 ng/million cells (graph 3.4.4.1.). H1299-Taxol and DLKP-A, had maximum accumulations 2600 and 2375 ng/million cells. The maximum accumulation for the DLKP and HL60/mxr cells were 1231 and 899 ng/million cells. The DLKP-SQ/mitox cells had the lowest accumulation (156 ng/million cells).The difference in accumulation between all the cell lines may be due to a difference in cell size, MDR transport protein expression or permeability.

We determined if celecoxib was a substrate for any of the MDR pumps. Using the lowest concentration of celecoxib (2.5 µM) we quantified the accumulation of celecoxib in the presence and absence of MDR inhibitors. For MRP1, 5 µM sulindac sulphide was used and for both P-gp and BCRP, 2.5µM elacridar was used. There was a 3-fold increase in celecoxib accumulation in the presence of sulindac sulphide (an MRP1 inhibitor) in both of the MRP1 cell lines, DLKP and 2008/MRP1 (see graph 3.4.4.2.). There was no increase in celecoxib accumulation in the presence of elacridar in DLKP-A cells. Nevertheless, the other P-gp-expressing cell line, H1299-Taxol, experienced a 3 fold increase in celecoxib accumulation in the presence of the same dose of elacridar. The cells were pre-treated with the MDR inhibitor to determine if pre-treatment would enhance celecoxib accumulation to a greater extent than the direct combination of celecoxib with the MDR inhibitor (see graph 3.4.4.2 and table 3.4.4.2. for details). The results were very similar; therefore pre-treating the cells with the MDR inhibitor did not enhance celecoxib accumulation to a greater extent then the co-incubation. A 2 fold increase resulted from the introduction of elacridar to both

of the BCRP-expressing cell lines, DLKP-SQ/mitox and HL60/mxr. This work suggests that celecoxib could be a substrate for MRP1, P-gp and BCRP.

To confirm whether celecoxib is a substrate of the MDR transporter pumps, we carried out efflux assays in all cell lines. The cells were exposed to 10μM celecoxib for 3 hours. At this point the drug was removed and fresh media (± MDR inhibitor) was added. We found that celecoxib is rapidly effluxed from all cells. The presence of an MDR-inhibitor did not alter this. However, there was a slight decrease in the efflux of celecoxib from the DLKP cells in the presence of sulindac sulphide (see graph 3.4.4.3.A). Yet, the effect is not observed with the 2008/MRP1 cells.
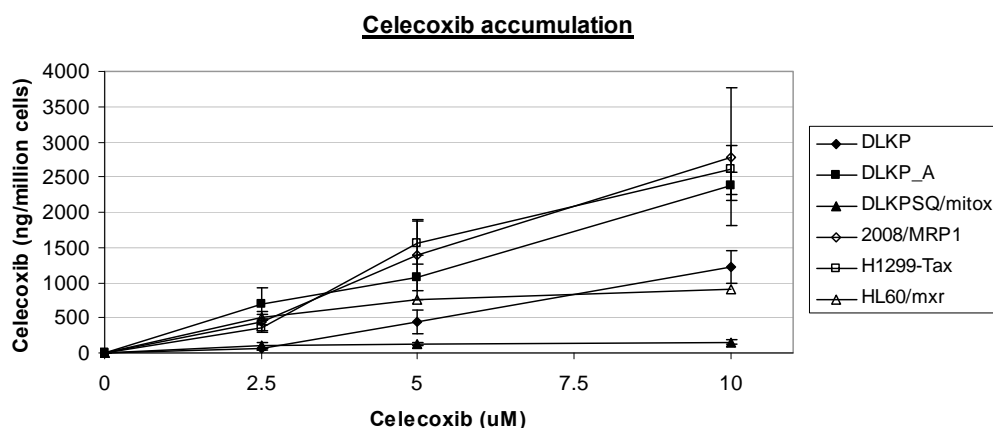
Graph 3.4.4.1.: Accumulation of celecoxib in two MRP1 (DLKP (◆) and 2008/MRP1 (◇)), P-gp (DLKP-A (■) and H1299-Taxol (□) and BCRP (DLKP-SQ/mitox (▲) and HL60/mxr (△)) expressing cell lines. This graph is the result of a triplicate intraday assay.
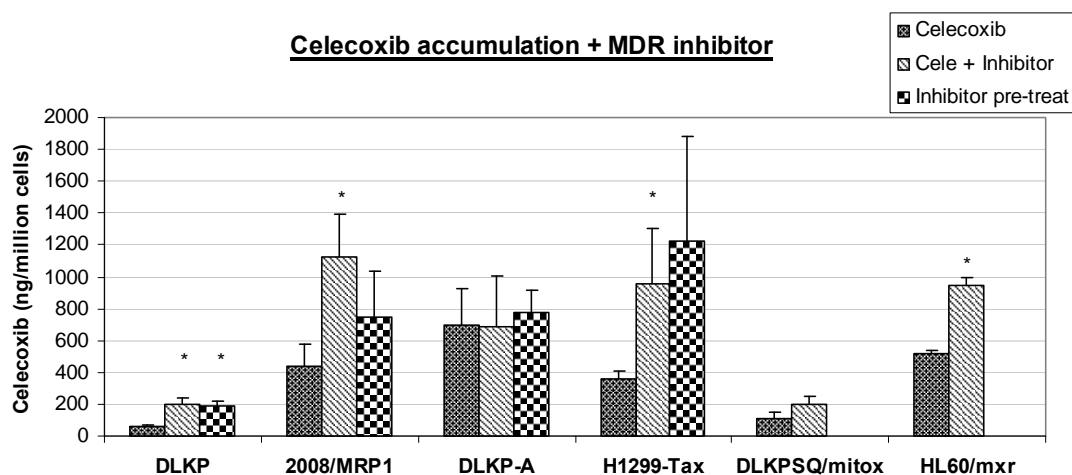
Graph 3.4.4.2.: This bar chart outlines the accumulation of 2.5μM celecoxib in the presence or absence of the appropriate multidrug resistance transport protein inhibitor in a panel of MDR-expressing cell lines. These accumulation assays involved the exposure of MRP1-expressing cell lines (DLKP and 2008/MRP1) to 2.5μM celecoxib alone and in combination with 5μM Sulindac sulphide (a known MRP1-inhibitor). This graph also depicts the accumulation of celecoxib in P-gp (DLKP-A and H1299-Taxol) and BCRP (DLKP-SQ/mitox and HL60/mxr) expressing cell lines in the presence or absence of 2.5μM elacridar (a known P-gp and BCRP inhibitor). This bar chart is one of two independent determinations, with triplicate intra-day results. Significane differences (P < 0.05) between celecoxib accumulation alone and in the presence of a MDR-inhibitor in indicated by *. Table 3.4.4.2 below depicts the quantity of celcoxib (ng/million cells), the standard deviations and significance values for this graph.

Table 3.4.4.2.: Data for the accumulation of celecoxib (ng/million cells) in the presence or absence of the appropriate MDR-inhibitor in the MRP1, P-gp and BCRP cells. This table includes the standard deviation and significance (P<0.05) values for graph 3.4.4.2.

Celecoxib (ng/million cells)	Celecoxib	Stdev	Cele + Inhibitor	StDev	P value	Inhibitor pre-treat	StDev	P value
DLKP	61	±11	201	±41	0.005	187	±32	0.003
2008/MRP1	434	±146	1127	±269	0.017	742	±288	0.174
DLKP-A	695	±235	685	±323	0.965	779	±142	0.627
H1299-Taxol	363	±41	957	±348	0.042	1219	±666	0.09
DLKP-SQ/mitox	106	±42	200	±46	0.061			
HL60/mxr	516	±23	949	±47	0.007			
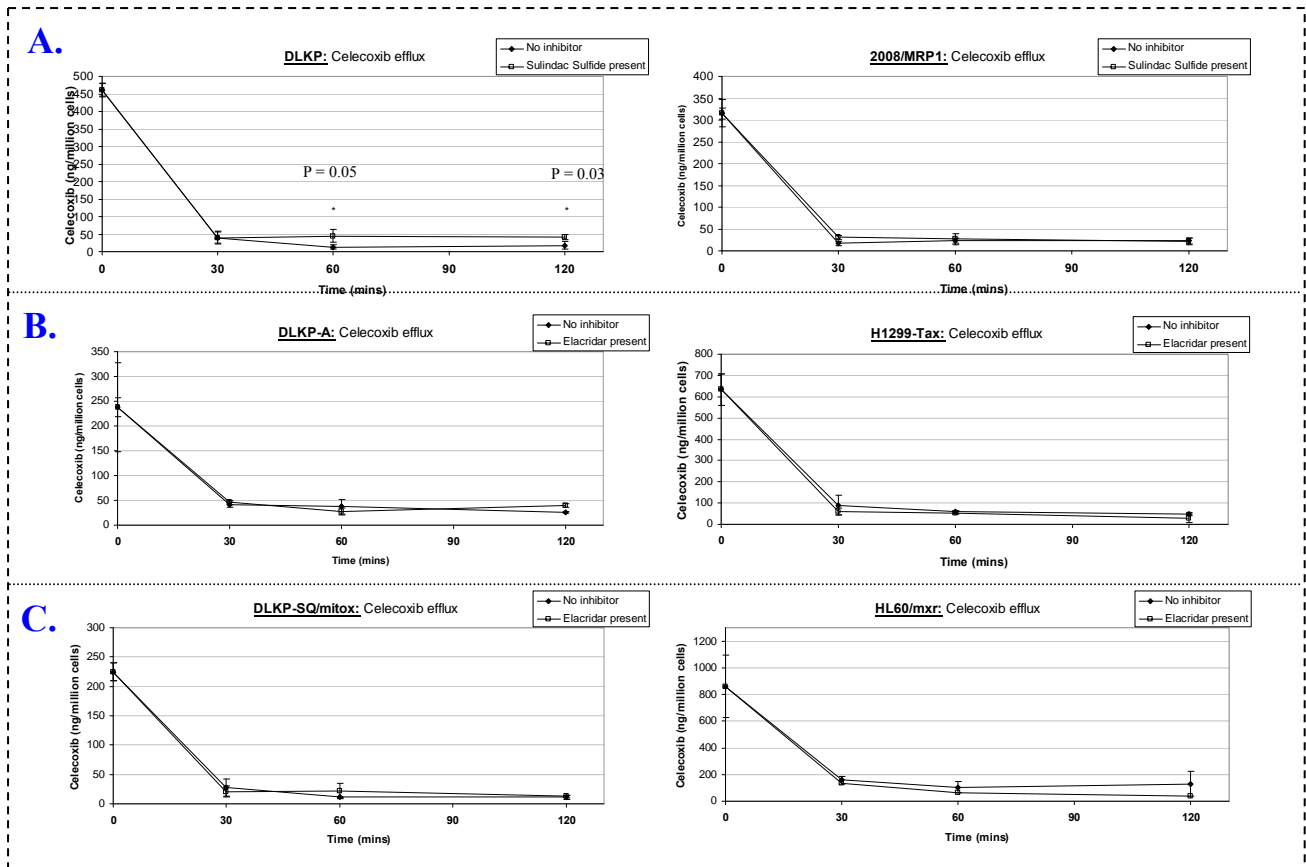
Graph 3.4.4.3.: The efflux of celecoxib in the presence (□) or absence (◆) of MDR-inhibitors in MRP1 (**A**: DLKP and 2008/MRP1), P-gp (**B**: DLKP-A and H1299-Tax) and BCRP (**C**: DLKP-SQ/mitox and HL60/mxr) expressing cells. The cells were exposed to 10μM celecoxib for 3 hours. At this time celecoxib was decanted, the cells were rinsed with warmed PBS and replaced with warm media (± the MDR-inhibitor) and samples were extracted after 30, 60 and 120 minutes. These graphs are results of triplicate intra-day determinations and * denotes significant differences (P < 0.05) between celecoxib efflux in the presence and absence of the appropriate MDR-inhibitor.

3.4.5. Effect of celecoxib on epirubicin accumulation in MDR-expressing cell lines.

We investigated the effect of celecoxib on the pharmacokinetics of MDR substrates in a panel of MDR-expressing cell lines, to establish if celecoxib can directly inhibit the efflux of MDR substrates via their appropriate transporter pump. For example, a heightened epirubicin accumulation was observed when celecoxib was present in MRP1 or P-gp cells, therefore suggesting that celecoxib can inhibit pump function. The best methods to determine this are accumulation or efflux assays (for experimental details see section 2.12.2). For this assay, all cells were exposed to $2\mu M$ epirubicin (± MDR inhibitor) for 2 hours. At this time, the cells were removed from their flasks, washed, counted and prepared for drug extraction.

Accumulation of epirubicin in the DLKP cells was higher than in the 2008/MRP1 cells (see graph 3.4.5.1). When 0.5, 2 and $10\mu M$ celecoxib was introduced there was a 1.3, 1.6 and 1.7 fold increase in epirubicin accumulation in the DLKP cells. Celecoxib had a greater impact on epirubicin accumulation in 2008/MRP1 cells. Fold increases of 1.3, 3.9 and 4.9 occured with the addition of 0.5, 2 and $10\mu M$ celecoxib (see graph 3.4.5.1 and table 3.4.5.1.).

As expected, there was very little accumulation of epirubicin in the DLKP-A cells. 2 and $10\mu M$ celecoxib increased this accumulation by 1.5 and 2.3 fold. Celecoxib had a similar impact on epirubicin accumulation in H1299-Taxol cells. 2 and $10\mu M$ celecoxib increased accumulation by 2.2 and 2.5 fold (see graph 3.4.5.2. and table 3.4.5.2.).

Unexpectedly, we also observed an increase in epirubicin accumulation in the presence of celecoxib in the BCRP expressing cells, DLKP-SQ/mitox. The addition of 0.5, 2 and $10\mu M$ celecoxib caused a 1.5, 1.7 and 1.5 fold increase in epirubicin accumulation (see graph 3.4.5.3. and table 3.4.5.3.).

These results would suggest celecoxib directly inhibits all three MDR pumps. The greatest effect was seen in the MRP1-expressing cell line 2008/MRP1, followed by the P-gp expressing cells and finally the BCRP cells. This order of impact could be due to the degree of inhibition or to the affinity the pump has for the substrate.

221

MRP1: Epirubicin accumulation
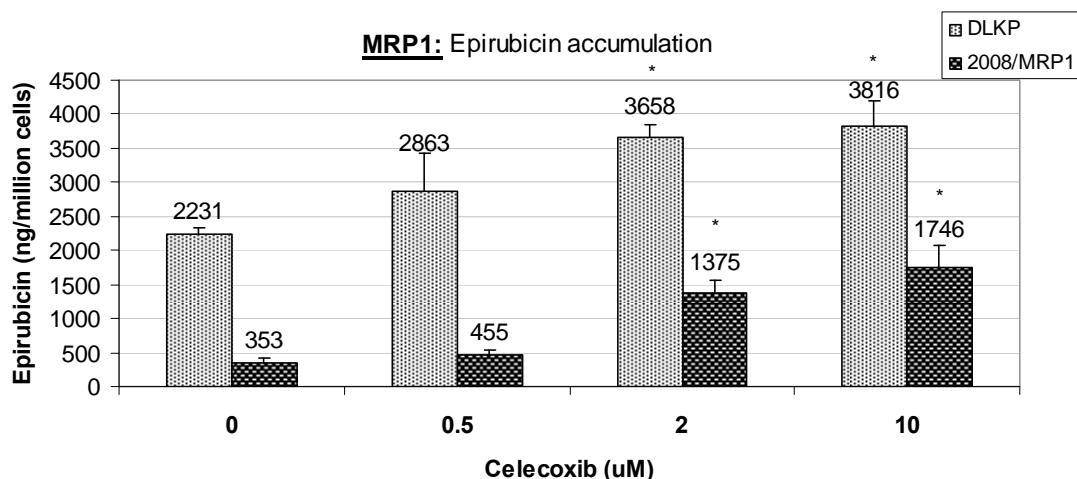
Graph 3.4.5.1.: The accumulation of epirubicin, in the presence or absence of celecoxib, in the two MRP1-expressing cell lines, DLKP and 2008/MRP1. The bars in this graph represent the quantity (ng) of epirubicin accumulated per million cells. Significance relative to the 0 μM celecoxib is indicated by * (p value below 0.05). The value for each bar is located above the error bars. This bar chart represents two independent determinations with triplicate intra-day results. Table 3.4.5.1. below provide the fold increases in epirubicin accumulation and the p values for each sample.

Table 3.4.5.1.: Data for the accumulation of epirubicin in the presence and absence of celecoxib in the DLKP and 2008/MRP1 cells. This table provides the fold changes and significance/P values for the cells exposed to both epirubicin and celecoxib relative to cells exposed to epirubicin alone.

Cell line	Celecoxib (μM)	Fold change	P value
DLKP	0	1.0	N/A
	0.5	1.3	0.13
	2	1.6	0.0003
	10	1.7	0.002
2008/MRP1	0	1.0	N/A
	0.5	1.3	0.17
	2	3.9	0.0008
	10	4.9	0.002
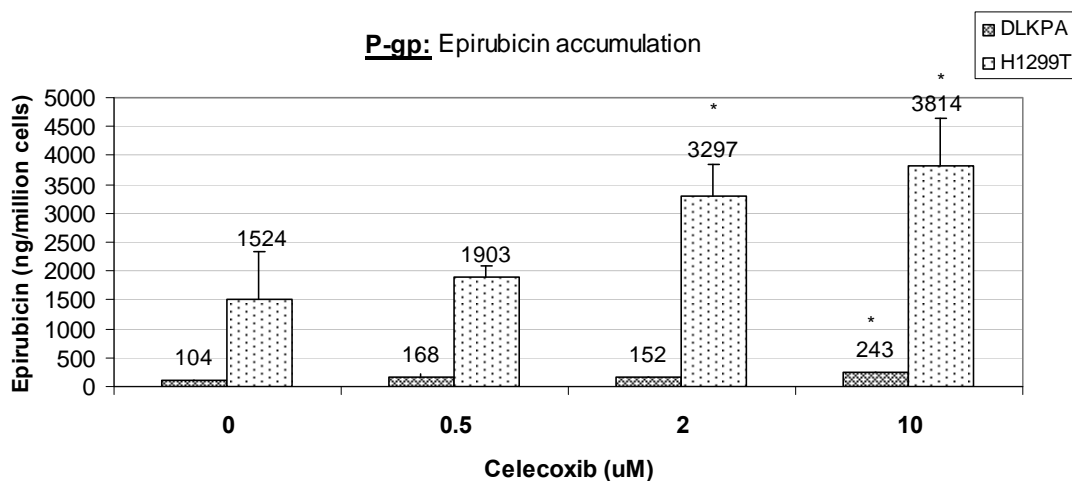
Graph 3.4.5.2.: The accumulation of epirubicin, in the presence or absence of celecoxib, in the two P-gp expressing cell lines, DLKP-A and H1299-Taxol. The bars in this graph represent the quantity (ng) of epirubicin accumulated per million cells. Significance is indicated by * (p value below 0.05). The value of each bar is located above the error bars. This bar chart represents two independent determinations with triplicate intraday results. Table 3.4.5.2. below provide the fold increases in epirubicin accumulation and the p values for each sample.

Table 3.4.5.2.: Data for the accumulation of epirubicin in the presence or absence of celecoxib in the DLKP-A and H1299-Taxol cells. This table provides the fold changes and significance values relative to 0µM celecoxib for graph 3.4.5.2. above.

Cell line	Celecoxib (µM)	Fold change	P values
DLKP-A	0	1	N/A
	0.5	1.6	0.06
	2	1.5	0.02
	10	2.3	0.001
H1299-Taxol	0	1	N/A
	0.5	1.2	0.58
	2	2.2	0.04
	10	2.5	0.03
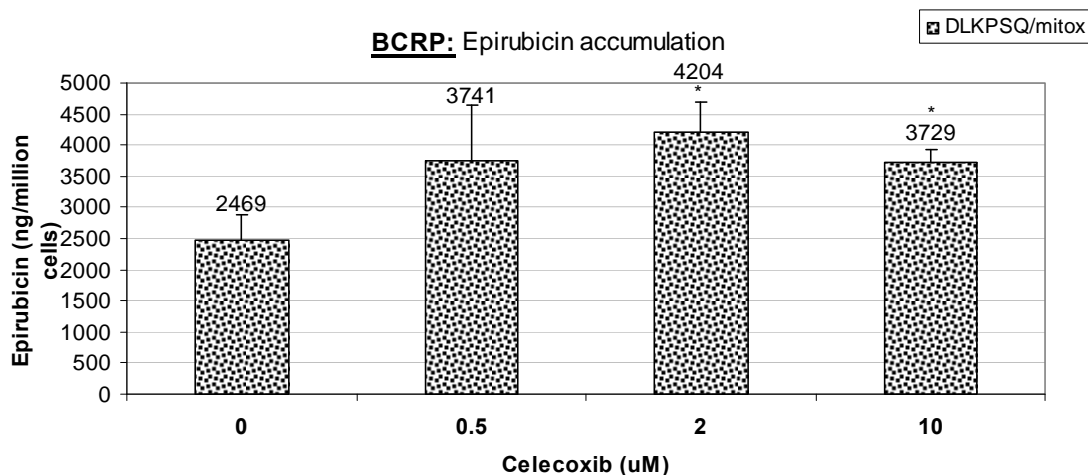
Graph 3.4.5.3.: The accumulation of epirubicin, in the presence and absence of celecoxib, in the BCRP expressing cell line, DLKP-SQ/mitox. The bars in this graph represent the quantity (ng) of epirubicin accumulated per million cells. Significance is indicated by * (p value below 0.05). The value for each bar is located above the error bars. This bar chart represents two independent determinations with triplicate intraday results. Table 3.4.5.3. below provide the fold increases in epirubicin accumulation and the p values for each treatment.

Table 3.4.5.3.: Data for the accumulation of epirubicin in the presence and absence of celecoxib in the DLKP-SQ/mitox cells. This table provides the fold changes and significance values for graph 3.4.5.3. above.

Cell line	Celecoxib (µM)	Fold change	P value
DLKP-SQ/mitox	0	1	N/A
	0.5	1.5	0.09
	2	1.7	0.009
	10	1.5	0.010

Section 4.

Discussion

General discussion

Multidrug resistance (MDR) proteins are expressed in a wide variety of tissue types, including, liver [42], gastrointestinal tract [35] and blood brain barrier, and help regulate the influx and efflux of substances required for normal cellular functioning [38] [39]. However, long-term treatment with chemotherapeutic drugs can lead to the over-expression of the MDR proteins and the development of the MDR phenotype. This phenotype and enhanced expression can be a major cause of treatment failure for conventional and modern anti-cancer drugs that are effluxed by MDR transporter proteins.

The search for agents that overcome this phenotype has been investigated for at least 30 years. An extensive range of MDR modulators has been identified (listed in tables 1.4.2.1, 1.4.3.1., 1.4.4.1, and 3.1.6.1.) and some of these have reached phase III of clinical trials [291] [180] [376]. However, the lack of improved outcome [291] [180] [376] and increased toxicity associated with the use of these agents [291] has hampered their entry into common clinical use.

There are a number of ways an agent can alter MDR expression and function:

1. post-translational modification, such as inhibition of MDR phosphorylation which can prevent the efflux of its substrates (directly inhibiting its function) and/or prevent the intermediate MDR protein from returning to its original state,

2. differences in affinity for the MDR protein can reduce and even prevent the efflux of anti-cancer agents by MDR transporter proteins.

3. amplification of the MDR gene by SP1 (mdr1, MRP1), PXR (mdr1), NF-Y (mdr1), YB-1 (mdr1), p53 mutation (mdr1) and the activation NF-kappaB (mdr1) by down-stream signalling of the AKT signalling pathway,

4. negative transcriptional regulation by a NF-KappaB/P63 and r-fos protein complex interaction with the CAAT region of the gene promoter and by c-jun and *p*-c-jun (JNK pathway affected by MEK/ERK pathway)

5. post-transcriptional control such as the use of an alternative promoter (5'UTR), post-transcriptional destabilisation of MDR1 mRNA, and translational blockade of P-gp expression at the ribosomal level.

In the past, a few functional inhibitors were tested in clinical trial [291] [180]. However, due to the lack of improvement in superior outcomes and toxicity, the focus shifted from inhibitors and competitive substrates to agents that could down-regulate or

eradicate MDR protein expression (by method 4 mentioned above). This shift in focus coincided with an increase in interest to identify an MDR modulator that could also inhibit oncoproteins (i.e. EGFR, HER2, COX-2, Hsp90) and cell signalling pathways (i.e. P13K/Akt, ERK/MEK) essential for tumour growth.

One such agent, 17-AAG (Hsp90 inhibitor and P-gp protein down-regulater), showed significant anti-tumour activities against a broad spectrum of cancers in pre-clinical studies, with growing clinical trial information [reviewed in 392]. To date, the modulation of MDR by 17-AAG has not been investigated in clinical trials.

The main aim of this project was to identify the optimum drug combination that would target multidrug resistance, oncoproteins and/or cell signalling pathways essential for tumour cell growth. For this, we compared the ability of COX, EGFR, HER2 and Hsp90 inhibitors to modulate MDR and determined their optimum treatment regimen. Also, we sought to identify a new MDR modulator by screening a panel of novel compounds derived from anti-cancer and cancer preventative agents as well as investigating a delivery system. The impact serum transport proteins have on the accumulation of epirubicin in normal and cancer cells *in vitro* was also evaluated.

4.1. Screening of potential novel anti-cancer agents

Despite the broad range of MDR modulators (anti-MDR agents), the search for better, safer, more efficient and less toxic modulators continues [reviewed in [393]]. In this section, we tested a panel of 61 novel compounds, ranging from plant derivatives to metal agents, for anti-cancer and anti-MDR potential. These compounds (listed in table 2.9.1.) along with other modern small molecule agents (listed in table 3.1.6.1.) that, according to the literature, interact with the MDR pumps (see section 1.4. for review on multidrug resistance), were tested for their anti-MDR potential. As described in section 2.10., the compounds were combined with MRP1 and P-gp substrates in non-small cell lung carcinoma cell models, DLKP and DLKP-A (MRP1 and P-gp cell models [369]). The small molecule agents were tested (see section 2.7. and 2.11. for methodology) in the lung cell lines; A549 (MRP1 expressing), A549-Taxol (paclitaxel-selected P-gp expresser) and DLKP-SQ/mitox (mitoxantrone-selected BCRP expresser).

Four families of derivatives were tested along with a polymer vehicle for daunorubicin delivery. Two potential P-pg modulators were identified, RBM15, a fluorinated resveratrol derivative, and KG104, an open hydrolysed macrocycle.

Nine small molecule agents were tested in P-gp, MRP1 and BCRP-expressing cell lines. 17-AAG was identified as a BCRP modulator. The majority of small molecule agents altered MDR protein expression. The level of MDR protein down-regulation was not significant enough to overcome resistance. However, with the range of small molecule agents tested, the optimum treatment regimen to overcome MDR in tumours was identified as the concurrent combination therapy of these small molecule agents with chemotherapeutic drugs that are effluxed by MDR transport proteins. This combination would enhance the cytotoxicity of the chemotherapeutic drugs and could increase survival rates and decrease mortality.

4.1.1. Polyamine derivatives

Polyamines are a group of organic compounds, with two or more amino groups, that are important in the regulation of gene expression, translation, cell proliferation, modulation of cell signalling, protein synthesis, and membrane stabilization in all known cell types [377] [378]. Adequate cellular polyamine levels are achieved by a careful balance between biosynthesis, degradation, and uptake of amines from the surrounding environment. Polyamines affect numerous processes in carcinogenesis. Increased polyamine levels are associated with increased cell proliferation, decreased apoptosis and increased expression of genes affecting tumour invasion and metastasis. Conversely, suppression/depletion of polyamine levels is associated with decreased cell growth [379], increased apoptosis and decreased expression of genes affecting tumour invasion and metastasis [380] [381]. Polyamines are often present at increased concentrations in tumour cells and tissues, for example, breast and colon cancer.

Several hundred polyamine synthesis inhibitors have been developed over the past 30 years. These drugs have focused on the key polyamine biosynthetic enzymes, catabolic enzymes, polyamine uptake, transport systems, and various downstream DNA, RNA, proteins, enzymes, and specific regulatory control systems. These inhibitors mainly concentrated on decreasing cell growth by inhibiting polyamine transport and synthesis. Selective inhibitors of the enzymes involved in polyamine

biosynthesis did not result in practically useful anti-cancer drugs [394] [395], but a selective inactivator of ornithine decarboxylase (ODC; an enzyme that partakes in the urea cycle), 2-(difluoromethyl) ornithine (DFMO) is currently being developed as a cancer chemopreventive agent [396]. For review see Marra M., *et al.* [154].

Over 10 years ago, it was reported that 50 μM of a polymeric conjugate of spermine was shown to reverse P-gp-mediated resistance to doxorubicin, etoposide, vinblastine and paclitaxel in the MDR variants (Dx5 cells) of the human sarcoma cell line MES-SA., [397]. Gosland MP., *et al.* [397], also suggested there may be a link between the polyamine influx pump and the P-gp efflux pump. This theory was confirmed by Aziz SM., *et al.* [398]. They suggest that functional polyamine transport may be required for P-gp transport activity and that increased expression of functional P-gp reduced polyamine transport in mdr1-transfected CHO cells. Since this time, there has been little work in the development of anti-MDR polyamine derivatives. In this section, we investigated the possibility that spermine and 5 polyamine derivatives might overcome P-gp and MRP1-mediated resistance in two non-small cell lung carcinoma cell lines, DLKP and DLKP-A (methodology described in section 2.7.1., 2.7.3. and 2.10.).

We found that, compared to spermine, the analogues were less toxic. The most toxic derivative was PA1; IC$_{50}$ values of 10 ± 4 μM in the DLKP cell line and 15 ± 2 μM in the DLKP-A cell line (section 3.1.1., table 3.1.1.1.). A concentration of 5 μM PA1 was the only analogue to interfere with the normal functioning of MRP1 and P-gp. This was shown by a mild enhancement of the anti-proliferative potential of epirubicin in MRP1-expressing, DLKP, and P-gp-expressing cell lines, DLKP-A (section 3.1.1., table 3.1.1.1.). This effect was very mild compared to the 42-fold reduction in doxorubicin resistance in the presence of 50 μM of a polymeric conjugate of spermine in the MDR variants (Dx5 cells) of the human sarcoma cell line MES-SA [399]. We noticed that spermine was significantly less toxic in the P-gp expressing cell line (section 3.1.1., table 3.1.1.1.). This was expected as spermine accumulation is lower in P-gp expressing cell lines compared to non-P-gp expressing parental cell lines [399]. This difference in sensitivity was eliminated by the modifications used to make PA1. Despite being a less effective P-gp modulator than the polymeric conjugate, its toxicity was independent of P-gp expression. There is no pharmacological data relating to the levels of this agent found in the blood. These two findings (MDR modulation and MDR independence) show that there may be potential

for the development of a polyamine derivative whose toxicity is independent of MDR expression while modulating MDR and still inhibiting polyamine production and/or transport. Future work in this field could involve polyamine transport studies to determine if PA1 alters influx or efflux of polyamines, synthesis of polyamines, expansion of the panel of P-gp expressing cell lines and their parental cell lines to determine if PA1 toxicity is independent of P-gp in multiple cell types, and modification of the PA1 structure with the aim of maintaining its MDR-independent toxicity while enhancing its toxicity and MDR modulation.

4.1.2. Resveratrol Analogues

Resveratrol is a polyphenol derived from nature and *in vitro,* has been shown to interfere with tumour initiation, promotion and progression. Research interest to date has been focused on cancer prevention and only slightly on its anti-cancer potential. Tolomeo M., *et al.* [400], found that resveratrol and other stilbenes overcame P-gp-mediated Imatinib resistance in lymphoma cell lines (HL60 and K562 cell lines). However, a major limitation of resveratrol use is its *in vivo* metabolic stability. Therefore, in this section, the collaborating chemists (Dr. Frankie Anderson and Dr. Brian Morgan) developed and synthesised a range of fluorinated analogue in the hopes of improving its metabolic stability [401] as well as its cytotoxicity and anti-MDR potential. We focused on MDR modulation and toxicity (methodology described in section 2.7.1., 2.7.3. and 2.10.).

The RF1 and RF3 compounds were slightly more toxic than resveratrol, while RBM15 was the most effective compound at overcoming P-gp-mediated resistance (section 3.1.2, and table 3.1.2.1). A concentration of 10 μM of the ditrifluoroacetyl derivative (2 μM above levels of resveratrol achievable in plasma [402]), RBM15, caused a 15% decrease in cell growth alone, but enhanced the cytotoxicity of 1.5 μM epirubicin from 15% to 80% (section 3.1.2, graph 3.1.2.1., and table 3.1.2.2.). It was through the enhancement of epirubicin toxicity, in the DLKP-A cell line, that RBM15 was identified as a potential P-gp modulator. The chemopreventive activity of resveratrol has been linked to its ability to block the NF-KappaB pathway through IkappaB kinase inhibition [403]. NF-KappaB is known to amplify the transcription of the mdr1 gene. Therefore, if RBM15 has the same mechanism of action, blocking

NK-KappaB activation could lead to the down-regulation in P-gp protein expression via eliminating the amplification of mdr1 gene transcription, thereby, sensitising P-gp-mediated resistant cells to the cytotoxic effects of chemotherapeutic drugs. This RBM15 compound had a number of superior characteristics to the original resveratrol compound as it was less toxic and potentiated the cytotoxicity of the P-gp substrate, epirubicin, to a much greater extent than resveratrol did (section 3.1.2., graph 3.1.2.1, and table 3.1.2.2). However, RBM15 does not overcome P-gp-mediated resistance to the same degree as other P-gp-modulators, such as elacridar, lapatinib or cyclosporine A, but is less toxic than the P-gp modulators. Therefore, further investigations into RBM15's MDR modulatory properties could be of interest. For example, expansion of the P-gp substrate chemotherapeutics panel as well as the panel of P-gp expressing cell lines (and not just lung cell lines) could be the first step. If these findings prove positive in many tumour types, a closer look at its effect on protein expression and alteration in pharmacokinetics of P-gp substrates in the presence of RBM15 would elucidate its mechanism of action. This body of work has shown that RBM15 does not overcome MRP1-mediated resistance (see section 8, graph 8.1.2.1.); however, its ability to overcome BCRP-mediated resistance has not been evaluated. A BCRP expressing cell line, which has been used successfully to demonstrate BCRP-modulation by small molecule agents in this project, is the squamous lung cancer cell line, DLKP-SQ/mitox. This would be an ideal cell line to evaluate any BCRP modulation by RBM15.

The cancer-preventative properties of resveratrol are still the main focus of researchers but its anti-cancer potential is beginning to emerge. This body of work is a step forward in bringing resveratrol closer to the clinic and was published by Moran BM., *et al.* [385]. However, significant work to examine bioavailability, toxicity and the anti-MDR potential of resveratrol is required before it can be considered seriously as an anti-cancer agent.

4.1.3. Macrocycle compounds

Macrocyclic compounds, such as cyclosporine A, are effective P-gp modulators *in vitro* [184] [404] [405], however, this drug did not improve the outcome of patients presenting the P-gp phenotype in phase II clinical trials [406] [399] (for further discussion

see section 3.1.3.). Despite increasing the AUC (area under the curve, drug level in the blood) of doxorubicin, etoposide and tenoside these macrocyclic agents were unsuitable for use in the clinic due to their undesirable side-effects. For example, cyclosporine's side effects include nephrotoxicity [407].

In this study, we tested a range of macrocyclic compounds for their toxicity and anti-MDR potential in two cell lines, DLKP and DLKP-A (methodology described in section 2.7.1., 2.7.3. and 2.10.). No MRP1 modulation occurred with these compounds. The IC_{50} for all tested compounds, in both cell lines, was in the micromolar range (i.e. reasonably non-toxic) (section 3.1.3., and table 3.1.3.5.). A number of compounds enhanced the cytotoxic potential of epirubicin in the P-gp expressing cell line, DLKP-A. The combination proliferation assays of KG3, KG4, KG103, KG104, KG105 and KG405 with epirubicin (section 3.1.3, graph 3.1.3.2 and table 3.1.3.2), and in many cases also with docetaxel, resulted in a large reduction in DLKP-A cell proliferation (graph 3.1.3.3. and graph 3.1.3.4). KG3 and KG4 were the first macrocycles designed and synthesised by our collaborators for anti-cancer testing. We found that both of these agents overcame P-gp-mediated resistance in the DLKP-A cell line. KG3 and KG4 have ether groups and are labile in aqueous solution. To determine if KG4 was broken down in the media and cells, our collaborators hydrolysed KG4 (see figure 3.1.3.1.) and we found that two of these hydrolysed compounds, KG103 and KG104 (graph 3.1.3.2), overcame P-gp-mediated resistance to a greater extent than the parent macrocycle, KG4. It was also hoped that the addition of the cytotoxic to the ether location on the closed KG3 or KG4 structure would improve drug delivery to the tumour, while hydrolysis of the compound inside the cell would release the cytotoxic drug and the KG metabolite would inhibit MDR transporter pumps.

KG104 strongly potentiated the anti-proliferative effect of epirubicin in the P-gp expressing cell line, DLKP-A, at the lowest concentration. The mechanism of P-gp modulation by these KG compounds could be through direct functional inhibition as demonstrated by other macrocyclic compounds, such as cyclosporine A. Compared with a similar combination in the same cell line carried out by Heenan M., *et al.* [369], of 1.7 μM adriamycin and 1.6 μM cyclosporine A, KG104 was only slightly less effective at modulating P-gp but was less toxic. This result could be very interesting for potential use in the clinic but requires further investigation to determine its mechanism of action and side effects. However, variations in interbatch synthesis led

to inconsistencies in the solubility of this compound which became a seriously limiting issue (see section 8, graph 8.1.3.1 and table 8.1.3.1). Extensive synthesis and solubility investigations in to the materials and vehicles used took place, however, with no success. This issue is currently being investigated in the chemistry department in the NICB, DCU.

4.1.4. Metal agents

The development of drugs with a metal platinum core, such as cisplatin and carboplatin, has had huge impact on current cancer treatment therapies. However, the range of cancers that can be treated with these platinum drugs is limited and the development of other metal drugs is being investigated. Other complexes include, iron, cobalt, gold, titanium, ruthenium, and gallium. Many of these complexes are undergoing pre-clinical studies as well as phase I and II clinical trials. For example, a metallocene titanocene dichloride was active in a broad spectrum of cancerous tissues in pre-clinical studies and showed promising results in phase I clinical trial. In 40 patients with refractory solid malignancies a lyophilized formulation of titanocene dichloride afforded two minor responses (in bladder carcinoma and in non-small cell lung cancer), the dose-limiting side effect was nephrotoxicity. For review see Ott I., and Gust R. [408].

Normally metal-based drugs, i.e. cisplatin, do not interact with multidrug resistance transport proteins (mentioned in section 1.0 in tables 1.4.1, 1.4.2, and 1.4.3). However, it was unknown if titanium based complexes can overcome multidrug resistance. In this section, we evaluated the potential that the Titanocene Y compound could overcome MRP1 and P-gp-mediated drug resistance in cancer cells. The cytotoxicity of Titanocene Y was moderate in both the DLKP (25 ± 3 μM) and DLKP-A (18 ± 4 μM) cell lines (section 3.1.4, table 3.1.4.1 and for method see section 2.10.). These IC_{50} values are 10 times less toxic than other metal agents for example; cisplatin has an IC_{50} of 1.1 ± 0.24 μM in DLKP and 2.0 ± 0.17 μM in the DLKP-A cells [207]. As expected, the combination proliferation assay of Titanocene Y with epirubicin in both the DLKP and DLKP-A cell lines resulted in no alteration in cell proliferation (section 3.1.4. and table 3.1.4.1). Metallic agents, such as cisplatin or carboplatin, rarely interact with multidrug resistance proteins; therefore, this result was expected.

The modulation of MDR by this compound is no longer of interest. However, an interesting point arises from this data. The cytotoxic effects of the titanocene compound are independent of MDR expression, i.e. the presence P-gp or MRP1-mediated drug resistance does not alter the compounds ability to reduce cell growth. Therefore, this type of compound could be significantly effective in tumours presenting the P-gp/MRP1 multidrug resistant phenotype. However, in these non-small cell lung carcinoma cell lines this titanocene analogue would not be the first choice of treatment as cisplatin is more effective. Comparing the cytotoxicity of this compound to cisplatin or carboplatin in a wider variety of cancer types would evaluate its true value. Following on from this investigation, other aspects, such as pro-apoptotic properties, are currently being investigated by Professor Tache of the Conway Institute.

4.1.5. Nano-particulate modified drugs

The use of biocompatible and biodegradable polymer nano-particules to enhance anthracycline delivery and distribution [409] while reducing cardiotoxicity as well as evade P-gp-dependent efflux [387] [388] *in vitro* has given some promising results [396]. Evasion of MRP1-mediated resistance, using a similar delivery system, daunorubicin nano-sphere, occurred in a breast cell line, MCF7 [410]. In this section, we investigated the potential that surrounding daunorubicin with a *n*-butylcyanacrylate nano-particle could evade daunorubicin MDR-mediated resistance. We carried out proliferation assays (described in section 2.7.) of daunorubicin, nano-particle polymerised daunorubicin, daunorubicin plus the nano-particle, and the nano-particle without drug in both the DLKP and DLKP-A cell lines. We found that the modification of daunorubicin in this manner did not enhance its cytotoxicity (section 3.1.5. and table 3.1.5.1). In fact, at high concentrations its potency was reduced in the P-gp-over-expressing cell line, DLKP-A (graph 3.1.5.1). Other similar nano-particulates have been shown to evade P-gp-mediated efflux in a large number of cell lines and short-term *in vitro* proliferation assays have shown an increase in the toxicity of the nano-particulate polymerised daunorubicin [388] [411]. However, the nanoparticulate used was a **polyalkyl**cyanoacrylate, which has many more carbons then the ***n*-butyl**cyanoacrylate, used in this project, which is limited to four carbons. The

difference in size could explain the lack of effect by the *n*-butylcyanoacrylate-daunorubicin polymer in P-gp and MRP1-expressing cell lines. However, the findings with this nano-particle discussed here are interesting, as there is strong evidence in favour of long-term retention of significant quantities of daunorubicin in the nano-particulate carrier in the cellular environment, if not within the cells themselves. The development of this type of system, remains an important goal for researchers working in the area of drug delivery. This body of work was published in Simeonova M., *et al.* [389].

4.1.6. MDR down-regulation

To date, the most effective multidrug resistance (MDR) inhibitors have been functional inhibitors. While many of these have shown promise *in vitro*, no inhibitors have proven successful in the clinic. For example, PSC-833 (valspodar) alone or in combination with vincristine, doxorubicin, and dexamethasone (VAD) did not increase the progress-free survival period (7 months for VAD alone reduced to 4.9 months for PSC-833 combined with VAD) [291] and when combined with cytarabine, daunorubicin and etoposide (ADE) it actually increased mortality (0% for ADE_2 alone increased to 18% for ADE combined with PSC-833) [412] for multiple myeloma patients compared to VAD or ADE_2 alone.

In this section, our aim was to identify a panel of MDR modulators that down-regulate the expression of MDR proteins while targeting other important signalling pathways and oncoproteins. We examined whether these small molecule agents caused the greatest anti-cancer outcome in combination (see section 2.7.2. for methodology) with chemotherapeutic drugs or as a pre-treatment (see section 2.7.3 for methodology) for the chemotherapeutic drugs. To the best of our knowledge an extensive study like this has not been carried out before. The selection of the small molecule agents was based on the availability of information in the literature, anti-MDR status and availability for use in a clinical trial. The panel included tyrosine kinase inhibitors (TKI; lapatinib, erlotinib and gefitinib), non-steroidal anti-inflammatory drugs (NSAID; celecoxib, sulindac sulphide, ibuprofen and indomethacin), an Hsp90 inhibitor (17-AAG) and an established MDR modulator (elacridar) (list summarised in table 3.1.6.1). Information published on the modulation

of MDR function and expression by these small molecule agents is summarised in section 1.4.5. The concentrations of the small molecule agents used for this work are equivalent and lower to their plasma AUC values (see section 1.4.5 and table 3.1.6.1. for details).

To determine if the small molecule agents listed in table 3.1.6.1 affected the expression of P-gp, MRP1 or BCRP we exposed the cells to the small molecule agents for 24 hours and carried out Western blots using the cell lysates (for methodology see section 2.11.). Small molecule agents that reduced the MDR protein expression by more than 20% were selected for examination of the stability of this alteration (section 2.11.), toxicity and combination/scheduling proliferation assay (section 2.7.) testing. The expression stability and toxicity of the selected small molecule agents testing involved; exposing the cells to the small molecule agents for 24 hours, removal of the drug and a further incubation of 24 and 48 hours in drug-free media. Western blotting was carried out on these lysates (section 2.11.) and the toxicity of the small molecule agents was evaluated using an end-point assay, PNP (section 2.7.2). Finally, the small molecule agents were either combined with MDR substrates (combination proliferation assay, see section 2.7.1.) or used as a pre-treatment for the MDR substrate (scheduled proliferation assay, see section 2.7.2.).

4.1.6.1. P-gp downregulation

We found that pharmacologically relevant concentrations of lapatinib, erlotinib, gefitinib, elacridar and sulindac sulphide increased P-gp expression in the P-gp moderately-expressing cell line, A549-Taxol. Densitometric analysis of these Western blots supported the visual findings (figure 3.1.6.1.1 and table 3.1.6.1.2). Long-term treatment with agents that up-regulate P-gp expression could lead to the development and amplification of multidrug resistance in cancer and, therefore, reduce the effectiveness of chemotherapy in patients. No information is published on the affect erlotinib, gefitinib or elacridar have on P-gp protein expression. But the data suggests that drug treatment with these targeted therapies may affect drug resistance mechanisms resulting in tumours with a higher degree of drug resistance. Using ATPase activity assays, it has been shown that lapatinib [147], erlotinib [148] and gefitinib [97] are functional inhibitors of P-gp. Contrary to results presented here and

demonstrated by other members of our group, where P-gp was up-regulated in the presence of lapatinib, Dai CL., *et al.* [147], demonstrated that lapatinib does not effect the expression of P-gp protein at the transcriptional or translational level in doxorubicin selected MCF7 cells following exposure to similar concentrations for 48 hours. However, this cell model was not developed using paclitaxel and was not a non-small-cell lung carcinoma cell line. Therefore, the effects observed here or in the publication may be cell line/tissue specific or due to a difference in the development in P-gp resistance. However, in agreement with our result, P-gp up-regulation with the same and higher concentrations of lapatinib [197] [112], erlotinib [112] and gefitinib [112] was reported by members of our group. Elacridar, which also up-regulated P-gp protein expression was found to inhibit P-gp-mediated resistance and increase intercellular accumulation while reducing efflux of rhodamine in acute leukemia and multiple myeloma cells lines RPMI 8226/Dox1, /Dox4, /Dox6 and /Dox40 compared to the wild-type 8226/S [191].

The only small molecule agent which was tested and found not to affect P-gp protein expression was ibuprofen.

Indomethacin and 17-AAG-treated A549-Taxol cells caused a decrease in P-gp protein expression at and below pharmacologically relevant concentrations (figure 3.1.6.1.1 and table 3.1.6.1.2). Celecoxib also down-regulated P-gp protein expression but only at concentrations above levels achievable in the body. These results indicate that indomethacin, celecoxib and 17-AAG could reduce the degree of resistance caused by P-gp in these cells by reducing its expression at the cell membrane. This reduction in resistance could result in enhanced toxicity of chemotherapeutic drugs and thus, increase the rate of tumour cell kill during treatment resulting in increased survival and decreased mortality in the clinic. This also suggests that long-term treatment with these small molecule agents may not result in P-gp-mediated resistance in later tumours.

With a closer look at down-regulation; we showed that indomethacin affected expression at 1 and 2 μM (20% and 50% reduction) but not at 0.4 μM in the A549-Taxol cell line (figure 3.1.6.1.1 and table 3.1.6.1.2.). It is thought that indomethacin down-regulates P-gp protein expression through activation of c-jun N-terminal kinase [181]. However, Zrieki A., *et al.* [96], found that a 90% down-regulation in P-gp protein expression occurred in CaCo-2 cells following exposure to the same concentration for the same time period. A difference in the type and level of P-gp expression, culturing

conditions and handling may explain the discrepancy in the degree of effect between the two cell lines.

The highest concentration of celecoxib (10 µM) down-regulated the expression of P-gp by 20% (table 3.1.6.1.2). Celecoxib inhibits Akt activation which could also lead to inactivation of the NF-kappaB promoter [333] and thus reduction in P-gp protein expression. Arunasree K.M. *et al.* [160], demonstrated a 50% decrease in P-gp expression in imatinib-resistant leukemic cells following a 24 hour exposure to 10 µM celecoxib but did not provide an explanation for its mechanism of action. Following a 24 hour exposure to 0.3, 0.5 and 1 µM of the Hsp90 inhibitor, 17-AAG, down-regulation of P-gp expression occurred in the A549-Taxol cell line, by 20%, 10% and 40% (figure 3.1.6.1.1 and table 3.1.6.1.2). Katayama K., *et al.* [3], also observed a down-regulation in P-gp protein expression and found that it was caused by 17-AAG inhibiting the MAPK signalling pathway. However, they also found that 0.1 µM of 17-AAG for 12 hours caused a 90% reduction in P-gp protein expression in colon cells (SW620 MDR selected) and breast cell lines (MCF7 and MDA-MB-231 MDR induced). The discrepancies in the degree of down-regulation by celecoxib and 17-AAG presented here versus results published may be due to the difference in cell type, difference in the growth rate of the cells, expression levels of P-gp, the method of P-gp induction or a difference in their dependence of signalling pathways for gene regulation, culturing conditions or handling. To determine if the down-regulation by these small molecule agents is tissue or cell line specific, the small molecule agents should be tested, in the same manner, on a panel of P-gp expressing cell lines that originate from a variety of tissues.

Indomethacin and 17-AAG had greatest effect on P-gp levels and were selected for further testing of their stability of down-regulation, toxicity and proliferation assays. The P-gp expression stability analysis showed that protein down-regulation by indomethacin recovered after 48 hours (figure 3.1.6.1.2) in a drug-free environment and that the concentrations were non-toxic under these conditions (see section 8, graph 8.1.6.1.1.A) (6-well plate with a cell seeding density of 7×10^4 cells/ml). On the other hand, the effect 17-AAG had on P-gp protein expression remained for a period of 48 hours following drug removal (figure 3.1.6.1.2). This may suggest that different mechanisms of down-regulation are caused by the two small molecule agents. The concentrations were also found to be non-toxic under these conditions (see section 8,

graph 8.1.6.1.1.B). Therefore, due to the sustained down-regulation of P-gp, 17-AAG was the best candidate for future work.

Neither the co-treatment nor pre-incubation with indomethacin enhanced the anti-proliferative potential of the chemotherapeutic drug (P-gp substrate), docetaxel (graph 3.1.6.1.1). The expression of P-gp recovered once indomethacin was removed, therefore, restoring full P-pg expression and function. This would explain the lack of effect in the scheduled proliferation assay. These results indicate that even though indomethacin down-regulated the expression of P-gp protein it does not alter its level of activity in these cells. Therefore, when considering its use in the treatment of cancer it will not overcome P-gp-mediated resistance but could reduce the risk of P-gp related resistance developing or amplifying in later tumours. Draper MP., *et al.* [413], also found that indomethacin did not inhibit the efflux of the P-gp substrate rhodamine 123 in the HL60/Vinc P-gp over-expressing cell line, however they did not look at protein expression. In contrast to both our results and Draper's results, Zrieki A., *et al.* [96], demonstrated a decrease in both expression and activity of P-gp in Caco-2 cells with the same concentrations. However, the degree of P-gp protein down-regulation in their cell line was significantly higher and this may account for the lack of effect observed in our combination proliferation assays. The concentrations of 17-AAG employed were extremely toxic in the combination proliferation assays (graph 3.1.6.1.2.A). The difference in toxicity between the 6-well plates (toxicity study) and the 96-well plates (combination and scheduled proliferation assay) was due to the large reduction in cell density required for the 7-day proliferation assays in the 96-well plates. While these concentrations were still very toxic in the scheduled proliferation assay, a toxicity curve for docetaxel in their presence was obtained (graph 3.1.6.1.2.B). This curve demonstrated that while 17-AAG may down-regulate P-gp protein expression (as shown in figure 3.1.6.2.1 and 3.1.6.2.2) it does not overcome P-gp-mediated resistance in this cell line (i.e. it doesn't enhance the cytotoxicity of docetaxel, the P-gp substrate). The IC_{50} of docetaxel was decreased in its presence but this was more likely due to the joint anti-proliferative effects of both 17-AAG and docetaxel and not due to P-gp modulation by 17-AAG. To date, the ability of 17-AAG to overcome P-gp-mediated resistance has not been investigated. For the scheduled proliferation assay, it would be expected that down-regulation of P-gp protein with 1 μM 17-AAG would help overcome MDR. However, as described by Breen L., *et al.* [370], treatment with chemotherapeutic drugs such as docetaxel can

cause stress induction and thus up-regulation of P-gp expression, especially in this cell line as it is a taxane-selected cell line. Therefore, the docetaxel effect on P-gp expression could potentially override any down-regulation caused by 17-AAG. Also, the down-regulation and stability of down-regulation of P-gp by 17-AAG was only looked at in the absence of docetaxel. However, recovery of P-gp expression could have occurred rapidly in the proliferation assays due to the presence of docetaxel. Also, it has been shown that 17-AAG resistance could be due to heat shock response and the up-regulation of P-gp [414]. Providing further evidence of up-regulation of P-gp following the removal of 17-AAG. Mechanistically, docetaxel induces apoptosis by promoting the phosphorylation and thus inactivation of bcl-2 [29], while 17-AAG down-regulates bcl-2 [414]. Down-regulation of bcl-2 prior to docetaxel exposure might initially slow docetaxel induced apoptosis. To date, the ability of 17-AAG to overcome P-gp-mediated resistance has been investigated only with regard to heat shock response.

This evidence indicates that the co-administration or pre-treatment of 17-AAG or indomethacin with chemotherapeutic drugs, does not overcome P-gp-mediated and thus a clinical trial is not indicated. It also suggests that the optimal method for overcoming P-gp-mediated resistance does not lie in the down-regulation of its protein.

In summary; five small molecule agents (lapatinib, erlotinib, gefitinib, sulindac sulphide and elacridar) up-regulated the expression of P-gp protein. This could have implications for their use in long-term treatment of cancer as they may induce or amplify drug resistance, due to P-gp activity, in secondary or advanced tumours. Two small molecule agents (indomethacin and 17-AAG) reduced the expression of P-gp in the A549-Taxol cell line at and below pharmacologically relevant concentrations. The affect of indomethacin on P-gp expression was not sustained once removed while 17-AAG's effects were maintained. Neither small molecule agent overcame P-gp mediated resistance in this cell line and should not be included in anti-P-gp clinical trials.

4.1.6.2. MRP1 down-regulation

The regulation of MRP1 expression is not fully understood but tenuous links between transcription factors, nrf2, n-myc and c-myc (important in P13K pathway), and MRP1 transcriptional regulation have been suggested. Hypoxic conditions increase the phosphorylation of ERK/MAPK and increase HIF-1 activity. These factors cause the up-regulation of MRP1.

We found that up-regulation of MRP1 expression occurred in the A549 cells following a 24 hour exposure to erlotinib, gefitinib, ibuprofen, indomethacin and elacridar (figure 3.1.6.2.1 and table 3.1.6.2.1.). Long-term treatment with these agents could lead to the development and amplification of MRP1-mediated drug resistance in cancer and, therefore, reduce the effectiveness of chemotherapy in patients.

We also found that four small molecule agents (lapatinib, celecoxib, sulindac sulphide and 17-AAG) down-regulated the expression of MRP1 protein in these cells (figure 3.1.6.2.1 and table 3.1.6.2.1). Lapatinib (the dual EGFR/HER2 tyrosine kinase inhibitor), 17-AAG (the Hsp90 inhibitor), and celecoxib (COX-2 specific inhibitor) could potentially down-regulate MRP-1 expression by reducing the active levels of Akt and thus inactivation of n-myc or c-myc or by preventing the phosphorylation of ERK/MAPK. High concentrations of sulindac were shown to increase MRP1 protein expression due to n-myc [207], however, the down-regulation observed here may be due to lower, less non-specific effects of sulindac sulphide on transcription factors such as n-myc or c-myc. These results indicate that lapatinib, sulindac sulphide and 17-AAG could reduce the degree of resistance caused by MRP1 in these cells by reducing it's expression at the cell membrane. This reduction in resistance could result in enhanced toxicity of chemotherapeutic drugs and thus, increase the rate of tumour reduction during treatment resulting in increased survival and decreased mortality in the clinic. This also suggests that long-term treatment with these small molecule agents may not result in MRP1-mediated resistance in secondary or advanced tumours.

With a closer look at down-regulation; a 20% decrease in MRP1 protein expression was caused by the highest concentration of celecoxib (10 μM, table 3.1.6.2.1). Kang HK., *et al.* [174], found that a 24 hour exposure to 5 μM celecoxib had no effect while 50 μM decreased the expression of MRP1 protein in a COX-2 independent manner. This does not contradict our result as they did not use the same concentrations as

those used in this project (concentrations listed in table 3.1.6.1.). Celecoxib was not selected for further testing as the percentage reduction was not significant enough and the change only occurred at a concentration greater then that achievable in the body (about 2 µM [25]) (see section 1.4.5). For all concentrations of lapatinib, significant down-regulation of MRP1 protein expression occurred (between 80% and 60%) (table 3.1.6.2.1). There are no publications in this area; however, this finding was replicated in the same cell line, with the same concentrations and experimental design by a member of our group, Dunne G., thesis [197]. Concentrations of 2 and 5 µM sulindac sulphide reduced MRP1 expression by 30% and 40%, while 17-AAG caused a reduction at all concentrations used (70% to 40%) (figure 3.1.6.2.1 and table 3.1.6.2.1.). These are novel observations that have not previously been reported. As the MRP1 down-regulation by these small molecule agents was partially inconsistent with some publications or novel findings, it would be important to evaluate if their effect is cell/tissue specific. For this, expanding the panel of MRP1-expressing cell lines to include a wide variety of tissue types would be essential.

The most efficient MRP1 protein down-regulator was lapatinib, followed closely by 17-AAG and finally sulindac sulphide. As their effect on protein expression occurred below pharmacologically relevant concentrations (less than 1.5 - 3.8 µg/ml for lapatinib [25], 0.15 - 17 µM for 17-AAG [212] and 4 - 6 µg/ml for sulindac sulphide [25]) and was greater than 20%, all three small molecule agents were brought forward for examination of the stability of their expression alterations, toxicity and proliferation assays.

The down-regulation of MRP1 by lapatinib, sulindac sulphide and 17-AAG was duplicated in biological replicates (figure 3.1.6.2.2.). However, after 24 hours MRP1 expression recovered following the removal of lapatinib or 17-AAG. The down-regulation caused by sulindac sulphide was stable for 48 hours following drug removal (figure 3.1.6.2.2). The concentrations were also found to be non-toxic under conditions in the 6-well plates (see section 8, graph 8.1.6.2.1).

The concurrent combination and scheduling proliferation assays of lapatinib with vincristine (the MRP1 substrate) found little significant change (graph 3.1.6.2.1 A and B). There was a slight reduction in the calculated IC_{50} of vincristine (graph 3.1.6.2.4 and table 3.1.6.2.3.) but this was more likely due to the combined anti-proliferative potential of lapatinib and vincristine rather than direct functional inhibition or protein down-regulation of MRP1. A partial recovery in MRP1 expression occurred after

lapatinib was removed for 48 hours therefore, partially restoring MRP1 expression and function. This would explain the lack of significant effect in the scheduled proliferation assay. These results indicate that even though lapatinib down-regulated the expression of MRP1 protein it does not alter its level of activity in these cells (also demonstrated by another member of our group). Or the down-regulation of MRP1 protein expression caused by lapatinib could be negated by stress induced factors due to the presence of vincristine. Therefore, when considering its use in the treatment of cancer it will not overcome MRP1-mediated resistance but could reduce the risk of MRP1 related resistance developing or amplifying in secondary or advanced tumours. The lack of effect can be explained to some degree by work carried out by Collins D., [112], who demonstrated, using ATPase assays, that lapatinib was a poor activator and inhibitor of MRP1 and does not overcome MRP1-mediated resistance to epirubicin in the A549 cell line [97]. Another MRP1 down-regulator, sulindac sulphide (the active metabolite for sulindac), caused very little toxicity itself and still reduced the IC$_{50}$ of vincristine in the combination proliferation assay (graph 3.1.6.2.2.A, graph 3.1.6.2.4 and table 3.1.6.2.3). This was expected as it was previously shown to overcome MRP1-mediated resistance in these cell lines [337] [172]. Whether down-regulation of MRP1 protein was involved is unclear. However, a slight drop in the IC$_{50}$ of vincristine was observed in the scheduled proliferation (graph 3.1.6.2.2.B, graph 3.1.6.2.4 and table 3.1.6.2.3). As the down-regulation of MRP1 protein expression was sustained for 48 hours following sulindac sulphide removal, the slight enhancement in vincristine cytotoxicity could potentially be due to this sustained down-regulation. To determine if this theory holds, MRP1 protein stability studies in the presence of vincristine would be required. The down-regulation of MRP1 protein expression by sulindac sulphide could reduce the efflux of chemotherapeutic drugs and thus improve their efficacy. The fact that the down-regulation of MRP1 is partially sustained following drug removal could have therapeutic implications. Not only could it overcome MRP1-mediated resistance but it could also prevent the induction or amplification of MRP1 by chemotherapy treatment in the clinic. In fact, combination of this non-specific COX inhibitor with another MRP1 substrate, epirubicin, has given promising results in xenograft models and is currently undergoing randomised melanoma phase II clinical trial [173].

When exposed to the cells for 5 days, all concentrations of 17-AAG were extremely toxic (graph 3.1.6.2.3.A and table 3.1.6.2.3). The difference in toxicity between the 6-

well plates (toxicity study) and the 96-well plates (combination and scheduled proliferation assay) was due to large reduction in cell density required for the 7-day proliferation assays in the 96-well plates. Therefore, a lower set of concentrations was employed for the combination and scheduling proliferation assays. However, no protein expression studies were carried out with these concentrations. A concentration of 0.02 μM 17-AAG allowed a 35% cell growth and it was this combination, with vincristine, that suggested that 17-AAG does not overcome MRP1-mediated resistance (graph 3.1.6.2.3.A). The drop in vincristine IC_{50} by their combination was due to the combined anti-proliferative potential of 17-AAG and vincristine and not due to changes in MRP1 protein expression (as protein expression was not effected with the higher concentration of 0.3 μM 17-AAG) or functional level by 17-AAG (graph 3.1.6.2.3.A and table 3.1.6.2.3). The lower concentrations of 17-AAG employed (0.02, 0.05 and 0.1 μM) were significantly less toxic (26%, 22% and 18% cell proliferation) when the cells were exposed to the drug for 24 hours of that 5 day period (scheduled proliferation assay) (graph 3.1.6.2.3.B). These concentrations caused a decrease in the IC_{50} of vincristine (graph 3.1.6.2.4 and table 3.1.6.2.3). In the scheduled proliferation assay with vincristine, the higher concentrations (0.3, 0.5 and 1 μM) resulted in over 60% growth inhibition but also reduced the overall cell proliferation. The toxicity of 0.5 and 1 μM 17-AAG were too high to evaluate. However, 0.3 μM was slightly less toxic but the reduction in the IC_{50} of vincristine can solely be attributed to the combined anti-proliferative potential of 17-AAG and vincristine and not due to MRP1 function or expression (no reduction in MRP1 expression occurred with this concentration) inhibition by 17-AAG. These combination and scheduled proliferation assay results indicate that 17-AAG does not overcome MRP1-mediated resistance. Therefore, when considering their use as part of cancer treatment in the clinic, they would not alter MRP1-mediated resistance but could help prevent the amplification or induction of MRP1 transporter proteins caused by chemotherapeutic drugs.

Of the three small molecule agents tested, sulindac sulphide was the only agent to overcome MRP1-mediated resistance in the A549 cell line and this only occurred in concurrent combination proliferation assays with vincristine. The combination proliferation assay result was not unexpected as sulindac is known to overcome MRP1-mediated resistance [337]. This body of work demonstrates that while all small molecule agents alter the expression of MRP1, the down-regulators, with the

exception of sulindac sulphide, do not overcome MRP1-mediated resistance. It also indicates that when using protein down-regulation as a mechanism of overcoming MDR in both *in vitro* and *in vivo* systems, a continuous exposure to the modulator is required to maintain the alteration. It also implies that lapatinib, sulindac sulphide and 17-AAG could be of therapeutic benefit in preventing the amplification or induction of MRP1 transporter proteins in cancer treated with chemotherapeutic drugs.

In summary; at and below pharmacologically relevant concentrations, five small molecule agents (erlotinib, gefitinib, ibuprofen, indomethacin and elacridar) up-regulated the expression of MRP1 in the A549 cell line. This could have implications for their use in long-term treatment of cancer as they may induce or amplify drug resistance due to MRP1 activity in secondary or advanced tumours. Three small molecule agents (lapatinib, sulindac sulphide and 17-AAG) down-regulated MRP1 protein expression, at and below pharmacologically relevant concentrations. Expression levels recovered following removal of 17-AAG or lapatinib. The regulatory effect of sulindac sulphide was stable for 48 hours. 17-AAG or lapatinib did not enhance the cytotoxicity of the MRP1 substrate, vincristine, through modulation of MRP1. Sulindac sulphide, which is also a non-specific COX inhibitor, overcame MRP1-mediated resistance when combined with the chemotherapeutic drug but its MRP1 inhibition was not sustained when absent. Therefore, these results indicate that only the concurrent combination of sulindac sulphide with MRP1 chemotherapeutic substrates is worth pursuing as an anti-cancer therapy. It also reveals that even with a 70% reduction of MRP1 protein expression, MRP1-mediated resistance is persistent or still susceptible to up-regulation by vincristine. Therefore, as reduction in MRP1 protein did not result in a reduction in MRP1-mediated resistance, two possible options remain for overcoming MRP1-mediated resistance; **a.** not partial but total elimination of MRP1 protein expression which would hopefully negate the stress induced effects of chemotherapeutic drugs, or, **b.** direct functional inhibition.

4.1.6.3. BCRP down-regulation

Little is known about the regulation of BCRP at the mRNA or protein level. However, a link between increased presence of porphyrin and heme in the cell leading to increase activated reactive oxygen species (ROS) and thus, increased BCRP protein expression has been suggested. BCRP expression is also up-regulated by heat shock response and the hypoxia-inducible transcription factor complex HIF-1 [138]. Also inactivation of the P13K/Akt pathway causes the translocation of BCRP from the apical surface of the membrane to the intracellular compartment. However, the physiological implications of this have not been established.

The cell line used in the section of the project was the mitoxantrone selected squamous lung cell line, DLKP-SQ/mitox, developed by Helena Joyce of the NICB, DCU.

By Western blotting (section 2.11.), we found that up-regulation of BCRP protein expression occurred in the DLKP-SQ/mitox cells following a 24 hour exposure to sulindac sulphide (figure 3.1.6.3.1). To date, up-regulation of BCRP is known to occur through increased activated reactive oxygen species, heat shock response or up-regulation of the transcription factor complex HIF-1. As the method for determining alterations in BCRP expression by the panel of small molecule agents is not under hypoxic condition (HIF-1) it can be theorised that up-regulation caused by sulindac sulphide is the result of increased ROS activity. This up-regulation of BCRP expression by sulindac sulphide implies that, use of this small molecule agent in the clinic could result in the amplification or induction of BCRP expression and thus, reduce efficacy of some chemotherapeutic drugs in secondary or advanced tumours. The up-regulation of BCRP by sulindac sulphide has not been explored previously in the literature.

A number of small molecule agents gave mixed results. For example, 0.3 and 0.5 μM of erlotinib slightly reduced BCRP expression, whereas, 1 μM increased BCRP expression in the DLKP-SQ/mitox cells. Celecoxib and ibuprofen both increased BCRP expression with low concentrations but decreased it with higher concentrations (figure 3.1.6.3.1 and table 3.1.6.3.1). These mixed results may be explained by the nature of MDR proteins and the specificity of small molecule agents over a broad concentration range. As the concentration of the small molecule agent increases in the cell its activities become less specific which could inadvertently induce a stress

response, inhibit or stimulate proteins, signalling pathways or transcription factors that regulate MDR protein expression and function. Due to the unstable regulation of BCRP protein expression by these small molecule agents they were not selected for further analysis.

Within the 24 hour exposure time, five small molecule agents down-regulated the expression of BCRP, in the DLKP-SQ/mitox cell line (figure 3.1.6.3.1 and table 3.1.6.3.1). These small molecule agents included (and in the order of efficacy); 17-AAG, lapatinib, indomethacin, elacridar and finally gefitinib. For each small molecule agent, concentrations used were well below and at the pharmacologically relevant levels (see section 1.4.5 for concentrations). They reduced BCRP protein expression by more than 20% in this cell line. It would be expected that the down-regulation in BCRP protein expression, by these small molecule agents, would reduce the efflux of BCRP substrates from BCRP-expressing cell lines. Therefore, enhancing the cytotoxic potential of these substrates resulting in increased cell death and improving treatment outcome. While others have demonstrated regulation of BCRP protein expression and mRNA levels, little is known to explain negative regulation of BCRP transcription, post-transcription, translation and post-translational modifications.

17-AAG caused a 50% decrease in protein expression with only 0.3 μM and to date, this not been published. The same concentration of lapatinib reduced BRCP expression by 40% (figure 3.1.6.3.1. and table 3.1.6.3.1.). However, Dai CL., *et al.* [147], found that lapatinib does not affect BCRP mRNA or protein expression levels. However, Dai CL., *et al.* [147], used a transfection induced colon cell line and even though the concentrations and exposure times are similar to those used in this project, a difference in tissue type, mutant/wild type and expression levels may explain the difference between their results and findings presented in this thesis. Concentrations of 0.3 and 0.4 μM of elacridar and indomethacin reduced expression by 30% (figure 3.1.6.3.1 and table 3.1.6.3.1). To date there are no publications stating the effect of elacridar on the expression of BCRP. The indomethacin result does not agree with Zrieki A., *et al.* [96]. They showed that exposure to 0.4 μM indomethacin for 24 hours increases BCRP expression by 10-40% in the colorectal cell line (CaCo-2). This disparity may be due to the expression of wild type BCRP in the CaCo-2 cells and the suspected expression of mutant BCRP in the DLKP-SQ/mitox cells (see section 1.4.4 for more details on amino acid substitution). Finally, gefitinib reduced expression by 50% at a concentration of 0.5 μM (figure 3.1.6.3.1 and table 3.1.6.3.1). There are no

publications to exemplify similar conditions; however, Meyer Zu Schwabedissen HE, *et al.* [170], suggested that anti-EGFR agents (such as gefitinib) could potentially reduce BCRP protein expression as they found that EGF stimulates BCRP expression. As the down-regulation by these small molecule agents was partially inconsistent with some publications, it would be important to evaluate if their effect is cell/tissue specific. The full panel of down-regulators were selected for further analysis as they reduced BCRP-expression by more than 20% and were well within biologically relevant concentrations. As summarised in table 3.1.6.1, none of the publications indicate that these agents alter BCRP protein expression.

Biological repetition of these Western blots (figure 3.1.6.3.2) generated results which were inconsistent with the lapatinib and elacridar BCRP protein down-regulation previously observed (figure 3.1.6.3.1). In these Western blots, it was clear that the two small molecule agents up-regulated the expression of BCRP. However, the down-regulation caused by gefitinib and 17-AAG, which is novel, was replicated and maintained for 48 hours following drug removal (figure 3.1.6.3.2). The effect by indomethacin was also replicated and maintained for 24 hours after the drug was removed. However, full recovery was achieved after 48 hours in a drug-free environment. For all five small molecule agents, the concentrations used were non-toxic under the described conditions (6-well plates seeded with 7×10^4 cells/ml) (see section 8, graph 8.1.6.3.1).

The next step in testing involved combination and scheduling proliferation assays (for methodology see section 2.7.1 and 2.7.2). In the combination proliferation assays, lapatinib, gefitinib, elacridar and 17-AAG caused a significant reduction in the IC_{50} of SN38 (graph 3.1.6.3.6 and table 3.1.6.3.2). This was expected for lapatinib [147] [97], gefitinib [150] and elacridar [415] as they were shown to functionally inhibit BCRP using ATPase activity assays. It is unclear if down-regulation of the BCRP protein expression influenced the small molecule agent's ability to overcome BCRP-mediated resistance. Lapatinib caused the greatest effect, followed by elacridar, gefitinib and finally 17-AAG. The degree by which these agents overcame BCRP-mediated resistance was substantial and could have significant implications in the treatment of BCRP-mediated resistant tumour. Their combination with BCRP substrate could significantly enhance the cytotoxic potential of the BCRP substrate, therefore increasing cell kill and improve treatment outcome. For the scheduled proliferation assay of 17-AAG, the higher concentrations (0.3, 05 and 1 µM) were extremely toxic

in these cells (graph 3.1.6.3.5.A.2). The difference in toxicity between the 6-well plates (toxicity study) and the 96-well plates (combination and scheduled proliferation assay) was due to large reduction in cell density required for the 7-day proliferation assays in the 96-well plates. However, the lower concentrations (0.02, 0.05 and 0.1 µM) were much less toxic but their effect on BCRP expression was not established. However, it was evident from the toxicity curves that 17-AAG modulates BCRP either through direct functional inhibition or reduction in protein expression (graph 3.1.6.3.5.A1, graph 3.1.6.3.6 and table 3.1.6.3.2). No literature could be found suggesting that 17-AAG modulates BCRP expression or function. Of all the small molecule agents tested in the combination and scheduled proliferation assays, indomethacin was the only one unable to overcome BCRP mediated resistance. At concentrations of 0.4, 1, and 2 µM, indomethacin was the only small molecule agent not to potentiate the cytotoxicity of SN-38 (graph 3.1.6.3.3.A, 3.1.6.3.3.B, 3.1.6.3.6 and table 3.1.6.3.2). As discussed in the P-gp down-regulation discussion, this inconsistency could be due to the stress induced BCRP expression (via ROS) by chemotherapeutic drugs such as irinotecan [416]. This combination proliferation assay results agrees with Nozaki Y., *et al.* [176], who found that 1 µM had no inhibitory effect on BCRP function, but 10 µM caused a 30% decrease in activity in human kidney slices. Therefore, it is possible that the concentrations of indomethacin used in this experiment were too low to induce an effect, however, it also suggests that down-regulation of BCRP protein expression by indomethacin is not an effective method of overcoming BCRP-mediated resistance. Despite its inability to overcome BCRP-mediated resistance, its ability to decrease BCRP protein expression still has a therapeutic benefit. The use of indomethacin might prevent the induction or amplification of BCRP in tumours treatment with chemotherapy.

Upon removal of lapatinib, elacridar, gefitinib or 17-AAG after a 24 hours pre-treatment (scheduling proliferation assay) the cytotoxic potential of SN-38 was still greatly enhanced (graph 3.1.6.3.1.B, 3.1.6.3.2.B., 3.1.6.3.4.B, 3.1.6.3.5.B, 3.1.6.3.6 and table 3.1.6.3.2.) As both lapatinib and elacridar regulation of BCRP protein expression was inconsistent (figure 3.1.6.3.2), the modulatory effect on BCRP could be due to a consequence of lasting BCRP functional inhibition, the presence of lapatinib in the cells 48 hours after removal even though it is a BCRP substrate (as described by our group in Dunne G., thesis [197]) or due to a change in protein expression. Conversely, 17-AAG's down-regulation of BCRP protein expression was

stable for 48 hours (figure 3.1.6.3.1 and 3.1.6.3.2.), but whether the potentiation of SN38 (graph 3.1.6.3.6) was due to protein down-regulation or direct and persistent functional inhibition has yet to be established (method involving exposure of the cells to 17-AAG for 24 hours, removal 17-AAG followed by the addition of various concentration of SN38. BCRP protein expression would be monitored over a 72 hour period to determine if SN38 reversed the down-regulation of BCRP by 17-AAG). The scheduling proliferation assay with gefitinib as the pre-treatment small molecule agent was much less effective compared to the combination proliferation assays (graph 3.1.6.3.2.A and 3.1.6.3.2.B). SN38 cytotoxicity was still enhanced but to a much lesser extent. This could be due to the down-regulation of BCRP protein in the first 24 hours or to mild sustained inhibition of BCRP function. This work also indicates that when using protein down-regulation as a mechanism of overcoming MDR in both *in vitro* and *in vivo* systems, a continuous exposure to the modulator is required to maintain the alteration. Of all the small molecule agents tested in BCRP-expressing cell lines, lapatinib was the most effective at overcoming BCRP-mediated resistance which caused a huge reduction in cell growth. This has significant therapeutically potential as lapatinib is also a dual EGFR/HER2 tyrosine kinase inhibitor [417] and P-gp functional inhibitor [418]. Therefore, tumours presenting multiple MDR, as well as, amplified EGFR/HER2 phenotypes could benefit greatly from the combination of lapatinib with chemotherapeutic drugs (that are P-gp and/or BCRP substrates).

In summary; one small molecule agent (sulindac sulphide) up-regulated the expression of BCRP protein while three small molecule agents (erlotinib, celecoxib and ibuprofen) caused up-regulation and down-regulation depending on their dose. These small molecule agents provide the potential for the induction and amplification of BCRP transporter protein expression in secondary or advanced tumours treated with them. Three small molecule agents (indomethacin, gefitinib and 17-AAG) consistently reduced the expression of BCRP in the DLKP-SQ/mitox cell line. For both gefitinib and 17-AAG, this down-regulation was sustained following drug removal but the effect by indomethacin recovered within 48 hours. Initially, two other small molecule agents, lapatinib and elacridar, down-regulated BCRP protein expression but these effects were not reproducible. However, when compared to the down-regulators, both small molecule agents had a greater impact on BCRP-mediated resistance in both co-treatment and pre-incubation proliferation assays. Gefitinib and

17-AAG were highly effective when combined with the chemotherapeutic drug but upon removal their anti-MDR potential was significantly reduced. This may suggest that 17-AAG does not only down-regulate BCRP protein expression but also inhibits its function. Therefore, once 17-AAG was removed, in the pre-treatment proliferation assays, its functional inhibitory effects on BCRP are significantly reduced but 17-AAG still overcomes BCRP-mediated resistance due to down-regulation of BCRP-protein expression. These small molecule agents could be of significant interest in the treatment of BCRP expressing tumours as not only do they overcome BCRP-mediated resistance but they could also prevent the amplification or development of BCRP.

To date, there are no clinical trials investigating BCRP modulation by lapatinib but results presented in this project suggest it could be beneficial. Phase I and II clinical trials of gefitinib with irinotecan (a BCRP substrate) in patients with advanced fluoropyrimidine-refractory colon cancer have been completed but gefitinib did not appear to add substantial efficacy to irinotecan [419]. There is a phase II clinical trial combining 17-AAG and irinotecan in solid tumours [420] however, their focus was on down-regulating checkpoint kinase 1 (Chk1) and not on overcoming BCRP-mediated resistance which is commonly induced in solid tumours. Therefore, the result of this clinical trial could be interesting considering we identified 17-AAG as a BCRP modulator. A pharmacological study (phase I clinical trial) was completed for the combination of elacridar with topotecan [421].

Key take-home points from MDR down-regulation experiments:

1. 17-AAG modulates BCRP expression and overcomes BCRP-mediated resistance.

2. Drugs can dynamically effect MDR protein expression

3. A single drug can differentially alter the expression of MDR proteins; therefore, understanding mechanisms of regulations for each MDR protein is important.

4. For the small molecule agents tested, combination therapy is the optimum treatment regimen.

5. Full and permanent eradication of MDR protein expression that is stable in the presence of chemotherapeutic drugs is essential when considering a combination or pre-treatment schedule.

6. Agents can be inhibitors, down-regulator and up-regulators of MDR transporter proteins.

7. When using protein down-regulation as a mechanism of overcoming MDR in both *in vitro* and *in vivo* systems, a continuous exposure to the modulator is required to maintain the alteration.

4.2. Cellular Pharmacokinetics of Epirubicin

The distribution and elimination of intravenously and orally administered anti-cancer drugs are influenced by biological factors such as multi-drug resistance transporter proteins and serum transport proteins. Serum transport proteins, such as serum albumin and α_1-acid glycoprotein (AAG) play a major role in the distribution, and thus efficacy, of anti-cancer agents by binding and transporting them through the circulatory system [48]. Albumin is crucial for the distribution, elimination and effectiveness of drugs such as digoxin, NSAIDs [49], midazolam, warfarin, thiopentone, tamoxifen, digitoin and anti-cancer drugs such as, anthracyclines [50] and taxanes etc. [50] [51]. AAG also plays an important role in the transport and delivery of many drugs. In a solution containing 50 µM AAG, 31% of a fixed concentration of epirubicin was bound [59]. Chassany O., *et al.* [59], also stated that 61 – 94% of epirubicin was bound to a solution containing 40 mg/ml of albumin. However, the impact of this binding on epirubicin transport, availability to the cell and the length of time spent in the body has not been investigated. On reaching the cell, the accumulation of these protein bound drugs is dependent on the molecular size of the protein, level of serum transport protein binding and the phenotype of the cancer cells.

In this study, we investigated the role that two serum proteins (serum albumin and α_1-acid glycoprotein) play in the accumulation of epirubicin in both normal and cancer cells. While the binding affinity of serum albumin and AAG to anthracyclines has been investigated, the impact of this binding on drug accumulation has never been explored. *In vitro,* varying levels of FCS are required for culturing different types of cancer cells. This body of work was undertaken to characterise the impact of varying levels of FCS on the cytotoxic potential of anti-cancer drug in difference cancer cells.

As expected, over 99% of epirubicin was free in a solution of water (UHP) or PBS, while 94% was free in cell growth media (ATCC) (graph 3.2.1.1.1 and for method see section 2.12.1). The decrease in free drug in cell culture media may be due to the presence of sugars and salts altering the pH and potentially have a small effect on drug solubility. Use of cell growth media without proteins resulted in varying levels of drug accumulation in the three different cell types. The largest drug accumulation, of 6281 ± 911 ng/million cells, was found in the MCF7 cells, followed by 3150 ± 184

ng/million cells in the normal HMEC cells and finally 1025 ± 529 ng/million cells in DLKP cells (graph 3.2.1.2.1, table 3.2.1.2.1 and see method section 2.12.2.1.).

The introduction of low levels of FCS or albumin increased epirubicin accumulation in all cells types (graph 3.2.1.2.1, 3.2.1.2.2 and 3.2.1.2.3 and method in section 2.12.). However, above 20% FCS, and the equivalent 8 mg/ml albumin, and with less then 60% of free epirubicin, the level of epirubicin accumulation reduced in all cells (graph 3.2.1.2.1, 3.2.1.2.2. and table 3.2.1.2.1., 3.2.1.2.2.). The proportion of bound epirubicin at this point was 48% in FCS (graph 3.2.1.1.2. and table 3.2.1.1.2) and 40% in albumin (graph 3.2.1.1.3 and table 3.2.1.1.3). At 100% FCS or 40 mg/ml serum albumin (with 0 to 20% free epirubicin), the level of epirubicin accumulation was halved, compared to 0% FCS or 0 mg/ml albumin, in the MCF7 and HMEC cells (graph 3.2.1.2.1, 3.2.1.2.2. and table 3.2.1.2.1., 3.2.1.2.2.). However, with the highest concentration of FCS, drug accumulation in the DLKP cells was double (2431 ± 171 ng/million cells) that of cell growth media without proteins (1025 ± 529 ng/million cells) (graph 3.2.1.2.1 and table 3.2.1.2.1). But with the equivalent concentration of albumin (40 mg/ml) the accumulation was only slightly higher (1564 ± 212 ng/million cells) (graph 3.2.1.2.2. and table 3.2.1.2.2). With 100% FCS, 100% of epirubicin was bound while 80% was bound in the presence of 40 mg/ml serum albumin. This accumulation data suggests that low levels of FCS and serum albumin aid epirubicin entry into the cells while higher levels restrict entry to these cells. This reduction in accumulation could be due to the protein sequestering the drug so it's not free to enter the cell. In the case of DLKP, the presence of FCS or serum albumin heightened epirubicin accumulation across the board. This may be due to a difference in tissue type, membrane drug permeability or protein influx pumps (expression of OATP's, etc.). Pharmacologically, this body of work indicates that serum albumin and the protein cocktail in serum do not differentially alter the accumulation of epirubicin in normal or cancer cells. The level of epirubicin-protein binding correlates with Chassany O., *et al.* [59], who used HPLC with fluorescent detection to discover that 61 – 94% of epirubicin, was bound to a solution containing 40 mg/ml of albumin. However, no publications have investigated the effect drug-protein binding has on drug accumulation in the cell.

At levels found in the body (0.08 mg/ml up to 0.8 mg/ml (20 µM)) only 6% to 14% of epirubicin was bound in the presence of AAG (graph 3.2.1.1.4, table 3.2.1.1.4 and method in section 2.12.1). This correlated with results described by Chassany O., *et al.*

[59], using HPLC with fluorescent detection, there was a 31% reduction of free epirubicin in the presence of 50 μM AAG. With the lowest level of AAG (0.08 mg/ml) epirubicin accumulation doubled in the DLKP cells (from 1025 ± 529 to 2670 ± 150 ng/million cells) and only slightly increased (from 3150 ± 184 to 4586 ± 495 ng/million cells) in the HMEC cells (graph 3.2.1.2.3., table 3.2.1.2.3 and method 2.12.2.1). MCF7 cells demonstrated the most dramatic epirubicin accumulation in the presence of AAG (graph 3.2.1.2.3 and table 3.2.1.2.3), which did not occur in the presence of FCS or albumin. In the presence of 0.8 mg/ml AAG, the accumulation of epirubicin increased 2-fold from 6281 ± 911 to 14011 ± 2537 ng/million cells in these cells. As drug-protein binding was very low even with the highest concentration of AAG, this could suggest that delivery of epirubicin by AAG is a more efficient compared to serum albumin. Therefore, one would expect that the presence of AAG in FCS would result in improved delivery and greater accumulation. However, in this case the level of AAG may be low in serum, while the levels of serum albumin would be set at 40 mg/ml and therefore, the binding of serum albumin to the cell membrane could not only inhibit the accumulation of albumin bound drug but also AAG bound drug . There are some disease states where the levels of AAG increase (280-fold) to the same levels as serum albumin. This can occur as a result of an acute inflammatory response and neoplasia. Inflammation has been linked with tumour initiation, promotion and progression [422] [423]. This project dealt with normal or non-inflammatory response levels of AAG. However, to determine the true impact of AAG on anthracycline accumulation, further pharmacokinetic studies using levels up to 280-fold higher need to be carried out. Other avenues, such as identifying the true impact serum proteins have on the efficacy of epirubicin could also be investigated. Apoptosis assays carried out in DLKP, MCF7 and HMEC cells in presence of varying levels of FBS, serum albumin and α_1-acid glycoprotein in serum-free media over a 3 day period would evaluate this. Also to investigate whether serum albumin and/or AAG levels in patients correlate with outcome would also be of great interest as it could potentially identify a patient sub-population that would respond better to anthracycline treatment. There has been very little research published on this area. The only article relating anthracycline-AAG binding was published by Chassany O., et al. [59]. The level of AAG used in their publication is more than double the highest concentration of AAG used in this project. However, their results demonstrate that epirubicin binding to AAG is low.

In summary, FCS and albumin bind free epirubicin. This binding aids epirubicin accumulation at low protein concentrations but hinders it at high protein concentrations. This is most likely due to bound drug being sequestering by the protein and unable to pass into the cell. AAG, at low levels found in blood under normal conditions, does not bind a lot of epirubicin but causes a 2-fold increase in the accumulation of epirubicin in all three cell lines. These serum proteins do not alter the availability of epirubicin for normal cells any differently than they do for the cancer cells.

4.3. Effect of tyrosine kinase inhibitors on the function and expression of epidermal growth factor receptors, EGFR and HER2, multidrug resistance transporter and cyclooxygenase proteins.

The epidermal growth factor receptor (EGFR) family (for review see section 1.5.) is composed of cell surface receptors with tyrosine kinase functionality that are involved in the regulation of cellular proliferation, survival and differentiation during development, tissue homeostasis, and tumourigenesis of epithelial cells. Activation of these receptors leads to stimulation of signal transduction pathways including phosphtidylinositol 3'-kinase (P13K/Akt/mTOR), Erk1/2 mitogen-activated protein kinase (MAPK) and Jak/Stat. HER2 over-expression or amplification occurs in a third of breast tumours and confers an aggressive clinical course, worse survival and is responsible for a quarter of all cancer-related deaths in women [215]. The outcome of these highly aggressive tumours has markedly improved with the development of anti-HER2 therapies. For example, the combination of trastuzumab with docetaxel in HER2 metastatic breast cancer patients resulted in better response (60% vs. 34%), increased survival (31.2 vs. 22.7 months), increased disease-free response (11.7 vs. 6.1 months) and longer duration of response (11.7 vs. 5.7 months) compared to docetaxel alone [217]. EGFR over-expression is found in many tumour types, such as lung, colon, kidney and head and neck carcinoma, which are mostly resistant to conventional chemotherapy [424]. Anti-EGFR, small molecule agents have been identified and several are now approved for treatment of late stage, advanced cancers [425]. We examined three such small molecule inhibitors, lapatinib (a dual EGFR and HER2 inhibitor), erlotinib and gefitinib (both specific EGFR inhibitors). We compared the efficacy of lapatinib, erlotinib and gefitinib, to sensitise EGFR/HER2-amplified breast cancer cell models to the chemotherapeutic agents, epirubicin and docetaxel (for methodology see section 2.7.1., 2.11. and for results see section 3.3.1.). As many tumours, such as breast, lung and colon, co-express EGFR/HER2, MDR and COX-2, we also compared the efficacy of lapatinib, erlotinib and gefitinib to overcome P-gp, MRP1 and BCRP-mediated resistance (see sections 2.7.1., 2.11., and 3.3.5.) aswell as determining their effect on COX expression and function (see sections 2.7.1., 2.11., 2.13., and 3.3.4).

Using combination proliferation assays (described in section 2.7.1), there were no alterations in cell proliferation when the three TKIs were combined with epirubicin or docetaxel in the EGFR-amplified cells (MDA-MB-231) (graph 3.3.1.1 and table 3.3.1.1), in HER2-amplified breast cancer cells (MDA-MB-453) (graph 3.3.1.2 and table 3.3.1.2) or in the moderately-expressing EGFR/HER2 breast cell model (MCF7) (see graph 3.3.1.3 and table 3.3.1.2.). This is surprising as sensitivity lapatinib decreased the active levels of both EGFR and HER2 (pEGFR and pHER2) in both lapatinib sensitive and insensitive breast cell lines [426].. Furthermore, in the clinic a HER2 inhibitor, trastuzumab, increased the benefit of first-line chemotherapy in metastatic breast cancer that overexpress HER2 [216]. Their combination resulted in a longer time to disease progression (median, 7.4 vs. 4.6 months; P<0.001), a higher rate of objective response (50 percent vs. 32 percent, P<0.001), a longer duration of response (median, 9.1 versus 6.1 months; P<0.001), a lower rate of death at 1 year (22% versus 33%, P=0.008), longer survival (median survival, 25.1 versus 20.3 months; P=0.01), and a 20% reduction in the risk of death. Therefore, this data provides biological rationale for the lack of clinical efficacy with lapatinib when used in EGFR or dual EGFR/HER2 over-expressing breast cancer patients.

By immunoblotting, Sakai K., *et al.* [390], demonstrated that 2 μM of gefitinib reduced phosphorylated (activated) EGFR levels in 293(W) cells transfected with wild-type EGFR. In invasive human bladder cells lines, Wallerand H., *et al.* [351], also demonstrated this effect by gefitinib using Western blotting techniques. There is no data to show the same for either erlotinib but it would be expected that erlotinib would have the same effect on pEGFR and that lapatinib would affect both pEGFR and pHER2. By ELISA (see section 2.11.6.) preliminary results indicate that lapatinib has no affect on the active levels of EGFR (see section 8, graph 8.3.2.1. and table 8.3.2.1.A.) but decreases HER2 activation levels (see section 8, graph 8.3.3.1 and table 8.3.3.1.A) at 24 hours and had little impact at 48 and 72 hours. As the effect was only observed for 24 hours it suggests that the effect on HER2 activity by lapatinib is only short term. The preliminary pHER2 result correlates with Zhang D., *et al.* [1], who demonstrated a reduction in pHER2 in BT-474 and SK-BR-3 breast cell lines following a 24 hour exposure to 0.1 and 1 μM lapatinib (using Western blotting techniques). However, the pEGFR result does not correlate with their result. This may be due to a difference in cell line, culturing techniques and handling. There are no

publications demonstrating *p*EGFR reduction in the MDA-MB-231 cell line. The positive controls for this experiment were MDA-MB-453 and MDA-MB-231 cells exposed to the EGF ligand for the same time periods as lapatinib. Sakai K., *et al.* [390], showed that short term exposure to the EGF ligand had little effect on EGFR expression in 293(W) cells transfected with wild-type EGFR, while Zhang D., *et al.* [1], also observed little change in EGFR protein expression but an increase in its phosporylated active form in BT-474 and SK-BR-3 breast cell lines. We also found that EGF had little effect on HER2 expression and only moderately increased its active state (see section 8, graph 8.3.3.1 and table 8.3.3.1.B). This has not been reported in the literature. This data helps explain why lapatinib did not sensitise the EGFR over-expressing cell line (MDA-MB-231) to epirubicin or docetaxel and instead why it sensitised the HER2 amplified cell line (MDA-MB-453) to the chemotherapeutic drugs.

Several studies reported that COX-2 (an enzyme involved in the PGE_2 pathway) production occurs along side EGFR activation [338] and HER2/HER3 heterodimerisation [340] [342]. COX-2 activity produces PGE_2 which in turn rapidly phosphorylates EGFR and triggers ERK2. Therefore, it is thought that through PGE_2's activity, which leads to the transactivation of EGFR and promotion of the Akt pathway, that COX2 causes an increase in tumour cell number and thus, volume as well as changes in morphological architecture and organisation [359]. Targeting EGFR, Gadgeel SM., *et al.* [327], showed that both erlotinib and gefitinib down-regulate the expression of COX-2 in the non small cell lung carcinoma cell lines, H1650 and H1781. In some cases, the combination of COX-2 inhibitors (celecoxib/NS-398) with erlotinib or gefitinib increased apoptosis in non-small cell lung carcinoma cell lines [362] and decreased cell number, tumour size and number in colorectal xenograft tumours in mice [324]. As both EGFR and HER2 have been linked with COX-2 production and COX2 activity has been linked with the transactivation of EGFR, a COX inhibitor (i.e. sulindac/celecoxib) could potentiate the pro-apoptotic of a dual EGFR/HER2 inhibitor (i.e. lapatinib). Therefore, in this section, we investigated the effect lapatinib has on the expression and activity of COX in the COX-1, COX-2, EGFR and HER2 expressing squamous lung cell line, A549 (for methodology see section 2.11. and 2.13. and for results see section 3.3.4.).

Firstly, we examined the effect a 48 hours exposure to each TKI (lapatinib, erlotinib and gefitinib) had on COX-2 protein expression in the A549 cell lines. We included 10 µM celecoxib as a negative control. We found that, as expected, erlotinib, gefitinib and celecoxib down-regulated COX-2 protein expression in the A549 cells (figure 3.3.4.3.). However, when compared to the EGFR-specific TKI's, erlotinib and gefitinib, lapatinib (the dual EGFR/HER2 TKI) had the opposite effect. It caused a large increase in COX-2 protein expression (figure 3.3.4.3.). As COX-2 protein expression was only increased following exposure to the dual EGFR/HER2 inhibitor and not by the EGFR-specific inhibitors, it is clear that the lapatinib-mediated up-regulation of COX-2 protein is independent of its EGFR tyrosine kinase inhibitory activity.

To determine if lapatinib up-regulated COX-2 protein expression through its HER2 inhibitory activity, we exposed the A549 cells to increasing concentrations of lapatinib, AG825 (HER1/2 TKI) and trastuzumab (HER2 antibody) and examined changes in COX-2 protein expression by Western blotting. We found that lapatinib consistently upregulated COX-2 protein expression while the HER1/2 TK inhibition, AG825, did not alter COX-2 protein expression (figure 3.3.4.2.). This indicates that COX-2 up-regulation by lapatinib is not through its HER2 tyrosine kinase activity. We also found that 0.75 and 1 µM trastuzumab down-regulated COX-2 protein expression (figure 3.3.4.2.). This also indicates that COX-2 up-regulation by lapatinib is not due to HER2 inhibition. Therefore, lapatinib-mediated up-regulation of COX-2 protein expression is independent of its EGFR/HER2 tyrosine kinase activity.

To establish whether the up-regulated COX-2 protein expressed by lapatinib was functionally active, we carried out COX activity assays on A549 protein lysates that were exposed to lapatinib for 48 hours prior to extraction. As a control, we included AG825 and trastuzumab treated A549 cell lysate. We found that A549 cells, when exposed to 2.5 and 5 µM lapatinib for 48 hours, up-regulated COX-2 protein expression and also increased its activity (graph 3.3.4.1.A.). This was mirrored by an increase in total COX activity (graph 3.3.4.1.A.). However, while 7.5 and 10 µM of lapatinib up-regulated COX-2 protein expression it did not alter COX-2 activity. This may suggest that concentrations of lapatinib below 5 µM stimulate COX-2 transcription and thus protein synthesis while concentrations above 5 µM interfere with post-transcription or translational modifications, thus rendering the new protein inactive.

As the up-regulation of COX-2 protein expression and activity by lapatinib has not been investigated before, a closer look into the signalling pathway, their down-stream transcription factors and effect on post-translational modifications, such as phosphorylation and folding, would be of considerable interest. Also, as the lapatinib-mediated COX-2 stimulation has only been studied in the A549 cell line, we do not know if the effect is cell specific, tissue specific or common in all COX-2 expression cancer cells. Also, as the concentrations used in this project were above achievable serum concentrations, repeating this study at lower concentrations would be essential to determine if the up-regulation of COX-2 by lapatinib would have consequences in the clinic, such as increased angiogenesis, metastasis or resistance to apoptosis. Interestingly, Huber LC., *et al.* [272], also looked at the effect of lapatinib on COX-2 expression and activity. However, they looked at it from a different perspective. They stimulated rheumatoid arthritis synovial fibroblasts with cytokines and pro-inflammatory mediators (TNFα, IL-1B and EGF ligand) which increased COX-2 mRNA and protein expression (quantified by ELISA). This increase was abrogated by the addition of 5 and 10 µM of lapatinib and the TKI also reduced PGE_2 production. In our system (the A549 cells), COX-2 expression occurs naturally and does not require induction/stimulation from external factors. To determine if the discrepancy in results is due to experimental design and type of COX-2 expression, the introduction of TNFα, IL-1B or EGF to proliferating A549 cells and examining any changes lapatinib has on this enhanced COX-2 would be important.

Incidentally, we also found that following a 48 hour exposure to the HER1/2 TKI, AG825 (graph 3.3.4.1.B.), and the HER antibody, trastuzumab (graph 3.3.4.1.C.), the activity of COX-2 in the A549 cells was more than halved. This provides further evidence to indicate that the stimulation of COX-2 expression and function by lapatinib was independent of its EGFR/HER2 TKI activity.

Work so far has demonstrated that, following a 48 hour exposure to lapatinib, COX-2 expression and function is increased significantly but the mechanism of action of this effect is not through tyrosine kinase inhibition of EGFR or HER2. At this stage, we examined the ability of lapatinib to directly stimulate COX-2 activity. We also included AG825, trastuzumab and celecoxib in this assay. To do this assay, we extracted untreated A549 lysate and included increasing concentrations of lapatinib into the assay plate. Before undertaking the assay we assessed whether lapatinib or its vehicle would interfere with the assay. Lapatinib has very little fluorescence (an

emission wavelength of 350-550 nm) even in strong organic solvents (as demonstrated by Dr. Brian Trummer, Department of Pharmaceutical Sciences, University at Buffalo) and therefore would not interfere in the assay. An excitation wavelength of 530 – 540 nm and emission wavelength of 585 – 595 nm were used to read the assay plates. Also, the lapatinib vehicle used was DMSO, and according to the assay manual, low levels of DMSO do not interfere with the assay. In this section, we found that lapatinib directly stimulated COX-2 activity readings in the A549 lysate (graph 3.3.4.2.A.). While AG825, trastuzumab (graph 3.3.4.2.B.) and celecoxib (graph 3.3.4.2.C.) directly inhibited COX-2 activity. Once again lapatinib stands apart from the HER2 TKI and antibody. The lapatinib-mediated COX-2 stimulation could lead to increased angiogenesis, metastasis, resistance to apoptosis and increased cell growth. However, it is unclear if other inhibitory activities of lapatinib would counter the increased COX-2 activity. Also, the concentrations of lapatinib used in this work are above pharmacologically relevant concentrations. Therefore, further investigations with lower concentrations would help determine if lapatinib-mediated COX-2 stimulation has therapeutic implications.

In summary, after short-term exposure, lapatinib up-regulates COX-2 protein and activity. It also directly stimulates COX-2 activity.

Finally, we examined whether lapatinib, AG825 or trastuzumab affected COX-1 expression and function aswell as directly interacting with COX-1. We found that with the highest concentration of lapatinib COX-1 protein expression was slightly reduced (figure 3.3.4.1.). AG825 had no effect on COX-1 expression (figure 3.3.4.1.) while 0.5, 0.75 and 1 uM of trastuzumab up-regulated COX-1 protein expression (figure 3.3.4.1.). Using the COX fluorescent activity assay, we found that a 48 hour exposure to lapatinib, AG825 or trastuzumab had little effect on COX-1 activity. Lapatinib had no effect, while both AG825 and trastuzumab slightly reduced COX-1 activity (graph 3.3.4.2.A, B and C.). Once again, lapatinib stands apart from the HER2 TKI and antibody. The highest concentration of lapatinib stimulates COX-1 activity while the highest concentration of AG825 and trastuzumab directly suppressed COX-1 activity (graph 3.3.4.2.B and C.). All the data combined indicates that lapatinib directly stimulates COX-1 activity but, following exposure to lapatinib for 48 hours, did not alter COX-1 protein expression of activity. AG825 had no effect on COX-1 protein expression but slightly decreases its activity directly and after a short-term treatment. Trastuzumab up-regulates COX-1 protein expression but

inhibits its activity directly and following short-term treatment. As COX-1 expression has been linked with early stage tumourigenesis (in HCC patients) [290] the use of lapatinib for preventing or reducing tumour progression might not therefore be recommended. However, as the concentrations of lapatinib used in this section are above pharmacologically relevant concentrations, these experiments require repeating with lower lapatinib concentrations to determine if lapatinib, at therapeutically achievable levels, would stimulate COX-1. On the other hand, the trastuzumab concentrations used are pharmacologically relevant and would be capable of inhibiting COX-1 activity in these cells, and therefore, trastuzumab could inhibit a factor that is potentially involved in tumour initiation/progression. There are no publications demonstrating the effects of lapatinib, AG825 or trastuzumab on COX-1.

It has been demonstrated that breast tumours can co-express COX-2, EGFR, HER2 and in many cases MDR transport proteins. As we have shown that lapatinib increases COX-2 expression and activity, we considered the implications of this on cell growth and apoptosis. We wanted to determine if sulindac, a non-specific COX inhibitor, could enhance the anti-proliferative potential of lapatinib in breast cell lines by reducing COX activity in these cells. We selected a panel of breast cell lines that were sensitive and insensitive to lapatinib and, while determining their COX-2 status, we carried out combination proliferation assays with both drugs. We found that sulindac could not sensitise the mild EGFR/HER2-expressing cell line, MCF7 (graph 3.3.4.3.(C) and table 3.3.4.2.), or the EGFR-amplified cell line, MDA-MB-231 (graph 3.3.4.3.(A) and table 3.3.4.2.), to lapatinib. But sulindac mildly sensitised the HER2-amplified breast cell line, MDA-MB-453, to lapatinib (graph 3.3.4.3.(B) and table 3.3.4.2.). However, in the meantime, we discovered that our panel of lapatinib sensitive and insensitive breast cell lines did not express COX-2. Therefore, even though a slight sensitisation of the HER2-expressing cell line, MDA-MB-453, occurred, the positive finding did not support the original hypothesis as this cell line does not express COX-2.

These novel results suggest that the effect of lapatinib on COX-2 is independent of its EGFR/HER2 targeted therapy activity. As COX-2 promotes angiogenesis, metastasis, cell proliferation and inhibit apoptosis (all negative outcomes for cancer treatment), the implications that lapatinib stimulates COX-2 could be detrimental in the clinic especially when combined with chemotherapeutic drugs that are already known to simulate COX-2 expression following long-term treatment. The combination of

lapatinib and a chemotherapeutic drug along with a NSAID/coxib would be worth serious consideration. We would also need to determine if the effect of lapatinib on COX-2 is cell specific by expanding testing to other COX-2 expressing cell lines, such as HL60, M14 and 2008/MRP1.

A number of anti-HER2 and anti-EGFR agents have been found to inhibit the function of multidrug resistant transporter proteins, such as P-gp and BCRP (discussed in section 1.4.5.). In this study, we compared the ability of the three tyrosine kinase inhibitors (lapatinib, erlotinib and gefitinib) to overcome (see section 2.7. for combination proliferation assay method) and alter the expression (see section 2.11. for Western blotting method) of P-gp, MRP1 and BCRP.

In three P-gp expressing cell lines (NCI/Adr-res, A549-Taxol and H1299-Taxol), lapatinib potentiated the anti-proliferative effects of two P-gp substrates (epirubicin and docetaxel) (graph 3.3.5.1.(A), 3.3.5.2.(A) and 3.3.5.3.(A)). Dai C-L., et al. [147], had similar findings in mdr1-transfected breast cell lines (MCF7 and S1) using combination proliferation assays. Using ATPase assays, they also showed that lapatinib directly inhibited the transport function of P-gp. Similar work by Collins D.M. et al. [97], in lung cancer cell lines also correlates with this finding. However, in two of three P-gp-expressing cell lines (NCI/Adr-res and H1299-Taxol (graph 3.3.5.1.(B&C) and 3.3.5.3.(B&C))), erlotinib and gefitinib did not overcome P-gp-mediated resistance. This does not correlate with Shi Z., et al. [148], who demonstrated that erlotinib sensitises the P-gp expressing colchicine-selected human epidermoid carcinoma cell line, KB-3-1, to P-gp substrates. Also, the gefitinib result does not correlate with work published by Yanase K., et al. [150], who found that 0.3 and 3 μM of gefitinib could sensitise an mdr1-transfected human myelogenous leukemia, K562, cell line to vincristine. Erlotinib (bar a mild affect with docetaxel in the H1299-Taxol cell line) and gefitinib did not inhibit P-gp function in these cells using the same combination proliferation assays employed in this thesis. The difference in results may be due to method of resistance selection/transfection or cell type. Comparing these results, lapatinib sensitises these P-gp expressing cell lines to the greatest extent. This finding is partially supported by ATPase assay results published by our group (Collins DM., et al. [97]), where lapatinib caused the greatest reduction in activated P-gp ATPase followed by erlotinib and finally gefitinib. All the TKIs caused an increase in the P-gp protein expression following a 48 hour exposure (figure 3.3.6.1.).

Contrary to our findings, Dai CL., *et al.* [147], found that lapatinib did not affect the mRNA or protein expression levels of P-gp in doxorubicin-selected MCF7 cells following exposure to similar concentrations for 48 hours. However, using the same cell line, similar drug concentrations and technique as used in this thesis, Collins DM., Thesis [112] demonstrated the same changes in protein expression presented in this thesis.

As all TKI's up-regulate the expression of P-gp, there is an increased risk that long-term treatment with the TKI's could amplify or induce P-gp protein expression and thus, P-gp-mediated resistance. This implies that the MDR phenotype could be presented in secondary or advanced tumours and would require consideration in treatment design. Lapatinib, below pharmacologically relevant concentrations, effectively overcame P-gp-mediated resistance, leading to an increased toxicity of the P-gp substrate chemotherapeutics, epirubicin and docetaxel. The inhibition of P-gp activity by lapatinib has two potential clinical applications, firstly sensitising P-gp-mediated multidrug resistance tumours to substrate chemotherapeutics and secondly improving the bioavailability of orally administered P-gp substrate anti-cancer agents. These results would suggest that the combination of lapatinib with epirubicin or docetaxel warrants clinical investigation in cancer.

In the transfected MRP1 cell line, 2008/MRP1, the three TKI's did not enhance MRP1 substrate toxicity or overcome resistance (graph 3.3.5.4 and table 3.3.5.4.). This correlates with a number of publications: (**a**) Yanase K., *et al.* [150], demonstrated this with gefitinib in MRP1-transfected human epidermoid carcinoma cells, KB-3-1, and (**b**) Collins D.M. *et al.* [97], found that lapatinib, erlotinib and gefitinib did not sensitise the endogenously expressing MRP1 lung cell line, A549, to epirubicin. With regard to MRP1 protein expression we found that the dual EGFR/HER2 TKI, lapatinib, had the opposite effect on MRP1 protein expression relative to erlotinib and gefitinib (figure 3.3.6.2.). Both erlotinib and gefitinib up-regulated MRP1 protein expression while lapatinib down-regulated it (also shown by Dunne G., Thesis [197]). Even though lapatinib down-regulated MRP1 protein expression it did not sensitise the A549 cells to epirubicin. This would not be unexpected, as work carried out by Collins D., [112] demonstrated, using ATPase assays, that lapatinib was a poor activator and inhibitor of MRP1. Also difference in MRP1 expression caused by lapatinib could be negated by stress response induced by the presence of vincristine.

The mechanism by which lapatinib down-regulated MRP1 protein expression has not been elucidated, however, from the proliferation combination assay discussed in this section, it is clear that this down-regulation does not alter the sensitivity to the MRP1 substrate, epirubicin. This finding has not been published in the literature.

The three TKI's do not overcome MRP1-mediated multidrug resistance, however, both erlotinib and gefitinib up-regulate MRP1 protein expression. Therefore, long-term treatment with erlotinib or gefitinib could amplify or induce MRP1 protein expression and thus, resistance to MRP1 substrate chemotherapeutic drugs including the anthracyclines or vincristine. However, this acquired resistance would not change the anti-proliferative potential of erlotinib or gefitinib. On the other hand, lapatinib down-regulates MRP1 protein expression and therefore lapatinib could suppress the subsequent development of MRP1-mediated resistance in tumours.

The greatest effect of the three TKIs occurred when combined with the BCRP substrate, SN-38, in the BCRP-expressing mitoxantrone-selected squamous lung cell line, DLKP-SQ/mitox (graph 3.3.5.5 and table 3.3.5.5.). With 0.3 µM lapatinib, 0.5 µM erlotinib and 0.5 µM gefitinib the anti-proliferative potential of SN-38 was increased from 4% to greater than 90%. Lapatinib caused the greatest effect, followed closely by erlotinib and finally gefitinib. In pre-clinical studies, a number of publications have shown enhanced sensitivity to BCRP substrates by lapatinib, erlotinib or gefitinib. However, a comparison between the three agents has never been published. Dai CL., et al. [147], sensitised the mitoxantrone-selected colon cell line, S1-M1-80, to topotecan and mitoxantrone with concentrations between 0.6 and 2.5 µM lapatinib. Using erlotinib, Shi Z., et al. [148], sensitised the flavopiridol-selected breast cell line, MCF7-BCRP, to mitoxantrone in combination proliferation assays. In combination proliferation assays, Yanase K., et al. [150], reversed BCRP-mediated resistance in human myelogenous leukemia (K562/BCRP), BCRP-transduced murine lymphocytic leukemia (P388-BCRP) and in the endogenous BCRP expressing human colon (HT-29) cancer cell lines with gefitinib. They also demonstrated an increase in substrate accumulation in the presence of gefitinib and indicated that the agent may be a functional inhibitor of the BCRP transporter protein (using ATPase assays).

The effect observed on BCRP protein expression by the three TKI's differed according to their concentrations (figure 3.3.6.3.). Down-regulation with lapatinib occurred; however, a biological repeat was not fully consistent. Dai CL., et al. [147],

showed that lapatinib does not affect the mRNA or protein expression levels of BCRP in a BCRP-transfected colon cell line. In our hands, the expression of BCRP was up-regulated with low concentrations of erlotinib but down-regulated at the higher concentration of 1 μM erlotinib. These mixed results may be explained by the nature of MDR proteins and the specificity of TKIs over a broad concentration range. As the concentration of the TKIs increases in the cell its activities become less specific which could inadvertently induce a stress response, inhibit or stimulate proteins, signalling pathways or transcription factors that regulate MDR protein expression and function. All three TKI's significantly overcame BCRP-mediated resistance. This was expected for lapatinib [147] [97], erlotinib [148] and gefitinib [150] as they were shown to functionally inhibit BCRP using ATPase activity assays. Lapatinib caused the greatest effect, followed by erlotinib and finally gefitinib. The degree by which these TKI's overcame BCRP-mediated resistance was substantial and could have significant implications in the treatment of BCRP-mediated resistant tumour. Their combination with BCRP substrate could significantly enhance the cytotoxic potential of the substrate, therefore increasing cell kill and improving treatment outcome.

In summary, lapatinib sensitised both HER2-expressing cell lines, MDA-MB-453 and MCF7, to chemotherapy treatment and overcame P-gp and BCRP mediated resistance to the greatest extent. However, lapatinib did not affect EGFR-expressing cells, while erlotinib inhibited both EGFR and BCRP to a greater extent than gefitinib. Thus, the use of lapatinib combined with P-gp substrates, such as epirubicin or docetaxel, or BCRP substrates, such as irinotecan, might decrease cell growth in tumours presenting an HER2 and/or MDR phenotype. Lapatinib may also enhance COX-2 expression and activity, therefore combining lapatinib with a COX-2 inhibitor could reduce tumour cell proliferation, angiogenesis, and metastasis and reduce the risk of later tumours presenting amplified levels of COX-2. The up-regulation of COX-2 protein expression and activity by lapatinib is not due to inhibition of EGFR and/or HER2. The combination of erlotinib or gefitinib with BCRP substrates, and potentially with a coxib, in EGFR$^+$, BCRP$^+$ and COX-2$^+$ cells could be beneficial as many solid tumours co-express BCRP and COX-2 due to the hypoxic environment inside the tumour mass. Also introducing a coxib, such as celecoxib (also an MRP1 inhibitor), into the combination would aid reduce the risk of the angiogenesis and metastasis. These combinations could have long term benefits in the treatment of

tumours commonly presenting intrinsic or acquired multidrug resistance, such as lung, digestive tract, lung, haemotopoeitic stem cells and brain tumours. In addition, these combinations might also prove beneficial in reducing solid tumour mass as BCRP [215] and COX-2 [428] expression is known to be upregulated in hypoxic conditions (observed in the solid tumours of ovarian, small-cell lung carcinoma, ewing sarcoma and prostate cancer).

There are no clinical trials investigating the anti-MDR potential of lapatinib. However, the anti-cancer properties presented in this project provide strong backing to support moving forward to animal models and potentially clinical trial. Erlotinib has not reached anti-MDR clinical trials but the pharmacokinetics erlotinib-mediated BCRP inhibition was investigated in Bcrp1-/-/Mdr1a/1b-/- (triple-knockout) and wild-type mice [229]. They found that erlotinib is actively transported by P-gp and BCRP *in vitro* and the lack of P-gp/BCRP significantly increased the blood plasma concentration of both i.p. and p.o. administered erlotinib in mice [198]. Phase I and II clinical trials of gefitinib with irinotecan in patients with advanced fluoropyrimidine-refractory colon cancer have been completed but gefitinib did not appear to add substantial efficacy to irinotecan [419]. This combination did not result in increased side-effects (grade 3-4).

4.4. Relationship between the COX-2 inhibitor, celecoxib, and expression and function of Multidrug resistant proteins.

Active components of the inflammatory response (COX-1 and COX-2 and their major metabolites) involved in tumour progression are frequently up-regulated in many cancer types. For review on this area see section 1.6. COX-1 is constitutively expressed in a wide variety of tissues and was been found to be over-expressed in breast [263], prostate [264], cervical [265] and ovarian [267] cancer. COX-2 on the other hand, is not detected in the majority of normal tissue but up-regulated in 80-90% of colorectal cancer [273], and is also commonly up-regulated in gastric [274], lung [275], prostate [264], breast, ovarian [276] [277], liver, bladder, osteosarcoma, melanoma [278] and bone cancer. PGE_2, a major metabolite of COX-2, has been shown to promote cell growth, inhibit apoptosis [239], increase angiogenesis [193] and enhance cell motility and adhesion [241] *in vitro*. COX-2 over-expression has been tentatively linked with poor prognosis, decreased survival and increased risk of re-occurrence in colorectal [286], ovarian [277] [287] and breast cancers [288].

A number of publications link COX-2 expression with multidrug resistance. For example, induced-COX-2 expression resulted in the enhancement in P-gp expression and functional activity in rat glomerular mesangial cells [326] and the breast cancer cell line, MCF7[328]. For review see section 1.6.3. and Sorkin A. [327]. Zatelli MC., *et al*. [175], provided evidence to support the hypothesis that the selective COX-2 inhibitor, NS-398, can prevent and reduce the development of the chemo-resistance phenotype in breast cancer cells by inhibiting P-gp function. Celecoxib, another selective COX-2 inhibitor, induced apoptosis by down-regulating the expression of COX-2 and P-gp via a mechanism involving the Akt pathway. Recently, Mazzanti R., *et al.* [429], restored apoptosis by inhibiting P-gp with celecoxib. They found that P-gp was involved in the HGF/MET autocrine loop which leads to increased Bcl-2 and mTor levels, inhibition of eIF2α, resistance to apoptosis, progression of cell cycle.
 On the other hand, Kang HK., *et al.* [174], showed that MRP1 expression was not necessarily due to the presence of COX-2, as induced COX-2 expression in the human H460 lung carcinoma cell line did not cause enhancement in MRP1 expression. Of further interest, they also showed that induced COX-2 expression did not increase P-

gp expression, suggesting that the P-gp up-regulation observed may not be true for all cells/tissue types. In human colorectal CaCo-2 cells, 6 μM naproxen [96], 0.4 μM indomethacin heptyl ester [96] and 10 μM nimesulide [96] reduced the expression and function of the P-gp pump. Puhlmann U., *et al.* [330], showed that doxorubicin-induced MDR1 over-expression was down-regulated by the COX-2-preferential inhibitor, meloxicam, in both HL-60 and primary AML blasts with subsequent improvement of cytostatic efficacy of doxorubicin. They suggested that the mechanism of P-gp down-regulation could be due to meloxicam directly inhibiting transcription factors, NF-KappaB and AP-1, which are known to positively regulate mdr1 transcription. For review on this area see section. 1.4.5., 1.6. and 1.6.3.

In this study, we established the effect celecoxib (above and below pharmacologically relevant concentrations) had on three multidrug resistance pumps, P-gp, MRP1 and BCRP. Firstly, we identified a panel of cell lines that only expressed one MDR protein (see section 3.4.1.). For example, DLKP-A expressed P-gp but does not express MRP1 or BCRP. Similar to finding published by Arunasree KM., *et al.* [160], where they showed that 10 μM celecoxib exposure for 24 hours down-regulated the expression of P-gp in the imatinib-selected K562 lymphoma cell line, we found that with the same concentration of celecoxib with the same exposure time, that celecoxib slightly down-regulated the expression of P-gp in the paclitaxel-resistant lung cell line, H1299-Taxol (see figure 3.4.3.1.(i) and for method see section 2.11.). The pharmacological studies revealed that celecoxib is a paclitaxel selected-P-gp substrate and inhibitor of both doxorubicin and paclitaxel selected P-gp. Accumulation of the P-gp substrate, epirubicin, increased in the presence of celecoxib at and above pharmacological concentrations in both cell lines (graph 3.4.5.2., table 3.4.5.2. and for method sees section 2.12.2.1.), while the P-gp inhibitor, elacridar, increased celecoxib accumulation in the same cell line (graph 3.4.4.2 and table 3.4.4.2.). This would suggest that celecoxib inhibits the transport function of P-gp and is effluxed by P-gp. An increase in celecoxib accumulation in the presence of elacridar did not occur in the DLKP-A cells, which is most likely due to the extremely high expression levels of P-gp in this cell line. Celecoxib was rapidly effluxed from both cell lines even in the presence of a functional inhibitor (graph 3.4.4.3.(B) and method in section 2.12.2.2.). This is most likely due to the expression of other mechanisms of efflux or experimental design. Keeping the pharmacological results in mind, it is not surprising

to find that celecoxib only slightly potentiated the anti-proliferative potential of two P-gp substrates, epirubicin and docetaxel, at and above pharmacologically relevant concentrations. This was observed in two of the three P-gp-expressing cell lines in our panel (graph 3.4.2.1., table 3.4.2.1. and method in section 2.7.1.). The inconsistency, for one of the cell lines, may be due to small nucleotide polymorphisms (SNP) differences [42] between the two drug selected-resistant cell lines and the transfected-resistant cell line.

Over-expression of MRP1 [349] and COX-2 but not P-gp [338] is frequently observed in lung cancers and has been associated with poor prognosis. Therefore, the second multidrug resistance protein we studied was MRP1. We found that only 10 μM celecoxib slightly reduced MRP1 expression (figure 3.4.3.1.(ii)). Partially consistent with these findings published work in this area found no alteration in MRP1 expression with 5 μM but an 80% decrease in expression with 50 μM celecoxib in the same cell line, A549 [174].

The pharmacological data strongly suggest that celecoxib inhibits the function of the MRP1 transporter protein. Celecoxib accumulation was increased 2 and 3 fold in the presence of sulindac sulphide, an MRP1 inhibitor, suggesting celecoxib may also be an MRP1 substrate (graph 3.4.4.2. and table 3.4.4.2.). However, contradicting with this point, the efflux of celecoxib occurred rapidly in the presence and absence of the MRP1 inhibitor (graph 3.4.4.3.(A)). There was a slight reduction in efflux at 60 minutes and 120 minutes in the presence of sulindac sulphide in the DLKP cells but not in the 2008/MRP1 cells. This may be due to the low levels of MRP1 expression in the DLKP cells. This contradiction may, in part, be due to slow inhibition of MRP1 by sulindac sulphide, but this fact has not been investigated. Looking at the efflux curve for shorter durations, between 0 and 30 minutes, would be the optimal method to determine if celecoxib is a substrate. Concentrations of 2 and 10 μM celecoxib increased the accumulation of the MRP1 substrate, epirubicin, in both of the MRP1-expressing cell lines, DLKP and 2008/MRP1 (graph 3.4.5.1.). In this case, the effect was 3 fold greater in the 2008/MRP1 cells compared to the DLKP cells. This significant increase (p = 0.008 and 0.002) in epirubicin accumulation was 2 fold greater than the effect observed in the P-gp-expressing cells. To date, publications in this area demonstrated that 50 and 100 μM celecoxib increases doxorubicin

accumulation following a 16 hour pre-treatment and enhances doxorubicin sensitivity in the A549 cells after 48hrs [174]. In this project, the dose of celecoxib used is at levels achievable in the blood which is 5 to 10 times lower than used by Kang HK., *et al.* [174], therefore, this work stands apart from their experiments. The pharmacological data indicates that celecoxib may be a weak substrate and is a direct functional transport inhibitor of MRP1. Therefore, it was not unexpected to find that celecoxib significantly enhanced the cytotoxicity of the two MRP1 substrates (epirubicin and vincristine) in all three MRP1-expressing cell lines (graph 3.4.2.2., table 3.4.2.2. and also see section 8, graph 8.4.2.1 and table 8.4.2.1.). Celecoxib did not alter the cytotoxicity of the two MRP1 non-substrates, docetaxel and 5FU, thus re-enforcing the statement that celecoxib overcomes MRP1-mediated resistance and that the mechanism of action is most likely through functional inhibition of the MRP1 transporter protein. Also, the enhancement in substrate cytotoxicity, during the combination proliferation assays, by celecoxib was significantly greater in the MRP1-expressing cells compared to the P-gp-expressing cells. As the anti-proliferative enhancement was observed at and below pharmacologically relevant concentrations and the cellular pharmacokinetic assays were conducted over 3 hours, the mechanism by which celecoxib overcomes MRP1-mediated resistance is unlikely to be through protein down-regulation (figure 3.4.3.1.(ii)) as protein down-regulation only occurred above pharmacologically relevant concentrations and over longer time periods. Therefore, this novel finding indicates that celecoxib is a functional inhibitor and weak substrate of MRP1 and thus overcomes MRP1-mediated resistance. The degree of inhibition by celecoxib in the MRP1-expressing cell lines was significantly larger than compared that of the P-gp-expressing cell lines. The inhibition of MRP1 activity by celecoxib has two potential clinical applications, firstly sensitising MRP1-mediated multidrug resistance tumours to substrate chemotherapeutics, and secondly, improving the bioavailability of orally administered MRP1 substrate anti-cancer agents. These results would suggest that the combination of celecoxib with epirubicin or vincristine warrants clinical investigation in cancer.

In 2008, Surowiak P., *et al.* [329], studied the correlation of COX-2, P-gp, MRP1 and BCRP expression in non-small cell lung carcinoma (NSCLC) in a cohort of 32 patients. They discovered that even though there was a very strong correlation between COX-2, P-gp and BCRP expression it had little prognostic value for

predicting outcome. However, this strong correlation prompted us to investigate the potential that celecoxib could additionally cause inhibition of BCRP-mediated drug resistance. Therefore, we carried out the same list of experiments as with P-gp and MRP1 in two BCRP expressing cell lines, DLKP-SQ/mitox (mitoxantrone-selected) and HL60/mxr (BCRP-transfected). Celecoxib had a mixed impact on BCRP protein expression (see figure 3.4.3.1.(iii)). At low levels, it appeared to increase expression, while at higher concentrations, BCRP protein expression was reduced. These mixed results may be explained by the nature of MDR proteins and the specificity of celecoxib over a broad concentration range. As the concentration of the small molecule agent increases in the cell its activities become less specific which could inadvertently induce a stress response, inhibit or stimulate proteins, signalling pathways or transcription factors that regulate MDR protein expression and function. Elacridar, a highly effective P-gp and BCRP functional inhibitor, caused a 2 fold increase in celecoxib accumulation in DLKP-SQ/mitox ($p<0.05$) and HL60/mxr ($p>0.05$) cells (see graph 3.4.4.2.). Once again celecoxib was promptly effluxed from both BCRP-expressing cell lines within 30 minutes (graph 3.4.4.3.). However, 2 μM celecoxib enhanced epirubicin accumulation by 1.7 fold ($P = 0.009$) in the DLKP-SQ/mitox cells (graph 3.4.5.3. and table 3.4.5.3.). The BCRP mutation status of this cell line is unknown, the enhanced accumulation of epirubicin in the presence of celecoxib could suggest that this cell line expresses the BCRP mutant form (see section 1.4.4.). This would suggest that celecoxib is also a weak substrate and inhibitor of BCRP. The combination proliferation assay of celecoxib and SN-38 confirmed this statement (graph 3.4.2.3. and table 3.4.2.3). At and above pharmacological concentrations (2 μM), celecoxib heightened the anti-proliferative potential of SN-38 in both of the BCRP-expressing cell lines, DLKP-SQ/mitox and HL60/mxr (graph 3.4.2.3. and table 3.4.2.3). Combining the protein expression work, the pharmacological data and the proliferation assay results, it is clear celecoxib is a weak substrate and inhibitor of BCRP at the pharmacological concentration of 2 μM and is a weak substrate, inhibitor and protein down-regulator at the higher concentration of 10 μM. This finding has not been noted in existing literature.

MDR inhibition by celecoxib was the greatest in MRP1-expressing cell lines, followed closely by BCRP-expressing cell lines and to a much lesser extent by the P-gp-expressing cell lines. The inhibition of BCRP activity by celecoxib has two

potential clinical applications, firstly sensitising BCRP-mediated multidrug resistance tumours to substrate chemotherapeutics and secondly improving the bioavailability of orally administered BCRP substrate anti-cancer agents. These results would suggest that the combination of celecoxib with irinotecan warrants clinical investigation in cancer.

In summary, celecoxib maybe a weak substrate of MRP1 and BCRP and inhibits the function of MRP1 and BCRP in these cell lines. Celecoxib is also a weak substrate and inhibitor of P-gp but not at pharmacologically relevant concentrations.

The uptake of celecoxib is heightened in the presence of the appropriate MDR inhibitor in all cell lines. Celecoxib slightly down-regulated MDR protein expression at 10 μM but this did not occur at achievable serum concentrations. The drug was rapidly removed from all cells within 30 minutes and increased MDR substrate accumulation in all cell lines. MDR substrate accumulation in the presence of celecoxib is particularly large in MRP1-expressing cells. Celecoxib enhanced the cytotoxic potential of MRP1 substrates the greatest extent, followed by BCRP and finally P-gp substrates. This evidence indicates that the combination of celecoxib with MRP1 or BCRP substrate chemotherapeutic drugs could potentially decrease tumour growth through direct pump inhibition and possibly through substrate competition. Tumours previously treated for prolonged periods with a traditional chemotherapy presenting MRP1 or BCRP phenotype along with COX-2 over-expression might be the best target for such therapy. The rationale behind this combination of traditional chemotherapy and the selective COX-2 inhibitor is further supported by the fact that chemotherapy itself induces COX-2 expression.

4.5. Overall summary and conclusion:

Pharmacokinetics of Epirubicin

•   Serum transport proteins alter epirubicin accumulation in cancer and normal cells.

•   Low levels of serum albumin and FCS aid epirubicin accumulation, but high levels hinder epirubicin accumulation.

• α_1-acidic glycoprotein (AAG) enhances the accumulation of epirubicin to the greatest extent.

•   Serum proteins do not alter epirubicin accumulation differently in normal versus cancer cells.

Screening of potential novel anti-cancer agents

•   Cytotoxicity of the polyamine derivative, PA1, and the titanium compound, Titanocene Y, are independent of P-gp expression and activity in the DLKP-A cell line.

•   The fluorinated resveratrol derivative, RBM15, and the hydrolysed macrocyclic compound, KG104, overcome P-gp-mediated resistance in the DLKP-A cell line.

MDR downregulation

•   Drugs dynamically alter MDR protein expression and understanding the pathways and transcription factors they inhibit or stimulate can help predict their effect.

•   The use of small molecule agents to overcome MDR-mediated resistance is most effective in combination with MDR substrate cytotoxics.

•   17-AAG overcomes BCRP-mediated resistance and down-regulates its protein expression.

•   As previously published; lapatinib, gefitinib, 17-AAG and elacridar overcome P-gp and BCRP-mediated resistance and could improve the bioavailability of orally administered.

•   Sulindac sulphide overcame MRP1-mediated resistance.

•   Agents can be inhibitors, down-regulator and up-regulators of MDR transporter proteins.

•   When using protein down-regulation as a mechanism of overcoming MDR in both *in vitro* and *in vivo* systems, a continuous exposure to the modulator is required to maintain the alteration.

Interactions of TKI activity

• Lapatinib sensitises HER2-expressing cells to chemotherapy in the presence or absence of EGFR expression in breast cancer cell lines.

• Lapatinib up-regulates the COX-2 protein expression and activity while also directly stimulating COX-2 activity in A549 cells. Its activity is independent of EGFR/HER2 tyrosine kinase inhibition.

• Lapatinib overcomes P-gp-mediated resistance to a greater extent than erlotinib or gefitinib.

Celecoxib interaction with MDR

• Celecoxib is a weak substrate for MRP1, BCRP and P-gp.

• Celecoxib down-regulates the expression of MRP1 and P-gp above plasma concentrations.

• Celecoxib inhibits MRP1 the greatest, followed closely by BCRP and to a much lesser degree P-gp, below plasma concentrations.

Considering novel results reported in this thesis, a number of drug combinations, which could potentially be therapeutically beneficial in the clinic, for targeting multiple oncoproteins and cell signalling pathway come to light:

• The concurrent combination of lapatinib and celecoxib or sulindac with a P-gp, MRP1 or BCRP chemotherapeutic substrate. This targets P-gp, MRP1, BCRP, COX-2 and HER2.

• The concurrent combination of erlotinib and celecoxib or sulindac with P-gp, MRP1 or BCRP chemotherapeutic substrate. This targets P-gp, MRP1, BCRP, COX-2 and EGFR.

• The concurrent combination of gefitinib and celecoxib or sulindac with a P-gp, MRP1 or BCRP chemotherapeutic substrate. This targets P-gp, MRP1, BCRP, COX-2 and EGFR.

• The concurrent combination of 17-AAG with irinotecan or another BCRP substrate.

• The concurrent combination of 17-AAG, lapatinib, celecoxib/sulindac with a P-gp, MRP1 or BCRP chemotherapeutic substrate. This targets all three MDR transporter proteins, COX-2, HER2 as well as heat shock protein 90.

Section 5.

Conclusion

5.1. Novel Compounds

Sixty one novel compounds were tested for their anti-cancer and anti-MDR potential in the two non-small cell lung carcinoma cell lines, DLKP and DLKP-A.

The polyamine compounds did not overcome MRP1 and P-gp-mediated drug resistance in the DLKP and DLKP-A cell lines.

The ditrifluoroacetyl resveratrol derivative, RMB15, and the open hydrolysed macrocycle compounds, KG104, are potentially modulators of P-gp, as shown in the DLKP-A cell line and could be therapeutically important.

The metallic agent, Titanocene Y, did not enhance the cytotoxic potential of MRP1 or P-gp cytotoxic substrates in the DLKP or DLKP-A cell lines. It has similar toxicity in both cell lines. Titanocene Y's cytotoxicity is independent of MDR expression which could be of significant therapeutic relevance similar to that of other metal-based anti-cancer agents.

Encapsulation of daunorubicin with a nano-particulate polymer was unsuccessful at evading pump-mediated efflux from MRP1 and P-gp-expressing cell models, DLKP and DLKP-A. However, there is strong evidence in favour of long-term retention of significant quantities of daunorubicin in the nano-particulate carrier in the cellular environment, if not within the cells themselves. This is of particular interest to researchers in the area of delivery development.

5.2. MDR down-regulation

Indomethacin and 17-AAG down-regulated the expression of P-gp in the A549-Taxol cell line but do not overcome P-gp-mediated resistance. Lapatinib, erlotinib, gefitinib, sulindac sulphide and elacridar up-regulate P-gp protein expression.

Lapatinib, sulindac sulphide and 17-AAG down-regulate MRP1 protein expression in the A549 cell line. MRP1 expression recovers following removal of lapatinib or 17-AAG. MRP1 protein reduction by sulindac sulphide is sustained for 48 hours. Sulindac sulphide overcame MRP1-mediated resistance in combination proliferation assays but not in scheduled proliferation assays. Lapatinib and 17-AAG did not overcome MRP1-mediated resistance. Erlotinib, gefitinib, ibuprofen, indomethacin and elacridar up-regulate MRP1 protein expression.

Gefitinib, indomethacin and 17-AAG down-regulate the expression of BCRP in the DLKP-SQ/mitox cell line. Down-regulation by gefitinib and 17-AAG is sustained for 48 hours following drug removal and both agents overcome BCRP-mediated resistance in the combination and scheduled proliferation assays. Indomethacin down-regulation recovered within 48 hours and it did not overcome BCRP-mediated resistance. Lapatinib and elacridar did not down-regulate the expression of BCRP but significantly overcame BCRP-mediated resistance in both the combination and scheduled proliferation assays. Sulindac sulphide up-regulated BCRP protein expression while erlotinib, celecoxib and ibuprofen up- and down-regated BCRP protein expression depending on their concentration.

Key take-home points from MDR down-regulation experiments:

8. 17-AAG down-regulates BCRP protein expression and overcome BCRP-mediated resistance.

9. Drugs can dynamically effect MDR protein expression

10. A single drug can differentially alter the expression of MDR proteins; therefore, understanding mechanisms of regulations for each MDR protein is important.

11. For the small molecule agents tested, combination therapy is the optimum treatment regimen.

12. Full and permanent eradication of MDR protein expression that is stable in the presence of chemotherapeutic drugs is essential when considering a combination or pre-treatment schedule.

13. Agents can be inhibitors, down-regulator and up-regulators of MDR transporter proteins.

14. When using protein down-regulation as a mechanism of overcoming MDR in both *in vitro* and *in vivo* systems, a continuous exposure to the modulator is required to maintain the alteration.

5.3. Pharmacokinetics of epirubicin

FCS and albumin causes a dose dependent reduction in free epirubicin. At low protein levels the binding epirubicin with FCS or serum albumin enhance epirubicin accumulation but high protein levels hinder epirubicin accumulation in all cell types. Binding to α_1-acid glycoprotein also enhances epirubicin accumulation in all cell types. Therefore, serum albumin and α_1-acid glycoprotein improve the availability of epirubicin to both normal and cancer cells. The true impact of AAG on anthracycline accumulation requires further investigating using AAG levels up to 280-fold higher.

5.4. Tyrosine kinase inhibitors

Lapatinib sensitises HER2 over-expressing cells to chemotherapy in the presence or absence of EGFR expression. Lapatinib slightly increases HER2 expression but reduced its active levels and does not alter EGFR expression or active levels. Lapatinib up-regulates the expression and function of COX-2 and down-regulates the expression of COX-1 protein but up-regulates its activity. This action is independent of EGFR and HER2 TKI inhibition but more likely due to the non-specific activities of lapatinib. Further work is needed to evaluate the possibility that COX inhibitors could sensitise breast cell lines to lapatinib. Lapatinib increases P-gp and BCRP protein expression and overcomes P-gp and BCRP-mediated resistance in the A549-Taxol and DLKP-SQ/mitox cell lines. Compared to erlotinib and gefitinib, lapatinib is the most potent inhibitor of P-gp and BCRP.

Erlotinib sensitises moderately-expressing EGFR/HER2 cells to chemotherapeutic drug to a greater extent than either lapatinib or gefitinib. Erlotinib down-regulates COX-2 protein expression. Erlotinib up-regulates the expression of P-gp, MRP1 and BCRP and in the DLKP-SQ/mitox cell line, overcomes BCRP-mediated resistance. Gefitinib down-regulates the expression of COX-2 and BCRP while up-regulating the expression of P-gp and MRP1. Gefitinib significantly overcomes BCRP-mediated resistance.

5.5. Celecoxib overcomes MDR resistance.

Pharmacological and proliferation assays indicate that celecoxib is a weak substrate and inhibitor of P-gp, MRP1 and BCRP. Celecoxib strongly overcomes MRP1 and BCRP-mediated resistance. Celecoxib also overcomes P-gp-mediated resistance but only non-pharmacologically relevant concentrations. Celecoxib reduces P-gp, MRP1 and BCRP protein expression at a concentration of 10 µM. Lower doses have no effect on their expression levels. The concurrent use of celecoxib with an MRP1 or BCRP substrate chemotherapeutic drug could be of value for the treatment of many tumours present multiple phenotypes (co-expression of COX-2 and MDR) and also because long-term treatment with chemotherapy often increases COX-2 expression.

Section 6.

Future plans

6.1. Modulation of Multidrug resistance

- Perform Western blotting to determine changes in P-gp expression, combination proliferation assays, P-gp substrate pharmacokinetic studies and ATPase assays to establish the nature of P-gp modulation by RBM-15 and KG104.

- The effects of RMB-15 and KG104 on the ATPase activity of other drug transporters, i.e. BCRP, MRP-2, 3 and 4, to develop a transporter profile.

- To expand on design and characterisation of the nano-particle polymer and to perform detailed *in vitro* examinations with other tumour cell lines and *in vivo* examinations on systemic drug toxicity of the new formulations.

- Perform Western blotting including more time points to determine changes in BCRP expression, combination proliferation assays with more substrates, BCRP substrate pharmacokinetic studies, confocal imaging of substrate accumulation and ATPase assays to establish the nature of BCRP modulation by 17-AAG.

- Identify a small molecule agent that causes full and stable eradication of MDR protein expression for pre-treatment schedule.

6.2. Pharmacokinetics of epirubicin

- Determine the amount of epirubicin bound to 280-fold higher α_1-acid glycoprotein and accumulation assays to show its affect on the availability of epirubicin to the normal and cancer cells.

- To determine if serum albumin and α_1-acid glycoprotein affect the cytotoxicity of epirubicin, carry out apoptosis assay with DLKP, MCF7 and HMEC cells in presence of varying levels of FBS, serum albumin and α_1-acid glycoprotein in serum-free media over a 3 day period.

- To identify, a possible link between serum albumin/α_1-acid glycoprotein blood levels and patient outcome following anthracycline treatment. Check the levels of serum albumin, and anthracyclines in patient's blood samples.

6.3. Tyrosine kinase inhibitors

- Further combination proliferation assay of the three tyrosine kinase inhibitors with a broader range of chemotherapeutic drugs in a larger panel of EGFR and HER2-amplified breast cell lines.

- Pharmacokinetics studies to determine if serum protein levels alter the availability of tyrosine kinase inhibitors to cancer cells.

- Determine if A549 cells produce TNFα, IL-1B or EGF in culture, and if the addition of TNFα, IL-1B or EGF to proliferating A549 cells changes the affect of lapatinib on this enhanced COX-2.

- Determine if a lapatinib-selected cell line expresses COX-2. Examine whether celecoxib can prevent COX-2 induction. Identify changes in the MDR and invasive status, including MMP production. Check for senescence.

6.4. Celecoxib, the MDR modulator

- COX activity assays, in the presence of celecoxib, on lysates that have been treated with lapatinib for 48 hours.

- Combination proliferation assays of lapatinib with celecoxib in breast cell models with induced (transfected) COX-2 expression, that are sensitive and insensitive to lapatinib.

- Determine if the enhancement of P-gp substrate cytotoxicity by celecoxib is due to P-gp inhibition or induction of apoptosis via P-gp involvement in the HGF/MET autocrine loop.

- The effects of celecoxib on the ATPase activity of MRP1, P-gp or BCRP, to conclusively determine if celecoxib is a functional inhibitor or substrate of these MDR transporter proteins.

Section 7.

References

1. Zhang D, Pal A, Bornmann WG, Yamasaki F, Esteva FJ, Hortobagyi GN, Bartholomeusz C, Ueno NT. Activity of lapatinib is independent of EGFR expression level in HER2-overexpressing breast cancer cells. Mol Cancer Ther. 2008 Jul;7(7):1846-50.
2. Kawano S, Tsuji S, Sawaoka H, Hori M, DuBois RN. Cyclooxygenase regulates angiogenesis induced by colon cancer cells. Cell. 1998 May 29;93(5):705-16.
3. Katayama K, Yoshioka S, Tsukahara S, Mitsuhashi J, Sugimoto Y. Inhibition of the mitogen-activated protein kinase pathway results in the down-regulation of P-glycoprotein. Mol Cancer Ther 2007;6(7):2092-102.
4. Evans HJ. Molecular genetic aspects of human cancers: The 1993 frank rose lecture. Br J Cancer 1993;68(6):1051-60.
5. Litman T, Druley TE, Stein WD, Bates SE. From MDR to MXR: New understanding of multidrug resistance systems, their properties and clinical significance. Cell Mol Life Sci 2001;58(7):931-59.
6. Robey RW, Shukla S, Steadman K, et al. Inhibition of BCRP-mediated transport by protein kinase inhibitors with a bisindolylmaleimide or indolocarbazole structure. Mol Cancer Ther 2007;6(6):1877-85.
7. Kuo MT. Roles of multidrug resistance genes in breast cancer chemoresistance. Adv Exp Med Biol 2007;608:23-30.
8. Bakos E, Homolya L. Portrait of multifaceted transporter, the multidrug resistance-associated protein 1 (MRP1/ABCC1). Pflugers Arch 2007;453(5):621-41.
9. Kruh GD, Belinsky MG. The MRP family of drug efflux pumps. Oncogene 2003;22(47):7537-52.
10. Nielsen D, Maare C, Skovsgaard T. Cellular resistance to anthracyclines. Gen Pharmacol 1996;27(2):251-5.
11. Nielsen D, Eriksen J, Maare C, Jakobsen AH, Skovsgaard T. P-glycoprotein expression in ehrlich ascites tumour cells after in vitro and in vivo selection with daunorubicin. Br J Cancer 1998;78(9):1175-80.
12. Johnson DH., Paul DM, Hande KR, DeVore RF. Paclitaxel plus carboplatin for advanced lung cancer: preliminary results of a Vanderbilt University phase II trial--LUN-46. Semin Oncol. 1995; Aug;22(4 Suppl 9):30-3.
13. Sinha, B.K., Topoisomerase inhibitors. A review of their therapeutic potential in cancer. Drugs, 1995. 49(1): p. 11-9.
14. Grem, J.L., 5-Fluorouracil: forty-plus and still ticking. A review of its preclinical and clinical development. Invest New Drugs, 2000. 18(4): p. 299-313.
15. Grollman AP, Moriya M. Mutagenesis by 8-oxoguanine: An enemy within. Trends Genet 1993;9(7):246-9.
16. Anderson RD, Berger NA. International commission for protection against environmental mutagens and carcinogens. mutagenicity and carcinogenicity of topoisomerase-interactive agents. Mutat Res 1994;309(1):109-42.
17. Dobbs NA, Twelves CJ. Comments on epirubicin. Ann Oncol 1994;5(1):98-9.
18. Myers CE. Anthracyclines. Cancer Chemother Biol Response Modif 1992;13:45-52.
19. Feig DI, Loeb LA. Oxygen radical induced mutagenesis is DNA polymerase specific. J Mol Biol 1994;235(1):33-41.
20. Bachur NR, Gee MV, Friedman RD. Nuclear catalyzed antibiotic free radical formation. Cancer Res 1982;42(3):1078-81.
21. Purmal AA, Kow YW, Wallace SS. Major oxidative products of cytosine, 5-hydroxycytosine and 5-hydroxyuracil, exhibit sequence context-dependent mispairing in vitro. Nucleic Acids Res 1994;22(1):72-8
22. Olson RD, Mushlin PS. Doxorubicin cardiotoxicity: Analysis of prevailing hypotheses. FASEB J 1990;4(13):3076-86.
23. .Hu XF, Slater A, Wall DM, Kantharidis P, Parkin JD, Cowman A, and Zalcberg JR. Rapid up-regulation of mdr1 expression by anthracyclines in a classical multidrug-resistant cell line. Br J Cancer 1995;71(5):931-6.

24. Hortobagyi GN. Anthracyclines in the treatment of cancer. an overview. Drugs 1997;54 Suppl 4:1-7.
25. www.rxlist.com >enter drug name into the system and go to pharmacological data<
26. Vaishampayan U, Parchment RE, Jasti BR, Hussain M. Taxanes: An overview of the pharmacokinetics and pharmacodynamics. Urology 1999;54(6A Suppl):22-9.
27. Gligorov, J. and J.P. Lotz, Preclinical pharmacology of the taxanes: implications of the differences. Oncologist, 2004. 9 Suppl 2: p. 3-8.
28. Francis PA, Kris MG, Rigas JR, Grant SC, Miller VA. Paclitaxel (taxol) and docetaxel (taxotere): Active chemotherapeutic agents in lung cancer. Lung Cancer 1995;12 Suppl 1:S163-72.
29. Haldar S, Basu A, Croce CM. Bcl2 is the guardian of microtubule integrity. Cancer Res 1997;57(2):229-33.
30. Blagosklonny MV, Schulte T, Nguyen P, Trepel J, Neckers LM. Taxol-induced apoptosis and phosphorylation of bcl-2 protein involves c-raf-1 and represents a novel c-raf-1 signal transduction pathway. Cancer Res 1996;56(8):1851-4.
31. Bradley G, Ling V. P-glycoprotein, multidrug resistance and tumor progression. Cancer Metastasis Rev 1994;13(2):223-33.
32. Gottesman MM, Pastan I. Biochemistry of multidrug resistance mediated by the multidrug transporter. Annu Rev Biochem 1993;62:385-427.
33. Cabral F, Barlow SB. Mechanisms by which mammalian cells acquire resistance to drugs that affect microtubule assembly. FASEB J 1989;3(5):1593-9.
34. Burzykowski T, Buyse M, Piccart-Gebhart MJ, Sledge G, Carmichael J, Lück HJ, Mackey JR, Nabholtz JM, Paridaens R, Biganzoli L, Jassem J, Bontenbal M, Bonneterre J, Chan S, Basaran GA, Therasse P.Evaluation of tumor response, disease control, progression-free survival, and time to progression as potential surrogate end points in metastatic breast cancer. J Clin Oncol. 2008 Apr 20;26(12):1987-92.
35. Suzuki H, Sugiyama Y. Role of metabolic enzymes and efflux transporters in the absorption of drugs from the small intestine. Eur J Pharm Sci 2000;12(1):3-12.
36. Goldstein GW, Betz AL. The blood-brain barrier. Sci Am 1986;255(3):74-83.
37. Hoffmeyer S, Burk O, von Richter O, et al. Functional polymorphisms of the human multidrug-resistance gene: Multiple sequence variations and correlation of one allele with P-glycoprotein expression and activity in vivo. Proc Natl Acad Sci U S A 2000;97(7):3473-8.
38. Thwaites DT, McEwan GT, Simmons NL. The role of the proton electrochemical gradient in the transepithelial absorption of amino acids by human intestinal caco-2 cell monolayers. J Membr Biol 1995;145(3):245-56.
39. Tsuji A, Tamai I. Carrier-mediated intestinal transport of drugs. Pharm Res 1996;13(7):963-77.
40. Stewart CF, Leggas M, Schuetz JD, et al. Gefitinib enhances the antitumor activity and oral bioavailability of irinotecan in mice. Cancer Res 2004;64(20):7491-9.
41. Fricker G, Drewe J, Huwyler J, Gutmann H, Beglinger C. Relevance of p-glycoprotein for the enteral absorption of cyclosporin A: In vitro-in vivo correlation. Br J Pharmacol 1996;118(7):1841-7.
42. Ayrton A, Morgan P. Role of transport proteins in drug absorption, distribution and excretion. Xenobiotica 2001;31(8-9):469-97.
43. Hagenbuch B. Molecular properties of hepatic uptake systems for bile acids and organic anions. J Membr Biol 1997;160(1):1-8.
44. LeBlanc GA. Hepatic vectorial transport of xenobiotics. Chem Biol Interact 1994;90(2):101-20.
45. Smith MD, Smirthwaite AD, Cairns DE, Cousins RB, Gaylor JD. Techniques for measurement of oxygen consumption rates of hepatocytes during attachment and post-attachment. Int J Artif Organs 1996;19(1):36-44.
46. Stieger B, Meier PJ. Bile acid and xenobiotic transporters in liver.. Curr Opin Cell Biol. 1998 Aug;10(4):462-7. Review.

47. Hooiveld GJ, van Montfoort JE, Meijer DK, Muller M. Function and regulation of ATP-binding cassette transport proteins involved in hepatobiliary transport. Eur J Pharm Sci 2000;12(1):13-30.

48. Kragh-Hansen U. Molecular aspects of ligand binding to serum albumin. Pharmacol Rev. 1981 Mar;33(1):17-53. Review.

49. Fiori M, Gunelli R, Mercuriali M, Bercovich E. Tension-free vaginal tape and female stress incontinence: further evidence of effectiveness. Urol Int. 2004;72(4):325-8.

50. Khan SN, Islam B, Yennamalli R, Sultan A, Subbarao N, Khan AU. Interaction of mitoxantrone with human serum albumin: spectroscopic and molecular modeling studies. Eur J Pharm Sci. 2008 Dec 18;35(5):371-82. Epub 2008 Aug 13.

51. Ojingwa JC, Spahn-Langguth H, Benet LZ. Reversible binding of tolmetin, zomepirac, and their glucuronide conjugates to human serum albumin and plasma. J Pharmacokinet Biopharm. 1994 Feb;22(1):19-40.

52. Khan SN, Islam B, Yennamalli R, Sultan A, Subbarao N, Khan AU. Interaction of mitoxantrone with human serum albumin: spectroscopic and molecular modeling studies. Eur J Pharm Sci. 2008 Dec 18;35(5):371-82. Epub 2008 Aug 13.

53. Magid E, Guldager H, Hesse D, Christiansen MS. Monitoring urinary orosomucoid in acute inflammation: observations on urinary excretion of orosomucoid, albumin, alpha1-microglobulin, and IgG. Clin Chem. 2005 Nov;51(11):2052-8. Epub 2005 Sep 15.

54. Shibata K, Okubo H, Ishibashi H, Tsuda-Kawamura K, Yanase T. Rat alpha 1-acid glycoprotein: Uptake by inflammatory and tumour tissues. Br J Exp Pathol 1978;59(6):601-8.

55. An MR, Hsieh CC, Reisner PD, et al. Evidence for posttranscriptional regulation of C/EBPalpha and C/EBPbeta isoform expression during the lipopolysaccharide-mediated acute-phase response. Mol Cell Biol 1996;16(5):2295-306.

56. Yiangou M, Scott SG, Rabek JP, An MR, Xiong W, Papaconstantinou J. Effects of mercuric chloride on the regulation of expression of the acute phase response components alpha(1)-acid glycoprotein and C/EBP transcription factors. Biochim Biophys Acta 2001;1518(1-2):47-56.

57. Pukhal'skii AL, Shmarina GV, Lyutov AG, Novikova LI, Shemyakin IG, Aleshkin VA. Alpha1-acid glycoprotein possesses in vitro pro- and antiinflammatory activities. Bull Exp Biol Med 2001;131(5):479-81.

58. Crown J. Smart bombs versus blunderbusses: High-dose chemotherapy for breast cancer. Lancet 2004;364(9442):1299-300.

59. Chassany O, Urien S, Claudepierre P, Bastian G, Tillement JP. Comparative serum protein binding of anthracycline derivatives. Cancer Chemother Pharmacol 1996;38(6):571-3.

60. Sham HL, Kempf DJ, Molla A, et al. ABT-378, a highly potent inhibitor of the human immunodeficiency virus protease. Antimicrob Agents Chemother 1998;42(12):3218-24.

61. Thomas H, Coley HM. Overcoming multidrug resistance in cancer: An update on the clinical strategy of inhibiting p-glycoprotein. Cancer Control 2003;10(2):159-65.

62. Fardel O, Lecureur V, Guillouzo A. The P-glycoprotein multidrug transporter. Gen Pharmacol 1996;27(8):1283-91.

63. Ambudkar SV, Dey S, Hrycyna CA, Ramachandra M, Pastan I, Gottesman MM. Biochemical, cellular, and pharmacological aspects of the multidrug transporter. Annu Rev Pharmacol Toxicol 1999;39:361-98.

64. Dean M, Allikmets R. Evolution of ATP-binding cassette transporter genes. Curr Opin Genet Dev 1995;5(6):779-85.

65. Hyde SC, Emsley P, Hartshorn MJ, et al. Structural model of ATP-binding proteins associated with cystic fibrosis, multidrug resistance and bacterial transport. Nature 1990;346(6282):362-5.

66. Dean M, Rzhetsky A, Allikmets R. The human ATP-binding cassette (ABC) transporter superfamily. Genome Res 2001;11(7):1156-66.

67. Lage H. An overview of cancer multidrug resistance: A still unsolved problem. Cell Mol Life Sci 2008;65(20):3145-67

68. Dean M. The human ATP-binding Cassette (ABC) Transporter Superfamily. (2002). www.ncbi.nlm.nih.gov/bookshelf/br.fcgi?book=mono_001&part=A137.

69. Riordan JR, Deuchars K, Kartner N, Alon N, Trent J, Ling V. Amplification of P-glycoprotein genes in multidrug-resistant mammalian cell lines. Nature 1985;316(6031):817-9.

70. Roninson IB, Chin JE, Choi KG, et al. Isolation of human mdr DNA sequences amplified in multidrug-resistant KB carcinoma cells. Proc Natl Acad Sci U S A 1986;83(12):4538-42.

71. Luker GD, Flagg TP, Sha Q, et al. MDR1 P-glycoprotein reduces influx of substrates without affecting membrane potential. J Biol Chem 2001;276(52):49053-60.

72. Roepe PD. The role of the MDR protein in altered drug translocation across tumor cell membranes. Biochim Biophys Acta 1995;1241(3):385-405.

73. Roepe PD, Wei LY, Cruz J, Carlson D. Lower electrical membrane potential and altered pHi homeostasis in multidrug-resistant (MDR) cells: Further characterization of a series of MDR cell lines expressing different levels of P-glycoprotein. Biochemistry 1993;32(41):11042-56.

74. Gottesman MM, Pastan I. Biochemistry of multidrug resistance mediated by the multidrug transporter. Annu Rev Biochem. 1993;62:385-427. Review.

75. Higgins CF, Gottesman MM. Is the multidrug transporter a flippase? Trends Biochem Sci 1992;17(1):18-21.

76. Shapiro AB, Ling V. Using purified P-glycoprotein to understand multidrug resistance. J Bioenerg Biomembr 1995;27(1):7-13.

77. Szakacs G, Paterson JK, Ludwig JA, Booth-Genthe C, Gottesman MM. Targeting multidrug resistance in cancer. Nat Rev Drug Discov 2006;5(3):219-34.

78. Leslie EM, Deeley RG, Cole SP. Multidrug resistance proteins: Role of P-glycoprotein, MRP1, MRP2, and BCRP (BCRP) in tissue defense. Toxicol Appl Pharmacol 2005;204(3):216-37.

79. Chang X-B. A molecular understanding of ATP-dependent solute transport by multidrug resistance-associated protein MRP1. Cancer Metastasis Rev 2007;26(1):15-37.

80. Kuwano M, Toh S, Uchiumi T, Takano H, Kohno K, Wada M. Multidrug resistance-associated protein subfamily transporters and drug resistance. Anticancer Drug Des 1999;14(2):123-31.

81. Chaudhary PM, Roninson IB. Expression and activity of P-glycoprotein, a multidrug efflux pump, in human hematopoietic stem cells. Cell 1991;66(1):85-94.

82. Mealey KL, Bentjen SA, Gay JM, Cantor GH. Ivermectin sensitivity in collies is associated with a deletion mutation of the mdr1 gene. Pharmacogenetics 2001;11(8):727-33.

83. Hu Z, Jin S, Scotto KW. Transcriptional activation of the MDR1 gene by UV irradiation. role of NF-Y and Sp1. J Biol Chem 2000;275(4):2979-85.

84. McCollum AK, TenEyck CJ, Stensgard B, Morlan BW, Ballman KV, Jenkins RB, Toft DO, Erlichman C. P-Glycoprotein-mediated resistance to Hsp90-directed therapy is eclipsed by the heat shock response. Cancer Res. 2008 Sep 15;68(18):7419-27.

85. Wei LY, Roepe PD. Low external pH and osmotic shock increase the expression of human MDR protein. Biochemistry 1994;33(23):7229-38.

86. Arceci RJ, Baas F, Raponi R, Horwitz SB, Housman D, Croop JM. Multidrug resistance gene expression is controlled by steroid hormones in the secretory epithelium of the uterus. Mol Reprod Dev 1990;25(2):101-9.

87. Piekarz RL, Cohen D, Horwitz SB. Progesterone regulates the murine multidrug resistance mdr1b gene. J Biol Chem 1993;268(11):7613-6.

88. Chin KV, Ueda K, Pastan I, Gottesman MM. Modulation of activity of the promoter of the human MDR1 gene by ras and p53. Science 1992;255(5043):459-62.

89. Burt RK, Garfield S, Johnson K, Thorgeirsson SS. Transformation of rat liver epithelial cells with v-H-ras or v-raf causes expression of MDR-1, glutathione-S-transferase-P and increased resistance to cytotoxic chemicals. Carcinogenesis 1988;9(12):2329-32.

90. Cai J, Wallace DC, Zhivotovsky B, Jones DP Separation of cytochrome c-dependent caspase activation from thiol-disulfide redox change in cells lacking mitochondrial DNA. Free Radic Biol Med. 2000 Aug;29(3-4):334-42.

91. Scotto KW. Transcriptional regulation of ABC drug transporters. Oncogene 2003;22(47):7496-511.

92. Ohga T, Uchiumi T, Makino Y, et al. Direct involvement of the Y-box binding protein YB-1 in genotoxic stress-induced activation of the human multidrug resistance 1 gene. J Biol Chem 1998;273(11):5997-6000.

93. Bahr O, Wick W, Weller M. Modulation of MDR/MRP by wild-type and mutant p53. J Clin Invest 2001;107(5):643-6.

94. El-Deiry WS. The role of p53 in chemosensitivity and radiosensitivity. Oncogene 2003;22(47):7486-95.

95. Ogretmen B, Safa AR. Negative regulation of MDR1 promoter activity in MCF-7, but not in multidrug resistant MCF-7/Adr, cells by cross-coupled NF-kappa B/p65 and c-fos transcription factors and their interaction with the CAAT region. Biochemistry 1999;38(7):2189-99.

96. Zrieki A, Farinotti R, Buyse M. Cyclooxygenase inhibitors down regulate P-glycoprotein in human colorectal caco-2 cell line. Pharm Res 2008;25(9):1991-2001.

97. Collins DM, Crown J, O'Donovan N, Devery A, O'Sullivan F, O'Driscoll L, Clynes M, O'Connor R. Tyrosine kinase inhibitors potentiate the cytotoxicity of MDR-substrate anticancer agents independent of growth factor receptor status in lung cancer cell lines. Invest New Drugs. 2009 Jun 5.

98. Sikic BI. Pharmacologic approaches to reversing multidrug resistance. Semin Hematol 1997;34(4 Suppl 5):40-7.

99. Coley HM. Mechanisms and strategies to overcome chemotherapy resistance in metastatic breast cancer. Cancer Treatment Reviews 2008;34(4):378-90.

100. Cole SP, Sparks KE, Fraser K, et al. Pharmacological characterization of multidrug resistant MRP-transfected human tumor cells. Cancer Res 1994;54(22):5902-10.

101. Majumder S, Dutta P, Mookerjee A, Choudhuri SK. The role of a novel copper complex in overcoming doxorubicin resistance in Ehrlich ascites carcinoma cells in vivo. Chem Biol Interact. 2006 Feb 1;159(2):90-103.

102. Lage H, Dietel M. Effect of the breast-cancer resistance protein on atypical multidrug resistance. The Lancet Oncology, 2000;1(3):169-75.

103. Cole SP, Bhardwaj G, Gerlach JH, et al. Overexpression of a transporter gene in a multidrug-resistant human lung cancer cell line. Science 1992;258(5088):1650-4.

104. Konig J, Hartel M, Nies AT, et al. Expression and localization of human multidrug resistance protein (ABCC) family members in pancreatic carcinoma. Int J Cancer 2005;115(3):359-67.

105. Borst P, Evers R, Kool M, Wijnholds J. A family of drug transporters: The multidrug resistance-associated proteins. J Natl Cancer Inst 2000;92(16):1295-302.

106. Brechot JM, Hurbain I, Fajac A, Daty N, Bernaudin JF. Different pattern of MRP localization in ciliated and basal cells from human bronchial epithelium. J Histochem Cytochem 1998;46(4):513-7.

107. Scheffer GL, Pijnenborg AC, Smit EF, et al. Multidrug resistance related molecules in human and murine lung. J Clin Pathol 2002;55(5):332-9.

108. Wright SR, Boag AH, Valdimarsson G, et al. Immunohistochemical detection of multidrug resistance protein in human lung cancer and normal lung. Clin Cancer Res 1998;4(9):2279-89.

109. Peng KC, Cluzeaud F, Bens M, et al. Tissue and cell distribution of the multidrug resistance-associated protein (MRP) in mouse intestine and kidney. J Histochem Cytochem 1999;47(6):757-68.

110. Gennuso F, Fernetti C, Tirolo C, et al. Bilirubin protects astrocytes from its own toxicity by inducing up-regulation and translocation of multidrug resistance-associated protein 1 (Mrp1). Proc Natl Acad Sci U S A 2004;101(8):2470-5.
111. Wijnholds J, Scheffer GL, van der Valk M, et al. Multidrug resistance protein 1 protects the oropharyngeal mucosal layer and the testicular tubules against drug-induced damage. J Exp Med 1998;188(5):797-808.
112. Collins DM., Docetaxel uptake and modulation of P-gp mediated docetaxel efflux by tyrosine kinase inhibitors in human lung carcinoma cell lines. 2007., Thesis.
113. Nagashige M, Ushigome F, Koyabu N, et al. Basal membrane localization of MRP1 in human placental trophoblast. Placenta 2003;24(10):951-8.
114. Leonessa F, Clarke R. ATP binding cassette transporters and drug resistance in breast cancer. Endocr Relat Cancer 2003;10(1):43-73.
115. Zaman GJ, Flens MJ, van Leusden MR, et al. The human multidrug resistance-associated protein MRP is a plasma membrane drug-efflux pump. Proc Natl Acad Sci U S A 1994;91(19):8822-6.
116. Lorico A, Rappa G, Flavell RA, Sartorelli AC. Double knockout of the MRP gene leads to increased drug sensitivity in vitro. Cancer Res 1996;56(23):5351-5.
117. Loe DW, Deeley RG, Cole SP. Biology of the multidrug resistance-associated protein, MRP. Eur J Cancer 1996;32A(6):945-57.
118. Renes J, de Vries EG, Nienhuis EF, Jansen PL, Muller M. ATP- and glutathione-dependent transport of chemotherapeutic drugs by the multidrug resistance protein MRP1. Br J Pharmacol 1999;126(3):681-8.
119. Cole SP, Deeley RG. Multidrug resistance mediated by the ATP-binding cassette transporter protein MRP. Bioessays 1998;20(11):931-40.
120. Coley HM, Sarju J, Wagner G. Synthesis and characterization of platinum(II) oxadiazoline complexes and their in vitro antitumor activity in platinum-sensitive and -resistant cancer cell lines. J Med Chem 2008;51(1):135-41.
121. Choudhuri S, Klaassen CD. Structure, function, expression, genomic organization, and single nucleotide polymorphisms of human ABCB1 (MDR1), ABCC (MRP), and ABCG2 (BCRP) efflux transporters. Int J Toxicol. 2006 Jul-Aug;25(4):231-59. Review.
122. Doyle LA, Yang W, Abruzzo LV, et al. A multidrug resistance transporter from human MCF-7 breast cancer cells. Proc Natl Acad Sci U S A 1998;95(26):15665-70.
123. Croop JM, Tiller GE, Fletcher JA, et al. Isolation and characterization of a mammalian homolog of the drosophila white gene. Gene 1997;185(1):77-85.
124. Spies T, Praznik W, Hofinger A, Altmann F, Nitsch E, Wutka R. The structure of the fructan sinistrin from urginea maritima. Carbohydr Res 1992;235:221-30.
125. Litman T, Jensen U, Hansen A, et al. Use of peptide antibodies to probe for the mitoxantrone resistance-associated protein MXR/BCRP/ABCP/BCRP. Biochim Biophys Acta 2002;1565(1):6-16.
126. Polgar O, Robey RW, Bates SE. BCRP: Structure, function and role in drug response. Expert Opin Drug Metab Toxicol 2008;4(1):1-15.
127. Kondo C, Suzuki H, Itoda M, et al. Functional analysis of SNPs variants of BCRP/BCRP. Pharm Res 2004;21(10):1895-903.
128. Chen ZS, Robey RW, Belinsky MG, et al. Transport of methotrexate, methotrexate polyglutamates, and 17beta-estradiol 17-(beta-D-glucuronide) by BCRP: Effects of acquired mutations at R482 on methotrexate transport. Cancer Res 2003;63(14):4048-54.
129. Mitomo H, Kato R, Ito A, et al. A functional study on polymorphism of the ATP-binding cassette transporter BCRP: Critical role of arginine-482 in methotrexate transport. Biochem J 2003;373(Pt 3):767-74.
130. Allen JD, van Loevezijn A, Lakhai JM, et al. Potent and specific inhibition of the breast cancer resistance protein multidrug transporter in vitro and in mouse intestine by a novel analogue of fumitremorgin C. Mol Cancer Ther 2002;1(6):417-25.

131. Miwa M, Tsukahara S, Ishikawa E, Asada S, Imai Y, Sugimoto Y. Single amino acid substitutions in the transmembrane domains of breast cancer resistance protein (BCRP) alter cross resistance patterns in transfectants. Int J Cancer 2003;107(5):757-63.

132. Volk EL, Farley KM, Wu Y, Li F, Robey RW, Schneider E. Overexpression of wild-type breast cancer resistance protein mediates methotrexate resistance. Cancer Res 2002;62(17):5035-40.

133. Janvilisri T, Shahi S, Venter H, Balakrishnan L, van Veen HW. Arginine-482 is not essential for transport of antibiotics, primary bile acids and unconjugated sterols by the human breast cancer resistance protein (BCRP). Biochem J 2005;385(Pt 2):419-26.

134. Doyle LA, Ross DD. Multidrug resistance mediated by the breast cancer resistance protein BCRP (BCRP). Oncogene 2003;22(47):7340-58.

135. Zhang W, Mojsilovic-Petrovic J, Andrade MF, Zhang H, Ball M, Stanimirovic DB. The expression and functional characterization of BCRP in brain endothelial cells and vessels. FASEB J 2003;17(14):2085-7.

136. Maliepaard M, Scheffer GL, Faneyte IF, et al. Subcellular localization and distribution of the breast cancer resistance protein transporter in normal human tissues. Cancer Res 2001;61(8):3458-64.

137. Van Aubel RA, Masereeuw R, Russel FG. Molecular pharmacology of renal organic anion transporters. Am J Physiol Renal Physiol 2000;279(2):F216-32.

138. Krishnamurthy P, Ross DD, Nakanishi T, Bailey-Dell K, Zhou S, Mercer KE, Sarkadi B, Sorrentino BP, Schuetz JD. The stem cell marker Bcrp/ABCG2 enhances hypoxic cell survival through interactions with heme. J Biol Chem. 2004 Jun 4;279(23):24218-25. Epub 2004 Mar 24.

139. Fedasenka UU, Shman TV, Savitski VP, Belevcev MV. Expression of MDR1, LRP, BCRP and bcl-2 genes at diagnosis of childhood all: Comparison with MRD status after induction therapy. Exp Oncol 2008;30(3):248-52.

140. Ross DD, Gao Y, Yang W, Leszyk J, Shively J, Doyle LA. The 95-kilodalton membrane glycoprotein overexpressed in novel multidrug-resistant breast cancer cells is NCA, the nonspecific cross-reacting antigen of carcinoembryonic antigen. Cancer Res 1997;57(24):5460-4.

141. Jiang XJ, Wang JS, Fang Q. Gene expression of breast cancer resistance protein in adult acute lymphocytic leukemia and its clinical significance. Zhongguo Shi Yan Xue Ye Xue Za Zhi. 2008 Feb;16(1):31-4.

142. Benderra Z, Faussat AM, Sayada L, et al. MRP3, BCRP, and P-glycoprotein activities are prognostic factors in adult acute myeloid leukemia. Clin Cancer Res 2005;11(21):7764-72.

143. Diestra JE, Scheffer GL, Català I, Maliepaard M, Schellens JH, Scheper RJ, Germà-Lluch JR, Izquierdo MA. Frequent expression of the multi-drug resistance-associated protein BCRP/MXR/ABCP/ABCG2 in human tumours detected by the BXP-21 monoclonal antibody in paraffin-embedded material. J Pathol. 2002 Oct;198(2):213-9.

144. Diestra JE, Condom E, Del Muro XG, Scheffer GL, Pérez J, Zurita AJ, Muñoz-Seguí J, Vigués F, Scheper RJ, Capellá G, Germà-Lluch JR, Izquierdo MA. Expression of multidrug resistance proteins P-glycoprotein, multidrug resistance protein 1, breast cancer resistance protein and lung resistance related protein in locally advanced bladder cancer treated with neoadjuvant chemotherapy: biological and clinical implications. J Urol. 2003 Oct;170(4 Pt 1):1383-7.

145. Hirschmann-Jax C, Foster AE, Wulf GG, et al. A distinct "side population" of cells with high drug efflux capacity in human tumor cells. Proc Natl Acad Sci U S A 2004;101(39):14228-33.

146. Dean M, Fojo T, Bates S. Tumour stem cells and drug resistance. Nat Rev Cancer 2005;5(4):275-84.

147. Dai CL, Tiwari AK, Wu CP, et al. Lapatinib (tykerb, GW572016) reverses multidrug resistance in cancer cells by inhibiting the activity of ATP-binding cassette subfamily B member 1 and G member 2. Cancer Res 2008;68(19):7905-14.

148. Shi Z, Peng X, Kim I, et al. Erlotinib (tarceva, OSI-774) antagonizes ATP-binding cassette subfamily B member 1 and ATP-binding cassette subfamily G member 2 mediated drug resistance. Cancer Res 2007;67(22):11012-20.
149. Nakamura Y, Oka M, Soda H, et al. Gefitinib ("iressa", ZD1839), an epidermal growth factor receptor tyrosine kinase inhibitor, reverses breast cancer resistance protein/BCRP-mediated drug resistance. Cancer Res 2005;65(4):1541-6.
150. Yanase K, Tsukahara S, Asada S, Ishikawa E, Imai Y, Sugimoto Y. Gefitinib reverses breast cancer resistance protein-mediated drug resistance. Mol Cancer Ther 2004;3(9):1119-25.
151. Ozvegy-Laczka C, Hegedus T, Varady G, et al. High-affinity interaction of tyrosine kinase inhibitors with the BCRP multidrug transporter. Mol Pharmacol 2004;65(6):1485-95.
152. Ozvegy-Laczka C, Varady G, Koblos G, et al. Function-dependent conformational changes of the BCRP multidrug transporter modify its interaction with a monoclonal antibody on the cell surface. J Biol Chem 2005;280(6):4219-27.
153. Houghton PJ, Germain GS, Harwood FC, et al. Imatinib mesylate is a potent inhibitor of the BCRP (BCRP) transporter and reverses resistance to topotecan and SN-38 in vitro. Cancer Res 2004;64(7):2333-7.
154. Marra M, Agostinelli E, Tempera G, Lombardi A, Meo G, Budillon A, Abbruzzese A, Giuberti G, Caraglia M. Anticancer drugs and hyperthermia enhance cytotoxicity induced by polyamine enzymatic oxidation products. Amino Acids. 2007 Aug;33(2):273-81.
155. Li H, Jin HE, Kim W, et al. Involvement of P-glycoprotein, multidrug resistance protein 2 and breast cancer resistance protein in the transport of belotecan and topotecan in caco-2 and MDCKII cells. Pharm Res 2008;25(11):2601-12.
156. Gottesman MM, Fojo T, Bates SE. Multidrug resistance in cancer: Role of ATP-dependent transporters. Nat Rev Cancer 2002;2(1):48-58.
157. Shi Z, Parmar S, Peng XX, et al. The epidermal growth factor tyrosine kinase inhibitor AG1478 and erlotinib reverse BCRP-mediated drug resistance. Oncol Rep 2009;21(2):483-9.
158. Rolff J, Dorn C, Merk J, Fichtner I. Response of Patient-Derived Non-Small Cell Lung Cancer Xenografts to Classical and Targeted Therapies Is Not Related to Multidrug Resistance Markers. J Oncol. 2009;2009:814140. Epub 2009 Jun 14.
159. Janneh O, Anwar T, Jungbauer C, Kopp S, Khoo SH, Back DJ, Chiba P. P-glycoprotein, multidrug resistance-associated proteins and human organic anion transporting polypeptide influence the intracellular accumulation of atazanavir. Antivir Ther. 2009;14(7):965-74.
160. Arunasree KM, Roy KR, Anilkumar K, Aparna A, Reddy GV, Reddanna P. Imatinib-resistant K562 cells are more sensitive to celecoxib, a selective COX-2 inhibitor: Role of COX-2 and MDR-1. Leuk Res 2008;32(6):855-64.
161. Chen Y, Agarwal S, Shaik NM, Chen C, Yang Z, Elmquist WF. P-glycoprotein and breast cancer resistance protein influence brain distribution of dasatinib. J Pharmacol Exp Ther. 2009 Sep;330(3):956-63.
162. Shukla S, Robey RW, Bates SE, Ambudkar SV. Sunitinib (Sutent, SU11248), a small-molecule receptor tyrosine kinase inhibitor, blocks function of the ATP-binding cassette (ABC) transporters P-glycoprotein (ABCB1) and ABCG2. Drug Metab Dispos. 2009 Feb;37(2):359-65.
163. Dai CL, Liang YJ, Wang YS, Tiwari AK, Yan YY, Wang F, Chen ZS, Tong XZ, Fu LW. Sensitization of ABCG2-overexpressing cells to conventional chemotherapeutic agent by sunitinib was associated with inhibiting the function of ABCG2. Cancer Lett. 2009 Jun 28;279(1):74-83.
    Abdul-Ghani R, Serra V, Gyorffy B, et al. The PI3K inhibitor LY294002 blocks drug export from resistant colon carcinoma cells overexpressing MRP1. Oncogene 2006;25(12):1743-52.

164. Garcia MG, Alaniz LD, Cordo Russo RI, Alvarez E, Hajos SE. PI3K/Akt inhibition modulates multidrug resistance and activates NF-kappaB in murine lymphoma cell lines. Leuk Res 2009;33(2):288-96.

165. Nakanishi T, Shiozawa K, Hassel BA, Ross DD. Complex interaction of BCRP/BCRP and imatinib in BCR-ABL-expressing cells: BCRP-mediated resistance to imatinib is attenuated by imatinib-induced reduction of BCRP expression. Blood 2006;108(2):678-84.

166. Yang JM, Vassil A, Hait WN. Involvement of phosphatidylinositol-3-kinase in membrane ruffling induced by P-glycoprotein substrates in multidrug-resistant carcinoma cells. Biochem Pharmacol. 2002 Mar 1;63(5):959-66.

167. Tazzari PL, Cappellini A, Ricci F, Evangelisti C, Papa V, Grafone T, Martinelli G, Conte R, Cocco L, McCubrey JA, Martelli AM. Multidrug resistance-associated protein 1 expression is under the control of the phosphoinositide 3 kinase/Akt signal transduction network in human acute myelogenous leukemia blasts. Leukemia. 2007 Mar;21(3):427-38. Epub 2007 Jan 11.

168. Takada T, Suzuki H, Gotoh Y, Sugiyama Y. Regulation of the cell surface expression of human BCRP/ABCG2 by the phosphorylation state of Akt in polarized cells. Drug Metab Dispos. 2005 Jul;33(7):905-9. Epub 2005 Apr 20.

169. Zhu H, Chen XP, Luo SF, Guan J, Zhang WG, Zhang BX, Mao CP. [The role of extracellular signal-regulated kinase/mitogen-activated protein kinase pathway in multidrug resistance of hepatocellular carcinoma] Zhonghua Wai Ke Za Zhi. 2007 Jul 1;45(13):917-20.

170. Meyer zu Schwabedissen HE, Grube M, Dreisbach A, Jedlitschky G, Meissner K, Linnemann K, Fusch C, Ritter CA, Völker U, Kroemer HK. Epidermal growth factor-mediated activation of the map kinase cascade results in altered expression and function of ABCG2 (BCRP). Drug Metab Dispos. 2006 Apr;34(4):524-33. Epub 2006 Jan 13.

171. Angelini A, Iezzi M, Di Febbo C, Di Ilio C, Cuccurullo F, Porreca E. Reversal of P-glycoprotein-mediated multidrug resistance in human sarcoma MES-SA/Dx-5 cells by nonsteroidal anti-inflammatory drugs. Oncol Rep 2008;20(4):731-5.

172. O'Connor R, Heenan M, Connolly L, Larkin A, Clynes M. Increased anti-tumour efficacy of doxorubicin when combined with sulindac in a xenograft model of an MRP-1-positive human lung cancer. Anticancer Res 2004;24(2A):457-64.

173. O'Connor R, O'Leary M, Ballot J, Collins CD, Kinsella P, Mager DE, Arnold RD, O'Driscoll L, Larkin A, Kennedy S, Fennelly D, Clynes M, Crown J. A phase I clinical and pharmacokinetic study of the multi-drug resistance protein-1 (MRP-1) inhibitor sulindac, in combination with epirubicin in patients with advanced cancer. Cancer Chemother Pharmacol. 2007 Jan;59(1):79-87. Epub 2006 Apr 27.

174. Kang HK, Lee E, Pyo H, Lim SJ. Cyclooxygenase-independent down-regulation of multidrug resistance-associated protein-1 expression by celecoxib in human lung cancer cells. Mol Cancer Ther 2005;4(9):1358-63.

175. Zatelli MC, Luchin A, Tagliati F, et al. Cyclooxygenase-2 inhibitors prevent the development of chemoresistance phenotype in a breast cancer cell line by inhibiting glycoprotein p-170 expression. Endocr Relat Cancer 2007;14(4):1029-38.

176. Nozaki Y, Kusuhara H, Kondo T, et al. Species difference in the inhibitory effect of nonsteroidal anti-inflammatory drugs on the uptake of methotrexate by human kidney slices. J Pharmacol Exp Ther 2007;322(3):1162-70.

177. Draper MP, Martell RL, Levy SB. Indomethacin-mediated reversal of multidrug resistance and drug efflux in human and murine cell lines overexpressing MRP, but not P-glycoprotein. Br J Cancer 1997;75(6):810-5.

178. Tsuruo T., and Tomida A., Multidrug resistance Anti-Cancer Drugs 1995, 6, pp. 213-218

179. Pick A., Müller H.,and Wiese M. Novel lead for potent inhibitors of breast cancer resistance protein (BCRP) Bioorg. & Med. Chem. Ltrs. Volume 20, Issue 1, 1 January 2010, Pages 180-183

180. Dalton WS, Crowley JJ, Salmon SS, Grogan TM, Laufman LR, Weiss GR, Bonnet JD. A phase III randomized study of oral verapamil as a chemosensitizer to reverse drug resistance in patients with refractory myeloma. A Southwest Oncology Group study. Cancer. 1995 Feb 1;75(3):815-20.

181. Loe D.W., Deeley R.G. and Cole S.P.C. Verapamil Stimulates Glutathione Transport by the 190-kDa Multidrug Resistance Protein 1 (MRP1). *JPET May 1, 2000 vol. 293 no. 2 530-538*

182. Yi Zhang[1], Anshul Gupta[1], Honggang Wang[1], Lin Zhou[1], R. Robert Vethanayagam[1], Jashvant D. Unadkat[1] and Qingcheng Mao1. BCRP Transports Dipyridamole and is Inhibited by Calcium Channel Blockers. Biomedical and Life Sciences, 2005, Oct 25., Vol 22, No.:12., pg.: 2023-2034.

183. Chaffman M, Brogden RN. Diltiazem: a review of its pharmacological properties and therapeutic efficacy. Drugs 1985; 29: 387–454.

184. Chen BA, Guo JJ, Cheng J. [Biomolecular mechanisms of cyclosporine A, tetrandrine and their combination on the reversion of multidrug resistance in human leukemia cell line] Zhongguo Zhong Xi Yi Jie He Za Zhi. 2008 Nov;28(11):1010-3. Chinese.

185. Qadir M, O'Loughlin KL, Fricke SM, Williamson NA, Greco WR, Minderman H, Baer MR. Cyclosporin A is a broad-spectrum multidrug resistance modulator. Clin Cancer Res. 2005 Mar 15;11(6):2320-6.

186. Arima H, Yunomae K, Hirayama F, Uekama K. Contribution of P-glycoprotein to the enhancing effects of dimethyl-beta-cyclodextrin on oral bioavailability of tacrolimus. J Pharmacol Exp Ther. 2001 May;297(2):547-55.

187. Gupta A, Dai Y, Vethanayagam RR, Hebert MF, Thummel KE, Unadkat JD, Ross DD, Mao Q. Cyclosporin A, tacrolimus and sirolimus are potent inhibitors of the human breast cancer resistance protein (ABCG2) and reverse resistance to mitoxantrone and topotecan. Cancer Chemother Pharmacol. 2006 Sep;58(3):374-83.

188. Schrickx JA, Fink-Gremmels J. Danofloxacin-mesylate is a substrate for ATP-dependent efflux transporters. Br J Pharmacol. 2007 Feb;150(4):463-9. Epub 2007 Jan

189. Brooks T., Minderman H., O'Loughlin K.L., Pera P., Ojima I., Baer M.R., and Bernacki1 R.J.Taxane-based reversal agents modulate drug resistance mediated by P-glycoprotein, multidrug resistance protein, and breast cancer resistance protein. (Mol Cancer Ther. 2003;2:1195–1205).

190. Menefee M. E., Fan C., Edgerly M., Draper D., Chen C., Robey R., Balis F., Figg W. D., Bates S. and Fojo A. T.. Tariquidar (XR9576) is a potent and effective P-glycoprotein (Pgp) inhibitor that can be administered safely with chemotherapy *J. of Clinical Oncol.*, 2005 Vol 23, No 16S

191. Ebert B, Seidel A, Lampen A. Phytochemicals induce breast cancer resistance protein in caco-2 cells and enhance the transport of benzo[a]pyrene-3-sulfate. Toxicol Sci 2007;96(2):227-36.

192. Evers R, Kool M, Smith AJ, van Deemter L, de Haas M, Borst P. Inhibitory effect of the reversal agents V-104, GF120918 and pluronic L61 on MDR1 P-gp-, MRP1- and MRP2-mediated transport. Br J Cancer 2000;83(3):366-74.

193. den Ouden D, van den Heuvel M, Schoester M, van Rens G, Sonneveld P. In vitro effect of GF120918, a novel reversal agent of multidrug resistance, on acute leukemia and multiple myeloma cells. Leukemia. 1996 Dec;10(12):1930-6.

194. Ramanathan RK, Trump DL, Eiseman JL, Belani CP, Agarwala SS, Zuhowski EG, Lan J, Potter DM, Ivy SP, Ramalingam S, Brufsky AM, Wong MK, Tutchko S, Egorin MJ. Phase I pharmacokinetic-pharmacodynamic study of 17-(allylamino)-17-demethoxygeldanamycin (17AAG, NSC 330507), a novel inhibitor of heat shock protein 90, in patients with refractory advanced cancers. Clin Cancer Res. 2005 May 1;11(9):3385-91.

195. Arora A, Seth K, Kalra N, Shukla Y. Modulation of P-glycoprotein-mediated multidrug resistance in K562 leukemic cells by indole-3-carbinol. Toxicol Appl Pharmacol 2005;202(3):237-43.

196. Schlessinger J. Common and distinct elements in cellular signaling via EGF and FGF receptors. Science 2004;306(5701):1506-7.
197. Dunne G., Characterisation and modulation of drug resistance in cancer cell lines. 2009. Thesis
198. Marchetti S, de Vries NA, Buckle T, et al. Effect of the ATP-binding cassette drug transporters ABCB1, BCRP, and ABCC2 on erlotinib hydrochloride (tarceva) disposition in in vitro and in vivo pharmacokinetic studies employing Bcrp1-/-/Mdr1a/1b-/- (triple-knockout) and wild-type mice. Mol Cancer Ther 2008;7(8):2280-7.
199. Nagashima S, Soda H, Oka M, et al. BCRP/BCRP levels account for the resistance to topoisomerase I inhibitors and reversal effects by gefitinib in non-small cell lung cancer. Cancer Chemother Pharmacol 2006;58(5):594-600.
200. Chang F, Steelman LS, Lee JT, et al. Signal transduction mediated by the Ras/Raf/MEK/ERK pathway from cytokine receptors to transcription factors: Potential targeting for therapeutic intervention. Leukemia 2003;17(7):1263-93.
201. Mantovani I, Cappellini A, Tazzari PL, Papa V, Cocco L, Martelli AM. Caspase-dependent cleavage of 170-kDa P-glycoprotein during apoptosis of human T-lymphoblastoid CEM cells. J Cell Physiol 2006;207(3):836-44.
202. Zuidervaart W, van Nieuwpoort F, Stark M, et al. Activation of the MAPK pathway is a common event in uveal melanomas although it rarely occurs through mutation of BRAF or RAS. Br J Cancer 2005;92(11):2032-8.
203. Basta D, Todt I, Eisenschenk A, Ernst A. Vestibular evoked myogenic potentials induced by intraoperative electrical stimulation of the human inferior vestibular nerve. Hear Res 2005;204(1-2):111-4.
204. Ji HB, Liao G, Faubion WA, et al. Cutting edge: The natural ligand for glucocorticoid-induced TNF receptor-related protein abrogates regulatory T cell suppression. J Immunol 2004;172(10):5823-7.
205. Sauvant C, Nowak M, Wirth C, et al. Acidosis induces multi-drug resistance in rat prostate cancer cells (AT1) in vitro and in vivo by increasing the activity of the p-glycoprotein via activation of p38. Int J Cancer 2008;123(11):2532-42.
206. Jue Wang, Hironao Ueno, Takashi Masuko and Yoshiyuki Hashimoto. Binding of Serum Albumin on Tumor Cells and Characterization of the Albumin Binding Protein. J. Biochem, 1994, Vol. 115, No. 5 898-903.
207. Tatebe S, Sinicrope FA, Kuo MT. Induction of multidrug resistance proteins MRP1 and MRP3 and gamma-glutamylcysteine synthetase gene expression by nonsteroidal anti-inflammatory drugs in human colon cancer cells. Biochem Biophys Res Commun 2002;290(5):1427-33.
208. Gedeon C, Behravan J, Koren G, Piquette-Miller M. Transport of glyburide by placental ABC transporters: Implications in fetal drug exposure. Placenta 2006;27(11-12):1096-102.
209. Kim SK, Lim SY, Wang KC, et al. Overexpression of cyclooxygenase-2 in childhood ependymomas: Role of COX-2 inhibitor in growth and multi-drug resistance in vitro. Oncol Rep 2004;12(2):403-9.
210. Zhang H, Burrows F. Targeting multiple signal transduction pathways through inhibition of Hsp90. J Mol Med 2004;82(8):488-99.
211. Maloney A, Workman P. HSP90 as a new therapeutic target for cancer therapy: The story unfolds. Expert Opin Biol Ther 2002;2(1):3-24.
212. Zhang H, Neely L, Lundgren K, Yang YC, Lough R, Timple N, Burrows F. BIIB021, a synthetic HSP90 inhibitor, has broad application against tumors with acquired multidrug resistance. Int J Cancer. 2009 Aug 12.
213. Ejendal KF, Hrycyna CA. Differential sensitivities of the human ATP-binding cassette transporters BCRP and P-glycoprotein to cyclosporin A. Mol Pharmacol 2005;67(3):902-11.
214. Yarden Y, Sliwkowski MX. Untangling the ErbB signalling network. Nat Rev Mol Cell Biol 2001;2(2):127-37.

215. Slamon DJ, Godolphin W, Jones LA, et al. Studies of the HER-2/neu proto-oncogene in human breast and ovarian cancer. Science 1989;244(4905):707-12.

216. Slamon DJ, Leyland-Jones B, Shak S, et al. Use of chemotherapy plus a monoclonal antibody against HER2 for metastatic breast cancer that overexpresses HER2. N Engl J Med 2001;344(11):783-92.

217. Marty M, Cognetti F, Maraninchi D, et al. Randomized phase II trial of the efficacy and safety of trastuzumab combined with docetaxel in patients with human epidermal growth factor receptor 2-positive metastatic breast cancer administered as first-line treatment: The M77001 study group. J Clin Oncol 2005;23(19):4265-74.

218. Piccart-Gebhart MJ, Procter M, Leyland-Jones B, Goldhirsch A, Untch M, Smith I, Gianni L, Baselga J, Bell R, Jackisch C, Cameron D, Dowsett M, Barrios CH, Steger G, Huang CS, Andersson M, Inbar M, Lichinitser M, Láng I, Nitz U, Iwata H, Thomssen C, Lohrisch C, Suter TM, Rüschoff J, Suto T, Greatorex V, Ward C, Straehle C, McFadden E, Dolci MS, Gelber RD; Herceptin Adjuvant (HERA) Trial Study Team. Trastuzumab after adjuvant chemotherapy in HER2-positive breast cancer. N Engl J Med. 2005 Oct 20;353(16):1659-72.

219. Murata H, Kawano S, Tsuji S, Tsuji M, Sawaoka H, Kimura Y, Shiozaki H, Hori M. Cyclooxygenase-2 overexpression enhances lymphatic invasion and metastasis in human gastric carcinoma. Am J Gastroenterol. 1999 Feb;94(2):451-5.

220. http://www.medscape.com/viewarticle/495752_6

221. Lee SH, Soyoola E, Chanmugam P, Hart S, Sun W, Zhong H, Liou S, Simmons D, Hwang D. Selective expression of mitogen-inducible cyclooxygenase in macrophages stimulated with lipopolysaccharide. J Biol Chem. 1992 Dec 25;267(36):25934-8.

222. Asano TK, McLeod RS. Non steroidal anti-inflammatory drugs (NSAID) and Aspirin for preventing colorectal adenomas and carcinomas. Cochrane Database Syst Rev. 2004;(2):CD004079. Review.

223. Fitzpatrick FA. Inflammation, carcinogenesis and cancer. Int Immunopharmacol. 2001 Sep;1(9-10):1651-67. Review.

224. Patrono C, Patrignani P, García Rodríguez LA. Cyclooxygenase-selective inhibition of prostanoid formation: transducing biochemical selectivity into clinical read-outs. Clin Invest. 2001 Jul;108(1):7-13. Review.

225. Boehncke S, Boehncke WH. Tolerance to coxibs in patients with intolerance to non-steroidal anti-inflammatory drugs (NSAIDs). Dtsch Med Wochenschr. 2005 Oct 7;130(40):2249-52. German.

226. Davis KA, Fabian TC, Croce MA, Proctor KG. Prostanoids: early mediators in the secondary injury that develops after unilateral pulmonary contusion. J Trauma. 1999 May;46(5):824-31;

227. Morris AJ, MacKenzie JF. Small-bowel enteroscopy and NSAID ulceration. Lancet. 1991 Jun 22;337(8756):1550.

228. Chan AL. Celecoxib-induced deep-vein thrombosis. Ann Pharmacother. 2005 Jun;39(6):1138.

229. Vane JR. The Croonian Lecture, 1993. The endothelium: maestro of the blood circulation. Philos Trans R Soc Lond B Biol Sci. 1994 Jan 29;343(1304):225-46. Review.

230. Graham DJ, Campen D, Hui R, Spence M, Cheetham C, Levy G, Shoor S, Ray WA. Risk of acute myocardial infarction and sudden cardiac death in patients treated with cyclo-oxygenase 2 selective and non-selective non-steroidal anti-inflammatory drugs: nested case-control study. Lancet. 2005 Feb 5-11;365(9458):475-81.

231. Tegeder I, Geisslinger G. Cardiovascular risk with cyclooxygenase inhibitors: general problem with substance specific differences? Naunyn Schmiedebergs Arch Pharmacol. 2006 Apr;373(1):1-17. Review.

232. Okie S. What ails the FDA? N Engl J Med. 2005 Mar 17;352(11):1063-6.

233. Yoshimatsu K, Altorki NK, Golijanin D, Zhang F, Jakobsson PJ, Dannenberg AJ, Subbaramaiah K. Inducible prostaglandin E synthase is overexpressed in non-small cell lung cancer. Clin Cancer Res. 2001 Sep;7(9):2669-74.

234. Milne SA, Jabbour HN. Prostaglandin (PG) F(2alpha) receptor expression and signaling in human endometrium: role of PGF(2alpha) in epithelial cell proliferation. J Clin Endocrinol Metab. 2003 Apr;88(4):1825-32.

235. van Rees BP, Sivula A, Thorén S, Yokozaki H, Jakobsson PJ, Offerhaus GJ, Ristimäki A. Expression of microsomal prostaglandin E synthase-1 in intestinal type gastric adenocarcinoma and in gastric cancer cell lines. Int J Cancer. 2003 Nov 20;107(4):551-6.

236. Yoshimatsu K, Golijanin D, Paty PB, Soslow RA, Jakobsson PJ, DeLellis RA, Subbaramaiah K, Dannenberg AJ. Inducible microsomal prostaglandin E synthase is overexpressed in colorectal adenomas and cancer. Clin Cancer Res. 2001 Dec;7(12):3971-6.

237. Golijanin D, Tan JY, Kazior A, Cohen EG, Russo P, Dalbagni G, Auborn KJ, Subbaramaiah K, Dannenberg AJ. Cyclooxygenase-2 and microsomal prostaglandin E synthase-1 are overexpressed in squamous cell carcinoma of the penis. Clin Cancer Res. 2004 Feb 1;10(3):1024-31.

238. Cohen EG, Almahmeed T, Du B, Golijanin D, Boyle JO, Soslow RA, Subbaramaiah K, Dannenberg AJ. Microsomal prostaglandin E synthase-1 is overexpressed in head and neck squamous cell carcinoma. Clin Cancer Res. 2003 Aug 15;9(9):3425-30.

239. Amano H, Hayashi I, Endo H, Kitasato H, Yamashina S, Maruyama T, Kobayashi M, Satoh K, Narita M, Sugimoto Y, Murata T, Yoshimura H, Narumiya S, Majima M. Host prostaglandin E(2)-EP3 signaling regulates tumor-associated angiogenesis and tumor growth. J Exp Med. 2003 Jan 20;197(2):221-32.

240. Mutoh M, Watanabe K, Kitamura T, Shoji Y, Takahashi M, Kawamori T, Tani K, Kobayashi M, Maruyama T, Kobayashi K, Ohuchida S, Sugimoto Y, Narumiya S, Sugimura T, Wakabayashi K. Involvement of prostaglandin E receptor subtype EP(4) in colon carcinogenesis. Cancer Res. 2002 Jan 1;62(1):28-32.

241. Tsujii M, Kawano S, DuBois RN. Cyclooxygenase-2 expression in human colon cancer cells increases metastatic potential. Proc Natl Acad Sci U S A. 1997 Apr 1;94(7):3336-40.

242. Subbaramaiah K, Dannenberg AJ. Cyclooxygenase 2: a molecular target for cancer prevention and treatment. Trends Pharmacol Sci. 2003 Feb;24(2):96-102. Review.

243. Kanai N, Lu R, Satriano JA, Bao Y, Wolkoff AW, Schuster VL. Identification and characterization of a prostaglandin transporter. Science. 1995 May 12;268(5212):866-9.

244. Nishigaki N, Negishi M, Ichikawa A. Two Gs-coupled prostaglandin E receptor subtypes, EP2 and EP4, differ in desensitization and sensitivity to the metabolic inactivation of the agonist. Mol Pharmacol. 1996 Oct;50(4):1031-7.

245. Pai R, Soreghan B, Szabo IL, Pavelka M, Baatar D, Tarnawski AS. Prostaglandin E2 transactivates EGF receptor: a novel mechanism for promoting colon cancer growth and gastrointestinal hypertrophy. Nat Med. 2002 Mar;8(3):289-93.

246. Holla VR, Mann JR, Shi Q, DuBois RN. Prostaglandin E2 regulates the nuclear receptor NR4A2 in colorectal cancer. J Biol Chem. 2006 Feb 3;281(5):2676-82.

247. Shimada T, Kojima K, Yoshiura K, Hiraishi H, Terano A. Characteristics of the peroxisome proliferator activated receptor gamma (PPARgamma) ligand induced apoptosis in colon cancer cells. Gut. 2002 May;50(5):658-64.

248. Kurumbail RG, Stevens AM, Gierse JK, McDonald JJ, Stegeman RA, Pak JY, Gildehaus D, Miyashiro JM, Penning TD, Seibert K, Isakson PC, Stallings WC. Structural basis for selective inhibition of cyclooxygenase-2 by anti-inflammatory agents. Nature. 1996 Dec 19-26;384(6610):644-8.

249. Luong C, Miller A, Barnett J, Chow J, Ramesha C, Browner MF. Flexibility of the NSAID binding site in the structure of human cyclooxygenase-2. Nat Struct Biol. 1996 Nov;3(11):927-33.

250. Silverstein FE, Faich G, Goldstein JL, Simon LS, Pincus T, Whelton A, Makuch R, Eisen G, Agrawal NM, Stenson WF, Burr AM, Zhao WW, Kent JD, Lefkowith JB, Verburg KM, Geis GS. Gastrointestinal toxicity with celecoxib vs nonsteroidal anti-inflammatory drugs for osteoarthritis and rheumatoid arthritis: the CLASS study: A

randomized controlled trial. Celecoxib Long-term Arthritis Safety Study. JAMA. 2000 Sep 13;284(10):1247-55.

251. Cervello M, Montalto G. Cyclooxygenases in hepatocellular carcinoma. World J Gastroenterol. 2006 Aug 28;12(32):5113-21. Review.

252. Otto JC, DeWitt DL, Smith WL. N-glycosylation of prostaglandin endoperoxide synthases-1 and -2 and their orientations in the endoplasmic reticulum. J Biol Chem. 1993 Aug 25;268(24):18234-42.

253. Yokoyama C., Takai T., Tanabe T. Primary structure of sheep prostaglandin endoperoxide synthase deduced from cDNA sequence. FEBS lett. 1988 Apr 25;231 (2) 347-51.

254. Funk CD, Funk LB, Kennedy ME, Pong AS, Fitzgerald GA. Human platelet/erythroleukemia cell prostaglandin G/H synthase: cDNA cloning, expression, and gene chromosomal assignment. FASEB J. 1991 Jun;5(9):2304-12.

255. Kraemer SA, Meade EA, DeWitt DL. Prostaglandin endoperoxide synthase gene structure: identification of the transcriptional start site and 5'-flanking regulatory sequences. Arch Biochem Biophys. 1992 Mar;293(2):391-400.

256. Jones DA, Carlton DP, McIntyre TM, Zimmerman GA, Prescott SM. Molecular cloning of human prostaglandin endoperoxide synthase type II and demonstration of expression in response to cytokines. J Biol Chem. 1993 Apr 25;268(12):9049-54.

257. Tay A, Squire JA, Goldberg H, Skorecki K. Assignment of the human prostaglandin-endoperoxide synthase 2 (PTGS2) gene to 1q25 by fluorescence in situ hybridization. Genomics. 1994 Oct;23(3):718-9.

258. Hempel SL, Monick MM, Hunninghake GW. Lipopolysaccharide induces prostaglandin H synthase-2 protein and mRNA in human alveolar macrophages and blood monocytes. J Clin Invest. 1994 Jan;93(1):391-6.

259. Laporte JD, Moore PE, Lahiri T, Schwartzman IN, Panettieri RA Jr, Shore SA. p38 MAP kinase regulates IL-1 beta responses in cultured airway smooth muscle cells. Am J Physiol Lung Cell Mol Physiol. 2000 Nov;279(5):L932-41

260. Chen CC, Sun YT, Chen JJ, Chang YJ. Tumor necrosis factor-alpha-induced cyclooxygenase-2 expression via sequential activation of ceramide-dependent mitogen-activated protein kinases, and IkappaB kinase 1/2 in human alveolar epithelial cells. Mol Pharmacol. 2001 Mar;59(3):493-500.

261. Chandrasekharan NV, Dai H, Roos KL, Evanson NK, Tomsik J, Elton TS, Simmons DL. COX-3, a cyclooxygenase-1 variant inhibited by acetaminophen and other analgesic/antipyretic drugs: cloning, structure, and expression. Proc Natl Acad Sci U S A. 2002 Oct 15;99(21):13926-31. Epub 2002 Sep

262. Qin N, Zhang SP, Reitz TL, Mei JM, Flores CM. Cloning, expression, and functional characterization of human cyclooxygenase-1 splicing variants: evidence for intron 1 retention. J Pharmacol Exp Ther. 2005 Dec;315(3):1298-305.

263. Hwang D, Scollard D, Byrne J, Levine E. Expression of cyclooxygenase-1 and cyclooxygenase-2 in human breast cancer. J Natl Cancer Inst. 1998 Mar 18;90(6):455-60.

264. Kirschenbaum A, Klausner AP, Lee R, Unger P, Yao S, Liu XH, Levine AC. Expression of cyclooxygenase-1 and cyclooxygenase-2 in the human prostate. Urology. 2000 Oct 1;56(4):671-6.

265. Sales KJ, Katz AA, Millar RP, Jabbour HN. Seminal plasma activates cyclooxygenase-2 and prostaglandin E2 receptor expression and signalling in cervical adenocarcinoma cells. Mol Hum Reprod. 2002 Dec;8(12):1065-70.

266. Tiano HF, Loftin CD, Akunda J, Lee CA, Spalding J, Sessoms A, Dunson DB, Rogan EG, Morham SG, Smart RC, Langenbach R. Deficiency of either cyclooxygenase (COX)-1 or COX-2 alters epidermal differentiation and reduces mouse skin tumorigenesis. Cancer Res. 2002 Jun 15;62(12):3395-401.

267. Daikoku T, Wang D, Tranguch S, Morrow JD, Orsulic S, DuBois RN, Dey SK. Cyclooxygenase-1 is a potential target for prevention and treatment of ovarian epithelial cancer. Cancer Res. 2005 May 1;65(9):3735-44.

268. Kino Y, Kojima F, Kiguchi K, Igarashi R, Ishizuka B, Kawai S. Prostaglandin E2 production in ovarian cancer cell lines is regulated by cyclooxygenase-1, not cyclooxygenase-2. Prostaglandins Leukot Essent Fatty Acids. 2005 Aug;73(2):103-11.

269. Chulada PC, Thompson MB, Mahler JF, Doyle CM, Gaul BW, Lee C, Tiano HF, Morham SG, Smithies O, Langenbach R. Genetic disruption of Ptgs-1, as well as Ptgs-2, reduces intestinal tumorigenesis in Min mice. Cancer Res. 2000 Sep 1;60(17):4705-8.

270. Takeda H, Sonoshita M, Oshima H, Sugihara K, Chulada PC, Langenbach R, Oshima M, Taketo MM. Cooperation of cyclooxygenase 1 and cyclooxygenase 2 in intestinal polyposis. Cancer Res. 2003 Aug 15;63(16):4872-7.

271. Lampiasi N, Foderà D, D'Alessandro N, Cusimano A, Azzolina A, Tripodo C, Florena AM, Minervini MI, Notarbartolo M, Montalto G, Cervello M. The selective cyclooxygenase-1 inhibitor SC-560 suppresses cell proliferation and induces apoptosis in human hepatocellular carcinoma cells. Int J Mol Med. 2006 Feb;17(2):245-52.

272. Huber LC, Künzler P, Boyce SH, Michel BA, Gay RE, Ink BS, Gay S. Effects of a novel tyrosine kinase inhibitor in rheumatoid arthritis synovial fibroblasts. Ann Rheum Dis. 2008 Mar;67(3):389-94. Epub 2007 Jul 27.

273. Eberhart CE, Coffey RJ, Radhika A, Giardiello FM, Ferrenbach S, DuBois RN. Up-regulation of cyclooxygenase 2 gene expression in human colorectal adenomas and adenocarcinomas. Gastroenterology. 1994 Oct;107(4):1183-8.

274. Ristimäki A, Honkanen N, Jänkälä H, Sipponen P, Härkönen M. Expression of cyclooxygenase-2 in human gastric carcinoma. Cancer Res. 1997 Apr 1;57(7):1276-80.

275. Wolff H, Saukkonen K, Anttila S, Karjalainen A, Vainio H, Ristimäki A. Expression of cyclooxygenase-2 in human lung carcinoma. Cancer Res. 1998 Nov 15;58(22):4997-5001.

276. Steffensen KD, Waldstrøm M, Jeppesen U, Jakobsen E, Brandslund I, Jakobsen A. The prognostic importance of cyclooxygenase 2 and HER2 expression in epithelial ovarian cancer. Int J Gynecol Cancer. 2007 Jul-Aug;17(4):798-807.

277. Denkert C, Köbel M, Pest S, Koch I, Berger S, Schwabe M, Siegert A, Reles A, Klosterhalfen B, Hauptmann S. Expression of cyclooxygenase 2 is an independent prognostic factor in human ovarian carcinoma. Am J Pathol. 2002 Mar;160(3):893-903.

278. Denkert C, Köbel M, Berger S, Siegert A, Leclere A, Trefzer U, Hauptmann S. Expression of cyclooxygenase 2 in human malignant melanoma. Cancer Res. 2001 Jan 1;61(1):303-8.

279. Cao Y, Prescott SM. Many actions of cyclooxygenase-2 in cellular dynamics and in cancer. J Cell Physiol. 2002 Mar;190(3):279-86. Review.

280. Prescott SM. Is cyclooxygenase-2 the alpha and the omega in cancer? J Clin Invest. 2000 Jun;105(11):1511-3.

281. Buchanan FG, Wang D, Bargiacchi F, DuBois RN. Prostaglandin E2 regulates cell migration via the intracellular activation of the epidermal growth factor receptor. J Biol Chem. 2003 Sep 12;278(37):35451-7. Epub 2003 Jun 24.

282. Shaik MS, Chatterjee A, Jackson T, Singh M. Enhancement of antitumor activity of docetaxel by celecoxib in lung tumors. Int J Cancer. 2006 Jan 15;118(2):396-404.

283. Stolina M, Sharma S, Lin Y, Dohadwala M, Gardner B, Luo J, Zhu L, Kronenberg M, Miller PW, Portanova J, Lee JC, Dubinett SM. Specific inhibition of cyclooxygenase 2 restores antitumor reactivity by altering the balance of IL-10 and IL-12 synthesis. J Immunol. 2000 Jan 1;164(1):361-70.

284. Hull MA, Ko SC, Hawcroft G. Prostaglandin EP receptors: targets for treatment and prevention of colorectal cancer? Mol Cancer Ther. 2004 Aug;3(8):1031-9. Review.

285. Rigas B, Goldman IS, Levine L. Altered eicosanoid levels in human colon cancer. J Lab Clin Med. 1993 Nov;122(5):518-23.

286. Sheehan KM, Sheahan K, O'Donoghue DP, MacSweeney F, Conroy RM, Fitzgerald DJ, Murray FE. The relationship between cyclooxygenase-2 expression and colorectal cancer. JAMA. 1999 Oct 6;282(13):1254-7.

287. Ferrandina G, Lauriola L, Zannoni GF, Fagotti A, Fanfani F, Legge F, Maggiano N, Gessi M, Mancuso S, Ranelletti FO, Scambia G. Increased cyclooxygenase-2 (COX-2)

expression is associated with chemotherapy resistance and outcome in ovarian cancer patients. Ann Oncol. 2002 Aug;13(8):1205-11.

288. Ristimäki A, Sivula A, Lundin J, Lundin M, Salminen T, Haglund C, Joensuu H, Isola J. Prognostic significance of elevated cyclooxygenase-2 expression in breast cancer. Cancer Res. 2002 Feb 1;62(3):632-5.

289. Denkert C, Winzer KJ, Müller BM, Weichert W, Pest S, Köbel M, Kristiansen G, Reles A, Siegert A, Guski H, Hauptmann S. Elevated expression of cyclooxygenase-2 is a negative prognostic factor for disease free survival and overall survival in patients with breast carcinoma. Cancer. 2003 Jun 15;97(12):2978-87.

290. Koga H, Sakisaka S, Ohishi M, Kawaguchi T, Taniguchi E, Sasatomi K, Harada M, Kusaba T, Tanaka M, Kimura R, Nakashima Y, Nakashima O, Kojiro M, Kurohiji T, Sata M. Expression of cyclooxygenase-2 in human hepatocellular carcinoma: relevance to tumor dedifferentiation. Hepatology. 1999 Mar;29(3):688-96.

291. Friedenberg WR., Rue M., Blood EA., Dalton WS., Shustik C., Larson RA., Sonneveld P., Greipp PR. Phase III study of PSC-833 (valspodar) in combination with vincristine, doxorubicin, and dexamethasone (valspodar/VAD) versus VAD alone in patients with recurring or refractory multiple myeloma (E1A95), a trial of the Eastern Cooperative Oncology Group. Cancer. 2006. Feb 15, 106(4), 830-8.

292. Schmedtje JF Jr, Ji YS, Liu WL, DuBois RN, Runge MS. Hypoxia induces cyclooxygenase-2 via the NF-kappaB p65 transcription factor in human vascular endothelial cells. J Biol Chem. 1997 Jan 3;272(1):601-8.

293. Kaidi A, Qualtrough D, Williams AC, Paraskeva C. Direct transcriptional up-regulation of cyclooxygenase-2 by hypoxia-inducible factor (HIF)-1 promotes colorectal tumor cell survival and enhances HIF-1 transcriptional activity during hypoxia. Cancer Res. 2006 Jul 1;66(13):6683-91.

294. Gupta RA, Tan J, Krause WF, Geraci MW, Willson TM, Dey SK, DuBois RN. Prostacyclin-mediated activation of peroxisome proliferator-activated receptor delta in colorectal cancer. Proc Natl Acad Sci U S A. 2000 Nov 21;97(24):13275-80.

295. Howe LR, Crawford HC, Subbaramaiah K, Hassell JA, Dannenberg AJ, Brown AM. PEA3 is up-regulated in response to Wnt1 and activates the expression of cyclooxygenase-2. J Biol Chem. 2001 Jun 8;276(23):20108-15. Epub 2001 Mar 26.

296. Singh B, Lucci A. Role of cyclooxygenase-2 in breast cancer. J Surg Res. 2002 Nov;108(1):173-9.

297. Cheng AS, Chan HL, Leung WK, To KF, Go MY, Chan JY, Liew CT, Sung JJ. Expression of HBx and COX-2 in chronic hepatitis B, cirrhosis and hepatocellular carcinoma: implication of HBx in upregulation of COX-2. Mod Pathol. 2004 Oct;17(10):1169-79.

298. Leung WK, Wu KC, Wong CY, Cheng AS, Ching AK, Chan AW, Chong WW, Go MY, Yu J, To KF, Wang X, Chui YL, Fan DM, Sung JJ. Transgenic cyclooxygenase-2 expression and high salt enhanced susceptibility to chemical-induced gastric cancer development in mice. Carcinogenesis. 2008 Aug;29(8):1648-54.

299. Peng H, Chen P, Cai Y, Chen Y, Wu QH, Li Y, Zhou R, Fang X. Endothelin-1 increases expression of cyclooxygenase-2 and production of interlukin-8 in hunan pulmonary epithelial cells. Peptides. 2008 Mar;29(3):419-24.

300. Onoe Y, Miyaura C, Kaminakayashiki T, Nagai Y, Noguchi K, Chen QR, Seo H, Ohta H, Nozawa S, Kudo I, Suda T. IL-13 and IL-4 inhibit bone resorption by suppressing cyclooxygenase-2-dependent prostaglandin synthesis in osteoblasts. J Immunol. 1996 Jan 15;156(2):758-64.

301. Niiro H, Otsuka T, Izuhara K, Yamaoka K, Ohshima K, Tanabe T, Hara S, Nemoto Y, Tanaka Y, Nakashima H, Niho Y. Regulation by interleukin-10 and interleukin-4 of cyclooxygenase-2 expression in human neutrophils. Blood. 1997 Mar 1;89(5):1621-8.

302. **A.** Cok SJ, Acton SJ, Sexton AE, Morrison AR. Identification of RNA-binding proteins in RAW 264.7 cells that recognize a lipopolysaccharide-responsive element in the 3-untranslated region of the murine cyclooxygenase-2 mRNA. J Biol Chem. 2004 Feb 27;279(9):8196-205. Epub 2003 Dec 8.

B. Sengupta S, Jang BC, Wu MT, Paik JH, Furneaux H, Hla T. The RNA-binding protein HuR regulates the expression of cyclooxygenase-2. J Biol Chem. 2003 Jul 4;278(27):25227-33.

303. Chapple KS, Scott N, Guillou PJ, Coletta PL, Hull MA. Interstitial cell cyclooxygenase-2 expression is associated with increased angiogenesis in human sporadic colorectal adenomas. J Pathol. 2002 Dec;198(4):435-41.

304. Davies G, Salter J, Hills M, Martin LA, Sacks N, Dowsett M. Correlation between cyclooxygenase-2 expression and angiogenesis in human breast cancer. Clin Cancer Res. 2003 Jul;9(7):2651-6.

305. Kim MH, Seo SS, Song YS, Kang DH, Park IA, Kang SB, Lee HP. Expression of cyclooxygenase-1 and -2 associated with expression of VEGF in primary cervical cancer and at metastatic lymph nodes. Gynecol Oncol. 2003 Jul;90(1):83-90.

306. Chu J, Lloyd FL, Trifan OC, Knapp B, Rizzo MT. Potential involvement of the cyclooxygenase-2 pathway in the regulation of tumor-associated angiogenesis and growth in pancreatic cancer. Mol Cancer Ther. 2003 Jan;2(1):1-7.

307. Nagatsuka I, Yamada N, Shimizu S, Ohira M, Nishino H, Seki S, Hirakawa K. Inhibitory effect of a selective cyclooxygenase-2 inhibitor on liver metastasis of colon cancer. Int J Cancer. 2002 Aug 10;100(5):515-9.

308. Sheng H, Shao J, Hooton EB, Tsujii M, DuBois RN, Beauchamp RD. Cyclooxygenase-2 induction and transforming growth factor beta growth inhibition in rat intestinal epithelial cells. Cell Growth Differ. 1997 Apr;8(4):463-70.

309. Tomozawa S, Nagawa H, Tsuno N, Hatano K, Osada T, Kitayama J, Sunami E, Nita ME, Ishihara S, Yano H, Tsuruo T, Shibata Y, Muto T. Inhibition of haematogenous metastasis of colon cancer in mice by a selective COX-2 inhibitor, JTE-522. Br J Cancer. 1999 Dec;81(8):1274-9.

310. Kim HJ, Wu HG, Park IA, Ha SW. High cyclooxygenase-2 expression is related with distant metastasis in cervical cancer treated with radiotherapy. Int J Radiat Oncol Biol Phys. 2003 Jan 1;55(1):16-20.

311. Cervello M, Foderàa D, Florena AM, Soresi M, Tripodo C, D'Alessandro N, Montalto G. Correlation between expression of cyclooxygenase-2 and the presence of inflammatory cells in human primary hepatocellular carcinoma: possible role in tumor promotion and angiogenesis. World J Gastroenterol. 2005 Aug 14;11(30):4638-43.

312. Rahman MA, Dhar DK, Yamaguchi E, Maruyama S, Sato T, Hayashi H, Ono T, Yamanoi A, Kohno H, Nagasue N. Coexpression of inducible nitric oxide synthase and COX-2 in hepatocellular carcinoma and surrounding liver: possible involvement of COX-2 in the angiogenesis of hepatitis C virus-positive cases. Clin Cancer Res. 2001 May;7(5):1325-32.

313. Gallo O, Franchi A, Magnelli L, Sardi I, Vannacci A, Boddi V, Chiarugi V, Masini E. Cyclooxygenase-2 pathway correlates with VEGF expression in head and neck cancer. Implications for tumor angiogenesis and metastasis. Neoplasia. 2001 Jan-Feb;3(1):53-61.

314. Dai Y, Zhang X, Peng Y, Wang Z. The expression of cyclooxygenase-2, VEGF and PGs in CIN and cervical carcinoma. Gynecol Oncol. 2005 Apr;97(1):96-103.

315. Timoshenko AV, Rastogi S, Lala PK. Migration-promoting role of VEGF-C and VEGF-C binding receptors in human breast cancer cells. Br J Cancer. 2007 Oct 22;97(8):1090-8.

316. Masferrer JL, Leahy KM, Koki AT, Zweifel BS, Settle SL, Woerner BM, Edwards DA, Flickinger AG, Moore RJ, Seibert K. Antiangiogenic and antitumor activities of cyclooxygenase-2 inhibitors. Cancer Res. 2000 Mar 1;60(5):1306-11.

317. Mooteri S, Rubin D, Leurgans S, Jakate S, Drab E, Saclarides T. Tumor angiogenesis in primary and metastatic colorectal cancers. Dis Colon Rectum. 1996 Oct;39(10):1073-80.

318. Sawaoka H, Tsuji S, Tsujii M, Gunawan ES, Sasaki Y, Kawano S, Hori M. Cyclooxygenase inhibitors suppress angiogenesis and reduce tumor growth in vivo. Lab Invest. 1999 Dec;79(12):1469-77.

319. Leahy KM, Ornberg RL, Wang Y, Zweifel BS, Koki AT, Masferrer JL. Cyclooxygenase-2 inhibition by celecoxib reduces proliferation and induces apoptosis in angiogenic endothelial cells in vivo. Cancer Res. 2002 Feb 1;62(3):625-31.

320. Fujita T, Matsui M, Takaku K, Uetake H, Ichikawa W, Taketo MM, Sugihara K. Size- and invasion-dependent increase in cyclooxygenase 2 levels in human colorectal carcinomas. Cancer Res. 1998 Nov 1;58(21):4823-6.

321. Chen WS, Wei SJ, Liu JM, Hsiao M, Kou-Lin J, Yang WK. Tumor invasiveness and liver metastasis of colon cancer cells correlated with cyclooxygenase-2 (COX-2) expression and inhibited by a COX-2-selective inhibitor, etodolac. Int J Cancer. 2001 Mar 15;91(6):894-9.

322. Sheng H, Shao J, Morrow JD, Beauchamp RD, DuBois RN. Modulation of apoptosis and Bcl-2 expression by prostaglandin E2 in human colon cancer cells. Cancer Res. 1998 Jan 15;58(2):362-6.

323. Dohadwala M, Batra RK, Luo J, Lin Y, Krysan K, Pold M, Sharma S, Dubinett SM. Autocrine/paracrine prostaglandin E2 production by non-small cell lung cancer cells regulates matrix metalloproteinase-2 and CD44 in cyclooxygenase-2-dependent invasion. J Biol Chem. 2002 Dec 27;277(52):50828-33. Epub 2002 Oct 21.

324. Buchanan FG, Holla V, Katkuri S, Matta P, DuBois RN. Targeting cyclooxygenase-2 and the epidermal growth factor receptor for the prevention and treatment of intestinal cancer. Cancer Res. 2007 Oct 1;67(19):9380-8.

325. Yang SF, Hsieh YS, Lue KH, Chu SC, Chang IC, Lu KH. Effects of nonsteroidal anti-inflammatory drugs on the expression of urokinase plasminogen activator and inhibitor and gelatinases in the early osteoarthritic knee of humans. Clin Biochem. 2008 Jan;41(1-2):109-16. Epub 2007 Oct 26.

326. Patel VA, Dunn MJ, Sorokin A. Regulation of MDR-1 (P-glycoprotein) by cyclooxygenase-2. J Biol Chem 2002;277(41):38915-20.

327. Sorokin A. Cyclooxygenase-2: potential role in regulation of drug efflux and multidrug resistance phenotype. Curr Pharm Des. 2004;10(6):647-57. Review.

328. Ratnasinghe D, Daschner PJ, Anver MR, Kasprzak BH, Taylor PR, Yeh GC, Tangrea JA. Cyclooxygenase-2, P-glycoprotein-170 and drug resistance; is chemoprevention against multidrug resistance possible? Anticancer Res. 2001 May-Jun;21(3C):2141-7.

329. Surowiak P, Materna V, Matkowski R, Szczuraszek K, Kornafel J, Wojnar A, Pudelko M, Dietel M, Denkert C, Zabel M, Lage H. Relationship between the expression of cyclooxygenase 2 and MDR1/P-glycoprotein in invasive breast cancers and their prognostic significance. Breast Cancer Res. 2005;7(5):R862-70. Epub 2005 Aug 25.

330. Puhlmann U, Ziemann C, Ruedell G, Vorwerk H, Schaefer D, Langebrake C, Schuermann P, Creutzig U, Reinhardt D. Impact of the cyclooxygenase system on doxorubicin-induced functional multidrug resistance 1 overexpression and doxorubicin sensitivity in acute myeloid leukemic HL-60 cells. J Pharmacol Exp Ther. 2005 Jan;312(1):346-54. Epub 2004 Oct 22.

331. Awara WM, El-Sisi AE, El-Sayad ME, Goda AE. The potential role of cyclooxygenase-2 inhibitors in the treatment of experimentally-induced mammary tumour: Does celecoxib enhance the anti-tumour activity of doxorubicin? Pharmacological Research, 2004;50(5):487-98.

332. Hashitani S, Urade M, Nishimura N, Maeda T, Takaoka K, Noguchi K, Sakurai K. Apoptosis induction and enhancement of cytotoxicity of anticancer drugs by celecoxib, a selective cyclooxygenase-2 inhibitor, in human head and neck carcinoma cell lines. Int J Oncol. 2003 Sep;23(3):665-72.

333. van Wijngaarden J, van Beek E, van Rossum G, van der Bent C, Hoekman K, van der Pluijm G, van der Pol MA, Broxterman HJ, van Hinsbergh VW, Löwik CW. Celecoxib enhances doxorubicin-induced cytotoxicity in MDA-MB231 cells by NF-kappaB-mediated increase of intracellular doxorubicin accumulation. Eur J Cancer. 2007 Jan;43(2):433-42. Epub 2006 Nov 9.

334. Müller N, Riedel M, Scheppach C, Brandstätter B, Sokullu S, Krampe K, Ulmschneider M, Engel RR, Möller HJ, Schwarz MJ. Beneficial antipsychotic effects of celecoxib

add-on therapy compared to risperidone alone in schizophrenia. Am J Psychiatry. 2002 Jun;159(6):1029-34.

335. Subbaramaiah K, Hart JC, Norton L, Dannenberg AJ. Microtubule-interfering agents stimulate the transcription of cyclooxygenase-2. Evidence for involvement of ERK1/2 AND p38 mitogen-activated protein kinase pathways. J Biol Chem. 2000 May 19;275(20):14838-45.

336. Takaoka K, Kishimoto H, Segawa E, Otsu N, Zushi Y, Hashitani S, Noguchi K, Urade M. In vitro susceptibility to anticancer agents of the human KB carcinoma cell line transfected with COX-2 cDNA. Oncol Rep. 2008 Sep;20(3):645-9.

337. Duffy CP, Elliott CJ, O'Connor RA, Heenan MM, Coyle S, Cleary IM, Kavanagh K, Verhaegen S, O'Loughlin CM, NicAmhlaoibh R, Clynes M. Enhancement of chemotherapeutic drug toxicity to human tumour cells in vitro by a subset of non-steroidal anti-inflammatory drugs (NSAIDs). Eur J Cancer. 1998 Jul;34(8):1250-9.

338. Gore E. Celecoxib and radiation therapy in non-small-cell lung cancer. Oncology (Williston Park). 2004 Dec;18(14 Suppl 14):10-4. Review.

339. Wall R, McMahon G, Crown J, Clynes M, O'Connor R. Rapid and sensitive liquid chromatography-tandem mass spectrometry for the quantitation of epirubicin and identification of metabolites in biological samples. Talanta. 2007 Apr 15;72(1):145-54. Epub 2006 Nov 20.

340. Erkinheimo TL, Lassus H, Finne P, van Rees BP, Leminen A, Ylikorkala O, Haglund C, Butzow R, Ristimäki A. Elevated cyclooxygenase-2 expression is associated with altered expression of p53 and SMAD4, amplification of HER-2/neu, and poor outcome in serous ovarian carcinoma. Clin Cancer Res. 2004 Jan 15;10(2):538-45.

341. Vadlamudi R, Mandal M, Adam L, Steinbach G, Mendelsohn J, Kumar R. Regulation of cyclooxygenase-2 pathway by HER2 receptor. Oncogene. 1999 Jan 14;18(2):305-14.

342. Wang SC, Lien HC, Xia W, Chen IF, Lo HW, Wang Z, Ali-Seyed M, Lee DF, Bartholomeusz G, Ou-Yang F, Giri DK, Hung MC. Binding at and transactivation of the COX-2 promoter by nuclear tyrosine kinase receptor ErbB-2. Cancer Cell. 2004 Sep;6(3):251-61.

343. Dillon MF, Stafford AT, Kelly G, et al. Cyclooxygenase-2 predicts adverse effects of tamoxifen: A possible mechanism of role for nuclear HER2 in breast cancer patients. Endocr Relat Cancer 2008;15(3):745-53.

344. Nassar A, Radhakrishnan A, Cabrero IA, Cotsonis G, Cohen C. COX-2 expression in invasive breast cancer: correlation with prognostic parameters and outcome. Appl Immunohistochem Mol Morphol. 2007 Sep;15(3):255-9.

345. Zerkowski MP, Camp RL, Burtness BA, Rimm DL, Chung GG. Quantitative analysis of breast cancer tissue microarrays shows high cox-2 expression is associated with poor outcome. Cancer Invest. 2007 Feb;25(1):19-26.

346. Eltze E, Wülfing C, Von Struensee D, Piechota H, Buerger H, Hertle L. Cox-2 and Her2/neu co-expression in invasive bladder cancer. Int J Oncol. 2005 Jun;26(6):1525-31.

347. Edwards J, Mukherjee R, Munro AF, Wells AC, Almushatat A, Bartlett JMS. HER2 and COX2 expression in human prostate cancer. European Journal of Cancer, 2004;40(1):50-5.

348. Ferrandina G, Ranelletti FO, Gallotta V, Martinelli E, Zannoni GF, Gessi M, Scambia G. Expression of cyclooxygenase-2 (COX-2), receptors for estrogen (ER), and progesterone (PR), p53, ki67, and neu protein in endometrial cancer. Gynecol Oncol. 2005 Sep;98(3):383-9.

349. Young LC, Campling BG, Cole SP, Deeley RG, Gerlach JH. Multidrug resistance proteins MRP3, MRP1, and MRP2 in lung cancer: correlation of protein levels with drug response and messenger RNA levels. Clin Cancer Res. 2001 Jun;7(6):1798-804.

350. Ranger GS, Jewell A, Thomas V, Mokbel K. Elevated expression of cyclooxygenase-2 in breast cancer and ductal carcinoma in situ has no correlation with established prognostic markers. J Surg Oncol. 2004 Nov 1;88(2):100-3.

351. Wallerand H, Cai Y, Wainberg ZA, Garraway I, Lascombe I, Nicolle G, Thiery JP, Bittard H, Radvanyi F, Reiter RR. Phospho-Akt pathway activation and inhibition depends on N-cadherin or phospho-EGFR expression in invasive human bladder cancer cell lines.Urol Oncol. 2008 Dec 11.

352. Jüngel A, Distler O, Schulze-Horsel U, Huber LC, Ha HR, Simmen B, Kalden JR, Pisetsky DS, Gay S, Distler JH. Microparticles stimulate the synthesis of prostaglandin E(2) via induction of cyclooxygenase 2 and microsomal prostaglandin E synthase 1. Arthritis Rheum. 2007 Nov;56(11):3564-74.

353. Ferrandina G, Ranelletti FO, Lauriola L, Fanfani F, Legge F, Mottolese M, Nicotra MR, Natali PG, Zakut VH, Scambia G.Cyclooxygenase-2 (COX-2), epidermal growth factor receptor (EGFR), and Her- 2/neu expression in ovarian cancer. Gynecol Oncol. 2002 May;85(2):305-10.

354. Timotheadou E, Skarlos DV, Samantas E, Papadopoulos S, Murray S, Skrickova J, Christodoulou C, Papakostantinou C, Pectasides D, Papakostas P, Kaplanova J, Vrettou E, Karina M, Kosmidis P, Fountzilas G. Evaluation of the prognostic role of a panel of biomarkers in stage IB-IIIA non-small cell lung cancer patients. Anticancer Res. 2007 Nov-Dec;27(6C):4481-9.

355. Huh YH, Kim SH, Kim SJ, Chun JS. Differentiation status-dependent regulation of cyclooxygenase-2 expression and prostaglandin E2 production by epidermal growth factor via mitogen-activated protein kinase in articular chondrocytes. J Biol Chem. 2003 Mar 14;278(11):9691-7. Epub 2002 Dec 18.

356. Chen LC, Chen BK, Chang WC. Activating protein 1-mediated cyclooxygenase-2 expression is independent of N-terminal phosphorylation of c-Jun. Mol Pharmacol. 2005 Jun;67(6):2057-69. Epub 2005 Mar 16.

357. Pham H, Chong B, Vincenti R, Slice LW. Ang II and EGF synergistically induce COX-2 expression via CREB in intestinal epithelial cells. J Cell Physiol. 2008 Jan;214(1):96-109.

358. Xu K, Shu HG. EGFR activation results in enhanced cyclooxygenase-2 expression through p38 mitogen-activated protein kinase-dependent activation of the Sp1/Sp3 transcription factors in human gliomas. Cancer Res 2007;67(13):6121-9.

359. Al-Salihi MA, Terrece Pearman A, Doan T, et al. Transgenic expression of cyclooxygenase-2 in mouse intestine epithelium is insufficient to initiate tumorigenesis but promotes tumor progression. Cancer Letters,;In Press, 2008.

360. Brattström D, Wester K, Bergqvist M, Hesselius P, Malmström PU, Nordgren H, Wagenius G, Brodin O. HER-2, EGFR, COX-2 expression status correlated to microvessel density and survival in resected non-small cell lung cancer. Acta Oncol. 2004;43(1):80-6.

361. Van Dyke AL, Cote ML, Prysak GM, et al. COX-2/EGFR expression and survival among women with adenocarcinoma of the lung. Carcinogenesis 2008;29(9):1781-7.

362. Chen L, He Y, Huang H, Liao H, Wei W. Selective COX-2 inhibitor celecoxib combined with EGFR-TKI ZD1839 on non-small cell lung cancer cell lines: in vitro toxicity and mechanism study. Med Oncol. 2008;25(2):161-71. Epub 2008 Jan 3.

363. Gadgeel SM, Ruckdeschel JC, Heath EI, Heilbrun LK, Venkatramanamoorthy R, Wozniak A. Phase II study of gefitinib, an epidermal growth factor receptor tyrosine kinase inhibitor (EGFR-TKI), and celecoxib, a cyclooxygenase-2 (COX-2) inhibitor, in patients with platinum refractory non-small cell lung cancer (NSCLC). J Thorac Oncol. 2007 Apr;2(4):299-305.

364. Narayanan BA, Reddy BS, Bosland MC, et al. Exisulind in combination with celecoxib modulates epidermal growth factor receptor, cyclooxygenase-2, and cyclin D1 against prostate carcinogenesis: In vivo evidence. Clin Cancer Res 2007;13(19):5965-73.

365. Gadgeel SM, Ali S, Philip PA, Ahmed F, Wozniak A, Sarkar FH. Response to dual blockade of epidermal growth factor receptor (EGFR) and cycloxygenase-2 in nonsmall cell lung cancer may be dependent on the EGFR mutational status of the tumor. Cancer. 2007 Dec 15;110(12):2775-84.

366. O'Byrne KJ, Danson S, Dunlop D, Botwood N, Taguchi F, Carbone D, Ranson M. Combination therapy with gefitinib and rofecoxib in patients with platinum-pretreated relapsed non small-cell lung cancer. J Clin Oncol. 2007 Aug 1;25(22):3266-73.

367. Carlson JJ. Erlotinib in non-small-cell lung cancer: a review of the clinical and economic evidence. Expert Rev Pharmacoecon Outcomes Res. 2009 Oct;9(5):409-16.

368. Putnam KP, Bombick DW, Doolittle DJ. Evaluation of eight in vitro assays for assessing the cytotoxicity of cigarette smoke condensate. Toxicol In Vitro 2002;16(5):599-607.

369. Heenan M, O'Driscoll L, Cleary I, Connolly L, Clynes M. Isolation from a human MDR lung cell line of multiple clonal subpopulations which exhibit significantly different drug resistance. Int J Cancer. 1997 May 29;71(5):907-15.

370. Breen L, Murphy L, Keenan J, Clynes M. Development of taxane resistance in a panel of human lung cancer cell lines. Toxicol In Vitro. 2008 Aug;22(5):1234-41. Epub 2008 Apr 15.

371. Özvegy-Laczka C., Hegedűs T., Várady G., Ujhelly O., Schuetz J.D., Váradi A., Kéri G., Őrfi L., Német K. and Sarkadi B. High-Affinity Interaction of Tyrosine Kinase Inhibitors with the ABCG2 Multidrug Transporter. Molecular Pharmacology June 2004 vol. 65 no. 6 1485-1495

372. Ujhelly O, Ozvegy C, Varady G, Cervenak J, Homolya L, Grez M, Scheffer G, Roos D, Bates SE, Varadi A, Sarkadi B, Nemet K Application of a human multidrug transporter (ABCG2) variant as selectable marker in gene transfer to progenitor cells. Human gene therapy 2003 Mar 14;4 403-412.

373. Hooijberg JH, Broxterman HJ, Kool M, Assaraf YG, Peters GJ, Noordhuis P, Scheper RJ, Borst P, Pinedo HM, Jansen G. Antifolate resistance mediated by the multidrug resistance proteins MRP1 and MRP2. Cancer Res. 1999 Jun 1;59(11):2532-5.

374. Towbin H, Staehelin T, Gordon J. Electrophoretic transfer of proteins from polyacrylamide gels to nitrocellulose sheets: procedure and some applications. 1979. Biotechnology. 1992;24:145-9.

375. Satyanarayana U, Rao DS, Kumar YR, Babu JM, Kumar PR, Reddy JT. Isolation, synthesis and characterization of impurities in celecoxib, a COX-2 inhibitor. J Pharm Biomed Anal. 2004 Jun 29;35(4):951-7.

376. Greenberg PL, Lee SJ, Advani R, Tallman MS, Sikic BI, Letendre L, Dugan K, Lum B, Chin DL, Dewald G, Paietta E, Bennett JM, Rowe JM.Mitoxantrone, etoposide, and cytarabine with or without valspodar in patients with relapsed or refractory acute myeloid leukemia and high-risk myelodysplastic syndrome: a phase III trial (E2995). J Clin Oncol. 2004 Mar 15;22(6):1078-86. Erratum in: J Clin Oncol. 2004 Jul 1;22(13):2747.

377. Pegg AE. Effect of alpha-difluoromethylornithine on cardiac polyamine content and hypertrophy. J Mol Cell Cardiol. 1981 Oct;13(10):881-7.

378. Pegg AE. Polyamine metabolism and its importance in neoplastic growth and a target for chemotherapy. Cancer Res. 1988 Feb 15;48(4):759-74. Review.

379. Jänne J, Hölttä E, Kallio A, Käpyaho K. Role of polyamines and their antimetabolites in clinical medicine. Spec Top Endocrinol Metab. 1983;5:227-93. Review.

380. Ignatenko NA, Zhang H,Watts GS, Skovan BA, Stringer DE, Gerner EW. The chemopreventive agent a-difluoromethylornithine blocks K-ras dependent tumor formation and specific gene expression in Caco-2 cells. Mol Carcinog (2004) 39: 221–233.

381. Averill-Bates DA, Chérif A, Agostinelli E, Tanel A, Fortier G. Anti-tumoral effect of native and immobilized bovine serum amine oxidase in a mouse melanoma model. Biochem Pharmacol. 2005 Jun 15;69(12):1693-704.

382. Kobayashi Y, Furukawa-Hibi Y, Chen C, Horio Y, Isobe K, Ikeda K, Motoyama N. SIRT1 is critical regulator of FOXO-mediated transcription in response to oxidative stress. Int J Mol Med. 2005 Aug;16(2):237-43.

383. Athar M, Back JH, Tang X, Kim KH, Kopelovich L, Bickers DR, Kim AL. Resveratrol: a review of preclinical studies for human cancer prevention. Toxicol Appl Pharmacol. 2007 Nov 1;224(3):274-83. Epub 2007 Jan 3. Review.

384. de la Lastra CA, Villegas I. Resveratrol as an antioxidant and pro-oxidant agent: mechanisms and clinical implications. Biochem Soc Trans. 2007 Nov;35(Pt 5):1156-60. Review.

385. Moran BW, Anderson FP, Devery A, Cloonan S, Butler WE, Varughese S, Draper SM, Kenny PT. Synthesis, structural characterisation and biological evaluation of fluorinated analogues of resveratrol. Bioorg Med Chem. 2009 Jul 1;17(13):4510-22. Epub 2009 May 8.

386. Lo A, Burckart GJ. P-glycoprotein and drug therapy in organ transplantation. J Clin Pharmacol. 1999 Oct;39(10):995-1005.

387. Kattan J, Droz JP, Couvreur P, Marino JP, Boutan-Laroze A, Rougier P, Brault P, Vranckx H, Grognet JM, Morge X, et al. Phase I clinical trial and pharmacokinetic evaluation of doxorubicin carried by polyisohexylcyanoacrylate nanoparticles. Invest New Drugs. 1992 Aug;10(3):191-9.

388. Soma CE, Dubernet C, Barratt G, Nemati F, Appel M, Benita S, Couvreur P. Ability of doxorubicin-loaded nanoparticles to overcome multidrug resistance of tumor cells after their capture by macrophages. Pharm Res. 1999 Nov;16(11):1710-6.

389. Simeonova M, Ivanova G, Enchev V, Markova N, Kamburov M, Petkov C, Devery A, O'Connor R, Brougham D. Physicochemical characterization and in vitro behavior of daunorubicin-loaded poly(butylcyanoacrylate) nanoparticles. Acta Biomater. 2009 Jul;5(6):2109-21. Epub 2009 Jan 31.

390. Sakai K, Arao T, Shimoyama T, Murofushi K, Sekijima M, Kaji N, Tamura T, Saijo N, Nishio K. Dimerization and the signal transduction pathway of a small in-frame deletion in the epidermal growth factor receptor. FASEB J. 2006 Feb;20(2):311-3. Epub 2005 Dec 22.

391. Hooijberg JH, Jansen G, Assaraf YG, Kathmann I, Pieters R, Laan AC, Veerman AJ, Kaspers GJ, Peters GJ. Folate concentration dependent transport activity of the Multidrug Resistance Protein 1 (ABCC1). Biochem Pharmacol. 2004 Apr 15;67(8):1541-8.

392. Usmani SZ, Bona R, Li Z. 17 AAG for HSP90 inhibition in cancer--from bench to bedside. Curr Mol Med. 2009 Jun;9(5):654-64.

393. Leonard GD, Fojo T, Bates SE. The role of ABC transporters in clinical practice. Oncologist. 2003;8(5):411-24. Review.

394. Marton LJ, Pegg AE. Polyamines as targets for therapeutic intervention. Annu Rev Pharmacol Toxicol. 1995;35:55-91.

395. Seiler N. Thirty years of polyamine-related approaches to cancer therapy. Retrospect and prospect. Part 1. Selective enzyme inhibitors. Curr Drug Targets. 2003 Oct;4(7):537-64. Review.

396. Gerner EW, Meyskens FL Jr. Polyamines and cancer: old molecules, new understanding. Nat Rev Cancer. 2004 Oct;4(10):781-92.

397. Gosland MP, Gillespie MN, Tsuboi CP, Tofiq S, Olson JW, Crooks PA, Aziz SM. Reversal of doxorubicin, etoposide, vinblastine, and taxol resistance in multidrug resistant human sarcoma cells by a polymer of spermine. Cancer Chemother Pharmacol. 1996;37(6):593-600.

398. Aziz SM, Worthen DR, Yatin M, Ain KB, Crooks PA. A unique interaction between polyamine and multidrug resistance (P-glycoprotein) transporters in cultured Chinese hamster ovary cells transfected with mouse mdr-1 gene. Biochem Pharmacol. 1998 Jul 15;56(2):181-7.

399. Toffoli G, Sorio R, Gigante M, Corona G, Galligioni E, Boiocchi M. Cyclosporin A as a multidrug-resistant modulator in patients with renal cell carcinoma treated with teniposide. Br J Cancer. 1997;75(5):715-21.

400. Tolomeo M, Grimaudo S, Di Cristina A, Roberti M, Pizzirani D, Meli M, Dusonchet L, Gebbia N, Abbadessa V, Crosta L, Barucchello R, Grisolia G, Invidiata F, Simoni D.

Pterostilbene and 3'-hydroxypterostilbene are effective apoptosis-inducing agents in MDR and BCR-ABL-expressing leukemia cells. Int J Biochem Cell Biol. 2005 Aug;37(8):1709-26. Epub 2005 Apr 26.

401. Böhm HJ, Banner D, Bendels S, Kansy M, Kuhn B, Müller K, Obst-Sander U, Stahl M. Fluorine in medicinal chemistry. Chembiochem. 2004 May 3;5(5):637-43. Review.

402. Almeida L, Vaz-da-Silva M, Falcão A, Soares E, Costa R, Loureiro AI, Fernandes-Lopes C, Rocha JF, Nunes T, Wright L, Soares-da-Silva P. Pharmacokinetic and safety profile of trans-resveratrol in a rising multiple-dose study in healthy volunteers. Mol Nutr Food Res. 2009 May;53 Suppl 1:S7-15.

403. Holmes-McNary M, Baldwin AS. Chemopreventive properties of trans-resveratrol are associated with inhibition of activation of the IkappaB kinase. Cancer Res 2000 ; 60 : 3477-83.

404. Ouyang H, Andersen TE, Chen W, Nofsinger R, Steffansen B, Borchardt RT. A comparison of the effects of p-glycoprotein inhibitors on the blood-brain barrier permeation of cyclic prodrugs of an opioid peptide (DADLE). J Pharm Sci. 2009 Jun;98(6):2227-36.

405. Elgie AW, Sargent JM, Williamson CJ, Lewandowicz GM, Taylor CG. Comparison of P-glycoprotein expression and function with in vitro sensitivity to anthracyclines in AML. Adv Exp Med Biol. 1999;457:29-33.

406. Sarris AH, Younes A, McLaughlin P, Moore D, Hagemeister F, Swan F, Rodriguez MA, Romaguera J, North L, Mansfield P, Callendar D, Mesina O, Cabanillas F. Cyclosporin A does not reverse clinical resistance to paclitaxel in patients with relapsed non-Hodgkin's lymphoma. J Clin Oncol. 1996 Jan;14(1):233-9.

407. Busauschina A, Schnuelle P, van der Woude FJ. Cyclosporine nephrotoxicity. Transplant Proc. 2004 Mar;36(2 Suppl):229S-233S.

408. Ott I, Gust R. Non platinum metal complexes as anti-cancer drugs. Arch Pharm (Weinheim). 2007 Mar;340(3):117-26.

409. de Verdière AC, Dubernet C, Némati F, Soma E, Appel M, Ferté J, Bernard S, Puisieux F, Couvreur P. Reversion of multidrug resistance with polyalkylcyanoacrylate nanoparticles: towards a mechanism of action. Br J Cancer. 1997;76(2):198-205.

410. Aouali N, Morjani H, Trussardi A, Soma E, Giroux B, Manfait M. Enhanced cytotoxicity and nuclear accumulation of doxorubicin-loaded nanospheres in human breast cancer MCF7 cells expressing MRP1. Int J Oncol. 2003 Oct;23(4):1195-201.

411. Vauthier C, Dubernet C, Chauvierre C, Brigger I, Couvreur P. Drug delivery to resistant tumors: the potential of poly(alkyl cyanoacrylate) nanoparticles. J Control Release. 2003 Dec 5;93(2):151-60.

412. Baer MR, George SL, Dodge RK, O'Loughlin KL, Minderman H, Caligiuri MA, Anastasi J, Powell BL, Kolitz JE, Schiffer CA, Bloomfield CD, Larson RA. Phase III study of the multidrug resistance modulator PSC-833 in previously untreated patients 60 years of age and older with acute myeloid leukemia: Cancer and Leukemia Group B Study 9720. Blood. 2002 Aug 15;100(4):1224-32.

413. Draper MP, Martell RL, Levy SB. Indomethacin-mediated reversal of multidrug resistance and drug efflux in human and murine cell lines overexpressing MRP, but not P-glycoprotein. Br J Cancer. 1997;75(6):810-5.

414. Duus J, Bahar HI, Venkataraman G, Ozpuyan F, Izban KF, Al-Masri H, Maududi T, Toor A, Alkan S. Analysis of expression of heat shock protein-90 (HSP90) and the effects of HSP90 inhibitor (17-AAG) in multiple myeloma. Leuk Lymphoma. 2006 Jul;47(7):1369-78.

415. Maliepaard M, van Gastelen MA, Tohgo A, Hausheer FH, van Waardenburg RC, de Jong LA, Pluim D, Beijnen JH, Schellens JH. Circumvention of breast cancer resistance protein (BCRP)-mediated resistance to camptothecins in vitro using non-substrate drugs or the BCRP inhibitor GF120918. Clin Cancer Res. 2001 Apr;7(4):935-41.

416. Maliepaard M, van Gastelen MA, de Jong LA, Pluim D, van Waardenburg RC, Ruevekamp-Helmers MC, Floot BG, Schellens JH. Overexpression of the

BCRP/MXR/ABCP gene in a topotecan-selected ovarian tumor cell line. Cancer Res. 1999 Sep 15;59(18):4559-63.

417. Xia W, Mullin RJ, Keith BR, Liu LH, Ma H, Rusnak DW, Owens G, Alligood KJ, Spector NL. Anti-tumor activity of GW572016: a dual tyrosine kinase inhibitor blocks EGF activation of EGFR/erbB2 and downstream Erk1/2 and AKT pathways. Oncogene. 2002 Sep 12;21(41):6255-63.

418. Polli JW, Olson KL, Chism JP, John-Williams LS, Yeager RL, Woodard SM, Otto V, Castellino S, Demby VE. An unexpected synergist role of P-glycoprotein and breast cancer resistance protein on the central nervous system penetration of the tyrosine kinase inhibitor lapatinib (N-{3-chloro-4-[(3-fluorobenzyl)oxy]phenyl}-6-[5-({[2-(methylsulfonyl)ethyl]amino}methyl)-2-furyl]-4-quinazolinamine; GW572016). Drug Metab Dispos. 2009 Feb;37(2):439-42. Epub 2008 Dec 4.

419. Chau I, Cunningham D, Hickish T, Massey A, Higgins L, Osborne R, Botwood N, Swaisland A. Gefitinib and irinotecan in patients with fluoropyrimidine-refractory, irinotecan-naive advanced colorectal cancer: a phase I-II study. Ann Oncol. 2007 Apr;18(4):730-7. Epub 2007 Jan 20.

420. Tse AN, Klimstra DS, Gonen M, Shah M, Sheikh T, Sikorski R, Carvajal R, Mui J, Tipian C, O'Reilly E, Chung K, Maki R, Lefkowitz R, Brown K, Manova-Todorova K, Wu N, Egorin MJ, Kelsen D, Schwartz GK. A phase 1 dose-escalation study of irinotecan in combination with 17-allylamino-17-demethoxygeldanamycin in patients with solid tumors. Clin Cancer Res. 2008 Oct 15;14(20):6704-11.

421. Kuppens IE, Witteveen EO, Jewell RC, Radema SA, Paul EM, Mangum SG, Beijnen JH, Voest EE, Schellens JH. A phase I, randomized, open-label, parallel-cohort, dose-finding study of elacridar (GF120918) and oral topotecan in cancer patients. Clin Cancer Res. 2007 Jun 1;13(11):3276-85.

422. Coussens LM, Werb Z. Inflammation and cancer. Nature. 2002 Dec 19-26;420(6917):860-7.

423. Balkwill F, Mantovani A. Inflammation and cancer: back to Virchow? Lancet. 2001 Feb 17;357(9255):539-45. Review.

424. Lage A, Crombet T, González G. Targeting epidermal growth factor receptor signaling: early results and future trends in oncology. Ann Med. 2003;35(5):327-36. Review.

425. Pennell NA, Mekhail T. Investigational agents in the management of non-small cell lung cancer. Curr Oncol Rep. 2009 Jul;11(4):275-84. Review.

426. Konecny GE, Pegram MD, Venkatesan N, Finn R, Yang G, Rahmeh M, Untch M, Rusnak DW, Spehar G, Mullin RJ, Keith BR, Gilmer TM, Berger M, Podratz KC, Slamon DJ. Activity of the dual kinase inhibitor lapatinib (GW572016) against HER-2-overexpressing and trastuzumab-treated breast cancer cells. Cancer Res. 2006 Feb 1;66(3):1630-9.

427. Gadgeel SM, Ali S, Philip PA, Wozniak A, Sarkar FH. Genistein enhances the effect of epidermal growth factor receptor tyrosine kinase inhibitors and inhibits nuclear factor kappa B in nonsmall cell lung cancer cell lines. Cancer. 2009 May 15;115(10):2165-76.

428. Zhang H, Neely L, Lundgren K, Yang YC, Lough R, Timple N, Burrows F. BIIB021, a synthetic HSP90 inhibitor, has broad application against tumors with acquired multidrug resistance. Int J Cancer. 2009 Aug 12.

429. Mazzanti R, Platini F, Bottini C, Fantappiè O, Solazzo M, Tessitore L. Down-regulation of the HGF/MET autocrine loop induced by celecoxib and mediated by P-gp in MDR-positive human hepatocellular carcinoma cell line. Biochem Pharmacol. 2009 Jul 1;78(1):21-32. Epub 2009 Mar 24.

Section 8.

Appendix

8.1. Screening of potential novel anti-cancer agents

8.1.1. Polyamine derivatives
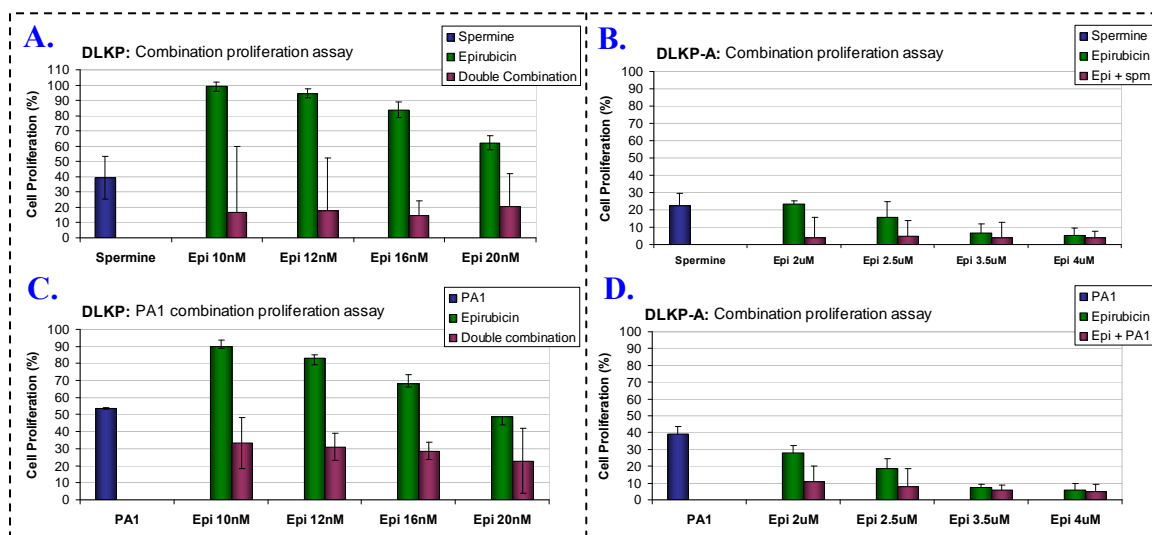
Graph 8.1.1.1.: The combination proliferation assays of spermine (**A** and **B**) or PA1 (**C** and **D**) with varying concentrations of epirubicin in the DLKP (**A** and **C**) and DLKP-A (**B** and **D**) cell lines. This graph is the result of a single determination.

8.1.2. Resveratrol Analogues
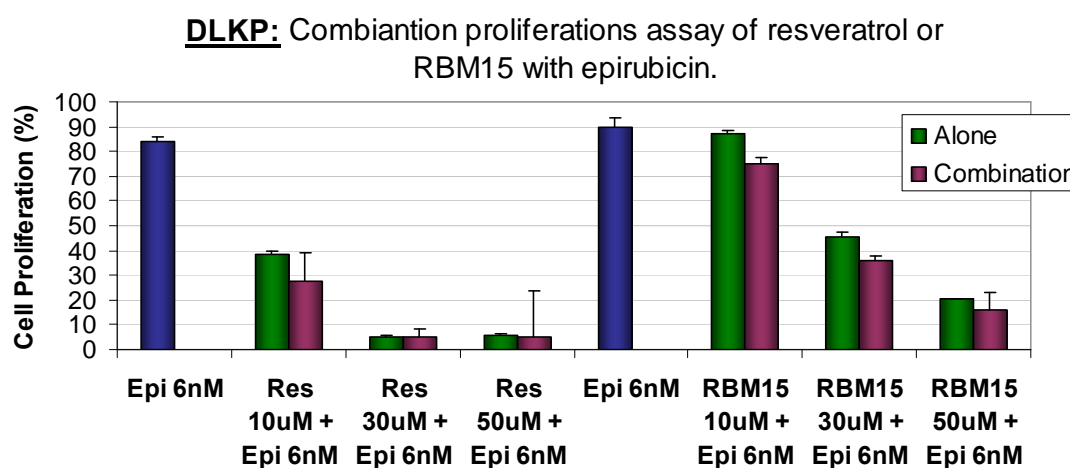
Graph 8.1.2.1.: The combination of resveratrol or RBM15 with the MRP1 substrate, epirubicin, in the DLKP cell line (MRP1 expressing cell line). The bar chart is the result of a single assay.

8.1.3. Macrocycle compounds
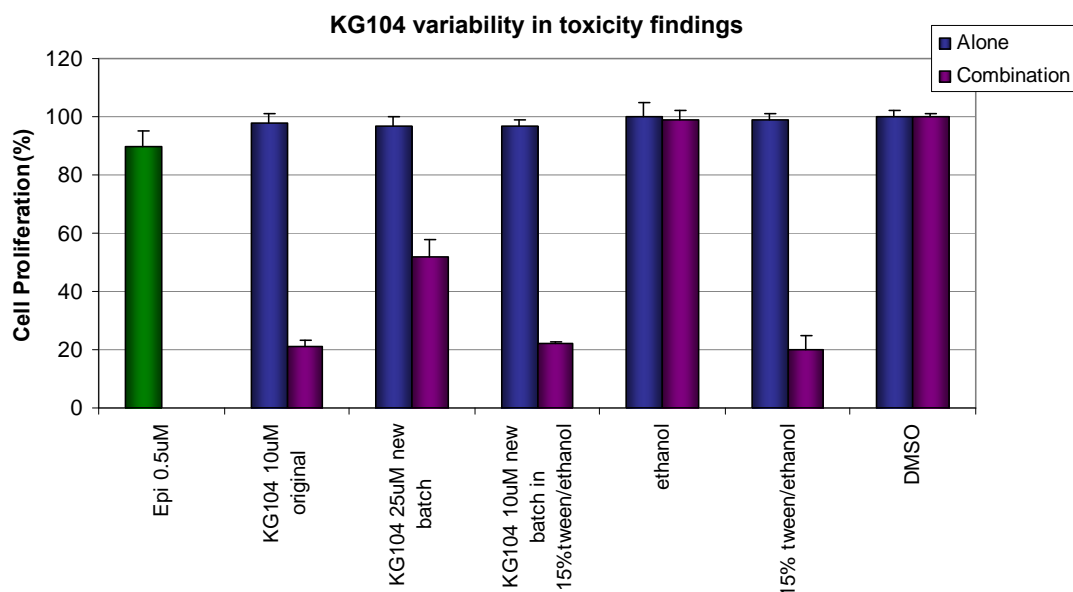
Graph 8.1.3.1: Cell proliferation associated with different KG104 batches, ethanol, DMSO and 15% tween80/ethanol (v/v) with epirubicin in the DLKP-A cell lines. This graph is the result of a single assay. Table 8.1.3.6 below depict the percentage cell proliferation and standard deviations for this graph.

Table 8.1.3.1: This table provides the combination data of epirubicin with a range KG104 batches and their vehicles.

Compounds	Cell Proliferation (%)			
	Alone	**St Dev (%)**	**Combination**	**St Dev (%)**
Epirubicin 0.5µM	90	±5		
KG104 10µM original	98	±3	21	±2
KG104 25µM new batch	97	±3	52	±6
KG104 10µM new batch in 15%tween/ethanol	97	±2	22	±0.8
Ethanol	100	±5	99	±3
15% tween80/ethanol	99	±2	20	±5
DMSO	100	±2	100	±1

8.1.6. MDR down-regulation

8.1.6.1. P-gp downregulation

A.

A549-Taxol: Indomethacin treatment

B.

A549-Taxol: 17-AAG treatment
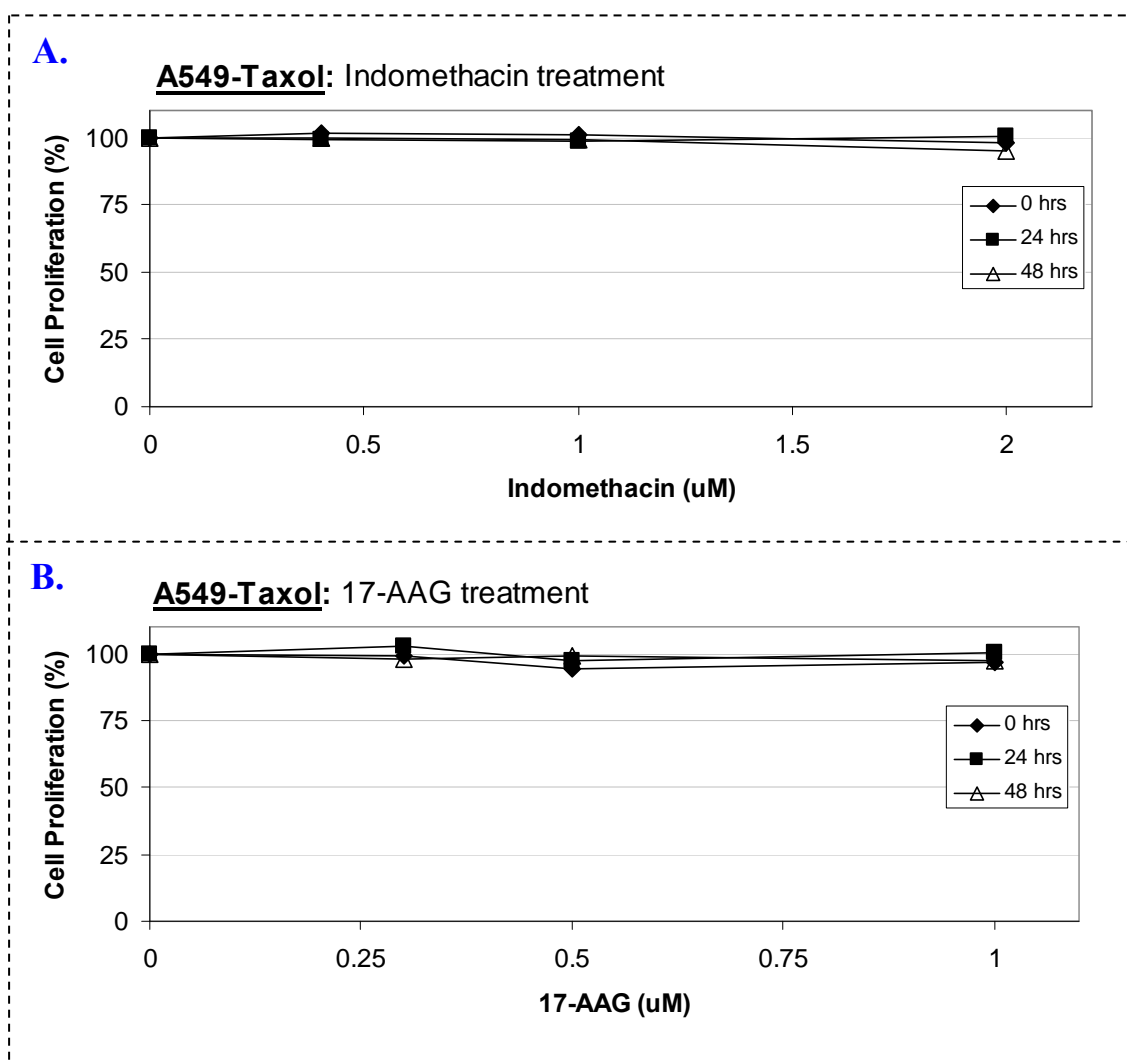
Graph 8.1.6.1.1.: The short-term treatment with A549-Taxol cells to indomethacin (**A**) or 17-AAG (**B**). The cells (at a density of 5×10^4 cells/ml) were exposed to each drug for 24 hours and the cell proliferation was determined at this point (0 (◆)), 24 (■) and 48 hours (Δ) later. Each graph is the result of a single assay.

8.1.6.2. MRP1 down-regulation
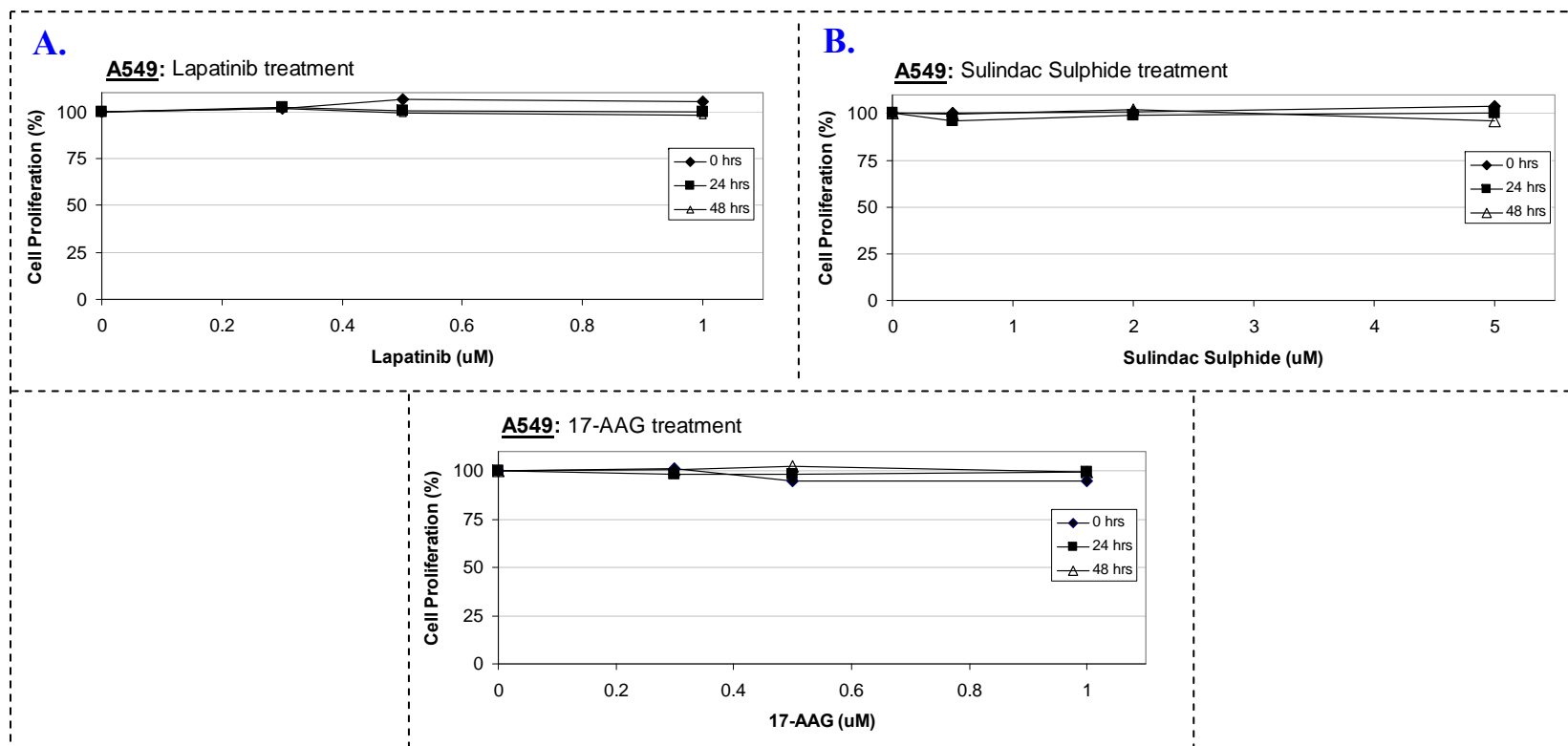
Graph 8.1.6.2.1.: The short-term treatment of A549 cells with lapatinib (**A**), sulindac sulphide (**B**) or 17-AAG (**C**). The cells (at a density of 5×10^4 cells/ml) were exposed to each drug for 24 hours and the cell proliferation was determined at this point (0 (◆)), 24 (■) and 48 hours (Δ) later. Each graph is the result of a single assay.

8.1.6.3. BCRP down-regulation

A. **DLKP-SQ/mitox:** Lapatinib treatment

B. **DLKP-SQ/mitox:** Gefitinib treatment

C. **DLKP-SQ/mitox:** Indomethacin treatment

D. **DLKP-SQ/mitox:** Elacridar treatment

E. **DLKP-SQ/mitox:** 17-AAG treatment
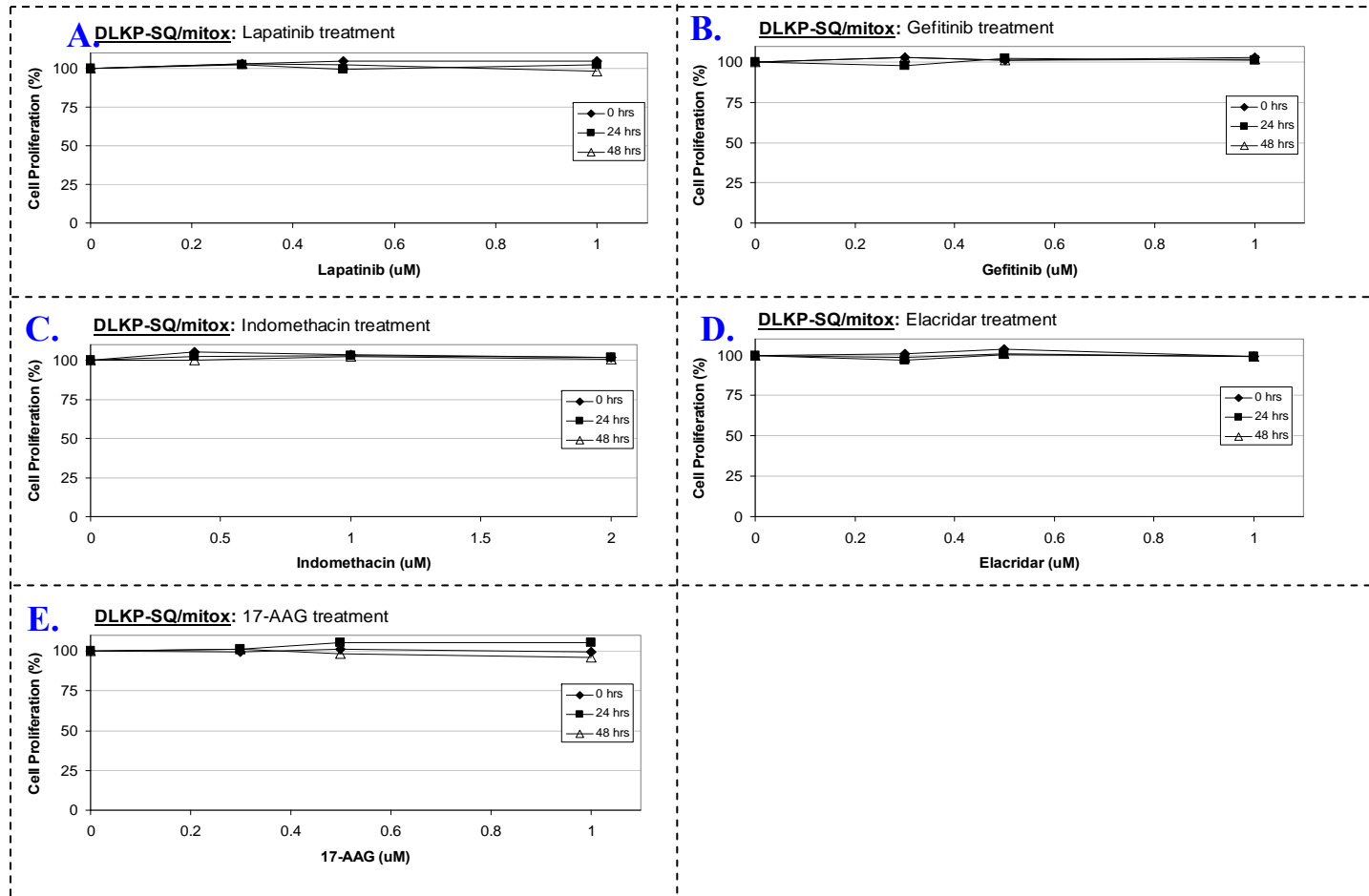
Graph 8.1.6.3.1.: The short-term treatment of DLKP-SQ/mitox cells with lapatinib (**A**), gefitinib (**B**), indomethacin (**C**), elacridar (**D**) or 17-AAG (**E**). The cells (at a density of 5×10^4 cells/ml) were exposed to each drug for 24 hours and the cell proliferation was determined at this point (0 (♦)), 24 (■) and 48 hours (Δ) later. Each graph is the result of a single assay.

8.3. Effect of tyrosine kinase inhibitors on the function and expression of epidermal growth factor receptors, EGFR and HER2, multidrug resistance transporter and cyclooxygenase proteins.

8.3.2. EGFR and phospho-EGFR protein quantification by ELISA

In section (3.3.1.) we found that lapatinib had no effect on the toxicity of epirubicin or docetaxel in the EGFR, HER2 or dual EGFR/HER2 expressing breast cell lines. In this section and in section 8.3.3., we quantified the effect lapatinib had on the expression and activation levels of EGFR and HER2/ErbB2. Quantitation employed ELISA assays. The EGFR and *p*EGFR ELISAs were carried out on MDA-MB-231 cell lysates while the ErbB2 and *p*ErbB2 ELISAs were carried out on MDA-MB-453 cell lysates. The MDA-MB-231 cells were exposed to lapatinib (2.5, 5 and 10 µM), EGF (10, 50 and 100 ng/ml) and DMSO (0.5 and 1 %) for 48 hours.

In the EGFR-amplified MDA-MB-231 cell line, we found that lapatinib had no effect on EGFR expression or active levels at 12 hours but caused a slight increase in both at 24 and 48 hours (see graph 8.3.2.1.**A** and table 8.3.2.1.**A**). Lapatinib's control, DMSO, caused no changes in EGFR expression or active levels at 12 and 24 hours but a slight increase at 48 hours (see graph 8.3.2.1.**C** and table 8.3.2.1.**C**).
EGF slightly decreased EGFR expression but greatly increased levels of phosphorylated EGFR (i.e. activity levels). The greatest increase in activation was seen after 12 hours (graph 8.3.2.1.**B** and table 8.3.2.1.**B**).
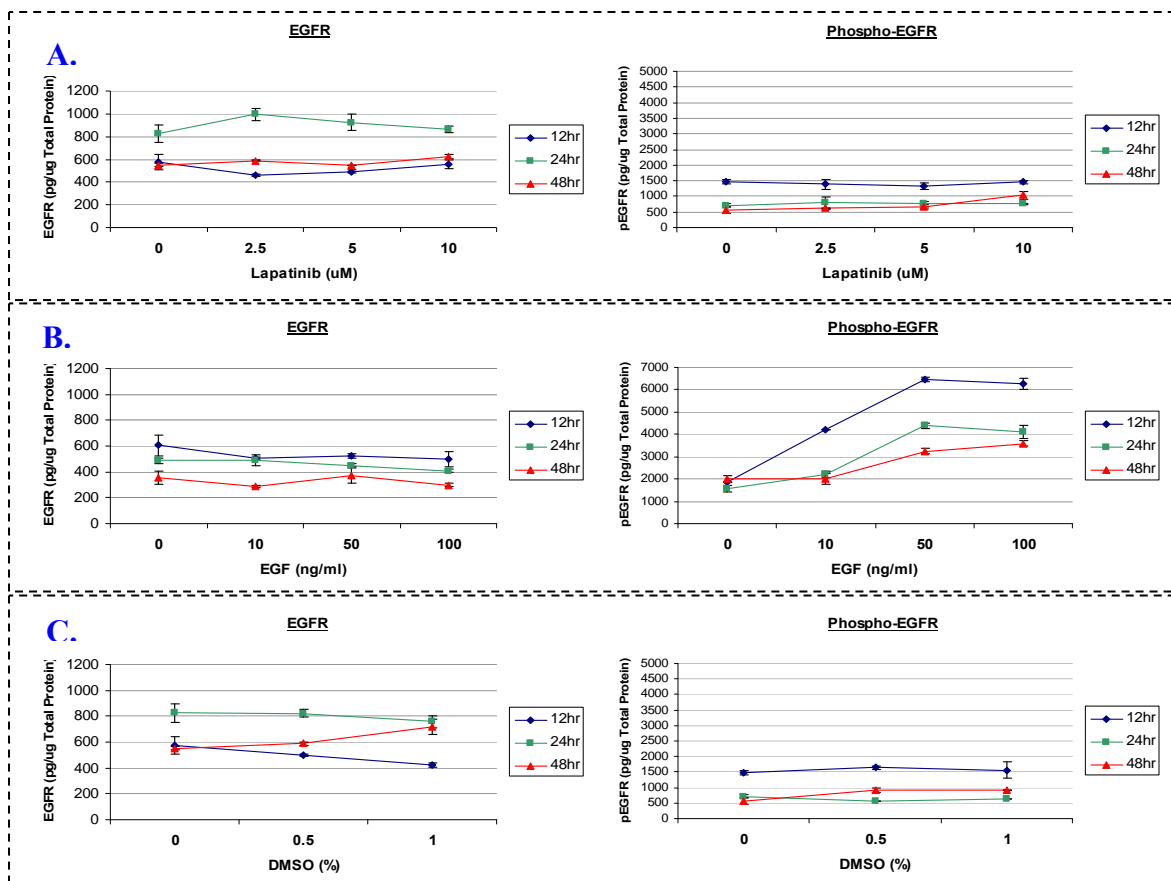
Graph 8.3.2.1: This set of graphs show the levels of EGFR and phosphor-EGFR in the MDA-MB-231 cell line following exposure to the tyrosine kinase inhibitor, Lapatinib (**A**), the EGFR ligand, EGF (**B**) and as a control, DMSO (**C**) for 12hrs (◆), 24hrs (■) and 48hrs (Δ). The data is representative of duplicate intraday results. The tables below provide the raw data illustrated in these graphs.

Table 8.3.2.1.A: This table outlines the expression levels of EGFR (pg/µg Total Protein) and *p*EGFR (pg/µg Total Protein) in MDA-MB-231 following a 12hr, 24hr and 48hr exposure to increasing concentrations of lapatinib. This data is illustrated in graph 8.3.2.1.**A**.

Lapatinib (µM)				
12hr	**EGFR (pg/µg Total Protein)**	StDev	***p*EGFR (pg/µg Total Protein)**	StDev
0	575	±65	1475	±71
2.5	457	±10	1387	±159
5	491	±15	1325	±106
10	559	±42	1463	±53
24hr				
0	826	±73	713	±53
2.5	995	±52	788	±194
5	925	±71	763	±88
10	864	±27	763	±18
48hr				
0	551	±11	575	±106
2.5	590	±6	613	±18
5	549	±2	650	±71
10	620	±25	1038	±124

Table 8.3.2.1.B: This table outlines the expression levels of EGFR (pg/µg Total Protein) and *p*EGFR (pg/µg Total Protein) in MDA-MB-231 following a 12hr, 24hr and 48hr exposure to increasing concentrations of EGF. This data is illustrated in graph 8.3.2.1.**B**.

EGF (ng/ml)				
12hr	**EGFR (pg/µg Total Protein)**	**Stdev**	***p*EGFR (pg/µg Total Protein)**	**Stdev**
0	605	±81	1850	±0
10	507	±8	4200	±0
50	525	±17	6450	±106
100	499	±62	6275	±247
24hr				
0	490	±21	1575	±141
10	490	±44	2213	±159
50	450	±12	4388	±124
100	410	±12	4100	±283
48hr				
0	358	±50	2013	±159
10	286	±10	2013	±230
50	370	±60	3250	±106
100	298	±12	3588	±124

Table 8.3.2.1.C: This table outlines the expression levels of EGFR (pg/µg Total Protein) and *p*EGFR (pg/µg Total Protein) in MDA-MB-231 following a 12hr, 24hr and 48hr exposure to increasing concentrations of DMSO. This data is illustrated in graph 8.3.2.1.**C**.

	DMSO (%)			
12hr	**EGFR (pg/µg Total Protein)**	**Stdev**	***p*EGFR (pg/µg Total Protein)**	**Stdev**
0	575	±65	1475	±71
0.5	501	±10	1638	±53
1	423	±15	1563	±265
24hr				
0	826	±73	712	±53
0.5	823	±27	575	±0
1	759	±48	650	±0
48hr				
0	551	±12	575	±106
0.5	588	±10	925	±71
1	721	±60	900	±0

8.3.3. ErbB2 and phospho-ErbB2 protein quantification by ELISA

As discussed in section 3.3.2 above, in this section we assessed the impact lapatinib had on the expression and activation levels of ErbB2.

The presence of lapatinib in MDA-MB-453 ErbB2-overexpressing cells resulted in a slight increase in ErbB2 expression and moderate decrease in its active level (graph 8.3.3.1.**A** and table 8.3.3.1.**A**.). DMSO caused a slight decrease at 12 and 24 hours but increased expression at 48 hours (graph 8.3.3.1.**C** and table 8.3.3.1.**C**). Similar to lapatinib, DMSO caused a slight decrease in the activity levels of ErbB2 and any effect at 48 hours can be eliminated by large error bars. However, the decrease in activity caused by lapatinib at 12 and 24 hours was greater than that of DMSO but no change at 48 hours.

EGF caused a slight increase in ErbB2 expression at 48 hours and activity at 12 and 24 hours. However, at 48 hours there was a sharp drop in pErbB2 present (graph 8.3.3.1.**B** and table 8.3.3.1.**B**.).
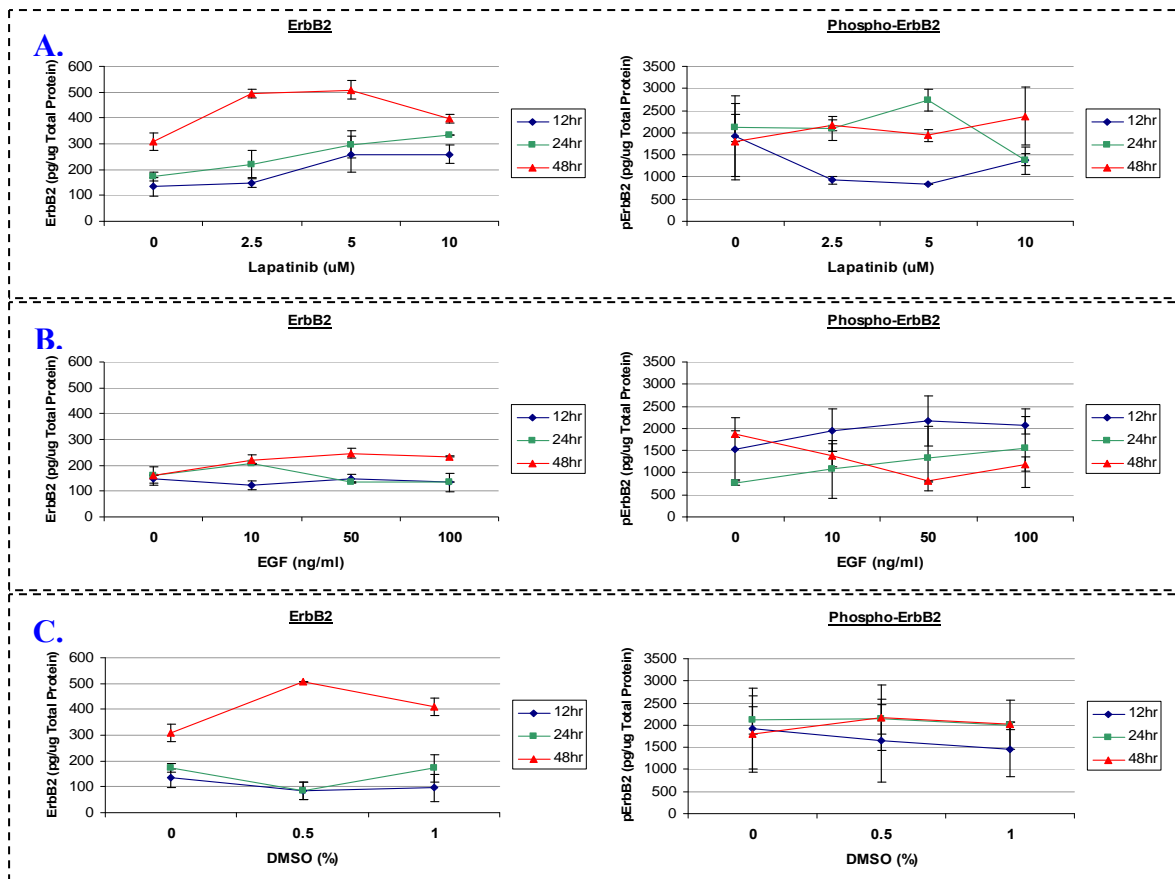
Graph 8.3.3.1: This set of graphs show the levels of ErbB2 and phosphor-ErbB2 in the MDA-MB-453 cell line following exposure to the tyrosine kinase inhibitor, Lapatinib (**A**), the EGFR ligand, EGF (**B**) and as a control, DMSO (**C**) for 12hrs (◆), 24hrs (■) and 48hrs (Δ). The data is representative of duplicate intraday results. The tables below provide the raw data illustrated in these graphs.

Table 8.3.3.1.A: This table outlines the expression levels of ErbB2 (pg/µg Total Protein) and *p*ErbB2 (pg/µg Total Protein) in MDA-MB-453 following a 12hr, 24hr and 48hr exposure to increasing concentrations of lapatinib. This data is illustrated in graph 8.3.3.1.**A**.

Lapatinib treatment (µM)				
12hr	**ErbB2 (pg/ug Total Protein)**	**StDev**	***p*ErbB2 (pg/ug Total Protein**	**StDev**
0	134	±35	1925	±912
2.5	147	±18	930	±85
5	259	±71	840	±0
10	259	±35	1370	±311
24hr				
0	172	±17	2115	±304
2.5	222	±53	2095	±262
5	297	±53	2730	±240
10	334	±0	1390	±141
48hr				
0	309	±35	1795	±856
2.5	496	±17	2175	±120
5	509	±35	1935	±134
10	397	±17	2370	±651

Table 8.3.3.1.B: This table outlines the expression levels of ErbB2 (pg/µg Total Protein) and *p*ErbB2 (pg/µg Total Protein) in MDA-MB-453 following a 12hr, 24hr and 48hr exposure to increasing concentrations of EGF. This data is illustrated in graph 8.3.3.1.**B**.

EGF Treatment (ng/ml)					
12hr	**ErbB2 (pg/µg Total Protein)**	**StDev**	***p*ErbB2 (pg/µg Total Protein)**	**StDev**	
0	147	±18	1525	±714	
10	122	±18	1955	±474	
50	147	±18	2165	±573	
100	134	±0	2065	±191	
24hr					
0	159	±0	775	±64	
10	209	±0	1080	±651	
50	134	±0	1320	±721	
100	134	±35	1560	±891	
48hr					
0	159	±35	1875	±64	
10	222	±18	1385	±262	
50	247	±18	805	±7	
100	234	±2	1195	±148	

Table 8.3.3.1.C: This table outlines the expression levels of ErbB2 (pg/µg Total Protein) and pErbB2 (pg/µg Total Protein) in MDA-MB-453 following a 12hr, 24hr and 48hr exposure to increasing concentrations of DMSO. This data is illustrated in graph 8.3.3.1.**C**.

	DMSO Control (%)				
12hr	**ErbB2 (pg/µg Total Protein)**	**StDev**	**pErbB2 (pg/µg Total Protein)**	**StDev**
0	134	±35	1925	±912
0.5	84	±35	1650	±948
1	97	±53	1455	±615
24hr				
0	172	±17	2115	±304
0.5	84	±35	2135	±332
1	172	±53	1985	±78
48hr				
0	309	±35	1795	±856
0.5	509	±0	2170	±750
1	409	±35	2015	±559

β-actin (48kDa)

8.4. Relationship between the COX-2 inhibitor, celecoxib, and expression and function of Multidrug resistant proteins.

8.4.2. Effect of celecoxib on the inhibition of multidrug resistance transporter proteins.
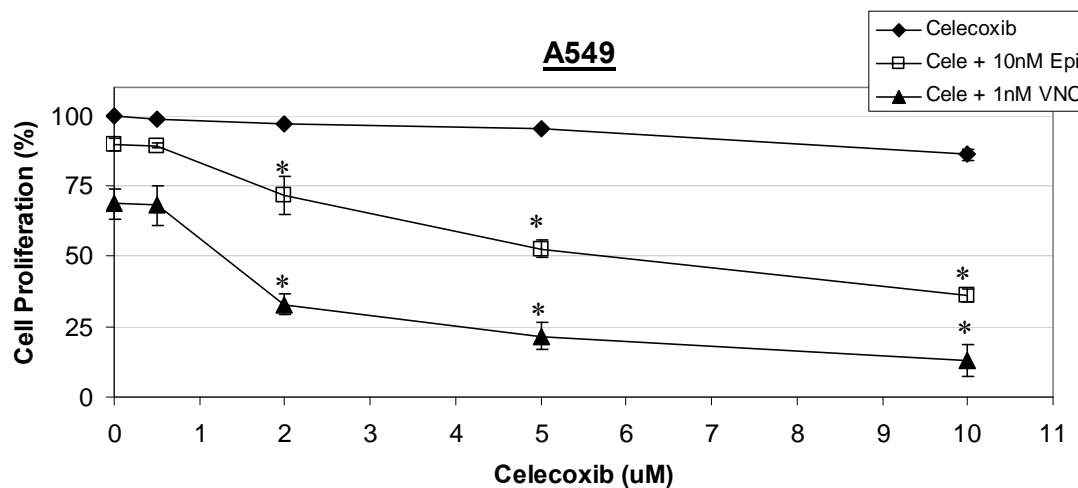
Graph 8.4.2.1.: Combination of epirubicin (□) or vincristine (VNC; ▲) with celecoxib (◆) in the A549 cell line. This proliferation assay involved the combination of one of 2 chemotherapeutic agents with celecoxib in a moderately expressing MRP1 cell line over a 5 day period. This graph is the result of a single determination with standard deviations, for that day, presented as error bars. Statistically significant ($p < 0.05$) results are indicated by (*). Table 8.4.2.1 below depicts the percentage cell proliferation and standard deviations for this graph.

Table 8.4.2.1.: The percentage cell proliferation and standard deviations for the combination proliferation assays of epirubicin or vincristine with celecoxib in the MRP1-expressing cell lines, A549. This table is illustrated in graph 8.4.2.1.

	Cell Proliferation (%)									
Celecoxib (µM)	**0**	StDev (%)	**0.5**	StDev (%)	**2**	StDev (%)	**5**	StDev (%)	**10**	StDev (%)
Celecoxib	100	±0	99	±0	97	±0	96	±0	86	±2
Cele + 10nM Epi	90	±2	89	±1	72	±7	53	±3	36	±2
Cele + 1nM Vinc	69	±5	68	±7	33	±4	22	±5	13	±6

Abbreviations

17-AAG	17-(Allylamino)-17-demethoxygeldanamycin
5-Fu	5-Fluorouracil
AAG	α_1-acid glycoprotein
ABC	ATP-Binding Cassette
ADE	Absorption, distribution and elimination
ADE_2	Cytarabine, daunorubicin and etoposide combination
ADP	Adenosine Diphosphate
ADR	Adriamycin
AML	Acute myeloid leukemia
ATCC	American Tissue Culture Collection
ATP	Adenosine Triphosphate
AUC	Area under the curve
BCA `	Bicinchoninic Acid
BCRP	Breast Cancer Resistance Protein
BSA	Bovine Serum Albumin
cDNA	Complementary DNA
CIN	Cervical intraepithelial neoplasia
COX	Cyclooxygenase
COX-1/-2	Cyclooxygenase-1/-2
C.P.M.	Counts Per Minute
DMEM	Dulbecco's Minimum Essential Medium
DMFO	2-(difluoromethyl) ornithine
DMSO	Dimethyl Sulfoxide
DNA	Deoxyribonucleic Acid
DOX	Doxorubicin (adriamycin)
EDTA	Ethylene diamine tetracetic acid
EGFR	Epidermal growth factor receptor
ELISA	Enzyme-linked Immunosorbant Assay
ERK	Extracellular signal-Regulated Kinase
ET	Endothelin
FCS	Fetal Calf Serum
FDA	Food and Drug Administration
GIT	Gastorintestinal tract

GSH	Glutathione
HBV	Hepatitis B
HCV	Hepatitis C
HCL	Hydrochloric Acid
HCC	Hepatocellular carcinoma
HGF	Hepatocyte growth factor
HEPES	4-(2-hydroxyethyl)-piperazine ethane sulphonic acid
HPLC	High Performance Liquid Chromatography
Hsp90	Heat shock protein 90
IC_{50}	Inhibitory Concentration 50%
ICG	Indocyanine Green
IgG	Immunoglobulin
IL	Interleukin
IMS	Industrial Methylated Spirits
JNK	Jun N-terminal Kinase
kDa	Kilo Daltons
MAPK	Mitogen Activated Protein Kinase
MDR	Multi-Drug Resistance
MEM	Minimum Essential Medium
$MgCl_2$	Magnesium Chloride
Mitox	Mitoxantrone
MRP	Multidrug Resistance-associated Protein
MMP	Metalloproteinase
mRNA	Messenger RNA
MW	Molecular Weight
N/A	Not appliacble
NaCl	Sodium Chloride
NBF	Nucleotide binding folds
$NaHCO_3$	Sodium Bicarbonate
NaOH	Sodium Hydroxide
NF-Y	Nuclear factor Y (transcription factor)
NSAID	Nonsteroidal anti-inflammatory drug
NSCLC	Non-small cell lung cancer
OCD	ornithine decarboxylase
OD	Optical Density
P450	Cytochrome P450
PAGE	Polyacrylamide Gel Eletrophoresis

PBS	Phosphate Buffered Saline
PCR	Polymerase Chain Reaction
PG	Prostaglandin
P-gp	P-glycoprotein
P13K	Phosphatigylinositol 3-kinase
PMSF	Phenylmethanesulphonyl Fluoride
RNA	Ribonucleic Acid
ROS	Reactive oxygen species
RT-PCR	Reverse Transcriptase-PCR
SD	Standard Deviation
SDS	Sodium Dodecyl Sulphate
siRNA	Small interfering RNA
SP1	Member of the SP/KLF transcriptor factor family
STAT	Signal transducers and activators of transcription protein
TBS	Tris Buffered Saline
TEMED	N, N, N', N'-Tetramethyl-Ethylenediamine
THF	Tetrahydrofuran
TKI	Tyrosine kinase inhibitor
TM	Transmembrane
Tris	Tris(hydroxymethyl)aminomethane
TXA	Thromboxanes
UTR	Untranslated region
UHP	Ultra high purity water
VAP	Vincristine, doxorubicin, and dexamethasone combination
Vp	Verapamil
VEGF	Vascular endothelial growth factor
PDGFR	Platelet-derived growth factor receptor
PXR	Pregnance X receptor
YB-1	Y box 1